Performance of Biological Filters for Drinking Water Treatment and Their Use for High Pressure Membrane Biofouling Control

by

Ahmed Mohamed Elsayed Elhadidy

A thesis
presented to the University of Waterloo
in fulfillment of the
thesis requirement for the degree of
Doctor of Philosophy
in
Civil and Environmental Engineering

Waterloo, Ontario, Canada, 2016

AUTHOR'S DECLARATION

This thesis consists of material all of which I authored or co-authored: see Statement of Contributions included in the thesis. This is a true copy of the thesis, including any required final revisions, as accepted by my examiners.

I understand that my thesis may be made electronically available to the public.

Statement of Contributions

This work is part of the project "Biofiltration as a Pre-treatment to Reduce Membrane Fouling" funded by the Ontario Research Fund (ORF), the Natural Sciences and Engineering Research Council of Canada (NSERC), the NSERC Chair in Water Treatment at the University of Waterloo and its partners. The Convergence automated membrane fouling simulator systems presented in Chapter 7 were purchased using the Southern Ontario Water Consortium (SOWC) funding.

The work presented in this thesis included valuable contributions of different individuals. The construction and operation of the biofiltration pilot plant used in the current study was a shared task with Brad Wilson, another graduate student in our group at the University of Waterloo. Several individuals in our group at the University of Waterloo helped with some of the sample analysis and collection tasks. Dr. Monica Tudorancea performed all the liquid chromatography organic carbon detector sample analysis and provided the raw data files used in further analysis. Fei Chen was responsible for performing all the fluorescence spectroscopy analysis and provided the raw data files used in further analysis. Jangchuck Tashi was responsible for doing dissolved organic carbon and ultraviolet adsorption analysis for all the water samples. The Region of Waterloo kindly provided information on some of the water quality parameters for the feed water to the Mannheim full scale water treatment plant as indicated in the relevant thesis chapters. Several undergraduate research assistants and exchange students including Yasser Sidaoui, José Mario Ferraz , Gary Tran, Kyong Jae Woo, John Cameron, Rachel Trower, Katarzyna Jaszczyszyn and Sylwia Kolaska provided valuable technical help in the lab over the course of the study.

Abstract

Biofiltration is a promising green drinking water treatment technology that can reduce the concentration of biodegradable organic matter (BOM) in water. Direct biofiltration or biofiltration without pretreatment (BF_{wp}) limits the use of chemicals such as coagulants or ozone commonly employed with conventional biofiltration, making BF_{WP} a more environmental friendly pre-treatment. BF_{WP} was proven to be an efficient pretreatment to reduce fouling of low pressure membranes, and can also improve the biological stability of the final treated drinking water to limit bacterial regrowth in the distribution system. One major operational problem for high pressure membranes (i.e. nanofiltration and reverse osmosis membranes) is membrane biofouling due to biofilm growth inside the feed channel of the membrane module, resulting in higher energy requirements and more frequent membrane cleaning. BF_{WP} can potentially be applied to reduce biofouling of nanofiltration membranes, which can reduce the energy requirements of high pressure membranes.

Three pilot-scale parallel biologically active filters with different empty bed contact times, and bench-scale nanofiltration membrane fouling simulators, were designed and constructed in this study. A challenging surface water source (the Grand River in Kitchener, ON) was used as source water for the investigation. Initial work assessed the effect of biofiltration on the treated water quality and how the biofilter performance is affected by changes in water temperature. A protocol was developed to better characterize the biofilter attached biomass and extracellular polymeric substances (EPS), in order to understand their possible relationship to biofilter performance. Flow cytometry was applied to measure both planktonic cell concentrations in water and also to perform assimilable organic carbon (AOC) analysis using a natural microbial inoculum. BF_{WP} was found to be an efficient pre-treatment for the removal of large molecular weight biopolymers and AOC over a wide range of water temperatures. Lower water temperatures had a significant impact on biopolymer removal, unlike AOC which was efficiently removed at lower water temperatures, and this proved the robustness of such a pre-treatment technology. Other fractions of the natural organic matter (NOM) such as humic substances, buildings blocks and low molecular weight organics were removed to a lower extent than biopolymers or AOC. Empty bed contact time (EBCT) as a design parameter had a limited effect on the biofilter performance. Most of the observed removal for BOM and total cell count happened at the shortest EBCT of 8 minutes, and increasing the EBCT up to 24 minutes had a significant but less proportional impact on biofilter performance. Regarding biofilter attached biomass, no direct linkage was found between biofilter performance and attached biofilter biomass characteristics using any of

the commonly used analytical methods such as adenosine triphosphate (ATP) or biofilm cell count, however, cellular ATP content was found to be indicative of biofilm activity. Biofilm EPS composition was not related to biofilter performance but it was largely affected by the water temperature. Through community level physiological profiling (CLPP) analysis it was evident that the microbial community was changing due to a drop in water temperature, however, this was a minor effect and it is likely that the overall drop in biomass activity was the main reason behind the drop in biofilter performance.

Finally, BF_{WP} was tested as a potential pre-treatment technology to control high pressure membrane biofouling, which is a major operational problem. BF_{WP} was able to reduce the amount of available nutrients measured as AOC, reduce the presence of conditioning molecules such as large molecular weight biopolymers, and modify the microbial community of the feed water. A 16 minute EBCT biofilter was able to extend the lifetime of nanofiltration membranes by more than 200% compared to the river water without biofiltration, both at low and high water temperature conditions. The 16 minute EBCT biofilter performance was also comparable to that of a full scale conventional biofilter with prior coagulation, sedimentation and ozonation. The biofiltration pre-treatment efficiently affected the amount of biomass present in the biofouling layer and affected the biofilm microbial community as determined using CLPP analysis.

The findings of this study provide the basis upon which further and larger scale testing of the BF_{WP} as a pre-treatment for membrane applications can be done. A sound technology could include a hybrid membrane system with a high pressure membrane proceeded with a low pressure membrane. BF_{WP} can then be used at the start of the treatment train to limit both low pressure membrane fouling at the same time limit the biofouling of the pressure membrane. This treatment train can provide a high water quality with limited footprint compared to conventional treatment trains and long service time. Monitoring of the treatment unit performance can be efficiently done using some of the proposed analytical methods presented in the study, such as AOC monitoring and flow cytometry to study microbiological water quality and biofilter biomass. Fluorescence spectroscopy and size exclusion chromatography can also be used to monitor large molecular weight biopolymers, which are responsible for several operational problems in water treatment in general and specifically for membrane applications.

Acknowledgements

Dedication

I dedicate my dissertation work to my family and many friends. A special feeling of gratitude to my loving parents, Mohamed Elhadidy and Boshra Elgendy and my wonderful wife Heba Dawood for their unconditional love and continuous support. They had endless faith in me and always encouraged me to achieve my dreams. My children Shorouk, Yahia and Yazid who made my life full of happiness and Joy. My brother Sherif and my sister Dina have never left my side and are very special. Also thanks to my friends Fei Chen, Mohamed Hamouda and Haitham Dawood for all the fruitful discussions we had on our research and life.

Table of Contents

List of Figures

xv

xvi

xviii

List of Tables

List of Abbreviations

BFwp	:	Biofiltration without pre-treatment
A	:	Maximum colour value
A.U	:	Arbitrary unit
AOC	:	Assimilable organic carbon
AP-PCR	:	Arbitrarily primed polymerase chain reaction
ATP	:	Adenosine triphosphate
BDOC	:	Biodegradable dissolved organic carbon
BSA	:	Bovine serum albumin
C/N	:	Carbon to nitrogen ratio
CER	:	Cation exchange resins
CFU	:	Coliform forming unit
CLPP	:	Community level physiological profiling
CLSM	:	Confocal laser surface microscope
CSUP	:	Carbon Substrate Utilization Pattern
Da	:	Dalton
DBP	:	Disinfection by product
DGGE	:	Denaturing gradient gel electrophoresis
DO	:	Dissolved Oxygen
DOC	:	Dissolved organic carbon
DOM	:	Dissolved organic matter
EBCT	:	Empty bed contact time
EDCs	:	Endocrine disrupting compounds
eDNA	:	Extracellular DNA
EDTA	:	Ethylenediaminetetraacetic acid
EfOM	:	Effluent organic matter
EPS	:	Extracellular polymeric substances
FEEM	:	Fluorescence excitation emission matrix
FEEM-A	:	Tryptophan-like substances
FEEM-B	:	Fulvic acid-like substances
FEEM-C	:	Humic acid-like substances
FL1	:	Green fluorescence
FL3	:	Red fluorescence
FSC	:	Forward scatter detector
GAC	:	Granular activated carbon
HMW EPS	:	High molecular weight EPS
HNA	:	High nucleic acid
HPC	:	Heterotrophic plate count
I.U	:	Intensity unit
IMW EPS	:	Intermediate molecular weight EPS

LC-OCD	:	Liquid chromatography organic carbon detector
LMW EPS	:	Low molecular weight EPS
LMWA	:	Low molecular weight acids
LMWN	:	Low molecular weight neutrals
LNA	:	Low nucleic acid
MFS	:	Membrane fouling simulator
MWCO	:	Molecular weight cut off
NF	:	Nanofiltration
NOM	:	Natural organic matter
NTU	:	Nephelometric Turbidity Units
OC	:	Organic carbon
ON	:	Organic nitrogen
PBS	:	Phosphate buffer saline
PC	:	Principal component
PCA	:	Principal component analysis
PEG	:	Polyethylene glycol
PES	:	Polyethersulfone
PhACs	:	Pharmaceutically active compounds
PI	:	Propidium iodide
PLFA	:	Phospholipid-derived fatty acids
PMMA	:	Poly(methyl methacrylate)
PMT	:	Photomultiplier tube
PP	:	Polypropylene
PTFE	:	Polytetrafluoroethylene
PVC	:	Polyvinyl chloride
RNA	:	Ribonucleic acid
RO	:	Reverse osmosis
RTD	:	Resistive temperature device
SCUPs	:	Sole carbon substrate utilization patterns
SDS	:	Sodium dodecyl sulfate
SPI	:	Strands per inch
SSC	:	Side scatter detector
SUVA	:	Specific UV absorbance
TEP	:	Transparent exopolymer particles
TFC	:	Thin film composite
TOC	:	Total organic carbon
TVAC	:	True volumetric absolute count
UF	:	Ultrafiltration
UPGMA	:	Unweighted pair-group method using arithmetic averages
UV	:	Ultraviolet

UV254	**:**	Ultraviolet light absorbance at 254 nm
ΔFCP	**:**	Feed Channel pressure drop
ΔFCP0	**:**	Initial Feed Channel pressure drop
$\mathbf{\mu_m}$	**:**	Rate of colour development

Chapter 1

Introduction

1.1 Problem Statement

Biological filtration is becoming more widely used in drinking water treatment. Biological filters were first used as a treatment step to ensure biological stability in distribution systems and the common practice in North America is to use biofiltration to remove both particles and BOM from water (Urfer et al., 1997). Conventional biofiltration includes the use of extensive pre-treatment such as coagulation/ sedimentation/ ozonation prior to the biofilter which acts as a final polishing step for the finished water. Several research studies reported that conventional biofiltration was able to improve the biological stability of the treated water and decrease its biofilm formation potential using different types of surface waters (Okabe et al., 2002; Urfer et al., 1997; Volk and LeChevallier, 1999). BF_{WP} is a modified approach as the raw water is directly treated by the biofilter without any pretreatment other than possibly roughing filtration. BF_{WP} was found to be an efficient pretreatment for ultrafiltration (UF) membranes due to its ability to degrade large molecular weight organics (i.e. proteins and polysaccharides) that can foul the membrane (Hallé et al., 2009). BF_{WP} has the potential of being used as a green pre-treatment technology for other application than UF membranes to limit the use of chemicals and reduce the energy requirement of the whole treatment process. BOM removal with biologically active filters in drinking water treatment is not well understood especially the role of the biofilter biomass in the observed BOM removal. Limited information is available about the biofilter biomass and only few single biomass parameters were used in biofiltration studies in literature with no obvious correlation to biofilter performance (Evans et al., 2013a). Few studies tried investigating the different compartments of the attached biofilm to the biofilter media in operational conventional biofilters and no direct correlation was observed between biofilter biomass characteristics and BOM removal. No studies have provided such information for BF_{WP} filters which are expected to be significantly different due to the differences in feed water quality in the absence of ozonation and prior coagulation.

In the past few decades, the demand for fresh water supplies has considerably increased due to the large increase in the world population. In addition, stringent drinking water quality guidelines along with the recent research on emerging contaminants have made it necessary to improve the efficiency of treatment processes. Newer technologies such as high pressure membrane filtration have been introduced to achieve higher water quality. Nanofiltration (NF) membranes are commonly used for softening applications, rejection of dissolved organic carbon (DOC) and rejection of emerging contaminants such as pharmaceutically active compounds (PhACs) and endocrine disrupting compounds (EDCs) (Bergman,

2007). One of the major operational problems of high pressure membranes including both NF and reverse osmosis (RO) membranes is biofouling. Biofouling can be defined as the growth of undesired microbial biofilm in the feed channel of the commonly used spiral wound configuration of high pressure membrane elements (Flemming et al., 1997). Biofouling increases the feed channel pressure drop which requires an increase of the feed pressure to maintain the overall permeability of the system. As a result, the energy requirements will increase. Preventive measures such as chemical cleaning will be required for biofouling control and retaining original permeability. This raises more concerns about the economic and environmental impacts of the treatment technology.

Biofilm growth on surfaces in direct contact with water is inevitable in any water system due to the presence of bacteria and nutrients. Biofouling was found to be directly related to the amount of available nutrients found in the feed water as indicated by AOC (Hijnen et al., 2009). Prevention of initial bacterial attachment to the membrane by surface modification and nutrient limitation through pretreatment are two possible approaches for biofouling control (van der Kooij et al., 2010). BF_{WP} is an attractive pretreatment technology for high pressure membranes to achieve nutrient limitation. This was reported by only few studies (Griebe and Flemming, 1998; van der Kooij et al., 2010), but they did not provide in depth analysis of the process performance and efficiency. Several factors that can affect the biofilter performance and its ability to biodegrade the available nutrients include the design contact time, water temperature and water quality (Urfer et al., 1997). These factors will also affect the biofouling potential of the biofilter effluent. More information about the biofiltration unit design and its performance will be essential to evaluate the proposed treatment train that is more robust and suitable for further testing at a larger scale.

1.2 Objectives

The overall objective of the research project was to evaluate the efficiency of BF_{WP} as a pre-treatment technology for membrane applications to remove BOM in general. A more specific application of BF_{WP} was to assess its ability to reduce biofouling of NF membranes. The effects of the main biofilter design parameters and feed water quality needed to be studied in depth to assess their relevance and to optimize the overall unit performance for biofouling control. This study was performed at a pilot scale biofiltration plant located at the Mannheim Water Treatment Plant, Kitchener, Ontario. The results of this study provide the basis to further test this pre-treatment technology on a larger scale. BF_{WP} is a green treatment technology that limits the use of chemicals that are required by other pretreatment technologies such as coagulation. Also, by reducing the biofouling rates, NF membranes will have lower energy requirements.

In order to reach the overall objectives the following sub-objectives were addressed:

1. Setup an automated pilot scale BF_{WP} facility including a downstream pilot-scale NF membrane system, suitable to perform the biofilter performance studies within a full scale treatment facility that employ biofiltration as well.

2. Develop a complete protocol to extract and characterize the attached biomass to biofilter media. The proposed protocol will be used to study the biofilter biomass characteristics during the proposed biofiltration studies.

3. Develop better analytical methods to study BOM and microbiological water quality in surface water sources

4. Evaluate the efficiency of several pilot scale biofilters with different EBCTs as a drinking water pretreatment technology to remove BOM.

   a. Investigate possible relationship between biofilter biomass levels and the observed BOM removal within the biofilters

   b. Evaluate the effect of seasonal changes in river water quality (temperature, NOM composition and AOC levels) on the BOM removal within the biofilters

   c. Identify the important biofilter design and operational parameters

   d. Characterization of the microbial community changes over the biofilter depth

   e. Characterization of the microbial community dynamics over different seasons

5. Test the performance of BF_{WP} as a pre-treatment to control NF membrane biofouling

   a. Evaluate the effect of biofiltration on biofouling of the NF membrane units

   b. Evaluate the effect of biofiltration on the biofilm microbial community composition growing on a NF membrane

   c. Compare BF_{WP} to conventional biofiltration with extensive pre-treatment (coagulation, flocculation and ozonation) to control biofouling of a NF membrane

1.3 Thesis structure

The literature review in **Chapter 2** includes an overview of published information related to the research area outlined above. A summary of different research gaps and detailed objectives of this research project are provided at the end of **Chapter 2**. The remainder of the thesis is in an integrated-article format. Each chapter was written as separate articles to describe the different phases of the project

in a more condensed way, and in order to explain the objectives and conclusions of each phase. Finally the overall objectives and contributions to knowledge are summarized in **Chapter 8**.

Chapter 3 includes a comprehensive protocol that was developed to quantify the attached biomass to the filter media. This protocol would replace single biomass parameters commonly used in biofiltration studies in the literature. The protocol aimed to characterize both the bacterial cells within the biofilm and the presence of EPS which constitute the support structure of the biofilm. The protocol was designed in a way that minimizes cell lysis and maximizes biomass extraction from the biofilter media. The protocol was tested on the same pilot scale biofilters which were used in the rest of the thesis.

Chapter 4 introduces an improved protocol to monitor surface water quality. A new method to measure AOC using indigenous bacteria and flow cytometry was adapted to the Grand River as a challenging water source. The developed method provided a reliable and accurate measurement of AOC as a main fraction of the NOM commonly removed by biofiltration and known to greatly affect NF membrane biofouling. The developed method was used to measure seasonal changes in river water AOC levels, and how they related to inorganic nutrient levels, NOM fractions and the river microbial community.

Chapter 5 provides the results of BOM removal by a pilot scale BF_{WP} study. The study employed the protocols and analytical methods presented in **Chapters 3** and **4** to monitor the biofilter performance. The effect of biofilter EBCT and seasonal water quality changes on the biofilter performance were studied. The attached biofilter biomass was also characterized to understand the seasonal changes in biofilter biomass and its relationship to biofilter performance.

Chapter 6 provides a study on the changes in the composition of the biofilter microorganisms using CLPP techniques. Sole carbon substrate utilization patterns (CSUPs) of the Biolog EcoPlates were used as indicators of community structure. Multivariate statistical analysis techniques i.e. hierarchical clustering and principal component analysis (PCA), were applied to determine differences in community composition over biofilter depth, and to detect possible changes in the dynamics of the microbial community due to changes in seasonal water quality.

Chapter 7 provides a study of BF_{WP} pre-treatment for biofouling control of NF membranes. Two different experiments were done to test the efficiency of BF_{WP} at two different seasons (with cold and warm water temperatures). The effect of biofilter EBCT on biofouling control was also tested, and BF_{WP} was directly compared to conventional biofiltration as a biofouling pre-treatment. The developed biofilter biomass characterization protocol in Chapter 3 was modified and used to characterize the developed

biofilms on the NF membranes. The effect of pre-treatment on the microbial community composition was also tested using the CLPP technique.

   Chapter 8 provides a summary of the findings of the study, and its general conclusions and contributions to the drinking water treatment knowledge. This chapter also presents the implication of this work for further testing of BF_{WP} as a drinking water pre-treatment technology, which can lay the foundation for full-scale implementation of this green pre-treatment technology.

Chapter 2
Literature Review

The literature review presents an overview of biofilm formation in general and specifically in the field of biofiltration, and biofouling formation of high pressure membranes for drinking water treatment. Biofiltration in drinking water treatment will also be discussed in the context of nutrient limitation and its potential for biofouling control.

2.1 Introduction

World water demand has seen a significant increase in the past few decades due to the rapid increase in the world population and changes in the living standards of people (Gleick, 2000) which has increased the stress on the available water resources. Another important aspect of the global water problem is the new categories of pollutants such as PhACs and EDCs. These contaminants were found in drinking water at trace levels in the United States and Canada (Heberer, 2002). Biological water treatment processes are on the rise in the drinking water treatment industry to have more environmental friendly technologies that can possibly deal with those contaminants along with the traditional contaminants. Biofiltration is the use of a granular media filter without any disinfectant residual, both in the feed and backwash water, which allows bacterial biofilms to grow on the media surface. The developed bacterial biofilm can degrade the biodegradable fraction of the NOM known as BOM. Biofiltration can efficiently remove BOM (Urfer et al., 1997), disinfection by-product (DBP) precursors, along with some of the emerging contaminants (Hallé et al., 2015; McKie et al., 2015). One recent application of biofiltration is using it as a pretreatment for membrane fouling control, specifically low pressure membranes (Hallé et al., 2009; Huck and Sozański, 2008).

Biofiltration may also have applications to control biofouling of high pressure membranes. High pressure membranes are one of the advanced water treatment technologies which are being used more recently. High pressure membranes, including both NF and RO membranes, are efficient treatment technologies to remove not only emerging contaminants but also other conventional organic contaminants, especially charged molecules (Kimura et al., 2003). NF membranes were developed in the late 1970s and have a lower operating pressure than the RO membranes, which are used mainly for water desalination. NF membranes can efficiently remove divalent cations, but unlike RO membranes, they do not reject monovalent ions. Applications of NF membranes in drinking water treatment include water softening, removal of synthetic organics and pathogens, DOC rejection and colour removal (Bergman, 2007). The use of high pressure membranes (NF/RO) is therefore expected to increase in the future in accordance with the increase in demand for higher quality water. However, membrane biofouling can increase the

cost and complexity of NF membrane operations. Therefore, more research will be needed to optimize their performance.

2.2 Bacterial biofilms in drinking water treatment

Most fresh water systems are favorable for bacterial cell growth and survival for many reasons including the availability of nutrients and the protection from extreme environmental conditions. Heterotrophic bacteria utilize available carbon in the water along with inorganic nutrients to produce new biomass (Sigee, 2004). BOM in water is commonly characterized using methods that are either based on consumption of DOC such as biodegradable dissolved organic carbon (BDOC) or biomass growth such as AOC. BDOC is the BOM fraction that is utilized by heterotrophic bacteria as measured by DOC consumption (Huck, 1990). AOC is the BOM fraction that is consumed by selected bacterial strains for biomass growth, and this growth is then related back to carbon concentration as acetate (van der Kooij, 1992). AOC measures mainly low molecular weight compounds and it is considered as the readily biodegradable fraction (Escobar and Randall, 2001). No direct correlations were found between DOC, BDOC and AOC concentrations for several waters (Huck 1990). AOC has a higher detection limit than BDOC (Escobar and Randall, 2001) and it was found to be more appropriate to represent the regrowth of biomass in the distribution systems (Huck, 1990). Inorganic nutrients required for bacterial growth include nitrogen and phosphorous, sulfur, calcium, potassium, magnesium and trace elements (iron, other metals), and sometimes growth factors which are specific to certain microorganisms (Bott, 2011). Carbon is commonly assumed to be the limiting nutrient for bacterial growth in water, however, phosphorous can be an important limiting nutrient in some special cases (Sathasivan and Ohgaki, 1999).

In any water system where the various nutrients are available, microorganisms tend to exist in larger communities of mixed species rather than individually (Flemming, 2002). A microbial biofilm is an ecosystem where various microorganisms can co-exist within a gelatinous structure of EPS excreted by the cells and used to bind them together (Sigee, 2004). In man-made systems such as pipelines or drinking water treatment units, bacteria are the major contributor to biofilm formation due the absence of light. Bacterial cells prefer to exist in the form of biofilms attached to solid surfaces rather than being suspended in the bulk liquid. A possible reason is the ease of delivering nutrients to the surface due to liquid turbulence, followed by nutrient diffusion inside the biofilm (Bott, 2011). Biofilms have an open structure as shown in **Figure 2-1,** where water can flow through the biofilm and deliver nutrients to the base of the biofilm (Lewandowski and Beyenal, 2005). Bacterial cells comprise only 10% of the dry biofilm mass, while the remaining 90% is mainly EPS (Flemming and Wingender, 2010). EPS consists of a heterogeneous mixture of compounds such as polysaccharides, proteins, lipids and/or nucleic acids (Flemming and Wingender, 2001). In addition to its role in biofilm cohesiveness, EPS also aids in

attaching the biofilm to the solid surface and provides adsorption sites for dissolved and colloidal nutrients for the bacteria (Flemming, 2002).
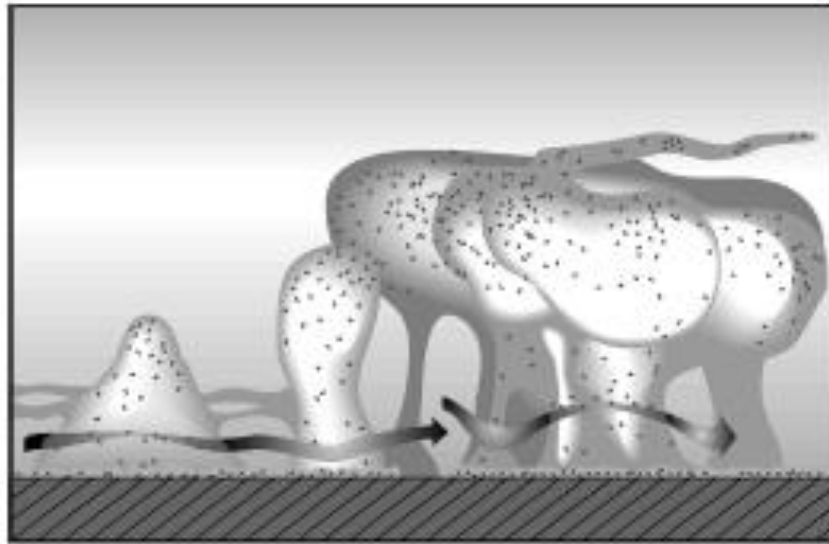
Figure 2-1 Schematic representation of the biofilm structure cross section (Lewandowski and Beyenal, 2005)

2.2.1 Biofilm formation mechanisms

Bacterial adhesion to solid surfaces is an organized process that happens in different stages which are similar for most bacterial strains. A schematic explaining the different steps of the biofilm formation process is shown in **Figure 2-2** (Bryers, 2008). The first stage is the initial attachment of bacterial cells to the surface. Cells continue to attach to open surfaces until a bacterial monolayer is developed. Deposited cells start communicating with each other through quorum sensing within a very short time frame of a few minutes (Bryers, 2008) and start excreting EPS to glue themselves to the surface (Costerton et al., 1999). The deposition of organisms will depend on the electrostatic and hydrophobic properties of both the surface and the bacterial cell along with hydrodynamic flow conditions (Bott, 2011). Also surface conditioning with organic macromolecules such as proteins along with some inorganic particles from the feed water can significantly improve the bacterial deposition as they can alter surface properties (Chamberlain, 1992). This phase is known as the induction phase of the biofilm growth (Flemming, 1997).
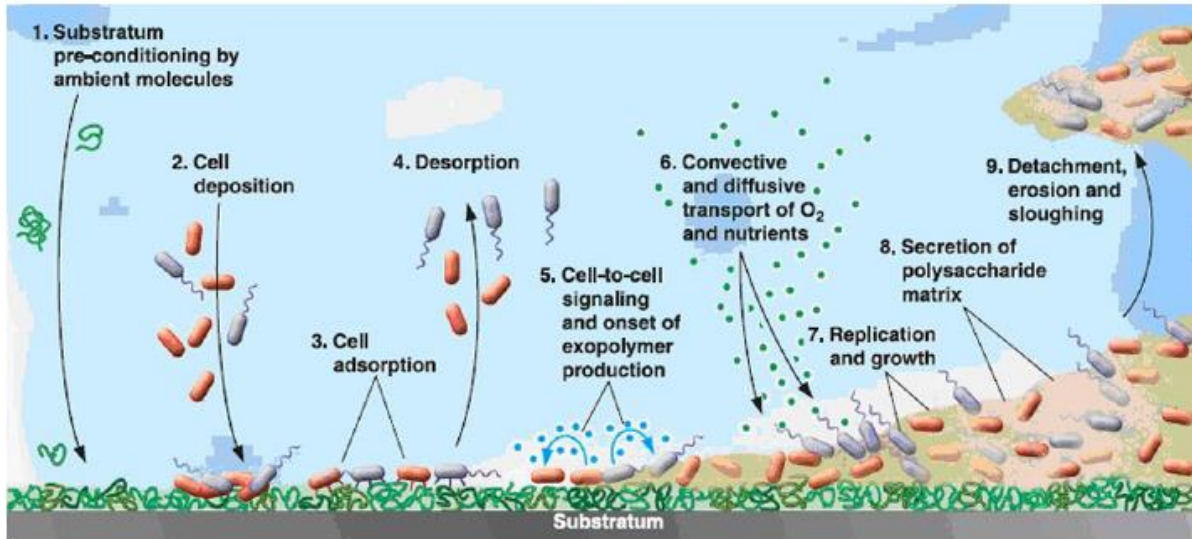
Figure 2-2 A schematic of the several steps for the biofilm formation process over time (Bryers and Ratner, 2004)

The second stage is biofilm maturation. Nutrients from the bulk liquid are delivered by diffusion to the bacterial cells attached to the surface. Attached bacteria consume the available nutrients and also use organic or inorganic compounds as an energy source for cell activity, multiplication and to produce additional EPS. This phase can be considered the logarithmic growth phase where the biofilm starts producing more new biomass than the deposited biomass (Flemming, 1997). Biofilm growth will be mostly reflected as an increase in biomass and biofilm thickness. The biofilm thickness will increase until oxygen and/or nutrients can no longer diffuse to the biofilm base, which weakens the biofilm. The fluid shear force then starts to break apart some of the biofilm (Characklis and Bryers, 2009). As a result, the biofilm growth reaches a steady state condition. Further growth of the biofilm is nearly matched by the biofilm decay and sloughing. The biofilm then starts its maintenance process by replacing weak parts of the structure and strengthening the overall structure to make it more amenable to detachment (Bott, 2011). This phase is usually named as the plateau phase (Flemming, 1997).

2.2.2 Biofilm EPS Composition and Function

Biofilm EPS is a group of different categories of molecules that vary greatly in nature and function, are actively excreted by living bacterial cells, and form approximately 90% of the biofilm mass (Wingender et al., 1999b). Biofilm EPS in general provide the biofilm with a protective barrier against antimicrobial agents and environmental factors and at the same time can act as a nutrient source if needed (Flemming and Wingender, 2010). Different EPS fractions include:

2.2.2.1 Polysaccharides

Biofilm polysaccharides are large molecular weight molecules consisting of different types of monomers such as monosaccharide, uronic acids and amino sugars (Wingender et al., 1999b). They have a wide range in molecular weight of $0.5 - 2 \times 10^6$ Da, which makes them vary greatly in composition and their chemical and physical properties (Sutherland, 2001a). Polysaccharides adhesive properties allow the biofilm to easily attach to surfaces and at the same time aggregate the bacterial cells together providing the biofilm with its cohesive strength (Flemming and Wingender, 2010). Detection of biofilm polysaccharides is commonly done using the carbohydrates phenol sulfuric acid method developed by DuBois and co-workers (1956).

2.2.2.2 Proteins

Biofilm extracellular proteins are believed to be the main fraction of the biofilm EPS (Sutherland, 2001b) as reported for wastewater activated sludge (Frølund et al., 1996), anaerobic sludge (Schmidt and Ahring, 1996), pure bacterial strains (Jahn et al., 1999) and drinking water biofilms (Michalowski, 2012; Stoquart et al., 2013). EPS proteins are commonly present as extracellular enzymes mainly responsible for the biofilms ability to degrade BOM fractions present in freshwater sources such as proteins, polysaccharides, lipids, cellulose and even organic particles trapped within the biofilm (Flemming and Wingender, 2010). Other forms of EPS proteins are structural proteins that help in providing the biofilm structural stability through electrostatic cross linkages or hydrophobic bonding (Dignac et al., 1998; Laspidou and Rittmann, 2002). The main building unit of EPS proteins are amino acids, and different standard analytical methods can be used for protein quantification such as the Lowry method, bicinchoninic acid assays and the Bradford method (Walker, 1996).

2.2.2.3 Humic Substances

Humic substances are commonly present in bacterial biofilms and they compromise up to 20% of the biofilm mass (Frølund et al., 1996; Jahn and Nielsen, 1998). The presence of humic substances in biofilms is attributed to adsorption of aquatic humic substances or due to partial enzymatic degradation and repolymerization of other types of molecules (Wingender et al., 1999b).

2.2.2.4 Extracellular DNA (eDNA)

eDNA was found to be one of the major fraction of biofilm EPS in wastewater activated sludge (Frølund et al., 1996; Palmgren and Nielsen, 1996), pure strain biofilm (Whitchurch et al., 2002) or environmental biofilms from soil and sediments (Pietramellara et al., 2009). The source of eDNA was believed to be cell lysis in the biofilm and the release of intercellular components (Sutherland, 2001b). However, several

studies found that eDNA is exerted by some bacterial strains and they have an important role in biofilm formation and structural properties (Whitchurch et al., 2002) or adhesion to surfaces (Das et al., 2010).

2.2.3 Biofilm EPS Extraction

A key step for EPS analysis and characterization is the EPS extraction and isolation method. For example, EPS composition for the same biofilm sample was found to vary when different types of extraction methods were used (Pellicer-Nàcher et al., 2013). This is because each fraction of the EPS has an optimum extraction method, and this especially true for biofilm from environmental samples, where mixed microbial populations will be present (Flemming and Wingender, 2010). Although there is no perfect EPS extraction method, the main objectives are to maximize the recovery while minimizing cell lysis and to prevent EPS contamination due to the release of intracellular components. A summary of different EPS extraction methods are shown in **Table 2-1**. Methods using cation exchange resins (CER) are common and were initially used for activated sludge biofilms (Frølund et al., 1996). The CER EPS extraction mechanism removes cations responsible for negatively charged functional groups in the extracellular polysaccharides, and this then causes the biofilm structure to collapse and dissolve the EPS (Nielsen and Jahn, 1999). CER extraction was successfully used on soil biofilms (Boretska et al., 2013), drinking water biofilms in high pressure membranes (Dreszer et al., 2013), drinking water distribution system biofilms (Michalowski, 2012) and biofilms from bacterial pure strains (Jahn et al., 1999). CER was also reported to cause a lower extent of cell lysis compared to other common EPS extraction methods such as formaldehyde/ NaOH treatment, sonication or Ethylenediaminetetraacetic acid (EDTA) treatment, both for wastewater activated sludge and drinking water biofilms (Michalowski, 2012; Pellicer-Nàcher et al., 2013). The dissolved EPS can then be separated from the bacterial cells using centrifugation or filtration, to be used for further EPS analysis. One main drawback of most of the EPS extraction techniques is that they mainly target EPS soluble molecules and neglect the insoluble EPS fractions such as cellulose (Flemming and Wingender, 2010).

Table 2-1 A list of the common EPS extraction methods that have been used in the literature (Michalowski, 2012; Nielsen and Jahn, 1999)

Physical EPS Extraction	Chemical EPS Extraction	Combined Chemical Physical EPS Extraction
• Heating / Boiling • Sonication • Centrifugation • Filtration	• NaOH treatment • EDTA treatment • Formaldehyde	• Cation exchange resin (CER) / Shear force

2.3 Biological Filtration in Drinking Water Treatment

Biological filtration is an interesting pretreatment technology for biofouling control. In principle, most granular media filters if operated without any disinfectant residual (e.g. chlorine) will perform as a biologically active filter. Due to the availability of nutrients and active biomass in the feed water, a bacterial biofilm starts to grow on the grains of the filter media. During filter operation, the biofilm consumes part of the BOM in the feed water as it passes through the filter. Conventional biological filtration is typically employed to control/biodegrade small organic molecules generated during ozonation from NOM. If left uncontrolled this spike in AOC concentration can enhance bacterial regrowth in the distribution system. The feed water to the ozonation step can either be raw water but is mostly clarified water after coagulation and flocculation. Biological filters were first used as a treatment step to ensure biological stability in the distribution systems and the common practice in North America is to use biofiltration to remove both particles and BOM from the water (Urfer et al., 1997). Several research studies reported that conventional biofiltration was able to improve the biological stability of the treated water and decrease its biofilm formation potential using different types of surface waters (Okabe et al., 2002; Urfer et al., 1997; Volk and LeChevallier, 1999). The main advantages of biological filtration are the reduced maintenance cost and high efficiency in BOM removal without the need for any chemicals (Fonseca et al., 2001).

BF_{WP} is a modified approach as the raw water is directly treated by the biofilter without any pretreatment other than possibly roughing filtration. This process has the same principle like the conventional biofiltration as a bacterial biofilm will be developed on the media surface to consume BOM. However, due to the process treatment objectives and operation the two processes will have some key differences. BF_{WP} is mainly intended as a pre-treatment technology to decrease particle and BOM loading on the subsequent treatment units, unlike conventional filtration which is a final polishing step in the treatment

train to consume ozonation by-products, disinfection by-products, organic trace contaminants, and taste and odor causing compounds. BF_{WP} was reported to be a good pretreatment to reduce BOM levels in the feed water, to improve water biological stability (Persson et al., 2006) at the same time remove taste and odor compounds (Persson et al., 2007) or organic trace contaminants (Hallé et al., 2015). One potential application for BF_{WP} is using it as a pretreatment for low pressure ultrafiltration membranes due to its ability to degrade large molecular weight organics (i.e. proteins and polysaccharides) that can foul the membrane. These results were reported both in bench scale (Hallé et al., 2009) and pilot scale studies (Peldszus et al., 2012).

Differences between the location of biofiltration in the treatment train may cause differences in the biofilm nature though this has not been studied yet. There will likely be differences in the nature of BOM reaching the biofilter, as BF_{WP} has no pre-ozonation or coagulation/sedimentation, unlike conventional biofiltration so BOM present in the surface water source will directly go into the BF_{WP} filter unlike conventional biofiltration. Pre-ozonation can actively increase the amount of easily biodegradable organics measured as AOC due to the breakup of large MW compounds such as humic substances (Hammes et al., 2006; Pharand et al., 2015). Additionally, the extensive pre-treatment in the case of conventional biofiltration can reduce the concentration of inorganic nutrients, especially phosphorous (Huck et al., 2015). Coagulation/sedimentation can also remove large MW biopolymers (i.e. proteins and polysaccharides) (Croft, 2012) and this biopolymer fraction was found to be a highly biodegradable fraction (Huber, 2002) in drinking water biofilters and act as a potential substrate. These differences in the types of nutrients can lead to changes in the biofilm community structure and function. Moll and co-workers (1998) reported significant differences in the microbial community structure of two parallel media filters fed using the same settled river water with or without prior ozonation step. These differences were also obvious in the number of utilizable organic substrates by the biomass in each filter as the filter without ozonation was able to utilize more carbon sources than the biomass from the filter with prior ozonation. Additionally, the biomass obtained deeper in the filter without ozonation was more similar to the biomass at the top of the same filter compared to the filter with prior ozonation where the biomass at the bottom of the filter could utilize fewer organic substrates compared to the biomass at the top of the same filter. This can show that ozonation affected the microbial community in the biofilter in general in addition to the microbial community profiling over the filter depth. Another difference between BF_{WP} and conventional biofiltration is presumably the amount and community structure of the fresh water biomass in the biofilter feed water. Pre-ozonation in the case of conventional biofiltration can act as a disinfectant and reduce the amount of bacterial cells present in the water (Hammes et al., 2008; Velten et al., 2011). Due to these differences, generalization of biofilter design criteria or biofilter performance expectations

among the two processes might not be appropriate regardless of the fact that both are similar biological processes in principle.

2.3.1 Operational parameters affecting biofilter performance

Biofiltration efficiency in BOM removal is affected by several operational parameters such as water temperature, filter media type, EBCT, and presence of a pre-oxidation step (Urfer et al., 1997). Three of these parameters which are applicable to BF_{WP} include biofilter media, EBCT and temperature.

2.3.1.1 Biofilter media

Commonly used biofilter media types include granular activated carbon (GAC), anthracite and sand. GAC has adsorptive capacity for organic molecules, unlike both anthracite and sand, and this can provide additional benefits over other types of media in the initial stages of operation. Therefore, a direct comparison between the different types of media cannot be obtained until the adsorptive capacity of the GAC is exhausted (Urfer et al., 1997). In a long term pilot scale experimental study using an anthracite sand filter and three different GAC filters, GAC had significant higher total organic carbon (TOC) removal, however AOC removal was only slightly higher (Wang et al., 1995). A major differences between sand and anthracite is that sand has a higher specific surface area (i.e. surface area per unit volume) than anthracite (Zhang, 1996). Dual-media filters such as anthracite/sand filters are commonly used in water treatment over mono-media filters such as sand only. Dual-media filters will help to mitigate head loss development, as the particles will be able to penetrate deeper into the filter bed without causing excessive head loss (Crittenden, 2005).

2.3.1.2 Biofilter EBCT

Biofilter EBCT is the ratio of the biofilter loading rate, or the downward flow velocity above the media (L. T^{-1}) divided by the filter depth (L), and it represents the hydraulic residence time of the empty biofilter. EBCT is considered a critical parameter for biofilter design as it largely affects BOM removal, which is believed to follow first order reaction kinetics. By increasing EBCT, the AOC removal within the filter will increase up to a maximum value (Urfer et al., 1997). As AOC is believed to be more easily removed by biological filters than BDOC, AOC will probably be removed at the top of the biofilter (at shorter EBCT) as has been reported by several studies in the literature (Prévost et al., 2005). Extending the biofilter EBCT beyond a certain value (i.e. very long EBCT) would results in a less proportional increase in BOM or AOC removal within the biofilter, according to some mathematical models to predict biofilter removal (Huck et al., 1994; Prévost et al., 2005; Zhang and Huck, 1996a, 1996b). Most of the studies reported here were done on conventional biofilters rather than BF_{WP} filters. Possible differences in the BOM nature between the two approaches are likely to exist due to preceding ozonation and/or

clarification steps in the conventional biofiltration and no prior steps in BF$_{WP}$. Limited information is available on the effect of BF$_{WP}$ biofilter EBCT on BOM removal in literature. Peldszus and co-workers (2012) showed that high MW biopolymers, DOC and turbidity removal increased significantly due to the increase in EBCT of anthracite/sand BF$_{WP}$ filters (EBCT of 5, 10 and 15 minutes). Similar results were reported for bench scale filters as well (Hallé et al., 2009).

2.3.1.3 Water temperature

Apart from the seasonal changes in NOM composition and AOC levels, the activity of the biofilter biomass and the mass transfer rates will increase with increasing temperature (Urfer *et al.* 1997). Laurent and co-workers (1999) showed that the activity of the attached biomass on GAC biofilter media as measured by the radiolabelled glucose respiration method (Servais et al., 1991) at 5°C was nearly 40% of the activity at a higher temperature of 23°C. Low water temperatures can also cause some changes in the microbial community of the attached biomass on the biofilter media (Moll et al., 1999). On the other hand, lower water temperature did not have a significant impact on the attached biofilter biomass when reported as ATP in full scale conventional filters (Evans et al., 2013a; Pharand et al., 2014). BOM removal would be expected to drop during cold seasons. However, some studies reported that conventional biofiltration could still provide high AOC removal at low temperatures (e.g. Prévost et al., 2005). Moll and co-workers (1999) reported that AOC was the least affected parameter when the temperature was dropped from 35 to 5°C in parallel conventional sand biofilters. They found that effluent AOC concentration dropped from 57 to 43 μg C/L, however, DOC, BDOC and chlorine demand had a higher drop in removal at the cold water temperature and overall BOM removal was reduced by 42% (Moll et al., 1999). Peldszus and co-workers (2012) reported simialr results for BF$_{WP}$ and showed that the DOC removal decreased from nearly 15% to 5% as the water temperature dropped below 10°C.

2.3.1.4 Attached Biofilter Biomass

Biofilter biomass is a key component of the biofiltration process which makes it a critical performance parameter. Several analytical techniques can be used to characterize the biofilm attached to biofilter media, and **Table 2-2** shows some of the common methods along with serveral biofiltration studies that applied those techniques. The methods vary from those that directly measure the attached biomass using hetrotrophic plate count, total direct cell count or flow cytomtry, to more indirect methods that estimate the amount of attached biomass using ATP or phospholipid fatty acids. Biomass activity can also be used as a biomass parameter, and analytical techniques include enzymatic assays or respirometric activity tests. One limitation of biomass monitoring is that steady state BOM removal can be achieved with a minmum amount of biomass, and beyond this biomass level BOM removal will not be affected (Urfer et al., 1997).

Wang and co-workers (1995) found that biofilters with different media types and attached biomass levels (measured as phospholipid fatty acids) had similar BOM removal measured as AOC. Measurement of a single biomass parameter such as ATP or biomass enzymatic activity also failed to explain the effect of water temperature, as these biomass parameters were not affected by the water temperatures regardless of the drop in DOC and AOC removals at decreased tempreatures (Evans et al., 2013a; Pharand et al., 2015). Wilson (2015) also showed similar biomass respirometric activity, measured as dissolved oxygen uptake rate, for two identical biofilters operated at different backwash routines. Based on these results, single biomass parameters can optimally be used to develop a seasonal baseline for the biofilter biomass to investigate any drastic changes in the amount of attached biomass, however their relationship to changes in the biofilter performance is not well established (Evans et al., 2013a).

Table 2-2 Different analytical methods used for monitoring biofilter biomass

Biomass Monitoring Tool	Sample Biofitlration studies from literature
Bulk ATP content	(Magic-Knezev and van der Kooij, 2004; Velten et al., 2007)
Biomass enzyme activity	(Fonseca et al., 2001; Le Bihan and Lessard, 1998)
Biomass respirometric activity (Dissolved Oxygen (DO) Consumption)	(Urfer and Huck, 2001)
Heterotrophic plate count (HPC) or total direct cell count	(Camper et al., 1985; Magic-Knezev and van der Kooij, 2004)
Extracellular polysaccharides	(Lauderdale et al., 2012)
Phospholipid fatty acids	(Peldszus et al., 2012; Wang et al., 1995)
Biomass cell count using flow cytoemtry	(Velten et al., 2011, 2007)

2.4 Nanofiltration membranes in drinking water

2.4.1 Surface characteristics and membrane selectivity

Thin film composite (TFC) membranes are commonly used for high pressure membranes (NF, RO) rather than the asymmetric membranes typical for micro and ultrafiltration membranes. TFC membranes were developed in the late 1970s and consist of a very thin salt barrier layer overlaying a more open microporous layer. Aromatic polyamide membranes are typically used due to their broad operational pH range and their resistance to biological degradation. NF membranes have a lower operational pressure

than RO membranes, and yet can still maintain salt rejection albeit only for divalent ions. The average molecular weight cut off (MWCO) of NF membranes is approximately 400 Daltons (Da) but can be lower. They commonly possess a negative surface charge (Bergman, 2007).

2.4.2 Module and process configuration

The commonly used module configuration of NF and RO membranes is the spiral wound configuration shown in **Figure 2-3**. In this configuration two membrane sheets are held together with their permeate sides facing each other and with a permeate spacer in between. Several of these membrane sandwiches are used and they are glued on all sides except one side that is connected to the central permeate collection tube. In between the feed side of each membrane sandwich, a feed spacer (i.e. plastic netting) is used to maintain a consistent feed chanel height and to create turbulence (Bergman, 2007). Feed water flows through the open side of the element to the flow chanel created by the feed spacer. The feed water then moves through the membrane under cross flow conditions, and the membrane permeate travels to the permeate collection chanel and then to the central collection tube. Retentate will be collected from the feed channels at the other end of the module. The full scale process includes several stages of high pressure membrane elements in series, where the concentrate/retentate from one stage is used to feed the next stage. The final concentrate can be either disposed of or mixed with the feed water to improve overall recovery.
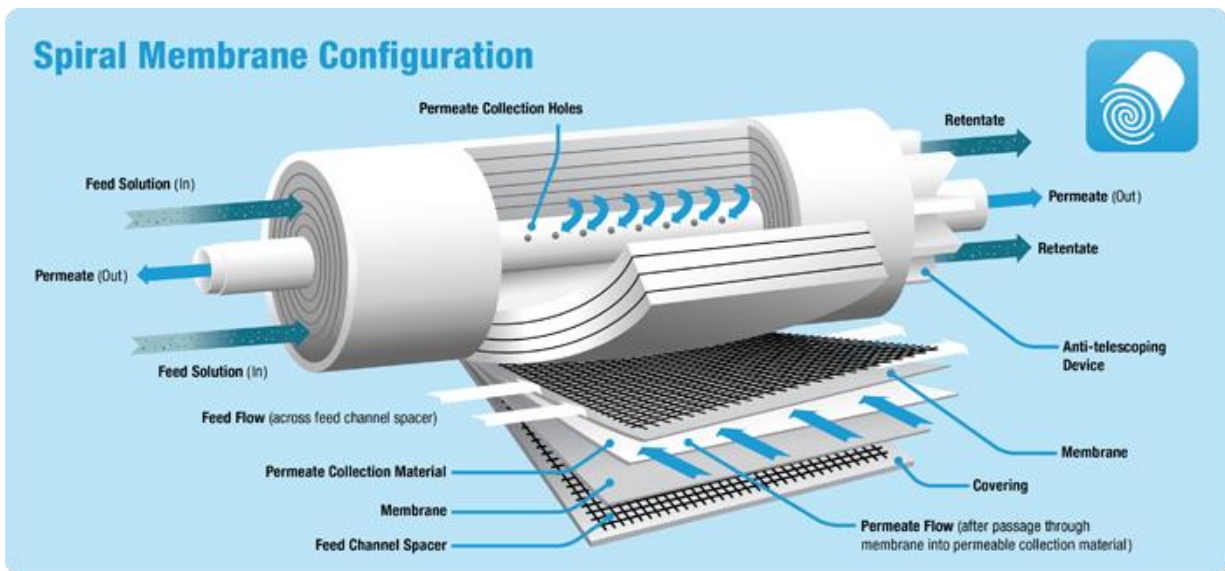
Figure 2-3 Spiral wound membrane configuration (Koch Membrane Systems Inc., USA)

2.4.3 Biofouling in high pressure membranes

One of the major problems with spiral wound membrane elements (e.g. NF or RO membranes) is the problem of biofouling. Biofouling can be defined as the development of unwanted bacterial biofilm inside the membrane module (Flemming, 1997). Due to the available nutrients and biomass found in the feed water, bacterial cells adhere to the walls within the feed channels (the membrane surface and the feed spacer), which initiates the biofilm formation process. No signs of biofilm growth have been found to occur on the permeate spacer (Vrouwenvelder et al., 2008). As described by Flemming (1997), biofouling within the feed channels can cause several problem to high pressure membrane elements such as:

1. Increased head losses within the feed channel, as measured by the feed channel pressure drop (ΔFCP), which will decrease the overall permeate production.

2. The developed biofilm will have a gel structure near the membrane surface that can enhance concentration polarization and decrease the salt rejection of the membrane.

3. The biofilm can eventually degrade the membrane material, especially for cellulous acetate membranes.

4. Increasing the demand for module cleaning, which can decrease the lifetime of the modules and more chemicals will be required.

5. Increased energy requirements and replacement costs.

2.4.4 Factors affecting high pressure membrane biofouling

The development of biofouling within the high pressure membrane element is a complex process and can depend on several factors. The raw water quality, nutrient availability, membrane surface properties and hydrodynamic flow conditions are the most important factors (Flemming, 1997).

2.4.4.1 Hydrodynamic flow conditions

After the initial deposition and attachment of bacteria to the substratum (i.e. solid surface where the biofilm will grow), the ambient flow conditions will control the biofilm growth and properties. The flow of water around the biofilm will increase the shear force, which can cause biofilm detachment. This will make the biofilm more compact and the adhesive strength of the biofilm will increase (Chen et al., 2005). In addition, biofilm formation can increase the surface roughness, which would increase the head loss (Stewart, 2012). Similar results were reported for high pressure membranes by only a few authors, who reported that the cross flow velocity increase caused an increase in the ΔFCP across a spiral wound membrane fouling simulator as well as biomass accumulation (Bucs et al., 2014; Vrouwenvelder et al., 2009b).

2.4.4.2 Membrane surface properties

Surface roughness is an important factor that can largely affect biofilm formation as it will enhance bacterial adhesion to the surface (Melo and Bott, 1997). Valleys in the membrane surface can provide shelter to the adsorbed bacterial cells from external flow conditions (Bott, 2011). Also, as mentioned earlier, development of the bacterial biofilm will increase the surface roughness and head loss (Stewart, 2012) and this will further increase biofilm thickness and growth (Bott, 2011).

2.4.4.3 Nutrient availability

Available nutrients in the aqueous phase are the driving force for biofilm formation and they also affect the biofilm characteristics. Nutrient limitation (e.g. low levels of the limiting substrate) can lead to a biofilm structure which is more dense and compact with a higher EPS content compared to an open structure in cases where nutrients are available (Garny et al., 2009; Melo and Bott, 1997). Under nutrient limiting conditions, biofilm growth will be slower, which can allow the applied shear force to erode external parts of the biofilm and make it more flat (Van Loosdrecht et al., 1995). Organic carbon or BOM is usually considered the primary substrate limiting the bacterial regrowth in the water systems as measured by the AOC test (Huck, 1990). AOC values below 10 µg C/L are considered as the minimum requirement for bacterial regrowth in distribution systems (van der Kooij, 1992). Typically, the required Carbon (C): Nitrogen (N): Phosphorus (P) ratio is 100:10:1 by weight (Toolan et al., 1991). While N is usually present in most surface waters in suitable concentrations, P can possibly be the limiting nutrient at concentrations below 5 µg P/L measured as PO_4^{-3} (Sathasivan et al., 1997).

The effect of nutrients on biofilm growth in spiral wound membrane systems have been reported by only a few authors. Severe biofouling was observed for NF/RO systems when the AOC values exceeded 80 µg C/L, based on data from more than 13 full scale plants (Vrouwenvelder and Van der Kooij, 2001). In experiments with synthetic model solutions Vrouwenvelder and co-workers (2009b) found that as the feed water acetate concentration (i.e. carbon as a limiting nutrient) increased, the biofilm biomass concentration and the ΔFCP significantly increased within membrane fouling simulators. However, Hijnen and co-workers (2009) reported in their modal solution experiments that increasing the acetate concentration beyond 25 µg C/L will reach a saturation value in terms of biofouling accumulation on NF membranes. They also reported that acetate concentrations as low as 1 µg C/L could still initiate biofouling (Hijnen *et al.* 2009). Sudden changes in substrate loading and/or concentration can also have a significant and rapid effect on the biofilm formation process. The biofilm response to changes in the substrate loading can be fast, and a sudden increase in the substrate loading can cause a large increase in ΔFCP within a few hours (Dreszer et al., 2013; Hijnen et al., 2009). Similarly removing the substrate

supply was found to cause a sudden exponential drop in the ΔFCP across a membrane simulator (Dreszer et al., 2013; Hijnen et al., 2009).

2.4.5 Biofilm microbial diversity

Bacterial biofilms typically contain many different types of microorganisms; however, heavily encapsulated bacterial strains with higher growth rates are more often associated with biofilm formation in water. These can include the bacterial groups *Aerobacter*, *Arthrobacter*, *Proteus*, *Bacillus*, and *Pseudomonas* (Bott, 2011). Members of the *Sphingomonas* genus were reported to be the main contributor to biofilm inside an RO membrane module in a full scale fresh water treatment plant, and these strains were found to have a high affinity for biofilm formation. They can survive at low nutrient concentrations and can even survive and grow after membrane chemical cleaning (Bereschenko et al., 2011).

2.4.6 Biofouling monitoring techniques

Development of biofouling monitoring systems is a major aspect of recent biofouling research. The use of biofouling monitors is beneficial as it allows the inspection of the developed biofouling layers without the need for membrane autopsies and destructive testing of the membrane elements. Available biofouling monitors include membrane fouling simulators (MFS) (Vrouwenvelder et al., 2006), and these are described in more detail below. Biofilm monitors (van der Kooij et al., 2010) have also been used to measure the formation of biofilms, but were originally developed to measure regrowth potential in drinking water distribution systems. The specific oxygen consumption rate has also been used to monitor biofilms, and involves measuring the dissolved oxygen consumption within the membrane modules as an indicator for biomass growth (Vrouwenvelder et al., 2003). Some advanced monitoring systems can include ultrasonic time domain reflectometry, biosensors or electric potential measurement (Nguyen et al., 2012). MFS were selected for the current study as they can simulate full scale membrane operation. MFS were successfully used to investigate biofouling of full scale spiral wound membranes (Vrouwenvelder et al., 2006). Biofilm formation potential as measured by the biofilm monitors was correlated to the biofouling rates of spiral wound membranes in full-scale treatment plants (van der Kooij et al., 2010).

2.4.6.1   MFS as a Biofouling Monitoring Tool

The MFS unit was first introduced by Dr. Hans Vrouwenvelder as a tool to simulate the flow conditions in spiral wound membrane elements (Vrouwenvelder et al., 2006). A 20 × 4 cm membrane sheet and feed spacer are installed in the unit for each experiment. The height of the MFS feed channel is identical to that

found in a typical spiral wound membrane element. By simulating the hydrodynamic conditions inside the spiral wound module, the development of the biofilm is assumed to be identical. The length of the MFS (20 cm) was selected as biofouling was found to usually happen with the first 20 cm of the spiral wound membrane element, even though the element usually has an approximate length of 1.0 m. The MFS unit has a low flow requirement of 15 to 25 L/h, so it can be used in parallel to full scale elements. The unit is equipped with a transparent window to allow visual inspection of the developed biofouling layer during operation. The ΔFCP is continuously monitored across the unit, and at the end of the study period the membrane and feed spacer can be sampled to analyze the developed biofilm. The unit is operated without membrane permeation, as it was shown that permeate production did not affect biofouling development (Vrouwenvelder et al., 2009c). The MFS was found to achieve a similar ΔFCP and biomass accumulation as a full- scale RO installation and a 4 inch diameter pilot test rig (Vrouwenvelder et al., 2006).

Figure 2-4 A photo of the membrane fouling simulator (MFS) units used for biofouling detection

2.5 Biofouling Control Strategies

A major research area related to membrane biofouling in drinking water treatment is biofouling prevention and control. Several strategies have been employed for biofouling mitigation and control using preventive measures such as pretreatment technologies and membrane cleaning strategies. Also, some innovative technologies were investigated such as membrane surface modification to limit biofilm attachment along with novel module design.

2.5.1 Membrane cleaning

Typical membrane cleaning procedures include preparation of the cleaning solution, heating it to the desired temperature and then circulating it through the modules for 30 to 60 minutes. The system is then

soaked in the cleaning solution for 1 to 12 hours before pumping out the cleaning solution and flushing the system. A common cleaning agent for biofouling includes caustic soda (NaOH) at high pH of 10 to 12 mixed with EDTA, sodium triphosphate or sodium dodecyl sulfate (SDS) (Bergman, 2007). A successful cleaning solution was obtained by mixing NaOH, EDTA, SDS and urea at a pH higher than 10 at 30°C, which efficiently removed the developed biofilm on glass and plastic rings used in biofilm monitoring units (van der Kooij et al., 2010). Hijnen and co-workers (2012) investigated the removal of biofilms using different cleaning chemicals for several spiral wound RO elements supplied with dechlorinated tap water. They found that removal efficiency of the EPS matrix (as measured by biofilm carbohydrate) was always lower than active biomass removal (as measured by ATP). This study also found that the cleaning efficiency was largely dependent on the biofilm characteristics as indicated by the ratio of carbohydrate to ATP, and as the ratio decreases to below 0.8 μg/ng (lower relative EPS concentration) it will be easier to clean the biofilm (Hijnen et al., 2012).

The main drawback of the cleaning process is that it will not be able to completely remove the biofilm from the membrane surface regardless of its effect on its structure. Cleaning can efficiently inactivate most of the biofilm active biomass and collapse the structure of the biofilm, but bacterial cells at the biofilm base can survive the cleaning process, as the EPS matrix can provide some protection (Bott, 2011). Rapid regrowth of the biofilm after the cleaning is likely being facilitated by the presence of the remaining EPS structure and viable cells, and in the case of full-scale RO membranes treating surface water, the *Sphingomonas* genus was responsible for this regrowth (Bereschenko et al., 2011). Moreover, frequent cleaning of the membrane will increase the overall cost for the produced water in addition to the environmental impact when disposing these waste chemicals. The cost of cleaning chemicals comprised up to 17% of the total operation and maintenance cost for a brackish ground water system (Bergman, 2007). The cleaning cost of NF/RO membranes was estimated to be in the range of 0.01 to 0.15 Euros/m^3 of produced water, based on the fouling rates and pretreatment technologies employed (van der Kooij et al., 2010).

2.5.2 Pretreatment of raw water

Most of the full-scale high pressure membrane filtration treatment plants will require adequate pretreatment before the NF step to reduce the turbidity and silt content of the feed water. Conventional treatment such as coagulation/flocculation, sedimentation and granular media filtration are often used. More advanced pretreatment technologies such as low pressure membrane filtration, advanced oxidation and ultraviolet (UV) disinfection can be combined with the conventional pretreatment trains to improve colloids removal, oxidize organic foulants and/or decrease the biomass loading on the NF membrane (Bergman, 2007). Regarding biofouling control, an efficient treatment technology should be able to

reduce the amount of nutrients reaching the NF membrane and/or reduce the amount of fresh biomass and biofilm conditioning macromolecules reaching the membrane. The choice of the proper pretreatment technology will depend on the raw water quality. Some of the different pretreatment options for biofouling control are discussed in section 2.6 in more detail.

Both feed water pretreatment and membrane cleaning are complementary to each other. By applying a more efficient pretreatment, operational cleaning cost of the membrane will be reduced significantly, however, the pretreatment costs are usually higher than the cleaning costs (van der Kooij et al., 2010). The effect of the cleaning chemicals on the life-time of the membrane would be another factor that would justify the additional cost of pretreatment. Frequent and intense cleaning of the membrane elements can compromise their integrity (Bergman, 2007).

2.5.3 Membrane surface modification

A more advanced biofouling mitigation option is the modification of the polymeric material of the membrane to prevent biofouling. The modified membranes can either have anti-adhesive surface properties to prevent the initial bacterial adhesion or antimicrobial properties to prevent further growth of the biofouling layer (Mansouri et al., 2010). Novel anti-adhesive polymeric materials such as polymeric-urea (Liu et al., 2006) or partially disulfonated poly(arylene ether sulfone) random copolymers (Paul et al., 2008) were introduced to produce more hydrophilic and smoother membrane surface than traditional membranes. Another approach is to coat the existing membranes with a layer of several types of organic macromolecules to achieve the same enhanced surface properties (Mansouri et al., 2010). On the other hand, antimicrobial membranes can be developed through nanosilver coating of the membrane and the feed spacer (Yang et al., 2009) or by incorporating silver nano-particles into the membrane base (Liu et al., 2010). Many other techniques for newer membrane materials or modification techniques are available in literature. Several concerns are raised around these techniques, as they have effects on the membrane separation properties, mechanical and chemical stability (Mansouri et al., 2010). These newly developed membranes still need to be studied over prolonged periods of time under varying test conditions to evaluate their biofouling resistance.

2.6 Pretreatment technologies for biofouling control

2.6.1 Conventional pretreatment

A conventional treatment train can include coagulation, flocculation, sedimentation and/or rapid granular media filtration. This pretreatment option is commonly used for brackish waters or river water with a high turbidity (Bergman, 2007). The coagulation step was found to be efficient in reducing the BDOC

concentration in several surface water sources in the US (Volk et al., 2000). However, this study also measured AOC removal and found that coagulation resulted in significant AOC reduction for only two of ten surface waters tested (Volk et al., 2000). Huck and co-workers (1991) reported high fluctuations in the observed AOC removal during the clarification step during a long term pilot scale study, where AOC removal ranged from 0% to 80% with a median of 38%. The removals dropped mainly in the fall and winter seasons (Huck et al., 1991).

Regardless of the above mentioned benefits of conventional pretreatment, it is not always effective for biofouling control of high pressure membrane filtration that uses surface water (van der Kooij et al., 2010). For example, Baker and co-workers (1995) still detected significant biofouling of their NF membranes supplied with Oise river water after coagulation, flocculation and rapid granular media filtration. In a different study of a freshwater RO plant of the Alberto Pasqualini refinery in Brazil, Schneider and co-workers (2005) reported that AOC had significantly increased after pre-chlorination, but coagulation was able to lower AOC by nearly 50%. This was attributed to the entrapment or biodegradation of the AOC fraction within the sludge blanket of the upflow clarifier. Subsequent rapid sand filtration had no effect on the AOC fraction regardless of its large effect on DOC, and as a result severe biofouling events were observed in the downstream RO units (Schneider et al., 2005).

2.6.2 Biological filtration

Few studies have investigated biofiltration as a pretreatment for high pressure membrane filtration. Griebe and Flemming (1998) have reported that a sand biofilter with an extended EBCT of 40 min was able to decrease the biofouling potential of flocculated surface water. The biofilm thickness developed on RO membranes dropped from 27 to 3 μm when fed with biofiltered water compared with flocculated water without biofiltration. EPS carbohydrates and proteins content and biofilm cell count had a similar decease as well. This was attributed to a significant drop in BDOC from 1.2 to 0.12 mg C/L. Persson and co-workers (2006) reported BDOC removals of 28% to 34% and AOC removal of 22 to 41% for direct treatment of coloured lake water in Sweden through GAC or expanded clay biofilters at an EBCT of 31 minutes and both raw and biofiltered water were used to feed flow through cells equipped with glass slides to test biofilm development. This was reflected in a reduction in the developed biofilm volume on the glass slides by 80% to 93% over several seasons. Generally, it was reported that single stage biofiltration resulted in an improved membrane cleaning frequency, and this could be further improved if a double stage biofiltration was employed (van der Kooij et al., 2010). Similar findings were observed in water reclamation systems as well. Hu and co-workers (2005) observed 45% AOC reduction for a pre-chlorinated reclaimed water using an activated clay biofilter with an EBCT of 30 min, and this was reflected in an extended operational time (96 to 384 h) of their RO modules before cleaning. Clearly, very

few studies used biological filtration as a pre-treatment for biofouling control and there are no studies using BF$_{WP}$ as a pre-treatment.

2.7 Knowledge gaps and research needs

After reviewing the current literature, several research gaps were identified and they were the motivation for this study. The purpose of my research was to gain in depth knowledge about the BF$_{WP}$ process and its performance. Also the ability of BF$_{WP}$ to control biofouling in high pressure membranes seems to be a promising pre-treatment technology that needed to be evaluated. The apparent research gaps are as follows:

2.7.1 Lack of a comprehensive biofilter biomass characterization protocol

As discussed in Section 2.3.1.4, the use of a single biomass parameter will provide limited information about the composition of the biofilm and to-date no single biomass parameter has been linked to biofilter performance. Additionally, EPS present in the biomass attached to the biofilter media were investigated only by few studies (Lauderdale et al., 2012; McKie et al., 2015; Stoquart et al., 2013). A comprehensive protocol for biofilter biomass characterization will be essential to properly evaluate the possible relationship between the biofilter performance and biofilter attached biomass as this can help in understanding the removal of BOM within the filters which can aid in optimizing biofilter performance. The proposed protocol should include different analytical methods that can be used individually or in combination to fully understand the state of the biofilter biomass. Ultimately a more representative and rapid method for studying biofilter performance can be developed. Additionally, more information about the biofilm composition and nature in complex environmental eco systems can be obtained.

2.7.2 Limitations in available water quality monitoring techniques

The main two aspects of water quality monitoring which are linked to biofilter performance are microbiological water quality and BOM characterization. To evaluate biofilter performance, proper water quality parameters for BF$_{WP}$ studies need to be determined. Performance of conventional biofilters is commonly evaluated by measuring DOC, BDOC and AOC removal. AOC is a very significant parameter for biofouling studies as AOC is regarded as a direct estimation of the bacterial regrowth potential (Hijnen et al., 2009; Huck, 1990). The standard AOC method (Van der Kooij et al., 1982) has some limitations. The method uses only two bacterial strains commonly found in surface waters so it neglects the heterogeneity of the natural microbial communities.

The standard AOC method requires a long incubation time which can limit the applicability of the method for extensive monitoring studies. Hammes and Egli (2005) presented a more recent AOC method that

employs a heterogeneous microbial community as AOC inoculum that can be easily detected using flow cytometry. Flow cytometry was also found to be a promising tool for microbiological water quality monitoring. Newer methods for NOM characterization methods such as LC-OCD and fluorescence spectroscopy can be used to study the removal of different NOM fraction in the biofilters. Adapting those new analytical methods to new surface water sources is important, especially if it represents a different ecological system compared to the one used in the original study. More information is needed on method optimization and testing the methods' adaptability for new applications.

2.7.3 Limited knowledge on the performance of BF$_{WP}$ filters, including the effect of biofilter operational and seasonal parameters

BF$_{WP}$ is a potential pretreatment technology to limit BOM and particulate matter reaching subsequent treatment units. This is especially of interest for nanofiltration membrane units and would reduce operational cost and chemical consumption. In order to efficiently employ BF$_{WP}$ as a pretreatment technology, a more in-depth understanding about the influence of biofilter design parameters on the biofilter performance is required. These parameters include design EBCT, which is a key factor affecting BOM removal. Water temperature is also an important operational parameter for biofiltration studies, especially if seasonal changes in water temperature can vary greatly over the year as they do in Canada. Robustness of any proposed pretreatment technology needs to be verified under these varying conditions. Such information was reported for BOM removal in conventional water treatment processes (Prévost et al., 2005), but it has not been evaluated for BF$_{WP}$ filters.

2.7.4 Limited information on the applicability of biofiltration as a pre-treatment for NF membrane biofouling control

In the literature to-date, only two studies investigated the use of BF$_{WP}$ for biofouling control (Griebe and Flemming, 1998) or to limit biofilm formation (Persson et al., 2006). The used EBCTs in these studies were longer than 30 minutes which are much longer than the EBCT range of 1 to 15 minutes used in drinking water treatment (Crittenden, 2005). More studies are needed to investigate the effect of commonly used EBCT values on biofilter performance as a pre-treatment for NF membrane biofouling. Other important parameters include the impact of seasonal changes in NOM composition and water temperature on biofilter performance as a NF pre-treatment were not evaluated to-date.

2.8 Summary

BF$_{WP}$ is a promising green pre-treatment technology for membrane applications which is being used more often in drinking water treatment. The use of such a pre-treatment technology can significantly reduce the

energy requirements, which is a main concern for high pressure membranes. By using a pretreatment strategy, fewer membrane chemical cleaning cycles will be needed as a result. More detailed information about BF_{wp} process performance is needed, including key design and operational parameters. This information would be essential for further testing of the process to eventually reach full scale implementation.

Chapter 3

Improved approach for the characterization of attached biomass and extracellular polymeric substances on granular media from biologically active drinking water filters

3.1 Summary

Biologically active granular media filters are widely used either as a pre-treatment or as a final step in drinking water treatment facilities. A protocol was developed to accurately measure and characterize the amount of biomass and the biofilm EPS composition attached to the filter media using variety of analytical techniques, to obtain a better understanding of the biofilm characteristics which may be linked to biofilter performance. A cation exchange resin extraction protocol was used to extract the biofilm cells and EPS directly from the filter media. Biomass was then measured using both ATP and true volumetric cell count using a flow cytometer. Biofilm EPS total protein and total carbohydrate content were determined, and more advanced analytical techniques including fluorescence spectroscopy and liquid chromatography organic carbon detector (LC-OCD) were used to further characterize the nature of the biofilm EPS. The developed protocol was applied to a pilot scale direct biofiltration pilot plant that pre-treats surface water for membrane applications. The developed protocol provided reliable results, and there were strong correlations between biomass and EPS components data. Proteins were found to be the major fraction of the biofilm EPS. Nearly 50% of the extracted EPS had a molecular weight larger than 2,000 Da and this fraction had a large contribution from protein-like substances. As well, there were differences between the sand and anthracite media used in the filter in terms of the relative EPS composition. The proposed protocol can potentially be applied to investigate biofilms on other surfaces, including those from natural and artificial systems such as membranes.

3.2 Introduction

Over the past few decades biological filtration has been used frequently in drinking water treatment as a tool to remove BOM commonly found in surface water sources, and it is often employed to simultaneously remove particles, colloids and pathogens instead of using a separate granular media filter. Biofiltration has other benefits such as reducing disinfection by-product precursors, chlorine demand and water corrosion potential (Urfer et al., 1997). Due to the absence of any disinfectant residual in both the feed and the backwash water, cells attach and a biofilm starts growing on the filter media, and BOM in the feed water serves as a substrate to maintain growth and activity of the biofilm. Accurate characterization of the different biofilm components, including bacterial cells and EPS, is necessary to better understand the biofilm matrix and how it may relate to biofilter performance.

The developed biofilm on the biofilter media surface is primarily responsible for the degradation of BOM, as dissolved compounds adsorb to or diffuse within the biofilm to be consumed by bacteria (Simpson, 2008). Bacterial cells comprise approximately 10% of the biofilm mass and the rest of the biofilm is mainly EPS along with water molecules that hydrate the biofilm. EPS contains various types of molecules, of which polysaccharides and proteins are particularly important (Flemming and Wingender, 2010). The EPS matrix gives the biofilm its 3-D structure, and other functions include cell adhesion to the surface, enhancing biofilm mechanical strength, providing sorption sites for bacterial nutrients from the feed water, degrading large molecular weight molecules through enzymatic activity, and being a protective barrier for the biofilm against environmental conditions (Flemming and Wingender, 2010). This highlights the importance of characterizing the biofilter biofilm EPS matrix to gain better understanding of its role in drinking water biofilters, particularly since limited information is available in this regard (Stoquart et al., 2013).Various methods have been used to assess the biofilter attached biomass in an attempt to use the data as indicators of biofilter performance. Several methods that have been used as a bulk measure for the available biomass include phospholipids content (Wang et al., 1995) and total direct cell count (Servais et al., 1994). ATP has also been used to quantify to the amount of available active biomass (Magic-Knezev and van der Kooij, 2004; Pharand et al., 2014; Velten et al., 2011), as it is an easy and reproducible method but ATP was not found to be a good indicator for biofilter performance (Pharand et al., 2014). One major problem with using ATP to quantify amount of attached of biomass is the possible variation of cellular ATP content due to environmental or operational conditions (Martin et al., 1980; Theron et al., 1987) and this value was found to have some variability in literature (Pharand et al., 2014). A more recent tool is the use of flow cytometry to determine the true volumetric cell count of bacteria from biofilter media (Velten et al., 2011). Flow cytometry is being used more frequently in drinking water studies due its rapid, accurate, true volumetric quantification of bacterial cells in water

(Hammes et al., 2008). As well, this method is able to count both culturable and non-culturable bacterial cells, unlike traditional methods like HPC.

EPS composition has been well studied for wastewater activated sludge (Wilderer et al., 2002) but limited information is available for drinking water biofilms. A critical step for accurate EPS characterization is EPS extraction from the substratum and separation from the bacterial cells while minimizing cell lysis. The objective of EPS extraction methods is to maximize the yield of extracted EPS and minimize EPS contamination by intercellular compounds due to cell lysis. EPS extraction methods vary from simple physical methods such as shaking or sonication, chemical methods such as acidic or alkaline treatment (Nielsen and Jahn, 1999). The different EPS extraction methods always need to be optimized based on the application of the EPS extraction process and the desired objectives. Therefore, new and existing EPS extraction methods need to be tested and evaluated to get better and more accurate data. Selection of the EPS extraction method is a critical step and new methods are being tested and existing methods are modified to optimize the extraction. Among the different extraction methods, the use of CER (Frølund et al., 1996), was found to give good EPS yields and to minimize cell lysis and possible contamination when applied to drinking water biofilms (Michalowski, 2012) and wastewater activated sludge (Pellicer-Nàcher et al., 2013). Boretska and co-workers (2013) used CER to extract EPS attached to soil media, but it was applied after physically detaching the biofilm from the soil media. There have been no studies that have applied CER extraction to granular media from drinking water biofilters.

In this study, we developed a comprehensive protocol to extract, quantify and characterize the attached biofilter biomass using different analytical methods. This was done to better understand how different methods can be used together to study the different biofilm components. A CER extraction procedure was developed to directly detach and separate biofilm cells and EPS material from biofilter media. ATP and true volumetric cell count using flow cytometry were used as alternative tools to quantify the biomass. EPS was characterized using photometric methods to quantify total proteins and total carbohydrates, and compared with newer NOM characterization techniques such as LC-OCD (Al-Halbouni et al., 2008; Meng et al., 2009; Stewart et al., 2013) and fluorescence spectroscopy (Domínguez et al., 2010; Sheng and Yu, 2006). The developed protocol was applied to samples taken from three different drinking water biofilters, and two different types of media (sand and anthracite) to determine possible effects of the media type on the biofilm composition. The benefit of this protocol is that it can be applied to other types of biofilms in water, for example membrane applications or distribution systems.

3.3 Materials and methods

3.3.1 Experimental setup and sample collection

Samples were collected from a direct biological filtration pilot plant employing dual media filters using sand and anthracite (media specifications are provided in **Appendix C**). Three clear polyvinyl chloride (PVC) columns were used in the study (**Figure 3-1**). Biofilter A had a 25.4 cm diameter and consisted of 20 cm of anthracite over 20 cm of sand. Biofilter B had a diameter of 25.4 cm and consisted of 20 cm of anthracite over 60 cm of sand. The effluent of biofilter B was used to feed biofilter C, which had a diameter of 20.3 cm and consisted of 40 cm of sand. Each filter had a 5 cm gravel base. A coarse media roughing filter made from 10 cm of crushed gravel preceded the biofilters, to reduce particle loading and prevent biofilter plugging.

The filters were fed using settled water from the Grand River, which is highly impacted by agricultural activities and treated wastewater effluents (Dorner et al., 2007). The pilot plant used the same feed water as the full scale Mannheim Water Treatment plant. The intake of the full scale plant is described in more detail in **Appendix C**. The filter media was pre-acclimated using the same surface water at a low flow rate for 6 months to accelerate the acclimation of the filters after the became in operation to reach steady state operation more quickly. The pilot plant was commissioned on April 2014 to operate at a loading rate of 5 m/h in a declining rate flow mode. The corresponding EBCTs were 5, 10 and 15 min for biofilters A, B and C, respectively. The filter filtration cycle lasted 48 h, and then the filters were backwashed using air and water to remove accumulated particles in the filters during operation to retain the initial bed porosity. A detailed description of the biofilter backwash procedure is provided in **Appendix C**. The biofilters were backwashed three times a week. Each biofilter had sampling ports that were used to collect media samples as shown in **Figure 3-1**.

A total of 21 samples were collected in four sampling events between April and June 2014. The media samples were collected in the middle of the filtration cycle, put in sterile 50 mL polypropylene (PP) tube, and kept wet using the biofilter feed water. The samples were stored at 4ºC and analyzed within 24 h. The upper media port in biofilter A and B was at the interface between sand and anthracite, and these two media types were gently separated using a 2 mm sieve. Sieving did not have any significant impact on the biofilm attached to the media (data not shown).
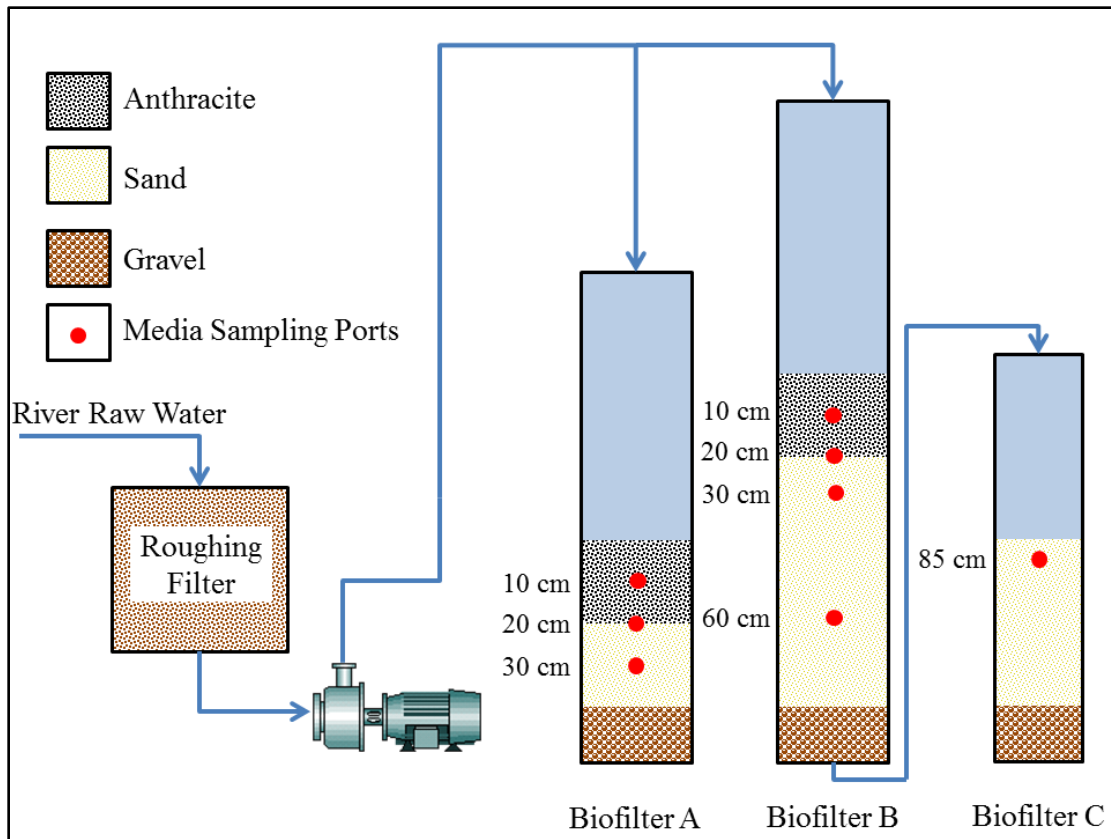
Figure 3-1 Schematic of the biological filtration pilot plant indicating the media sampling ports

3.3.2 Feed water quality

Temperature and turbidity were obtained from on-line measurements installed on the feed line of the used pilot plant. The used turbidity meter was a 1720E Low Range Process Turbidimeter (Hach Company, USA) and temperature was measured using a resistive temperature device (RTD) probe (Cole Parmer, Canada). Data for TOC, DOC, pH, conductivity, ortho-P, ammonia and nitrate were obtained from the Region of Waterloo. The total cell counts were measured using a Cube 6 flow cytometer (Sysmex – Partec, Germany) according to the Swiss Guideline for Drinking Water Analysis (SLMB, 2012). AOC was quantified using a modified method employing a flow cytometry method with a natural bacterial inoculum from the same river based on a previously published method (Hammes and Egli, 2005) which is also described in **Chapter 4**.

3.3.3 ATP measurement

A flowchart showing the steps used for media sample processing is shown in **Figure 3-2.** The separated media samples were rinsed three times using biofilter C effluent to remove loosely attached biomass. For ATP analysis, 1 g of media was added to 5 mL of a commercial cell lysis buffer (Ultralyse 7, LuminUltra

Technologies, NB, Canada) then vortexed for 20 s. After 10 minutes, 20 µL of each sample was added to a 96 well microplate. ATP quantification was done using a GloMax® 96 Microplate Luminometer (Promega Corporation, WI, USA). One hundred µL of luciferase (Promega ENLITEN ATP kit, Promega Corporation, WI, USA) was added to each well, and luminescence was measured over 10 s. A five point calibration curve was constructed using ATP standards (10^{-1}, 10^{-2}, 10^{-3}, 10^{-4}, 10^{-5} and 0 µM ATP). All standards were prepared in the same lysis buffer (Ultralyse 7). In addition, ATP remaining on the media samples after EPS extraction was evaluated for random samples (n=7) to determine the average biomass recovered from the media through the extraction process. After EPS extraction, the media samples (3 g media and 3 g CER) were rinsed three times with 6 mM phosphate buffered saline (PBS), samples were drained, then 5 mL of the cell lysis buffer was added and vortexed, and finally the ATP concentration was measured in the same way as described above. The ATP recovery through EPS extraction would then be quantified using the following equation.

$$Percent\ of\ biomass\ recovery\ as\ ATP = 100 * \frac{Bulk\ Media\ ATP - Media\ ATP\ after\ EPS\ extraction}{Bulk\ Media\ ATP}$$
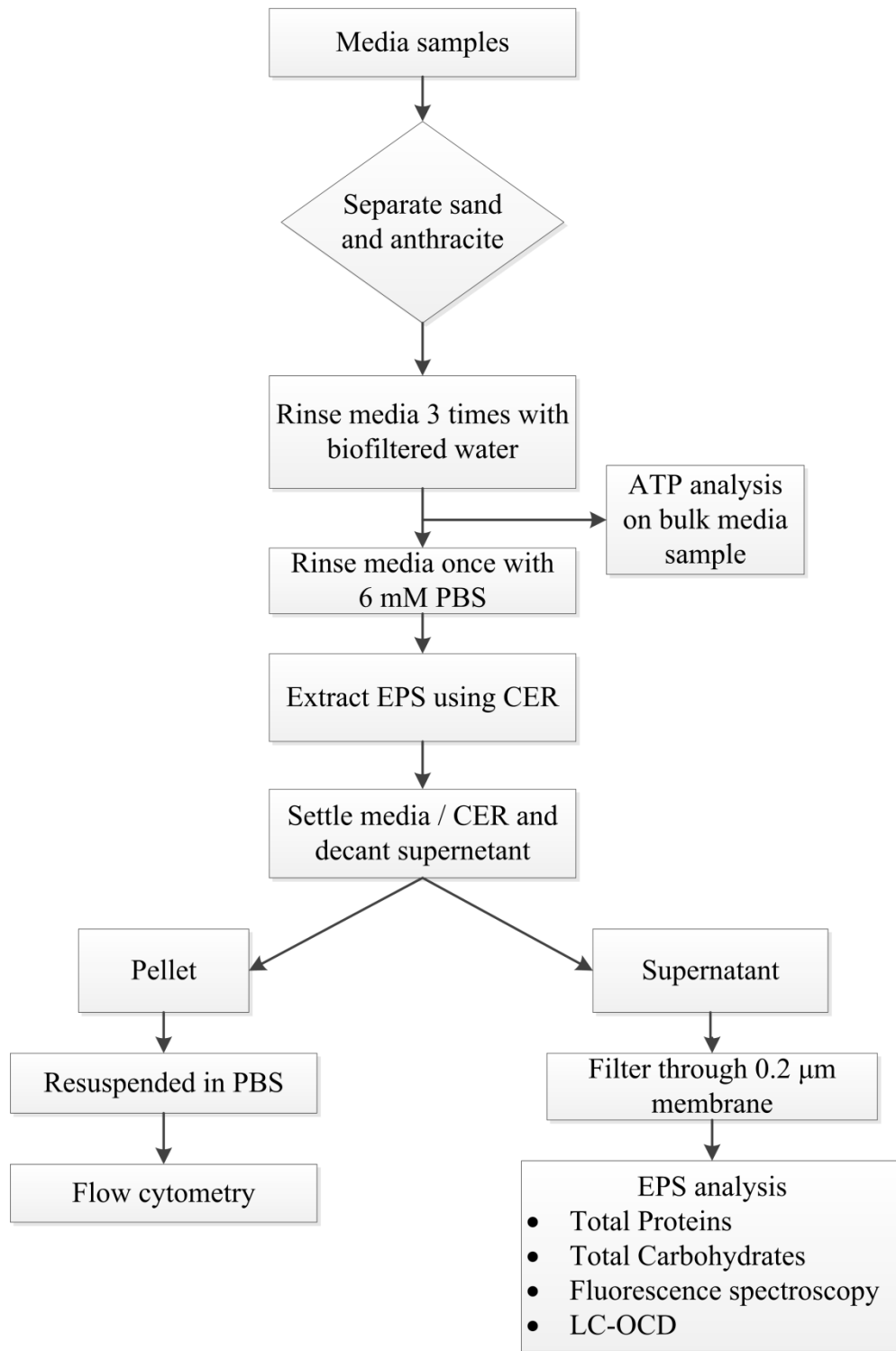
Figure 3-2 A flowchart of the sample preparation and analysis protocol

3.3.4 EPS Extraction

The media was rinsed three times with 6 mM PBS (pH 7.0) (Michalowski, 2012) to remove any remaining organic compounds. The PBS was filtered through a 0.2 μm PES filter (Pall) before use. Dowex Marathon C CER (Sigma Aldrich, USA) was used for the EPS extraction process (Frølund et al., 1996). CER was washed in an upflow reactor using Milli-Q water for at least 100 bed volumes before it was used for EPS extraction. Three g (wet weight) of rinsed media, 3 g (wet weight) of rinsed DOWEX CER and 20 mL of 6 mM PBS were added to a sterile 45 mL PP centrifuge tube. The tubes were loaded horizontally in an incubator and shaken at 350 rpm and 15°C for 1 h. A 1 h extraction time was used as it was previously reported to be a suitable for EPS extraction in drinking water biofilms (Michalowski, 2012), soil biofilms (Boretska et al., 2013) and for pure cultures (Takahashi et al., 2009; Ubertini et al., 2015). The media and CER were then left to settle and discarded. The supernatant was removed and added to a sterile 45 mL PP centrifuge tube, and centrifuged at 5,000 x g for 20 min to separate the detached cells from the dissolved EPS. The cell pellet was resuspended in 10 mL of 0.2 μm filtered PBS for cell counting using flow cytometry. The supernatant containing the EPS was filtered using 0.2 μm PES syringe filter (VWR, Canada) to remove any particles, and stored at 4°C for further analysis.

3.3.5 Cell counts using flow cytometry

The resuspended cells were filtered through a 10 μm CellTrics nylon mesh sterile filter (Partec NA, NJ, USA) to remove large particles that can interfere with the cell count. The cell count was performed as described in **Chapter 4** and based on (SLMB, 2012) using a Cube 6 flow cytometer (Sysmex-Partec, Germany). The flow cytometer is equipped with a 488 nm blue laser, forward scatter detector (FSC), side scatter detector (SSC) and three fluorescence detectors (FL1 – 536 ± 20 nm, FL2 – 590 ± 25 nm, FL3 > 615 nm). All samples were diluted 1:10 in 0.2 μm filtered 6 mM PBS, and 990 μL of the diluted sample was stained with 10 μL of diluted SYBR Green I nucleic acid stain (1:100 dilution in 0.2 μm filtered DMSO; Life Technologies). The samples were heated for 15 min at 35°C prior to analysis. The stained samples were further diluted 1:50 or 1:100 in 0.2 μm filtered Mili-Q water right before measurement. The instrument flow rate was 4 μL/s and the true volumetric absolute count (TVAC) was obtained using the instrument electrodes. FL1 detector was used to trigger the measurement. All data were processed using FCS Express 4 software (De Novo Software, CA, USA). Electronic gating on the density plots of both FL1 and FL3 was used to differentiate the cells from unwanted particles as described in **Chapter 4** and shown in **Figure 3-3-a**. The same gate was used to analyze all samples.
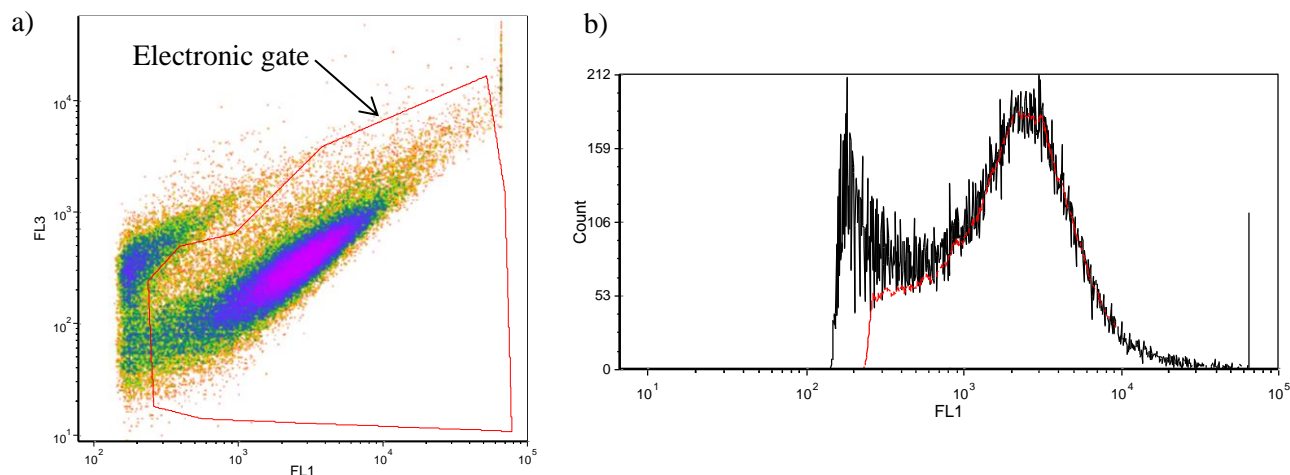
Figure 3-3 Typical (a) density plot of the biofilm extracted cells for green fluorescence (FL1) and red fluorescence (FL3) showing the electronic gate in red and (b) the corresponding FL1 histogram in black with the gated events in red colour

3.3.6 Protein and carbohydrate assays

The total carbohydrates content of the extracted EPS was determined using the phenol sulfuric acid method described by DuBois and co-workers (1956). In short, 0.5 mL of the EPS extract, 0.5 mL of 5% (in water) phenol solution (Sigma Aldrich, USA) and 2.5 mL of 98-99% sulfuric acid (Sigma Aldrich, USA) were added to acid washed (0.1 N HCl) glass test tubes. The tubes were gently shaken, capped and heated to 30 °C in a water bath for 15 minutes. The samples were left to cool to room temperature then analyzed on Cary 100 UV/VIS spectrophotometer (Agilent Technologies, USA) at 490 nm using a 1 cm glass cuvette. The measured absorbance values were calibrated against D-glucose standard solutions (0, 1, 2.5, 5, 7.5, 10 mg/L as D-glucose). All samples and standards were analyzed in triplicate.

The total protein content of the extracted EPS was determined using the bichronic acid method (Pierce micro-BCA protein kit, Thermo Scientific). A 2 mL sample of the EPS extract was added with 2 mL of the prepared reagent in an acid washed glass test tube. The solutions in the tubes were mixed gently and heated at 60 °C in a water bath for 1 h. The samples were left to cool to room temperature then measured at 562 nm using a Cary 100 UV/VIS spectrophotometer (Agilent Technologies, USA) in a 1 cm glass cuvette. The recorded absorbance values were calibrated using bovine serum albumin (BSA) standards (0, 1, 2.5, 5, 7.5 and 10 mg/L BSA). All samples and standards were analyzed in triplicate.

3.3.7 Fluorescence spectroscopy

Fluorescence spectroscopy is an analytical technique used to detect different types of organic molecules by detecting the presence of certain natural occurring fluorophores associated with different types of

organic molecules. The emission spectrum for different excitation wavelengths is being recorded to create a fluorescence excitation emission matrix (FEEM). FEEMs of each extracted EPS sample was measured using a Cary Eclipse Fluorescence Spectrophotometer (Agilent Technologies, USA). A typical FEEM plot of an extracted EPS sample is shown in **Figure 3-4**. All measurements were done using a quartz cuvette with 1 cm path length and a photomultiplier tube (PMT) voltage of 750 V. Each matrix included 301 individual emission intensity values (within the 300 – 600 nm emission range at 1 nm increments), and at sequential 10 nm increments at excitation wavelengths between 250 nm and 380 nm. These range values were used in previous studies to characterize the natural organic matter in the same surface water source (Grand River) that was used to feed the biofilters in this study (Chen et al., 2014; Peldszus et al., 2011). In the obtained FEEM plot, fulvic acid-like substances have a peak (FEEM-B) at an excitation / emission pair of 320/415 nm. The humic acid-like peak was measured at an excitation / emission pair of 270/460 nm (FEEM-C). Tryptophan-like substances have a peak maximum at an excitation / emission pair of 280/330 nm (FEEM-A), and intensity values at these coordinates were used as an indicator of the content of protein-like, humic acid-like and fulvic like-acid substances in the samples (Peiris et al., 2010). Note that carbohydrates or polysaccharides do not contain fluorophores and can therefore not be measured by FEEM. Raw data files were provided by fellow graduate student Fei Chen who did all the FEEM measurements and data analysis was done by me on MATLAB (MathWorks, USA).
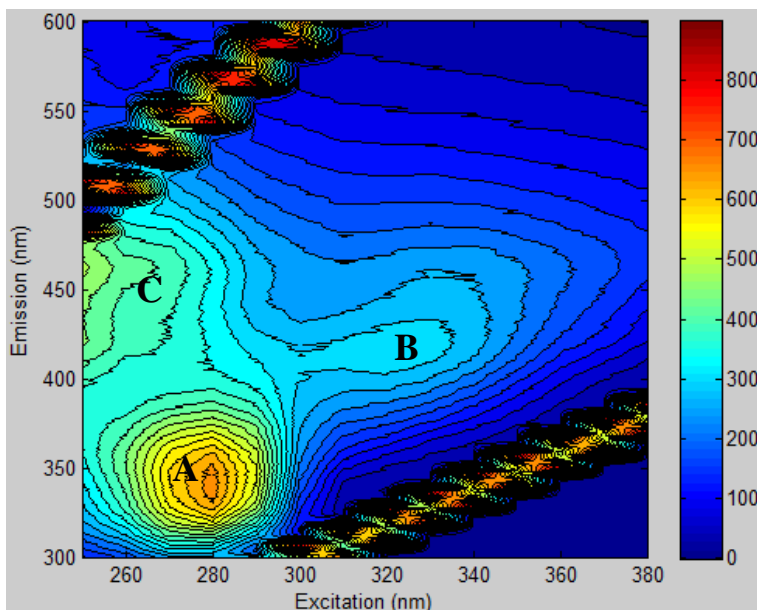
Figure 3-4 Typical FEEM contour plot of the extracted biofilm EPS

3.3.8 Size exclusion chromatography

Liquid chromatography - organic carbon detection (LC–OCD) was used to determine the molecular weight (MW) distribution of extracted EPS compounds. LC-OCD is a tool to separate the bulk natural organic matter in water into several fractions based on their apparent molecular weight (Huber et al., 2011). The system employs a size exclusion column (250 mm x 20 mm, TSK HW 50S, 3000 theoretical plates, Tosoh, Japan), with a column resin separation range of 0.1 to 18 kDa as polyethylene glycol (PEG) according to the resin supplier. The eluted, size separated organics from the column pass through three online detectors to determine their organic carbon (OC) content, organic nitrogen (ON) content and their ultraviolet light absorbance at 254 nm (UV254). To determine the relationship between MW and column retention time, 12 different PEG standards were injected to determine the peak retention time as shown in **Figure S-1** in **Appendix A**. Chromatograms of the bulk EPS showed three main fractions in all extracts, however, the evaluation criteria typically applied to LC/OCD based on Huber and co-workers (2011) seemed not quite suitable as it was based of the aquatic NOM present in water samples which was different than the EPS samples obtained in the current study. Instead high, intermediate, and low molecular weight fractions were defined based on retention times, as shown in **Figure 3-5.** Manual integration was used to determine the OC, ON and UV254 content of each fraction. The high molecular weight EPS (HMW-EPS) fraction elutes between 25 and 35 min, and contains compounds with a MW larger than 13 kDa according to the column retention calibration curve. Aquatic biopolymers including polysaccharides, proteins and amino sugars are reported to have similar elution time (Huber et al., 2011). The intermediate molecular weight EPS (IMW-EPS) fraction elutes between 35 and 45 min which corresponds to an apparent molecular weight range of 2 kDa to 13 kDa. Aquatic humic and fulvic like substances from surface water samples were reported to have a similar elution times (Huber et al., 2011). The low molecular weight EPS (LMW-EPS) compounds elute at a retention time higher than 45 min, which corresponds to apparent molecular weights of less than 2 kDa. This fraction may contain small peptides or degraded humic substances. Dr. Monica Tudorancea did the LC-OCD sample analysis and provided raw data files. Raw data files were numerically integrated by me using MATLAB (MathWorks, USA).
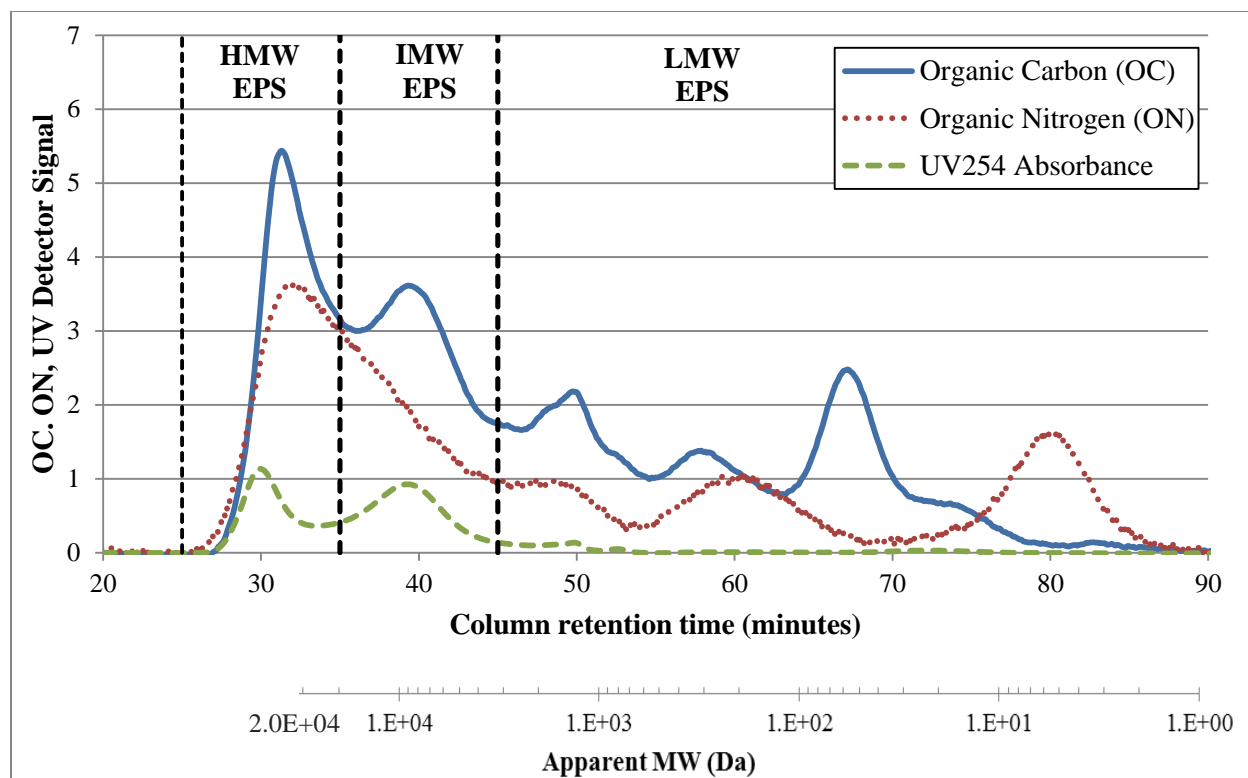
Figure 3-5 Typical LC-OCD chromatograph of extracted EPS samples showing the three user defined MW fractions: high MW (HMW), intermediate MW (IMW) and low MW (LMW)

3.3.9 Statistical analysis

All the obtained results are expressed per unit volume of dry biofilter media as explained in the supplementary material. A two tailed t-test was used to investigate the statistical significance of the observed differences between the sand and anthracite samples. Pearson (r) correlation coefficient matrix for all the measured parameters in all the samples collected (n=21) was used to determine the correlation between each pair of parameters.

3.4 Results and discussion

This study aimed at developing a comprehensive protocol for characterizing the biomass attached to the granular media used in drinking water biofilters. The filter was operated using water from an impacted river and a summary of the feed water quality is shown in **Table 3-1**. Different analytical methods were used to determine biofilm activity, biofilm cell count and EPS composition. Relationships among the different parameters were investigated to better understand the biofilm structure on the biofilter media, and the linkage between the different analytical methods. Good overall correlation among the different parameters would be expected if they are indicators of the same biological process (i.e. biofilm growth),

39

and a stronger correlation between a certain pair of parameters can indicate that they are measuring a similar process variable.

Table 3-1 Feed water quality as measured over the sampling period

Parameter	Unit	Range
Temperature	ºC	3 - 21
pH [a]		7.9 - 8.2
Conductivity [a]	μS/cm	550 - 650
Turbidity	NTU	4.5 - 5.5
Total cell count [1]	Cells / mL	1.5×10^6 - 2.7×10^6
TOC [a]	mg C/L	4.55 - 6.05
DOC [a]	mg C/L	4.40 - 5.75
AOC	μg C as acetate / L	220 - 240
Ortho-phosphate (O-PO$_3$) [a]	mg P / L	0.005 - 0.009
Nitrate (NO$_3$ – N) [a]	mg N / L	2.8 - 3.3
Ammonia/Ammonium (NH$_3$/NH$_4$-N) [a]	mg N / L	0.1[*] - 0.36

[*] Method detection limit

[a] These parameters were provided by the Regional Municipality of Waterloo as measured by the treatment plant staff

In the proposed protocol, the CER was directly mixed with the media samples unlike previous studies that have employed CER on soil biofilms (Boretska et al., 2013) which had a separate initial step to physically detach the bacterial biofilm from the media and then mixing it with CER. This is advantageous as it shortens the time of the overall extraction process and it reduces the shear force that has to be applied to the biofilm for detachment. This protocol has been successful in this study in detaching the biofilm from the media as indicated by a good biomass extraction yield measured as ATP recovery of 65 ± 15 % (n=7). This was determined by measuring the remaining ATP on the biofilter media after EPS extraction and comparing it to the bulk media ATP content. The use of CER treatment in the extraction is believed to minimize cell lysis (Frølund et al., 1996; Jahn and Nielsen, 1998; Michalowski, 2012; Pellicer-Nàcher et al., 2013) however this was not tested in this study. After the extraction, biofilm bacterial cells and EPS were separated by centrifugation to analyze each separately. Several analytical methods were used in order to characterize the biomass on the biofilter media. ATP was evaluated on the bulk media as an

indicator for biomass activity. A total of 21 samples were analyzed and the detailed results for all the parameters measured are shown in **Table S1** of **Appendix A**. The Pearson (r) correlation matrix among the different parameter pairs is shown in **Table 3-2**. Pearson (r) correlation values for all the parameters used ranged between 0.77 and 1 except for the UV absorbance of the low molecular weight EPS. This indicates that the used protocol provided reliable and consistent results.

Table 3-2 Pearson r correlation coefficient matrix among the different biofilm parameters measured (n = 21)

	Bulk Media ATP	Biofilm Cell count	Total Protein	Total Carbohydrates	FEEM Protein intensity (A)	FEEM Fulvic intensity (B)	FEEM Humic intensity (C)	High MW EPS OC	High MW EPS ON	High MW EPS UV	Intermediate MW EPS OC	Intermediate MW EPS ON	Intermediate MW EPS UV	Low MW EPS OC	Low MW EPS ON	Low MW EPS UV
Bulk media ATP	1.00															
Biofilm Cell count	0.96	1.00														
Total Protein	0.91	0.92	1.00													
Total Carbohydrates	0.88	0.90	0.91	1.00												
FEEM Protein intensity (A)	0.93	0.94	0.99	0.89	1.00											
FEEM Fulvic intensity (B)	0.81	0.79	0.80	0.81	0.80	1.00										
FEEM Humic intensity (C)	0.92	0.91	0.92	0.85	0.93	0.94	1.00									
High MW EPS OC	0.88	0.91	0.99	0.89	0.99	0.77	0.90	1.00								
High MW EPS ON	0.92	0.94	1.00	0.91	0.99	0.81	0.93	0.99	1.00							
High MW EPS UV	0.90	0.93	0.98	0.94	0.95	0.81	0.89	0.97	0.97	1.00						
Intermediate MW EPS OC	0.92	0.91	0.96	0.95	0.94	0.90	0.94	0.94	0.96	0.96	1.00					
Intermediate MW EPS ON	0.89	0.91	0.99	0.93	0.96	0.84	0.92	0.98	0.98	0.99	0.97	1.00				
Intermediate MW EPS UV	0.88	0.86	0.90	0.91	0.87	0.95	0.93	0.86	0.89	0.92	0.98	0.94	1.00			
Low MW EPS OC	0.91	0.91	0.99	0.93	0.97	0.88	0.94	0.97	0.98	0.97	0.99	0.98	0.95	1.00		
Low MW EPS ON	0.82	0.79	0.88	0.89	0.86	0.89	0.87	0.86	0.88	0.88	0.95	0.91	0.95	0.93	1.00	
Low MW EPS UV	0.29	0.33	0.61	0.49	0.56	0.43	0.49	0.62	0.58	0.54	0.52	0.62	0.49	0.58	0.55	1.00

Row groupings (left side): Fluorescence Spectroscopy covers FEEM Protein intensity (A), FEEM Fulvic intensity (B), FEEM Humic intensity (C); LC-OCD covers High MW EPS OC through Low MW EPS UV; Biofilm EPS spans Total Protein through Low MW EPS UV.

Legend:
- r ≥ 0.95 — Excellent correlation
- r ≥ 0.90 — Good correlation
- r ≥ 0.80 — Weak correlation
- r < 0.80 — No correlation

3.4.1 Biomass characterization

Bulk media ATP values ranged from 200 to 2200 ng ATP / cm^3 of media (i.e. cm^3 of reactor volume). These values are within the reported range of 100 -10,000 ng ATP / cm^3 of media for different full scale biofilters (Evans et al., 2013a; Pharand et al., 2014). The bulk media ATP content showed a good correlation with the biofilm cell count (Pearson (r) correlation = 0.96) as shown in **Table 3-2** and **Figure 3-6-a**. This indicates that bulk media ATP content was a suitable parameter to represent the biofilm total cell count, regardless of the broad range of their values (1×10^8 to 1.2×10^9 cells / cm^3 media). Differences in biomass due to sample depth in the biofilter, and differences in sampling time and in water quality and temperature, did not have an effect on the relationship between the media ATP and biofilm cell count, as the overall correlation among both parameters remained high over the course of the experiments.

Based on the biomass data, the average cellular ATP ratio was calculated to be $2.6 \times 10^{-15} \pm 1 \times 10^{-16}$ g ATP/cell. Hamilton and Holm-Hansen (1967) reported similar cellular ATP contents for different bacterial strains in the range of 1.3×10^{-15} to 4×10^{-15} g ATP/cell for the cells that were still in their growth phase. These values dropped one fold to nearly 2×10^{-16} to 5×10^{-16} g ATP/cell as the cells went into the stationary or the decay phase. Other studies on drinking water biofilters reported slightly lower values, including Velten and co-workers (2007) who reported an average value of 6.7×10^{-17} to 2.3×10^{-16} g ATP/cell for biofilms grown on GAC filters with prior ozonation. Similarly, Magic-Knezev and Van der Kooji (2004) reported a value of 2.1×10^{-17} g ATP/cell for GAC filters with prior ozonation. They also reported a higher value of 3.6×10^{-16} g ATP/cell for rapid sand filters which was attributed to a higher growth rate for the biomass in these filters. It is possible that this explanation can also account for the high cellular ATP content observed in the current study, as the biofilters were in their acclimation period. The other biofiltration studies were done on full scale filters that were already at steady state (Magic-Knezev and van der Kooij, 2004; Velten et al., 2007). Another source of variability can be the analytical methods that were used to obtain the ATP and cell count data. The CER extraction protocol combined with flow cytometry used in this study to determine true volumetric cell count of the bacterial suspension perhaps provided more accurate data compared to conventional total direct cell count used in previous studies (Magic-Knezev and van der Kooij, 2004). In addition, the method to directly lyse cells on the bulk media followed by ATP

measurement may have provided higher values compared to simple manual shaking followed by cell counting and ATP measurement of the detached cells used by Velten and co-workers (2007).
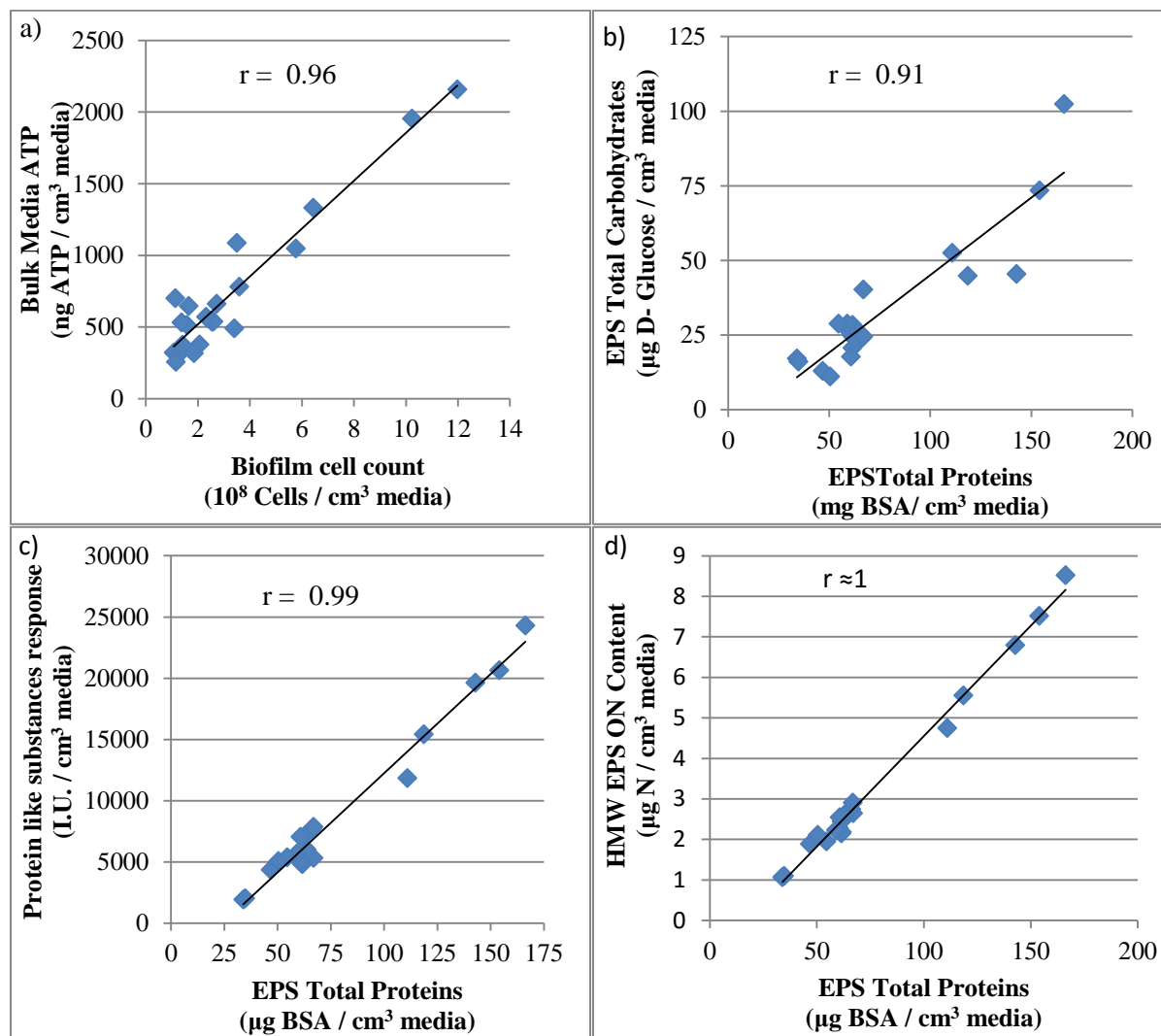
Figure 3-6 Correlation plots between (a) biofilm cell count and bulk media ATP content, (b) EPS total proteins and EPS total carbohydrates, (c) EPS total proteins and FEEM protein-like response (c), EPS total proteins and HMW EPS organic nitrogen content (LC-OCD) with the corresponding Pearson (r) correlation coefficient

3.4.2 EPS characterization

The chemical composition of the biofilm EPS was determined using conventional photometric assays to measure total proteins and total carbohydrates. EPS total protein and total carbohydrates content were used as general indicators of the biofilm EPS changes due the biofilm dynamic processes within the biofilter. In addition, these two fractions are believed to be the main components of the biofilm matrix (Flemming and Wingender, 2010). Only few studies have used these parameters in studying biofilms attached to drinking water treatment biofilter media. Both proteins and carbohydrates were highly correlated with the biofilm cell count (r = 0.92 and 0.9, respectively; **Table 3-2**), which indicates that all three parameters were controlled by the same biological process. In addition, this shows that the extraction and analysis protocols were able to accurately monitor such a process. The EPS total proteins ranged from 34 – 166 μg BSA/cm^3 media and the EPS total carbohydrates ranged from 11 to 102 μg D-Glucose/cm^3 media.

The protein component of the EPS is mainly present as extracellular enzymes, which play an important role in biofilm processes (Flemming and Wingender, 2010). Biofilm bacteria produce those extracellular enzymes to breakdown large organic macromolecules into low molecular weight fractions that are small enough to be transported through the cell walls to be utilized by the bacteria. These enzymes become trapped and accumulate within the biofilm matrix (Wingender et al., 1999a). On the other hand, the carbohydrate component of the EPS includes both high molecular weight polysaccharides along with monosaccharides and any other monomers such as D-Glucose or some uronic acids (Michalowski, 2012). The function of polysaccharides in bacterial biofilm is mainly being a structural component as they provide the biofilm with its mechanical and adhesive strength in addition to aggregating the bacterial cells. Total EPS including both proteins and carbohydrates acts as a protective barrier for bacterial cells and a sorption site for organic or inorganic molecules (Flemming and Wingender, 2010).

The ratio of the total protein to total carbohydrate content of the EPS was relatively stable over the whole study at 2.5 ± 0.7 g BSA/ g D-glucose. This indicates that proteins are the major component of the EPS in the investigated system. This is in agreement with the reported protein to carbohydrate ratio of approximately 1.5 g BSA/ g D-glucose for biological activated carbon samples from a drinking water treatment biofilter, and of over 4 g BSA/ g D-glucose for powdered activated carbon from a pilot testing facility (Stoquart et al., 2013) . Andersson and co-workers (2009) reported an

average EPS protein to carbohydrates ratio of 2.5 g BSA/ g D-glucose for a denitrifying bacteria biofilm grown using either minimal media or domestic wastewater. Similar results were reported for biofilms grown in drinking water distribution systems. Michalowski (2012) reported a value of 2 – 3 g BSA / g D-Glucose for 14 day old biofilms grown in different plumbing and distribution systems. Kilb and co-workers (2003) determined that the protein to carbohydrate ratio for biofilms on replaced valve seals in drinking water distribution systems ranged from 0.9 to 3.5. Much smaller values were reported for biofilms in soil (i.e. < 0.5) where nutrients would be limited (Leon Morales et al., 2007; Redmile-Gordon et al., 2014). Supplying nutrients to sand for several weeks was found to increase the protein to carbohydrates ratio of the biofilm from 0.25 to nearly 1(Leon Morales et al., 2007). This suggests that the observed high protein to carbohydrates ratio in the present study is indicative of a sufficiently high level of available nutrients in the biofilter feed water. Also, the biofilm extraction method has been reported to affect the observed values. Pellicer-Nàcher and co-workers (2013) found that the protein to carbohydrates ratio for 3 different types of wastewater mixed culture biomass from different full scale plants varied greatly based on the extraction method used. The reported ratio varied by 2 to 5 times for each type of biomass when different extraction methods were used. This variability needs to be considered when comparing observed values and with the literature when different EPS extraction methods have been used.

Further characterization of the EPS was carried out using size exclusion chromatography and fluorescence spectroscopy. The latter is a fast and reliable method to detect protein-like substances with high sensitivity as the amino acid tryptophan is a strong fluorophore. Results in **Table 3-2** show that the EPS total protein content had a very high correlation with the protein (i.e. tryptophan) like substances FEEM response (FEEM-A) as shown in **Figure 3-6-c.** Therefore, fluorescence spectroscopy can be a suitable method to monitor EPS proteins. A drawback of using fluorescence spectroscopy is that it is not a direct measure of absolute concentration but rather an indication of relative content if the composition of the matrix does not vary substantially. Hence, comparisons of FEEM intensity values are only meaningful within a certain matrix. For example, FEEM may be suitable for long term monitoring studies for a single biological system to determine variability in the protein content of the same biological reactor.

LC-OCD was also used to characterize the EPS constituents. LC-OCD consists of a size exclusion column followed by three online detectors namely organic carbon, organic nitrogen and UV absorbance detectors. Using LC-OCD, the bulk EPS can be divided into different size fractions and

their characteristics can be determined. LC-OCD has previously been used to determine large molecular weight fractions of activated sludge EPS (Al-Halbouni et al., 2008; Meng et al., 2009) or EPS from periphyton (Stewart et al., 2013). LC-OCD chromatograms of the biofilter EPS extracts showed three distinct peaks (**Figure 3-5**). Although Huber and co-workers (2011) propose a set of rules/peak identifiers to evaluate LC/OCD chromatograms, these are not really applicable to the EPS extracts as these rules are based on the evaluation of surface water NOM. Hence, the peaks were defined here as high, medium and low molecular weight fractions based on the general pattern of the peaks obtained in the samples obtained in this study as each fraction had a major peak and this pattern was reproducible in all samples. Overall, data from the HMW EPS fraction (i.e. MW $\geq$ 13 KDa) had the best correlation with the total protein content (**Table 3-2**). The ON content of this fraction had an essentially perfect correlation (r >0.99) with the EPS total protein content (**Figure 3-6-d)** and both the OC content and UV absorbance of this fraction also had an excellent correlation with the total protein content (r = 0.99 and 0.98 respectively). Several enzymes that are associated with bacterial biofilms (Michalowski, 2012) are listed in **Table S-2** of **Appendix A**. All have a molecular weight larger than 13 KDa and so they would fall in this fraction. HMW EPS organic carbon had a weak correlation with either humic acid-like (FEEM-C) or fulvic acid-like (FEEM-B) FEEM intensities indicating that this fraction has low contribution of those types of molecules and they are not linked to the observed UV absorbance. Also, most enzymes contain aromatic structures which would result in good UV absorbance. These results are in agreement with the findings of Tsai and co-workers (2008) who reported high UV absorbance and protein like substances content, determined using fluorescence spectroscopy, for high molecular weight soluble microbial products of wastewater sludge after fractionation using a similar size exclusion column to the one used in this study

The observed carbon to nitrogen ratio (i.e. C/N ratio) of the HMW EPS fraction was very consistent at 4.2 $\pm$ 0.3 g C/ g N, which is close to the theoretical C/N ratios for the enzymes listed in **Table S-2** of **Appendix A** (3.5 to 4.25 g C/ g N) or the experimentally determined C/N ratio of 3.3 g C/ g N for common proteins (Rouwenhorst et al., 1991). A similar C/N ratio of 4.3 $\pm$ 0.8 g C/ g N was also reported for the large MW LC-OCD fraction of EPS for freshwater biofilms (Stewart et al., 2013). The HMW EPS fraction had a much lower correlation with the EPS total carbohydrates content (r= 0.89) than with the EPS total protein content (r=0.99). So carbohydrates (i.e. polysaccharides) seem to play a secondary role in this fraction; biofilm polysaccharides are believed to have a MW of 500 to 2000 kDa (Flemming and Wingender, 2010) and so they would be expected to be present in this

fraction. In summary, the observed C/N ratio, along with the very strong correlation with EPS total protein content and FEEM protein-like response, suggests that the HMW-EPS is mostly composed of protein-like substances with a secondary contribution of other compounds such as polysaccharides. This is supported by Flemming and Wingender (2010), who stated that proteins are believed to be more abundant than polysaccharides in bacterial biofilms on mass basis (Flemming and Wingender, 2010).

For IMW EPS fraction (i.e. 2 to 13 kDa), the OC and ON content also had an excellent correlation with the EPS total protein content (r = 0.96 and 0.99 respectively; **Table 3-2**), and only a slightly lower correlation with EPS total carbohydrates (r = 0.95 and 0.93, respectively). This suggests that the IMW fraction includes both types of compounds, and that proteins are the main type of nitrogen containing molecules, possibly due to the presence of small peptides, disaccharides or amino sugars (Stewart et al., 2013). In addition, both humic acid-like (FEEM-C) and fulvic acid-like (FEEM-B) fluorescence responses had a good correlation with the LC-OCD UV absorbance, showing that humic acid-like and fulvic acid-like substances likely contributed to the IMW fraction. Aquatic humic substances from natural waters have been reported to elute at the same elution time window (Huber et al., 2011), and these compounds are sometimes considered as a part of the EPS matrix either by being absorbed from the water phase or being formed within bacterial biofilms due to enzymatic degradation and repolymerization (Wingender et al., 1999b). The observed C/N ratio of this IMW EPS fraction was 6.1 ± 1 g C / g N, which is higher than the C/N ratio of the HMW EPS fraction or the C/N of bacterial enzymes shown on **Table S-2 in Appendix A** indicating that more carbon containing molecule are present in this fraction compared to nitrogen containing molecules. This IMW EPS fraction seems quite complex as it includes different types of molecules including proteins, carbohydrates and humic like substances.

For LMW EPS fraction (i.e. ≤ 2 kDa), the organic carbon content had an excellent correlation with the EPS total protein content and protein like substances FEEM response (FEEM-A), but organic nitrogen content was only weakly correlated. This could be caused by the presence of inorganic nitrogen such as nitrate or ammonium that are known to elute in this window as described by Huber and co-workers (2011) and they would compromise the majority of the nitrogen content of this fraction. The LMW fraction would be expected to contain small peptides or free proteinogenic amino acids (Ishizawa et al., 2010) that can also be detected by the protein assay. Carbohydrates also had a

good correlation with this fraction so small peptides of proteins and carbohydrates (i.e. monosaccharides) are present in this fraction as well.

In general, the comparison of biofilm EPS characteristics and biomass showed good overall correlations for all parameters, except for the UV absorbance of the LMW EPS fraction. Values among the different pairs of parameters ranged from 0.75 to 1.0 (**Table 3-2**). The biofilm extraction and analysis protocol used here provided reliable results over four different sampling events, and the relative relationships among the various parameters remained similar regardless of the variability in the biofilter biomass over the course of the study. These parameters could characterize the biofilm within the studied biofilters regardless of the variability in the sampling time and/or location. Hence, the EPS extraction and analytical methods used here were shown to be reproducible and to accurately measure the biomass characteristics.

3.4.3 Biofilm differences between different media types

One of the important research topics is the effect of the biofilter media type on the biofilter performance. Sand and anthracite used in this study both represent non adsorptive media types unlike GAC which has significant adsorption capacity mainly at the start of the biofilter operation. Sand and anthracite were found to be a good combination in dual media biofilters which can provide BOM removals similar to GAC biofilters (Huck, 1990). But limited information is available about possible differences in the relative biomass composition attached to each type of media. In this study we collected both sand and anthracite samples from varying depth within the filters. Mixed media samples from the media interface in the biofilters were separated to get mono media samples prior to analysis.

Some differences were observed between the EPS relative composition of the two types of media as determined by LC-OCD and fluorescence spectroscopy (**Figure 3-7**). LC-OCD results of the HMW and IMW fractions measured by the organic carbon detector were compared as shown in **Figure 3-7-a**. For sand, the HMW EPS accounted for $22.9 \pm 2\%$ of the total OC content of the EPS (n=13) compared to $17.3 \pm 2\%$ for anthracite (n=8), and this difference was statistically significant (P≤0.05). As a result, sand would have relatively more HMW EPS, which is composed mainly of extracellular enzymes as discussed earlier. This means that sand will have a higher relative extracellular enzyme activity compared to the anthracite. On the other hand, results for the IMW organic carbon fraction showed the opposite trend. In this case, the IMW organic carbon fraction on sand was $25.9 \pm 2\%$ of

49

the EPS, and the value on anthracite was 29.8±2%, and this difference was statically significant (P≤0.05). In addition, results from fluorescence spectroscopy showed further significant differences between sand and anthracite (**Figure 3-7-b**). The average ratio of the fluorescence fulvic acid -like response (FEEM B) to the protein-like response (FEEM A) was 0.72±0.38 for anthracite compared to 0.32±0.08 for the sand. Similarly, the ratio of the fluorescence humic acid -like response (FEEM C) to the protein-like response (FEEM A) was 1.27±0.57 for anthracite and 0.61±0.09 for sand. Both humic acid-like and fulvic acid-like substances are expected to elute in the IMW EPS fraction which can also explain the high ratio of IMW EPS OC to HMW EPS OC. These results show that anthracite had a statistically significant higher relative amount of humic- and fulvic-like substances than sand, presumably due to a difference in uptake of these compounds, since sand and anthracite have different surface characteristics. These findings are valid for sand and anthracite samples collected at the same biofilter depth during the last two sampling events (i.e. May 29 and June 19), so these findings are not due to the differences in the depth of the sample collection port.

Figure 3-7 Relative EPS composition on both sand and anthracite samples measured using (a) LC-OCD and (b) fluorescence spectroscopy

3.4.4 Biofilm profiling over the biofilter depth

The biofilm profile over depth was investigated by collecting samples at three different locations in the same biofilter (biofilter C, 15 min EBCT) (20, 60 and 85 cm from the biofilter surface) in one sampling after 2 months of operation (**Figure 3-8**). For sand and anthracite samples collected at the

same depth, it is clear that sand had a much higher amount of biomass compared to the anthracite due to the higher specific surface area of the sand (Urfer et al., 1997). For the sand samples, all the biomass parameters decreased exponentially over the biofilter depth. Similar trend was observed for ATP content in GAC biofilters (Velten et al., 2011) and for biomass phospholipids (Urfer and Huck, 2001). Results also showed that both the biomass (ATP and cell count) and the biofilm EPS (total protein and carbohydrates) decayed at relatively similar rates within the biofilter, keeping the relative biofilm composition stable regardless of a possible nutrient gradient within the biofilter (Velten et al., 2011) and possible differences in the biofilter microbial community over the biofilter depth (Boon et al., 2011).
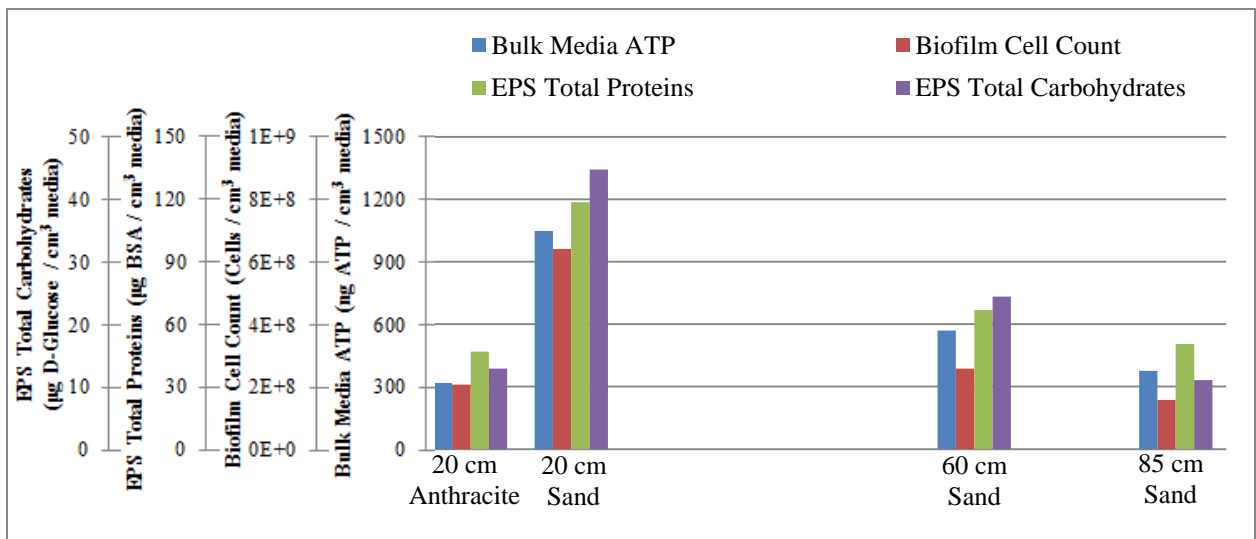
Figure 3-8 Profiling selected biomass parameters over the 120 cm depth of biofilter C (15 minute EBCT) in samples taken at 2 months of operation

3.5 Conclusions

The presented study aimed at developing a protocol for characterizing the biofilm attached to the media of biologically active drinking water treatment filters. The protocol was evaluated and applied to samples collected from a pilot scale testing facility fed directly by river water. Some of the measured parameters (i.e. cellular ATP content, EPS protein to carbohydrate ratio and carbon to nitrogen ratio) were relatively stable and seemed to be a fingerprint of the studied biological process. This can provide new parameters to be further studied to understand their possible relationship to

biofilm growth. These results show the possible advantages of using several analytical techniques similar to the ones used here. Moreover, the used protocol is suitable for studying biofilms from other origins such as biofilms on artificial surface (i.e. membranes) used in drinking water treatment applications. Depending of the objective of the biofilm monitoring process, some of the reported parameters might be of less importance and can be abandoned for that application. For example, fluorescence spectroscopy and LC-OCD can be indicative of biofilm protein content, and they are simpler so they can potentially replace some of the used photometric method. The developed protocol can be further applied to monitor the biofilm in drinking water biofilter in longer term studies to study possible relationships between biofilter biomass and biofilter performance and to assess how environmental or operational conditions can affect these.

- The proposed protocol provided reliable results for both sand and anthracite samples with varying amounts of attached biomass.
- Media ATP is a suitable parameter to measure the biofilm total cell count as the cellular ATP content was stable at $2.6 \times 10^{-15} \pm 1 \times 10^{-16}$ g ATP/cell within the same biofilter at varying depth and for parallel biofilters as well.
- Proteins were found to be the major component in the biofilm EPS pool and fluorescence spectroscopy was able to provide a reproducible indirect estimation of the EPS protein content.
- Size exclusion chromatography using LC-OCD separated EPS into three main fractions according to their molecular weight. Instead of using the regular interpretation of LC-OCD chromatographs presented by the supplier which was based on analysis of aquatic natural organic matter, a different criteria was developed specifically for extracted EPS based on the observed peak pattern in the obtained samples.
- HMW EPS was mainly composed of proteins unlike both IMW EPS and LMW EPS which had a combination of different types of substances.
- Potential parameters for biofilm monitoring include the total protein to total carbohydrate ratio and the carbon to nitrogen ratio of the extracted EPS. The ratio of the EPS protein to carbohydrates content was relatively stable at 2.5 ± 0.7 mg BSA/ mg D-Glucose regardless of media type, biofilter depth and biofilm age. Carbon to nitrogen ratio of the HMW EPS and IMW EPS fractions were 4.2 ± 0.3 and 6.1 ± 1 g C/ g N respectively. Long term monitoring

of such ratio can determine their possible significance for example in relation to biofilter performance parameters.

- The used protocol identified differences between sand and anthracite samples as the EPS extracted from sand samples had a higher relative content of high MW EPS (i.e. proteins) compared to anthracite samples which seemed to have higher content of humic like substances in the intermediate MW EPS fraction probably due to differences in media surface characteristics.

Chapter 4

Application of flow cytometry to monitor assimilable organic carbon (AOC) and microbial community changes in surface water

4.1 Summary

Flow cytometry is a promising monitoring tool for rapid cell counting, and can be applied to research on water quality and treatment. In this study, an established method that employs flow cytometry and a natural microbial inoculum to determine AOC was improved and adapted for use with a challenging surface water source. The required sample sterilization technique before adding the AOC inoculum was found to be membrane filtration combined with heat treatment. Conditions for preparing the natural river inoculum also required modification, since growth was limited in different types of inorganic minimal media and in natural spring water. The resulting flow cytometry AOC method was reliable and reproducible, and results were comparable to the standard plate count AOC method. Flow cytometry was used to monitor both AOC levels and total cells counts in a long term study to monitor the water quality of a river which was used as a drinking water source. AOC concentrations were related to the observed cell counts in the water source. Flow cytometry could distinguish between high nucleic acid (HNA) and low nucleic acid (LNA) groups of bacteria, and HNA bacteria responded much faster than LNA bacteria to nutrient spikes and changes in water temperature. Higher total cell counts in the river seemed to be related to the increased amounts of the biopolymer fraction of the natural organic matter, a linkage which may aid in our understanding of the nature and the origin of the biopolymers.

4.2 Introduction

Water quality monitoring is an important area of research in drinking water treatment. Efficient and reliable monitoring tools are necessary to understand how changes in incoming water quality affect the efficiency of treatment technologies. Monitoring tools are also instrumental in optimizing the performance of drinking water treatment unit processes. An important area for water quality monitoring research is BOM, which can affect drinking water treatment objectives as BOM can promote bacterial regrowth, increase chlorine demand, increase water corrosion potential and act as a precursor for disinfection by-products (Urfer et al., 1997). Of note is that bacterial regrowth can cause severe problems such as biofouling of high pressure membrane treatment units (Vrouwenvelder et al., 2009a), and biofilm formation in distribution systems (Prévost et al., 2005). Along with BOM quantification, accurate and reliable detection of bacterial cells in water and understanding their response to environmental factors is essential to develop a robust drinking water treatment train.

Standard methods that are used for the quantification of BOM in water are comprised of two main approaches. The first approach is to quantify the amount of dissolved organic carbon consumed due to biological activity, which is defined as BDOC (Joret and Levi, 1986; Servais et al., 1987). The second approach is to monitor the growth of bacterial cells on the BOM in the water samples as an estimate of the available substrate in these water samples. This approach is defined as AOC (Rice et al., 2012). AOC is the suitable parameter to interpret BOM concentration if bacterial regrowth the in treated water and biological stability in the distribution system is the objective of the work (Escobar and Randall, 2001; Huck, 1990). AOC is believed to include easily biodegradable organics that can be used by heterotrophic bacteria for producing new cells (Huck, 1990). AOC has been shown to include both high and low MW ranges of dissolved organic matter (DOM), with the majority in the low MW ranges (Hem and Efraimsen, 2001) and several studies found AOC in the effluent of high pressure membranes (Escobar et al., 2000; Meylan et al., 2007; Park et al., 2006).

AOC was first introduced by Van der Kooij and co–workers (1992; 1982), when two bacterial strains (NOX and P17) were used as inoculum for the sterilized water samples, which were then incubated and regrowth of these strains in these samples was determined using standard plate count techniques or ATP as indicator of biomass growth (LeChevallier et al., 1993). Measured biomass growth was converted into AOC using a standard growth yield on sodium acetate for each strain. Further AOC method development work has been done using different strains (Kemmy et al., 1989) or bioluminescent derivatives of the original AOC bacterial strains (Haddix et al., 2004). To account for

the diversity of the natural microbial community and their growth using various carbon sources, other AOC methods involved the use of an indigenous bacterial community as AOC inoculum. Cell growth in the samples can be determined using turbidity (Werner, 1985), ATP (Jago and Stanfield, 1989) or flow cytometry (Hammes and Egli, 2005; Stepanauskas et al., 2000). The application of a natural microbial inoculum and flow cytometry to determine AOC (Hammes and Egli, 2005) was found to result in a rapid method that is more representative of the BOM concentration in water samples compared to the traditional AOC method (Van der Kooij et al., 1982) due to the functional diversity of the natural microbial community.

One of the major areas that requires further development is the preparation and testing of the AOC inoculum, since this is a critical component of the AOC method as it directly affects the method reproducibility. The use of flow cytometry for enumeration of cell growth has been found to provide reliable results which correlated well with other AOC methods (Ross et al., 2013). However, the flow cytometry AOC method is relatively new and needs further optimization and testing on different types of water sources. Another application of flow cytometry is as a tool for rapid and true volumetric cell counts of aquatic bacteria (Hammes et al., 2008). Optimization of the flow cytometry protocol incorporating information on the nature of the microbial community by including a separation into high and low nucleic acid bacteria (De Roy et al., 2012; Prest et al., 2013) is highly desirable.

In this study, a detailed step-by-step optimization of an analytical flow cytometry AOC method using indigenous bacteria was performed, in order to adapt it to a challenging water source impacted by agricultural activities and treated wastewater. Simultaneously, a total cell count method was developed which was also able to enumerate HNA and LNA bacteria in water samples. Different aspects of the AOC method were investigated, including sample and inoculum preparation. Sample preparation involved comparing two different sample sterilization methods, including heat treatment (Van der Kooij et al., 1982) and membrane filter sterilization (Hammes and Egli, 2005). Also, AOC inoculum yield on acetate as a model substrate in different types of growth media were tested, as well as the effect of inoculum storage time and seasonal changes in the water source. Finally, a long term study was conducted in river water using the optimized flow cytometry AOC and total cell count methods, to study the changes in water quality and the river microbial communities. Size exclusion chromatography was also performed to study the relationship between observed AOC and total cells

count values and changes in the different dissolved organic matter (DOM) molecular weight fractions.

4.3 Materials and Methods

4.3.1 Preparation of AOC free glassware

For sample collection, one litre glass bottles were acid washed (0.1 N HCl) overnight then rinsed 3 times with Milli-Q water, capped with aluminum foil and dried at 105ºC. Plastic bottle caps were washed in a 10% w/w sodium persulfate solution at 60ºC for 1 h, then rinsed 3 times with Milli-Q water and dried at 105ºC. Glass AOC test vials (45 mL) were acid washed (0.1 N HCl) for more than 6 h, then rinsed three times with Milli-Q water. The vials were capped with foil, dried at 105ºC, and then baked at 450ºC for 6 h. Plastic AOC caps with Teflon septa were washed in a 10% w/w sodium persulfate solution at 60ºC for 1 h, then rinsed 3 times with Milli-Q water and dried at 105ºC.

4.3.2 Water source and sample collection

The water source used for this study was the Grand River, located in southern Ontario, Canada. The river is impacted by agricultural activities and treated municipal wastewater effluent. Nearly 93% of the river watershed is considered a rural area and a total of 29 sewage plants are present in the river watershed discharging their treated wastewater effluent into the river and its tributaries (GRCA, 2015). Rainfall or run off events were found to have a significant impact on the total bacteroidales (Lee et al., 2014) and fecal coliforms (Dorner et al., 2007) in the river water as they are possibly washed from the agricultural fields. The normal river flow is 15 - 30 m^3/s, but spring run-off and rainfall events can increase the river flow up to 100 – 150 m^3/s (Environment Canada, 2015).

For this study, river water samples were collected at the inlet point of a water treatment plant located in Kitchener, Ontario, The inlet point to the plant was preceded by natural settling in a storage reservoir. Samples were collected in AOC-free 1 litre glass bottles between January 2014 and April 2015. The samples were stored at 4ºC and analyzed within 24 h of collection. Turbidity, temperature, and pH at the sampling point were monitored using online sensors installed at the inlet of the water treatment plant. Data for DOC, ammonium, nitrate, ortho-phosphate and total phosphate were provided by the Region of Waterloo.

To study the difference between the flow cytometry AOC method and a standard plate count AOC method, water samples were collected from the City of Brantford full-scale water treatment plant.

This plant also uses the Grand River as a source, and its intake is located 50 km downstream of the Kitchener water treatment plant intake. The samples were collected after 1) coagulation\ sedimentation, 2) ozonation and 3) biologically active GAC filtration. Details of the Brantford treatment train are described elsewhere (Pharand et al., 2015).

4.3.3 Cell count using flow cytometry

Flow cytometry was used to measure cell concentrations in the AOC method, and also to measure total cell counts in river water samples. The water samples were filtered through a sterile 10 μm CellTrics nylon mesh filter (Partec NA, NJ, USA) to remove larger particles that can interfere with cell counting. SYBR Green I nucleic acid stain (Life Technologies) was used to stain the cells. A 1:100 dilution of SYBR Green I in 0.2 μm filtered DMSO was prepared and 10 μl was added to 990 ul of the filtered water sample. The stained samples were incubated in the dark at 37 ℃ for 15 min in a heating block. Prior to cell counting, the stained samples were further diluted in 0.2 μm filtered Milli-Q water to adjust the cell count to the instrument optimum detection range (1×10^5 to 2×10^5 cells/mL). Cells were counted using a Partec Cube 6 Flow Cytometer (Sysmex-Partec, Germany) equipped with a 488 nm blue laser, forward scatter detector (FSC), side scatter detector (SSC) and three fluorescence detectors (FL1 – 536 ± 20 nm, FL2 – 590 ± 25 nm, FL3 > 615 nm). The sheath fluid flow rate was 4 μL/s and the true volumetric absolute count (TVAC) was obtained using the instrument electrodes. FL1 detector was used as a trigger. All raw data files were processed using commercial software (FCS Express 4, De Novo Software, CA, USA). Selected samples were stained using both SYBR Green I and propidium iodide (PI) (Life Technologies). For these samples, 1 μL of PI was added to 999 μL of the sample and SYBR Green staining was done in the same way described above. The stained samples were incubated in the dark at 37 ℃ for 15 min in a heating block before running the samples on the flow cytometer under the same conditions as mentioned above.

4.3.4 Assimilable organic carbon (AOC)

The flow cytometer AOC method employing a natural microbial inoculum was based on the method developed by Hammes and Egli (2005). For the final method, water samples were sterilized by filtration through a 0.2 μm polyethersulfone (PES) filter, followed by heat treatment at 60°C for 30 min. To prepare the samples, a PES syringe filter (VWR Canada) was first rinsed with 120 mL of Milli-Q water, then the sample was filtered directly into AOC free clean 45 mL vials. Three 20 mL

replicates of each sample were prepared along with two 20 mL controls. For the first control, the sample was supplemented with 20 μL of an inorganic nutrient stock solution that included nitrogen, phosphorus, magnesium and trace elements to ensure that only carbon was limiting growth. The inorganic nutrient solution contained 12.8 g /L $Na_2HPO_4·2H_2O$, 3 g/L KH_2PO_4, 1.77 g/L $(NH_4)_2·SO_4$, 130 mg/L $MgCl_2·6H_2O$, 80 mg/L $CaCO_3$, 77 mg/L $FeCl_3·3H_2O$, 11 mg/L $MnCl_2·4H_2O$, 1.5 mg/L $CuSO_4·5H_2O$, 1.3 mg/L $CaCl_2$, 4 mg/L ZnO, 1.2 mg/L H_3BO_4, 10 mg/L $NaMoO_4·2H_2O$ and 790 mg/L $EDTA·Na_4·2H_2O$ and it was prepared in 1000× concentrated stock (Ihssen and Egli, 2004). The second control was supplemented with 20 ul of inorganic nutrients stock solution and 100 μg C/L sodium acetate as a growth control to determine if there were any inhibitors for bacterial growth in the sample. All the sample replicates and the controls were heat treated at 60ºC for 30 min in a water bath. The vials were then left to cool to room temperature. A natural bacterial inoculum was then added to each vial to achieve an initial cell count ($N_{initial}$) of approximately $1×10^4$ cells/mL. Preparation of the inoculum is described in the next section. The inoculated samples were gently mixed then incubated without shaking at 30ºC for 4 days. The final cell count (N_{final}) in each vial was measured by flow cytometry as previously described, and used to determine the AOC concentration according to **Equation 1**.

$$AOC \ (\mu g \ C \ as \ acetate \ / \ L) = \frac{\left(N_{final} - N_{intial}\right)\left(\frac{Cell}{L}\right)}{inncoulum \ yield \ \left(\frac{Cells}{\mu g \ C \ acetate}\right)} \ .... \textbf{Equation -1}$$

To test different sample sterilization techniques, a river water sample was collected and passed through a 10 um filter, followed by 0.2 um filtration and then heat treatment at 60ºC for 30 min. Sub-samples were collected before and after 0.2 um filtration and following heat treatment, and added in triplicate to 40 mL glass vials and incubated at 30ºC for 3 days. Vials were analyzed by flow cytometry at day 0 and day 3. To evaluate the effect of incubation time, a river water sample was tested in triplicate either undiluted, or diluted either by 66% or 33% in low DOC water (BDH Aristar Plus water, VWR International, Ontario). The samples were incubated at 30ºC for 4 days, and 1 mL from each vial was collected daily for cell counting by flow cytometry.

A comparison of the flow cytometry AOC method and the P17 and NOX plate count AOC method (Van der Kooij et al., 1982) was done using samples collected from the Brantford water treatment plant. Fellow graduate student Lizanne Pharand collected the samples and performed the NOX and P17 plate count AOC analysis, and these results are reported elsewhere (Pharand et al., 2015). The AOC plate count method was performed according to Standard Methods 9217B (2012) as described

by Pharand et al. (2015). Briefly, AOC-free clean vials were filled with 40 mL of each sample in triplicate, and the samples were heat treated at 60ºC for 30 min in a water bath. In addition, two controls were prepared (inorganic nutrient control and growth control). Each vial was then inoculated with 500 cells/mL each of *Pseudomonas fluorescens* strain P-17 (ATCC 49642) and *Spirillum* sp. strain NOX (ATCC 49643). The inoculated samples were incubated for 9 days at 15ºC. The number of colony forming units (CFU)/mL of each strain was determined on days 7, 8 and 9 using a spread plate technique onto R2A agar (BD, Sparks, Maryland). AOC concentration (µg C/L) was calculated using yield values of 4.6×10^6 CFU/µg C for P17 and 1.2×10^7 CFU/µg C for NOX.

To further compare the two AOC methods, a simple batch test was done to determine the DOC consumption. Water samples for this test were collected from the Grand River at the inlet of the Mannheim Water Treatment plant used in this study. The samples were sterilized and inoculated as described above for each method, with P-17 and NOX used for the standard plate count method and a natural inoculum used for the flow cytometry AOC method. Uninoculated controls were also prepared for each sample. Samples were incubated as described above according to each method, and following incubation all samples were then filtered through a 0.2 µm PES membrane to remove cells and to be consistent with the AOC method. Samples were then analyzed to measure DOM size fractions using LC-OCD as described later.

4.3.5 Preparation of natural microbial inoculum

For the flow cytometry AOC method, the indigenous bacterial community of the river was used as an inoculum. To prepare the inoculum, river water was collected and filtered through a 10 µm CellTrics nylon mesh sterile filter (Partec NA, NJ, USA) into an AOC-free 250 mL glass bottle. The river water was then incubated for 21 days at 30 ºC to ensure that any AOC in the sample was consumed. The cell count was monitored over this period by flow cytometry to monitor cell growth. The inoculum was then stored at 4ºC and used for the AOC test. AOC inoculum was stored for up to 4 months, as recommended by Hammes and Egli (2005).

AOC inoculum growth yield on sodium acetate was evaluated to convert measured biomass growth into AOC concentration. Growth yields were measured by adding sodium acetate to different types of aqueous solutions including 1) a synthetic water (A) composed of Milli-Q water with nitrogen (0.767 mg/L NH_4Cl, 1.44 mg/L KNO_3) and phosphorus (0.171 mg/L K_2HPO_4) compounds as described in standard methods (9217B) (2012), 2) synthetic water (B) containing a mixture of inorganic nutrients

as described by Ihssen and Egli (2004) described earlier in **section 3.3.4** as a minimal media for AOC method controls, 3) a natural spring water (Evian, Switzerland) as recommended by Hammes and Egli (2005) or 4) Grand River water collected from the effluent of a biofilter (15 min empty bed contact time). The pilot-scale dual media biologically active filter is further described in Chapter 5. Biofiltered water was further supplemented with the same minerals stock mentioned earlier in **section 3.3.4** to ensure enough inorganic nutrients and trace elements are present. Each standard was prepared in triplicate, then the river inoculum was added to each vial to reach a final concentration of 1×10^4 cells/mL and all were incubated at 30ºC for 4 days. The final cell count was determined in all vials by flow cytometry. The cell growth in each standard was corrected by subtracting the cell growth in the blank without acetate to account for any background AOC. The corrected cell growth was correlated to the acetate concentration to determine the inoculum yield. For some inoculum batches, the inoculum yield was evaluated after different storage times to assess the effect of inoculum storage on the yield values.

4.3.6 Liquid chromatography organic carbon detector (LC-OCD) analysis

LC-OCD (DOC-LABOR, Karlsruhe, Germany) was used to fractionate the DOM found in the river water samples based on their molecular weight as described by (Huber et al., 2011) and shown in **Figure S-1** of **Appendix B**. Manual integration using commercial software (ChromCALC, DOC-LABOR, Karlsruhe, Germany) was used to evaluate the chromatographs. DOM fractions are measured using 3 kinds of detectors that measure OC content, ON content and UV254 absorbance. Initially, the water samples were filtered through a pre-rinsed 0.45 μm PES membrane and stored in 45 mL glass vials at 4ºC until they were analyzed. Biopolymers are the largest MW fraction that elutes at a retention time of around 33 min and have a MW of more than 10 KDa. Since biopolymers are thought to contain both proteins and polysaccharides, there is a response for both the organic carbon and organic nitrogen detector (OND).The second and largest peak represents humic substances which elutes at 42 min and are characterized by their large UV absorbance. Humic building blocks show up as a shoulder to the humic substances peak. A third peak that elutes at around 50 min is composed of low molecular weight acids (LMWA), and this peak also has a response in the UV detector. The UV response is assumed to be mainly due to presence of small humic-like molecules with an aromatic structure (Huber et al., 2011). The last fraction is the LMW neutral compounds which elute after 54 min. LC-OCD was used to monitor the changes in the

concentration of the different DOM fractions in the river water over time. It was also used to measure the reduction in DOM fractions in the AOC test. Dr. Monica Tudorancea was responsible for operating the LC-OCD, and provided raw data files for further analysis.

4.4 Results and Discussion:

4.4.1 Flow cytometry method and electronic gating

Flow cytometry was used as a tool for counting the bacterial cells both directly in river water and also in the AOC samples after growth. The flow cytometer results for water from the Grand River after staining with SYBR Green I nucleic acid stain had three main populations (**Figure 4-1)** as shown by the three electronic gates (Gate 1, Gate 2 and Gate 3). SYBR Green I has a major peak in its emission spectrum at the wavelength of the FL1 detector (536 ± 20 nm), so stained cells would have a strong response using this detector and therefore it was used as a trigger. Combining the results of the FL1 and FL3 (> 615 nm) detectors was previously found to be a good approach to distinguish the bacterial cells from background noise (Hammes et al., 2008), and electronic gating of the density plots of FL1 versus FL3 were used to differentiate the cells from abiotic particles. According to Hammes and Egli (2005), the signal in Gate 1 is due to instrument noise, while Gates 2 and 3 would contain LNA bacteria and HNA bacteria, respectively. For the Grand River water, there is a visible population in the density plot of the 0.2 μm filtered sample, both in the Gate 1 and Gate 2 regions (**Figure 4-1-a)** while the Gate 3 population was only visible in unfiltered river water (**Figure 4-1-b)**. Since the Gate 2 population was present both in filtered and unfiltered samples, its presence could be due to instrument noise, background particles in the filtered water, or bacterial cells that can pass through the filter, as LNA bacteria were reported to pass through 0.2 μm filters (Wang et al., 2007).
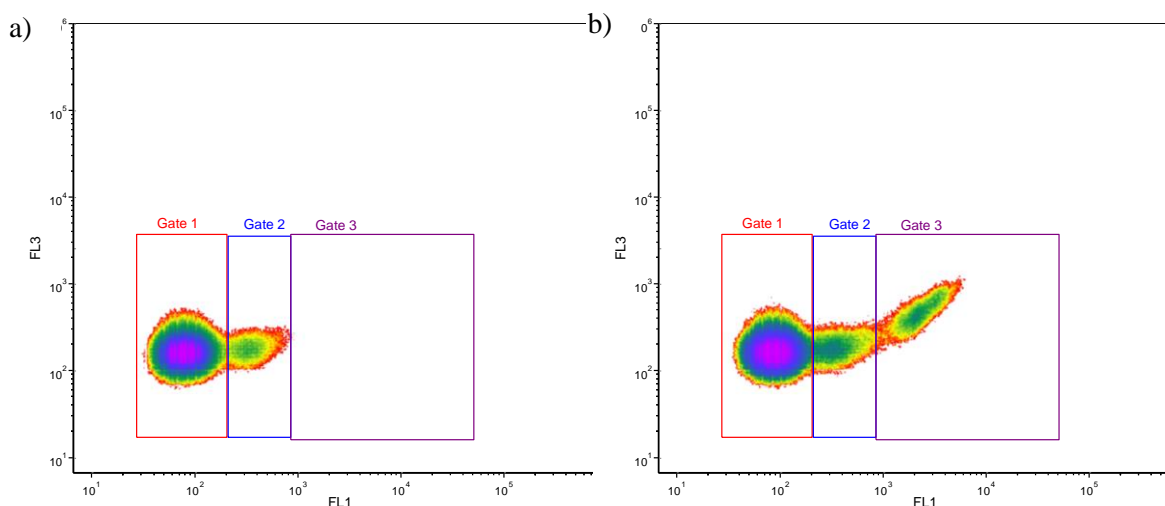
Figure 4-1 Density plot of green fluorescence (FL1) versus red fluorescence (FL3) for (a) filter sterile river water stained with SYBR Green and (b) after adding unfiltered river water as inoculum showing the three main gated populations Gate 1, Gate 2 and Gate 3

To understand the nature of the gate 2 signal in 0.2 μm filtered samples, both SYBR Green I and propidium iodide (PI) stains were used separately to stain both 0.2 μm filtered and unfiltered river water, as shown in **Figures 4-2** and **4-3**. SYBR Green I is a DNA stain that can pass through the cell membrane, and can therefore stain cells with both intact and compromised cell membranes, whereas PI is a DNA stain that cannot pass through intact membranes, and can only stain cells with compromised membranes or free DNA. A summary of the observed number of events in each of the three gates is shown in **Figure 4-4**. The signal in Gate 1 was not affected by staining using either SYBR Green or PI, so it was established that Gate 1 was due to instrument noise or particles with autofluorescence. In the 0.2 um filtered sample, there was a large signal in Gate 2 when SYBR Green I was used as a stain, but no signal when PI was used, showing that gate 2 did not contain dead cells or free DNA. In unfiltered water, the PI stain shows a very low signal in gate 2 and no signal in gate 3, showing that dead cells or free DNA did not influence the total count. Based on these results, the proper electronic gates to isolate the bacterial cells from the background noise peak is shown in **Figure 4-5-a**, and incorporates the signals from Gate 2 and Gate 3. By plotting the frequency histogram of the FL1 signal for the gated particles (**Figure 4-5-b**), the LNA and the HNA communities can be easily selected using the shown markers. The same electronic gate and markers were used to process all the samples in this study.

63
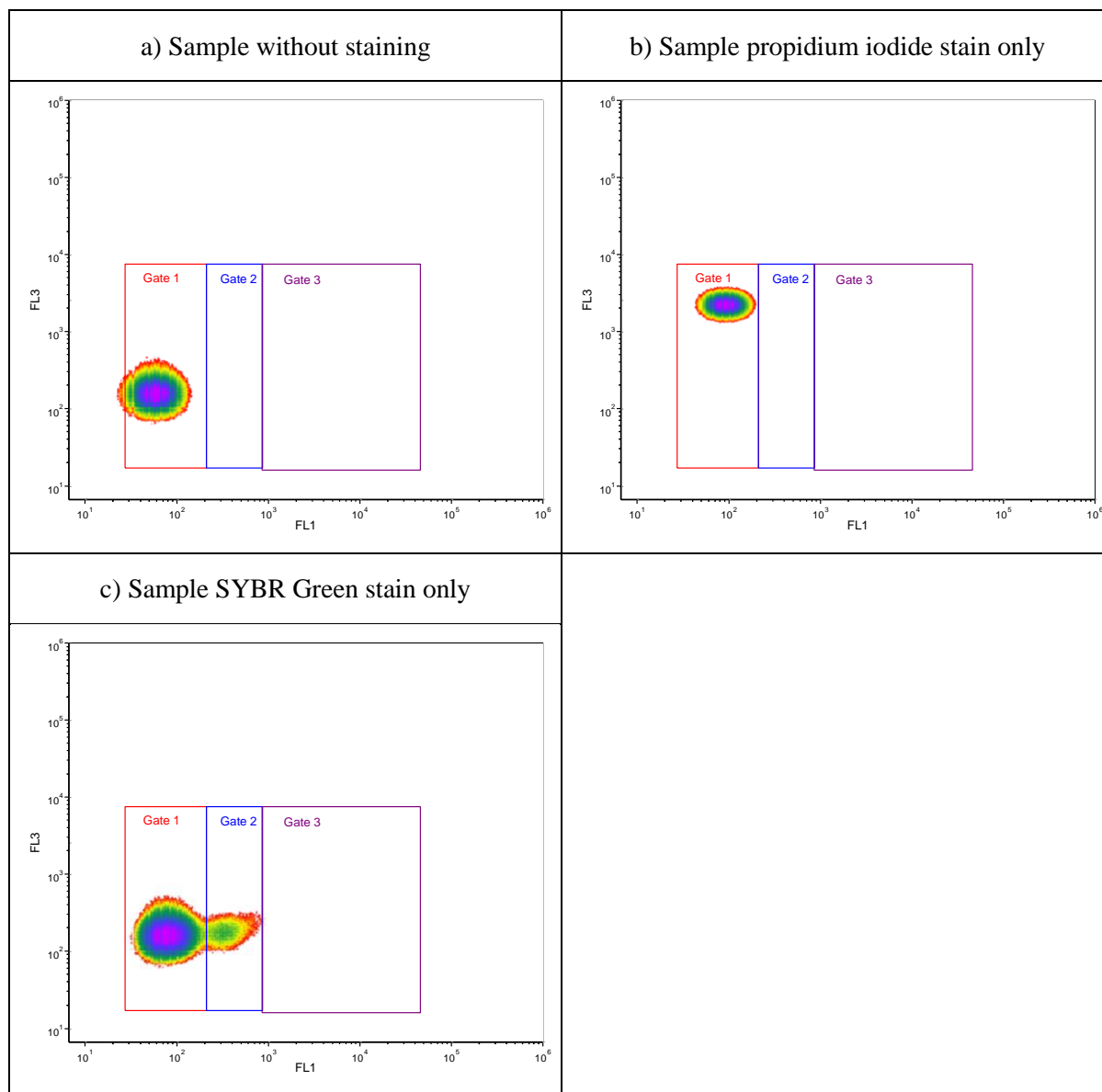
Figure 4-2 Density plots for green fluorescence (FL1) and red fluorescence (FL3) for (a) filter sterile river water without nucleic acid stains, (b) stained with propidium iodide (PI) or (c) SYBR Green
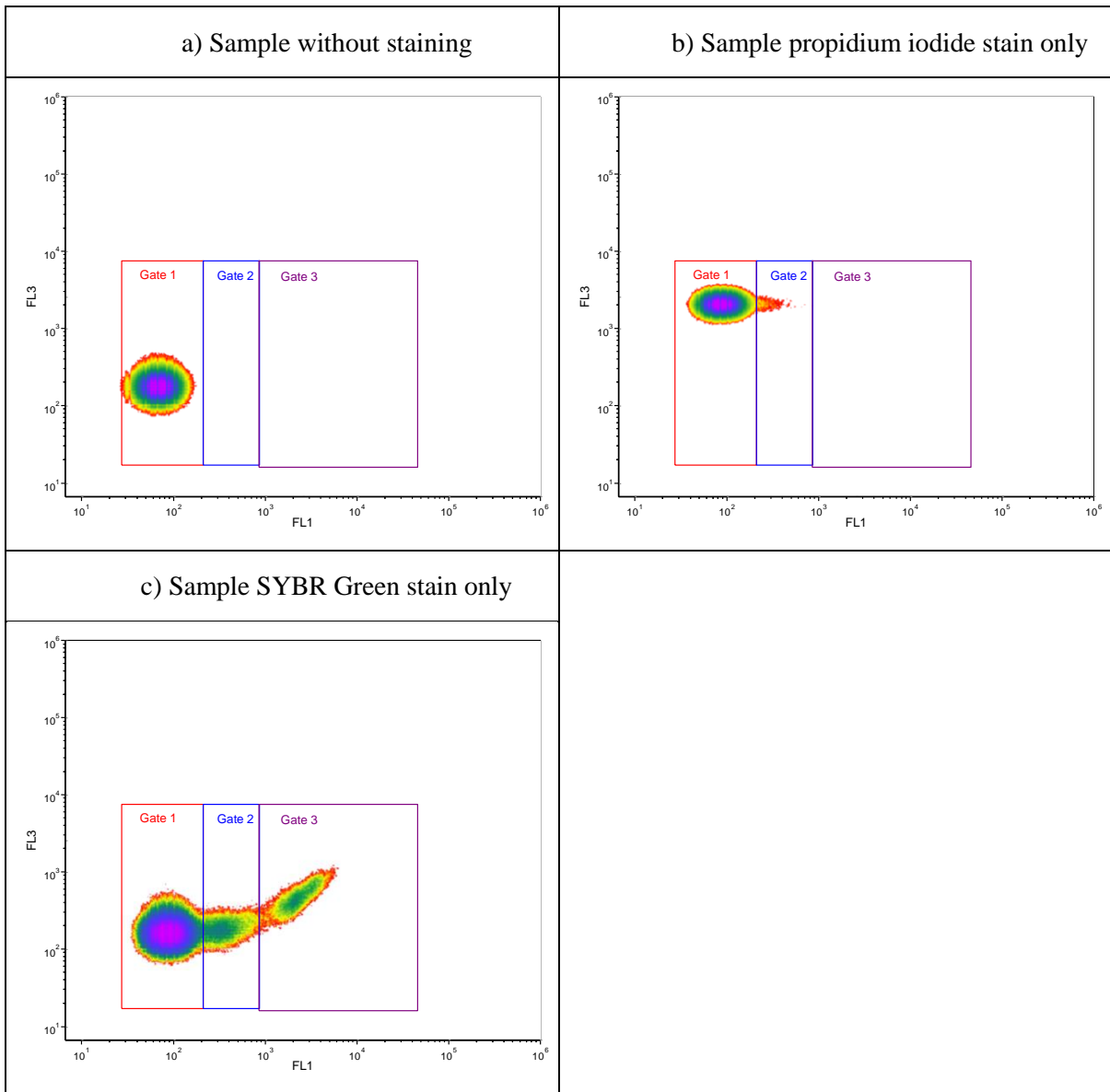
Figure 4-3 Density plots for green fluorescence (FL1) and red fluorescence (FL3) for (a) filter sterile river water after adding unfiltered river water without nucleic acid stains, (b) stained with propidium iodide (PI) or (c) SYBR Green
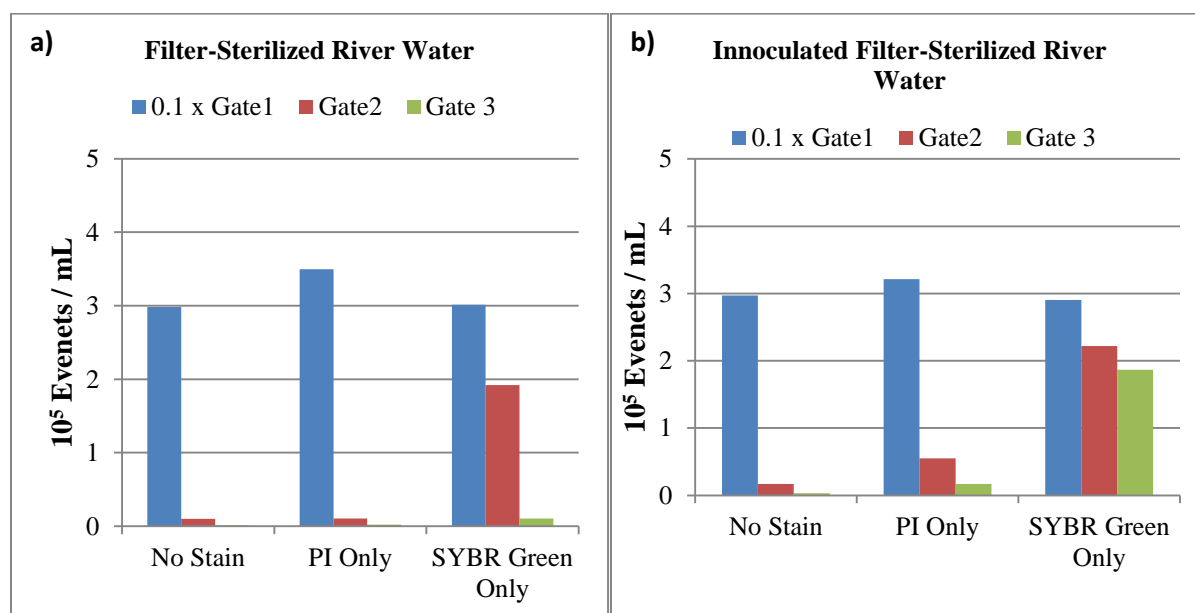
Figure 4-4 Number of events counted in each of the three gates defined on Figure 4-3 for 0.2 µm filtered river water (a) without nucleic acid stains, stained with propidium iodide (PI) or SYBR Green or both stains before adding unfiltered river water or (b) after adding unfiltered river water (b)
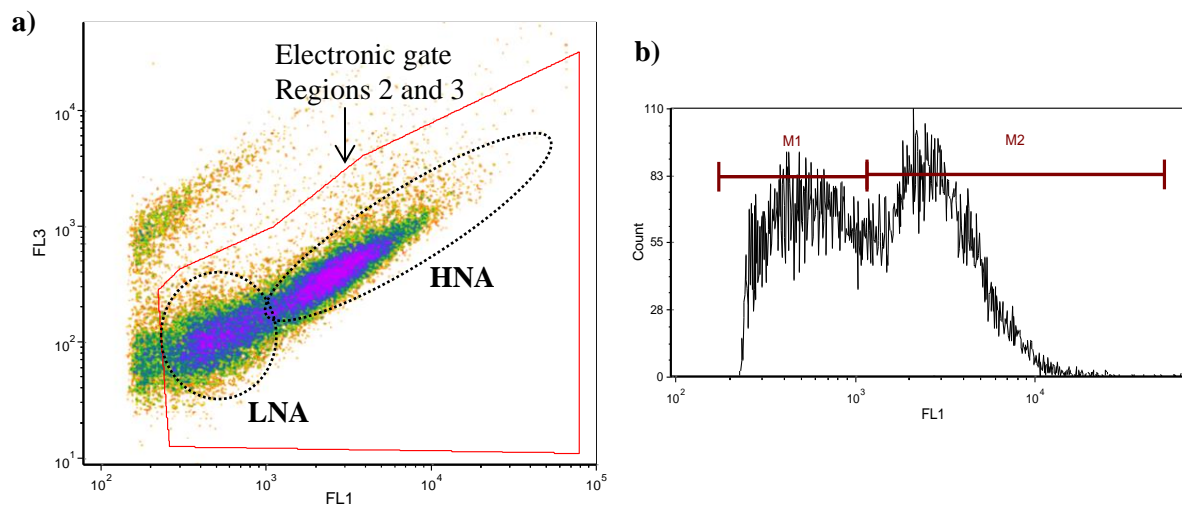
Figure 4-5 Typical density plot (a) of FL1 and FL3 for unfiltered river water along with the used electronic gate and (b) the gated cells frequency histogram of green fluorescence (FL1) showing markers for LNA bacteria (M1) and HNA bacteria (M2). The presented gate would include both gate 2 and gate 3 shown on Figure 4-2

66

To confirm the presence of bacteria cells in filter-sterilized river water samples, an experiment was done to compare sample sterilization protocols. For AOC analysis, microorganisms must first be removed or inactivated in the water sample. For the plate count AOC method, heat treating is the typical method used, as described by Standard Methods (Rice et al., 2012). However for the AOC method using flow cytometry, cells must be physically remove by filtration to remove any background interference. Filtration is considered a better sterilization method as it physically removes bacterial cells without affecting the organic molecules present in the water, whereas heating can potentially alter compounds such as proteins or cause precipitation of inorganic molecules such as carbonate (Ross et al., 2013). To evaluate the two different sterilization methods, Grand River water following10 μm filtration, 0.2 μm filtration, or 0.2 μm filtration combined with heat treatment (60°C for 30 min) were analyzed after sample preparation (day 0) and after incubating the samples at 30ºC for 3 days. FL1-FL3 density plots of all the samples before and after incubation are shown in **Figure 4-6**.
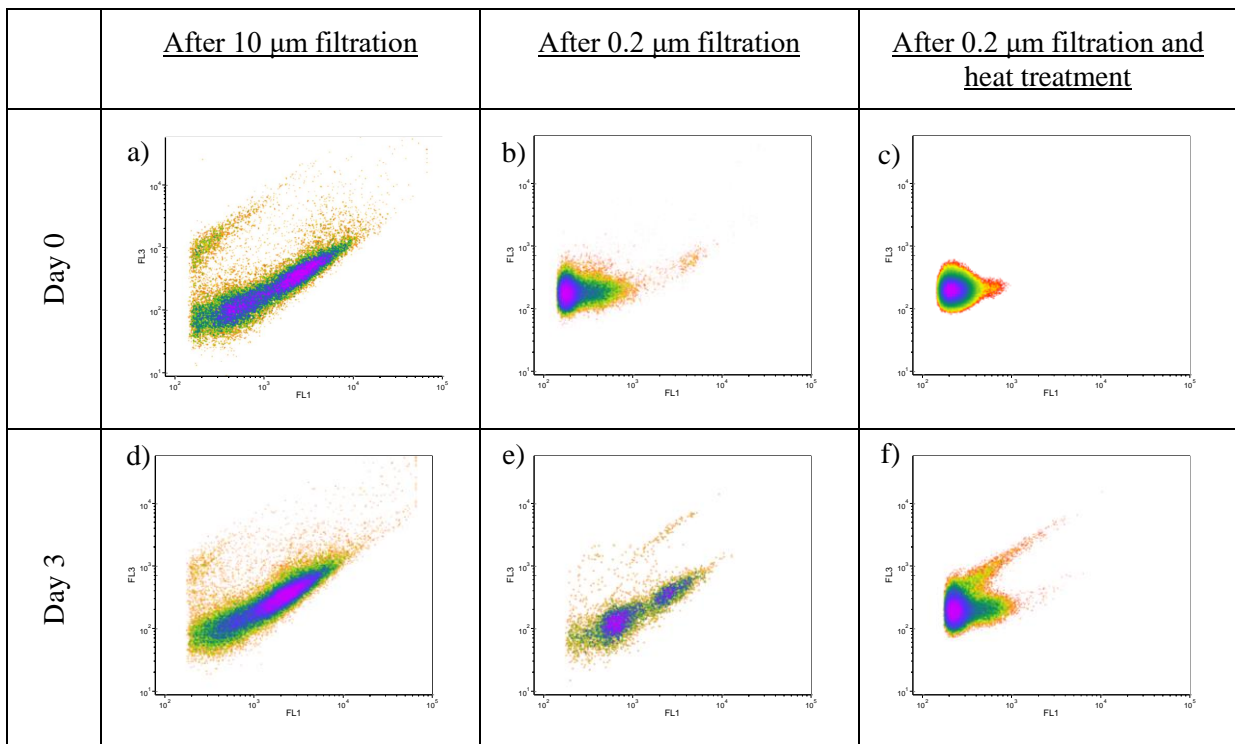
Figure 4-6 Density plots of (a,d) raw water samples, (b,e) raw water after sterilization by syringe filtration and (c,f) after syringe filtration and heat treatment (a,b,c) before incubation and (d,e,f) after 3 day incubation period

Filter sterilization using 0.2 μm filters was not found to be an absolute barrier for bacteria as some bacterial cells especially spirillum-shaped bacteria of different species were passing 0.2 μm filters (Wang et al., 2008, 2007). For the used river water after 0.2 μm filtration (**Figure 4-6-b**), HNA were completely removed as they were below the detection limit of the instrument and LNA were removed by 93%. The total cell count in the filtrate was 4×10^4 cell/mL. After 3 day incubation, the total cell count increased to 3.5×10^5 cell/ mL and both the HNA and LNA bacteria were present and compromised 35% and 65% respectively (**Figure 4-6-e**). HNA bacteria were possibly still present in the filtered water at a very low concentration below the flow cytometer detection limit in the filtrate and were able to grow in the sample after incubation. LNA bacteria were the major fraction in the incubated sample as it increased by 2×10^5 cell/mL over the 3 day incubation period. The presence of LNA bacteria in the incubated sample further proved that the LNA fraction consisted of actual bacterial cells that can grow in the water sample and remain in the LNA region after growth. This further validated the picked electronic gate shown on **Figure 4-5-a**. The 0.2 um filtered sample after 3 days incubation was plated onto an R2A agar plate and after 7 days of incubation, colonies were visible. The predominant colonies had the same morphology, and observation under the microscope showed that the colonies were composed of spirillum-shaped bacterial cells, similar to those previously reported by Wang and co-workers (2007).

Heat treatment at 60°C for 30 minutes was more efficient (**Figure 4-6-c)** and it was able to prevent regrowth in both the LNA and HNA regions as shown in **Figure 4-6-f**. There was one drawback with the use of heat treatment as the heat treatment of the river water caused a significant increase in the noise region defined as gate 1 in **Figure 4-1**. The increase in the noise region can interfere with the accurate quantification on the LNA bacteria however this effect will be less pronounced for the AOC test as HNA bacteria compromised the majority in the grown samples so they were easily separated from the noise. The noise increase is probably due to the formation of calcium carbonate crystals as the used water which had high total dissolved solids of 370 ± 71 mg/L. The interference of the noise region with the observed cell growth and the corresponding AOC value was found to be as low as 3 μg C/L as the total cell count after the sample incubation was 3×10^4 event/ mL. Heat sterilization at 60°C (**Figure 4-6-f**) was found to eliminate the LNA bacterial fraction usually present after filter sterilization but at the same time it did not lead to the formation of excessive amount of abiotic molecules (i.e. cell debris) as in the case of boiling for 30 min as shown in **Figure S-2** in **Appendix B** with minimum interference with the obtained cell count after cell growth within the AOC test.

Combined heat treatment and syringe filtration was recommended earlier by Kaplan and co-workers (1993) as filtration would remove particulate organic that are prone to AOC release upon heat treatment which is a more efficient sterilization technique than membrane filtration only. This is in agreement with our findings so combined membrane filtration and heat treatment was determined to be the best method for sample sterilization for the AOC test.

To evaluate the proper incubation time for the AOC test to ensure that the maximum cell growth was reached, AOC samples were incubated at 30ºC for 4 days and 1 mL samples were collected daily as shown on **Figure 4-7**. Also the sample was diluted by 2:3 and 1:3 in low DOC water to determine the effect of varying AOC concentration on incubation time. An incubation time of 3 days was recommended as the stationary phase of bacterial growth was reached at around 48 h (Hammes and Egli, 2007, 2005). Results from the current study showed that cell growth increased rapidly (2.3 log) in the first 2 days in the undiluted sample, and then the growth rate decreased, but still resulted in a 0.15 log increase in cell count on day 3 and 0.04 log on day 4. The effect of sample dilution did not affect the growth rate of the cells as they followed the same trend as the undiluted sample (**Figure 4-7-b**). These results, i.e. the specific rate of growth of the bacteria approached zero on day 4, indicate that 4 days is an appropriate incubation period using Grand River as the water matrix. For all the presented AOC results, AOC samples were incubated for 4 days.
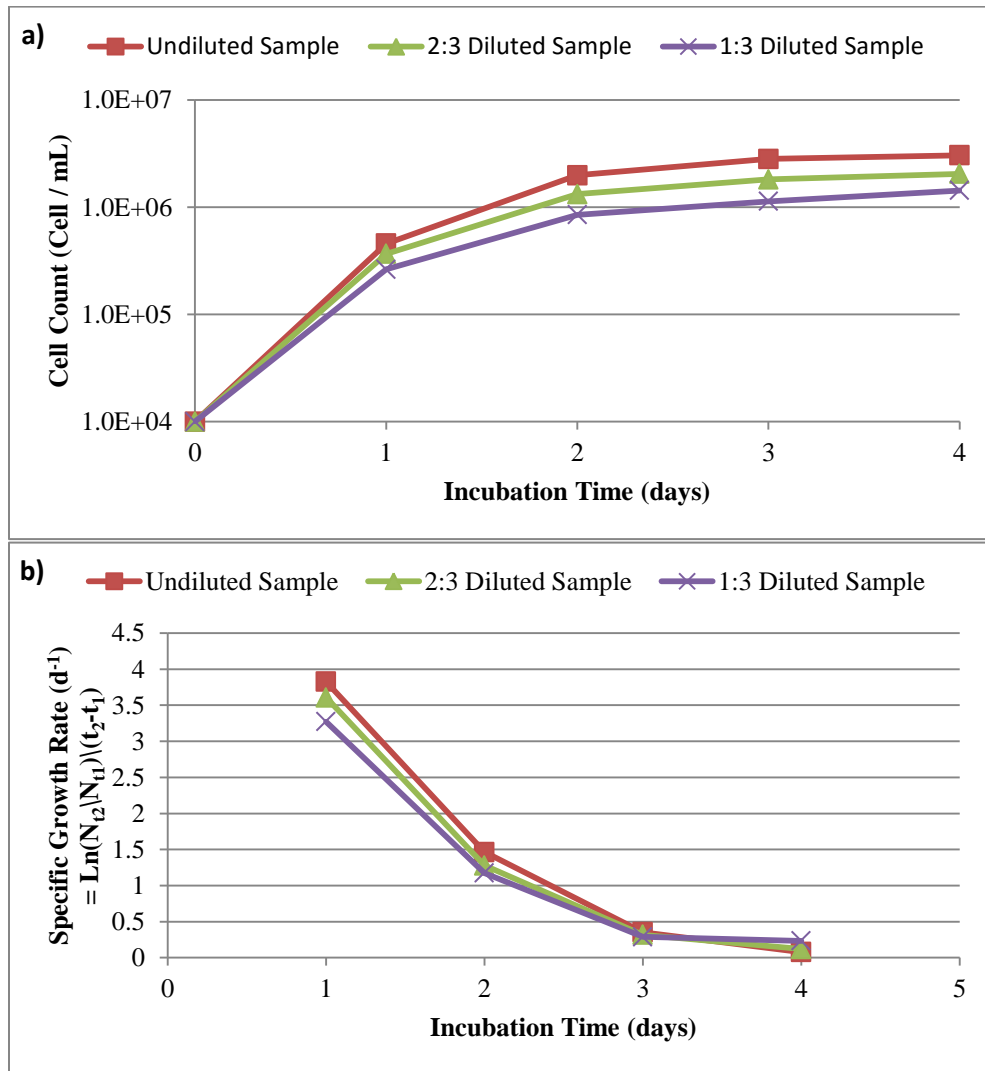
Figure 4-7 Growth of inoculated river bacteria in AOC samples over the 4 day incubation period

4.4.2 AOC inoculum

A critical step for any AOC method using an indigenous bacterial community is the preparation of the inoculum and monitoring the inoculum quality to ensure that the obtained results are valid. As well, determining the growth yield of the inoculum using model nutrients, usually acetate, is essential to convert bacterial growth into a carbon equivalent AOC concentration. Different methods have been used to prepare the natural microbial inoculum for AOC assays. Previous studies have used natural

spring water (Hammes and Egli, 2005; Hammes et al., 2006; Vital et al., 2007) or a minimal medium with sodium acetate as growth media for the indigenous bacteria, followed by incubation to allow cell growth and consumption of the carbon source. Alternatively, the inoculum can be prepared in the source water itself. Hammes and Egli (2005) used this procedure to prepare AOC inoculum by inoculating 0.2 μm filtered surface water with unfiltered water. This inoculum was then incubated for 14 days to consume background AOC, and the cells were then harvested by centrifugation and resuspended in an AOC-limited minimal media. This approach was used in the current study, but was modified to simply incubate the surface water for a long enough time to allow all the background AOC to be consumed. This simplified procedure involved first passing the river water sample through a 10 μm filter to remove any large particles or microorganisms other than bacteria. The sample was then incubated at 30 ℃ for a minimum of 21 d to ensure all the present AOC was consumed. The inoculum was stored at 4℃ and used for analysis.

In this study, we compared the growth yields of the natural river water bacterial community on different types of growth media using sodium acetate as a model substrate as shown in **Figure 4-8** and the obtained yield factors are listed in **Table 4-1**. By using a simple nutrient mixture including nitrogen (NH_4 and NO_3), phosphate (PO_4) and acetate (synthetic water A), the inoculated bacteria from the Grand River had a very low yield of 1.74×10^6 Cells / μg C. This is lower than the reported value of approximately 1×10^7 cells / μg C for a natural inoculum grown from lake Zurich, Switzerland (Hammes and Egli, 2007, 2005). P17 and NOX pure strains used for the traditional AOC method were reported to have yield values of 4.1×10^6 CFU / μg C and 1.20×10^7 CFU / μg C, respectively, using acetate as a substrate (van der Kooij, 1992). Such a low yield in synthetic water A was an indicator that a nutrient limitation condition could be present and carbon was not the limiting substrate in this case. Commercially available natural spring water was also tested using the same AOC inoculum used to test synthetic water (A) prepared on (February 2014). The bacterial yield in the natural spring water was 3.58×10^6 cells / μg C was higher than for the simple nutrient solution of synthetic water A, but the observed yield was still lower than the reported yield values in literature for natural microbial communities (Hammes and Egli, 2007, 2005), and indicated possible nutrient limitation. A more complex medium that included several trace elements (Ihssen and Egli, 2004) (synthetic water (B)) was also used. The observed yield in synthetic water B was 4.49×10^6 cells / μg C, which was slightly higher than the yield in the natural spring water, possibly due to the increased

number of minerals present in synthetic water (B) compared to synthetic water (A) and the spring water.

Table 4-1 Yield factors of different batches of AOC inoculum (and their age at the time of the test) on acetate

Inoculum age at time of test	Growth medium	Linear growth model (Bacterial growth = yield x AOC)	
		Inoculum yield Cells / µg C as acetate	Pearson R^2
1 month	Synthetic water A	1.74×10^6	0.73
2 months	Synthetic water B	4.49×10^6	0.99
2 months	Spring water	3.58×10^6	0.93
2 months	Biofiltered river water	1.22×10^7	0.99
2 months	Biofiltered river water	1.24×10^7	0.99
4 months	Biofiltered river water	1.14×10^7	0.94
7 months	Biofiltered river water	6.89×10^6	0.99
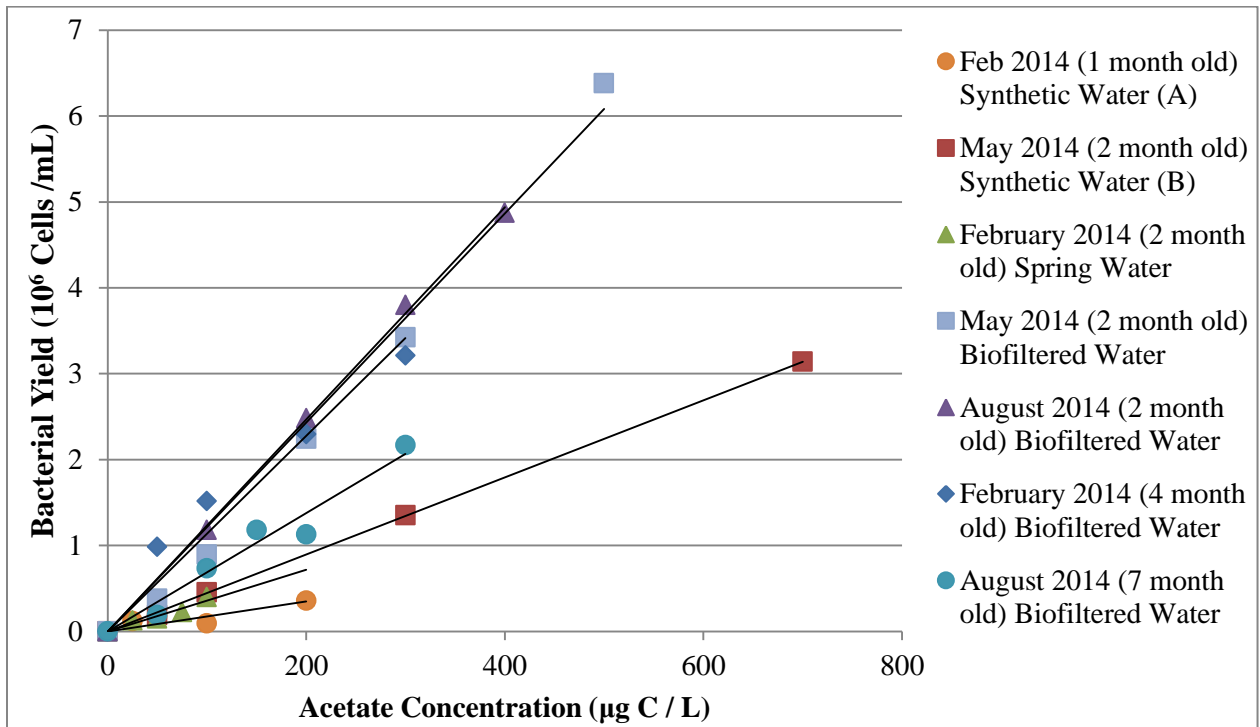
Figure 4-8 Growth yields of AOC inoculum on different types of growth media on acetate and their corresponding yield factors

The final growth medium tested was biofiltered river water. Biofiltered water was used instead of raw water to reduce the available background AOC in the water. Three different batches of the inoculum were prepared in three different seasons (February 2014, May 2014 and August 2014) and were tested to evaluate the effect of possible changes of the bacterial community on growth yields. The observed yield factors for the three batches were very similar, and were approximately 1.20×10^7 cells / μg C which is significantly higher than the previously obtained yield value in synthetic or natural spring water. This value is also similar to previously reported yield values for natural microbial inoculums (Hammes and Egli, 2005). Also the observed linear relation fitting was excellent ($R^2 = 0.94 – 0.99$) (**Table 4-1**). The high R^2 values indicated that the growth of the AOC inoculum was not affected by the present background AOC in the biofiltered water. Bacterial growth remained in the linear range even at the highest standard tested, which is higher than the normal AOC values encountered in drinking water treatment. Additionally, yield values were not affected by possible changes in the bacterial community of the river in different seasons. These results show that this AOC method is suitable for long term studies. Growing different batches of inoculum from the same source gave

73

AOC results that are reproducible and consistent. Storing the AOC inoculum for 7 months significantly affected the inoculum yield, which dropped to 6.9×10^6 cells / μg C. Other yield values obtained for different AOC inocula stored for up to 4 months had similar yield values, so storing the inoculum for up to 4 months is suitable and the AOC results will not be affected.

In summary, the observed inoculum yield obtained using natural water was two to three times higher than the yield of the same inoculum when it was grown in spring water or synthetic water. These differences could be due to nutrient limitation conditions that existed in any of the growth media tested except for the natural water. Also, the measured yield factors for the indigenous inoculum from river water in this study were similar to the yield of the natural inoculum grown from lake Zurich, Switzerland, suggesting that a major change in the ecological system of origin may not affect results, although this would need to be confirmed by testing other types of source waters. The theoretical yield factor of 1×10^7 cells / μg C suggested by Hammes and Egli (2005) which was also similar to the yield value obtained in this study was then used to determine the AOC concentration for all samples in this study.

4.4.3 Comparison of traditional and flow cytometry AOC method

The flow cytometry AOC method (using indigenous bacteria) was compared to the standard plate count AOC method (using P17 and NOX strains) to understand their relationship and to relate results of this method to the results in the literature which are commonly obtained using the standard AOC method. Water samples were collected from a full scale water treatment plant that also uses the Grand River as source water. Samples were collected on 2 occasions (July 1st and 14th, 2013) after clarification, ozonation and GAC biofiltration as described by Pharand and co-workers (2015). The results of the two AOC methods are shown in **Figure 4-9**. For the standard plate count AOC method, the AOC value is based on the sum both P17 and NOX strains, and the AOC fraction contributed by each of these strains is shown on **Figure 4-9-b**. A comparison of the AOC results from both methods (**Figure 4-9-a**) showed that the results of the standard plate count AOC method with the exception of one outlier were generally comparable to the flow cytometry method, unlike what was reported in the literature (Ross et al., 2013). An outlier in the regrowth of NOX in one of the post ozonation samples as shown of **Figure 4-9-b** resulted in weak correlation ($R^2 = 0.58$, n =6) between the methods and by excluding this point R^2 will be 0.85 (n=5). The P17 fraction of the traditional AOC results had a very good correlation with the flow cytometry AOC results ($R^2 = 0.77$, n=6), but the growth of NOX was

higher than that of the natural community in post ozonation samples. This is because NOX grows well on ozonation by-products such as organic acids, aldehydes and ketones (Hammes et al., 2006) which will be present in the two post ozonation samples causing the differences between the two methods. In general, AOC results obtained using the two methods should be compared with caution, as the two methods have different procedures that can affect the results; however the results for non-ozonated samples were quite similar.
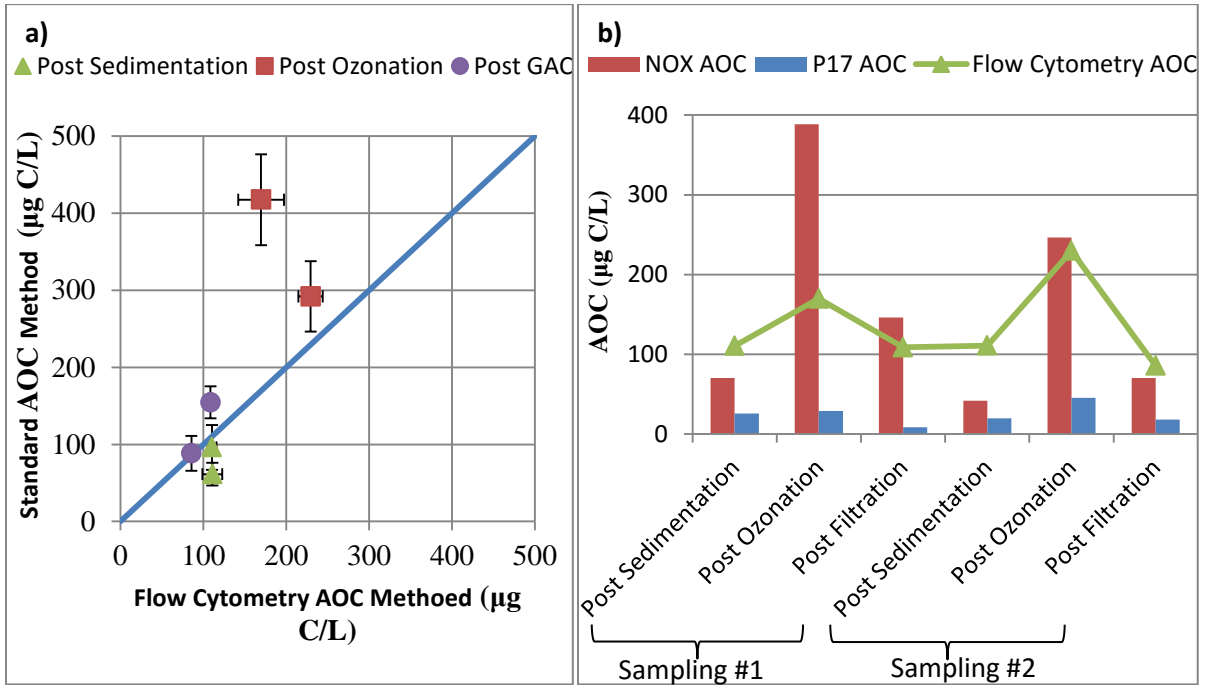
Figure 4-9 Comparison of (a) traditional AOC method (Van der Kooji et al. 1982) and flow cytometry AOC method , and (b) the relationship between flow cytometry AOC and both P17 and NOX strains AOC fractions from the traditional method

The differences between the two AOC methods were also investigated using LC-OCD to measure the NOM fractions consumed during the AOC batch tests (**Figure 4-10**). LC-OCD analysis can provide information on the different fractions of the natural organic matter. Two main fractions, biopolymers and LMWA, have significance for biological processes in the river as they have been shown to be degradable by aquatic bacteria (Huber, 2002). Biopolymers are thought to be composed of polysaccharides and proteins (Huber et al., 2011), which may originate either from effluent organic matter (EfOM) of treated wastewater or biological activities in the river, as they are a major component of the EPS in fresh water biofilms (Stewart et al., 2013). The LMWA fraction contains the

low molecular weight acids present in the sample along with some contribution from low molecular weight humic-like substances (Huber et al., 2011). Compounds such as acetate or pyruvate have retention time that match this peak (Ruhl and Jekel, 2012). For the standard AOC test using P17 and NOX, there was less than 10% removal of biopolymers (both organic carbon and organic nitrogen fractions) and of LWMA compounds (organic carbon and aromatic compounds) (**Figure 4-10-a**). In several cases the amount of these fractions showed an increase following incubation, presumably due to the production of these NOM fractions by bacterial growth in the vials. For the indigenous microbial community used for the flow cytometry AOC method, the LMWA organic carbon fraction was significantly reduced by approximately 20%, however the corresponding peak in the UV absorbance spectrum was not removed, indicating that the LMW aromatic compounds were not removed (**Figure 4-10-b**). Also, the biopolymers organic carbon fraction which has a higher molecular weight was consumed by an average value of about 10%, and for one sample it was consumed only by 2%. The biopolymers organic nitrogen fraction was also reduced, indicating that protein-like matter was utilized during the AOC test along with some polysaccharides. Overall results show that the indigenous microbial community had a higher consumption of both high and low molecular weight DOC fractions compared to P17 and NOX strains which is probably due to the diversity in the indigenous microbial community composition and its ability to consume a variety of organic molecules compared to the more limited substrate utilization range of the P17 and NOX pure cultures.
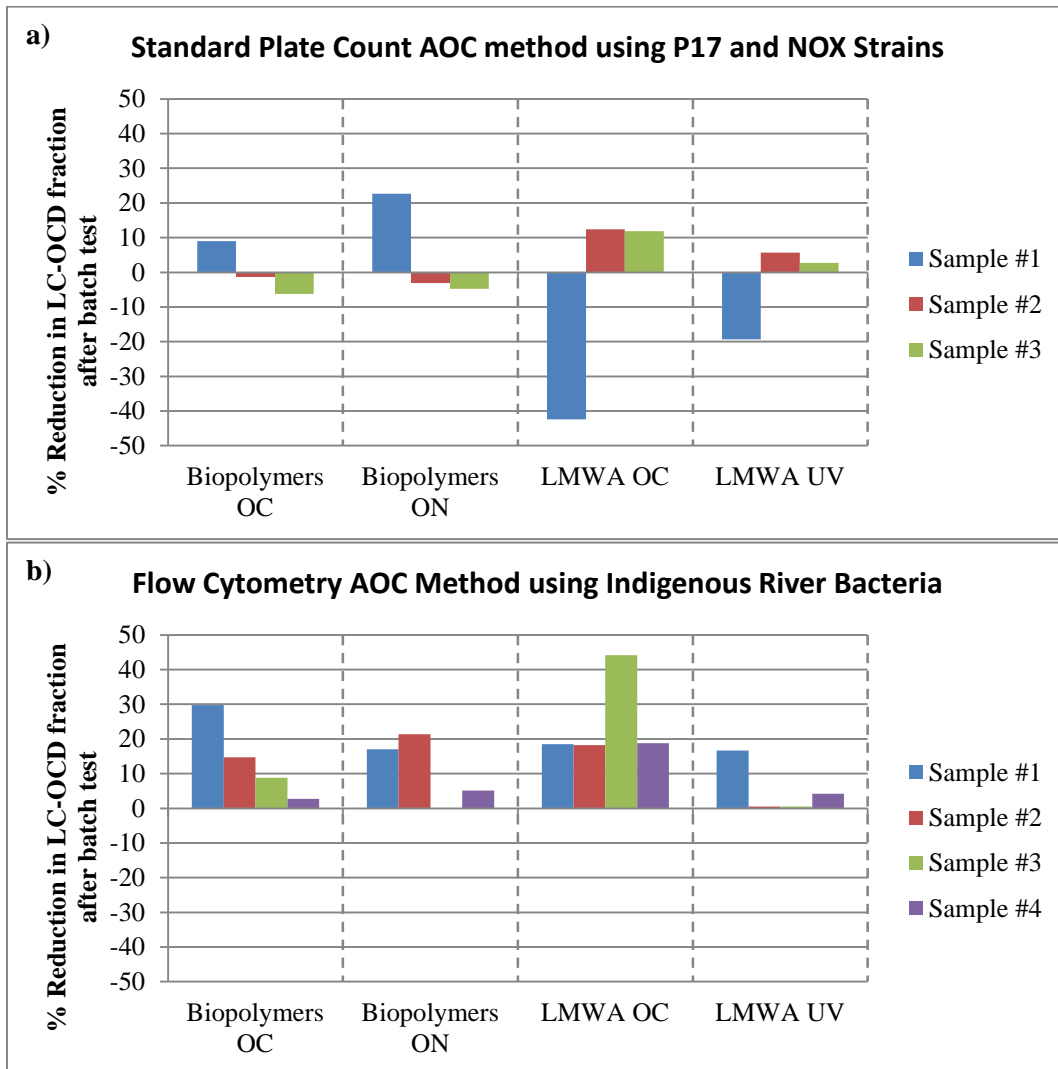
Figure 4-10 Consumption of different LC-OCD fractions following (a) the AOC test using P17 and NOX strains for the standard AOC method (10 days at 14ºC) and (b) the indigenous microbial inoculum for the flow cytometry method (4 days at 30ºc) the different presented samples are samples collected on different dates from the Mannheim Water Treatment plant intake

4.4.4 Monitoring seasonal water quality changes in the Grand River

The modified AOC method using indigenous bacteria and flow cytometry was used to monitor water quality in the Grand River over 16 months from January 2014 to April 2015. These results were

compared with the total cell count of the river water using flow cytometry, and also with a number of other water quality parameters including phosphorus and nitrogen levels, temperature, and turbidity. As well, overall DOC and NOM fractions were measured. The AOC results and the total cells counts for the HNA and LNA groups are shown on **Figure 4-11**. The AOC flow cytometry method provided reproducible results since the standard error of the three replicates for any of the samples was ≤ 12% over the study period. The normal range for the AOC values of the river was between 200 and 250 μg C acetate/L regardless of the changes in water temperature which ranged from 2 to 26°C over the study period. Two major spikes in the river AOC occurred during the spring run-offs in March 2014 and in March 2015, and were probably caused by large amounts of snow melting that washed nutrients from the soil into the river. Total and ortho-phosphate (**Figure 4-12**) also had large increases in concentration during the spring snow-melt events, but there was no spike in ammonia. Instead, ammonia followed a seasonal trend in the river with higher concentrations at cold temperatures as shown in **Figure 4-12** which is in agreement with the DOC data that was higher during the summer and spring seasons and lower during the winter season.
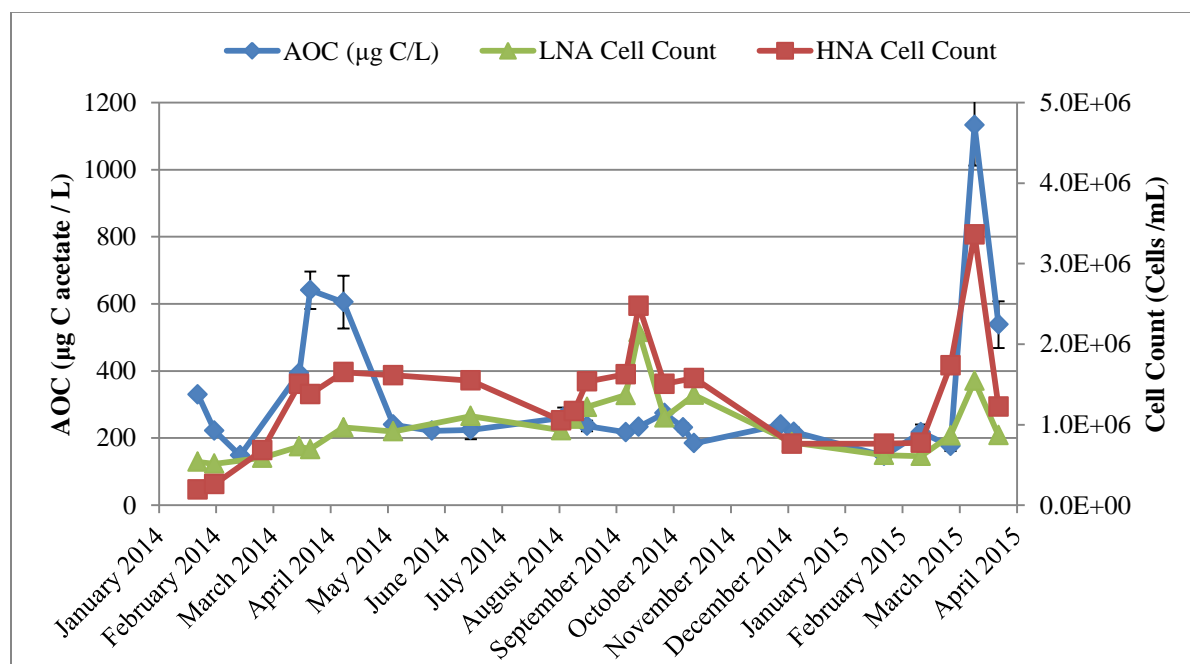
Figure 4-11 Seasonal changes in assimilable organic carbon (AOC) of the river raw water and the corresponding cell counts for LNA and HNA bacteria using flow cytometry with error bars indicating standard deviation of the AOC sample replicates (n=3)

78
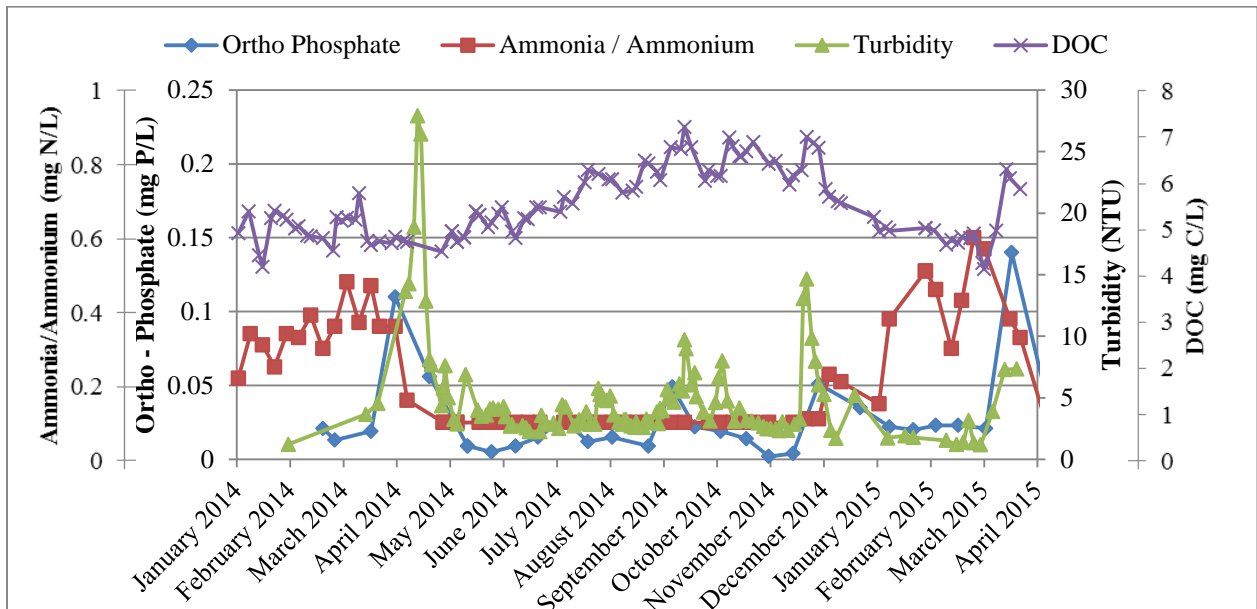
Figure 4-12 Seasonal changes in Ortho-phosphate, Ammonia/Ammonium, DOC and turbidity of the raw water over the study period

For the total cell count in the river, both LNA and HNA bacteria were present at similar concentrations over the study (**Figure 4-11**), except during the spring and summer seasons between March and August 2014. The HNA bacterial concentration increased at warmer water temperatures and became more dominant than LNA bacteria. The LNA bacteria also increased with warmer water temperatures, but at a much slower rate compared to HNA bacteria. As the water temperature started dropping after October 2014, both HNA and LNA bacteria were present at a similar concentration again. During a major rain event on September 2014 and during the spring run-off on March 2015, both HNA and LNA bacteria increased significantly along with the increase in nutrients. The observed increase is possibly due to washing out of bacterial cells from agricultural fields where manure is commonly spread during that time of the year. A similar increase in total bacteroidales (Lee et al., 2014) and fecal coliforms (Dorner et al., 2007) was previously observed during rain events in the Grand River. Another possible explanation is that the bacteria responded to the additional nutrients in the river during those runoff events.

LC-OCD was used to study the changes in the biopolymers and LMWA fractions in the Grand River. The biopolymers fraction had a relatively stable composition with a carbon to nitrogen ratio

79

consistently at 10 as shown in **Figure 4-13.** This is nearly three times the average carbon to nitrogen ratio of 3.3 as reported for the majority of proteins by (Rouwenhorst et al., 1991). Therefore, polysaccharides seem to be the major contributor to the biopolymers fraction in this river. Both, biopolymer organic carbon and organic nitrogen content followed a trend similar to the bacterial cell count in the river (**Figure 4-11**), and this suggests that the biopolymers in the river water are linked to the microbial activities in the river. The LMWA organic carbon content ranged between 60 and 290 μg C/L over the study (**Figure 4-13**). The average carbon content of LMWA was 160 μg C/L with some spikes during run-off or rainfall events. The LMWA UV response had a trend similar to the LMWA organic carbon. The specific UV absorbance (SUVA) of the LMWA peak was 3.56±0.6 L/mg C·M which is slightly lower than the SUVA value for the bulk humic substances in the same water (approximately 4 L/mg C·M). This points to that humic substances with aromatic structure contributed substantially to this LMWA peak along with organic molecules such as organic acids that do not have an aromatic structure. The spikes in LMWA organic carbon during rainfall or run-off events (**Figure 4-13**) may therefore be explained by humic like substances being washed away from the soil into the river during those events. None of the LC-OCD fractions were directly linked to AOC concentrations in the river water ($R^2 \leq 0.4$, n=19). These results are similar to those for the AOC batch test (**Figure 4-10**) as none of the LC-OCD fractions was completely consumed by the AOC inoculum. The reason is that biodegradable organic carbon as measured by AOC is a complex mixture of organics which seems to includes a wide size range of molecules (Hem and Efraimsen, 2001). Also, each LC-OCD fraction is composed of a pool of different molecules that have different biodegradability. Therefore, no specific LC-OCD fractions can be linked to the measured AOC values. The contribution of each fraction to the AOC might be variable making the relationship between AOC and LC-OCD fractions a very complex one.
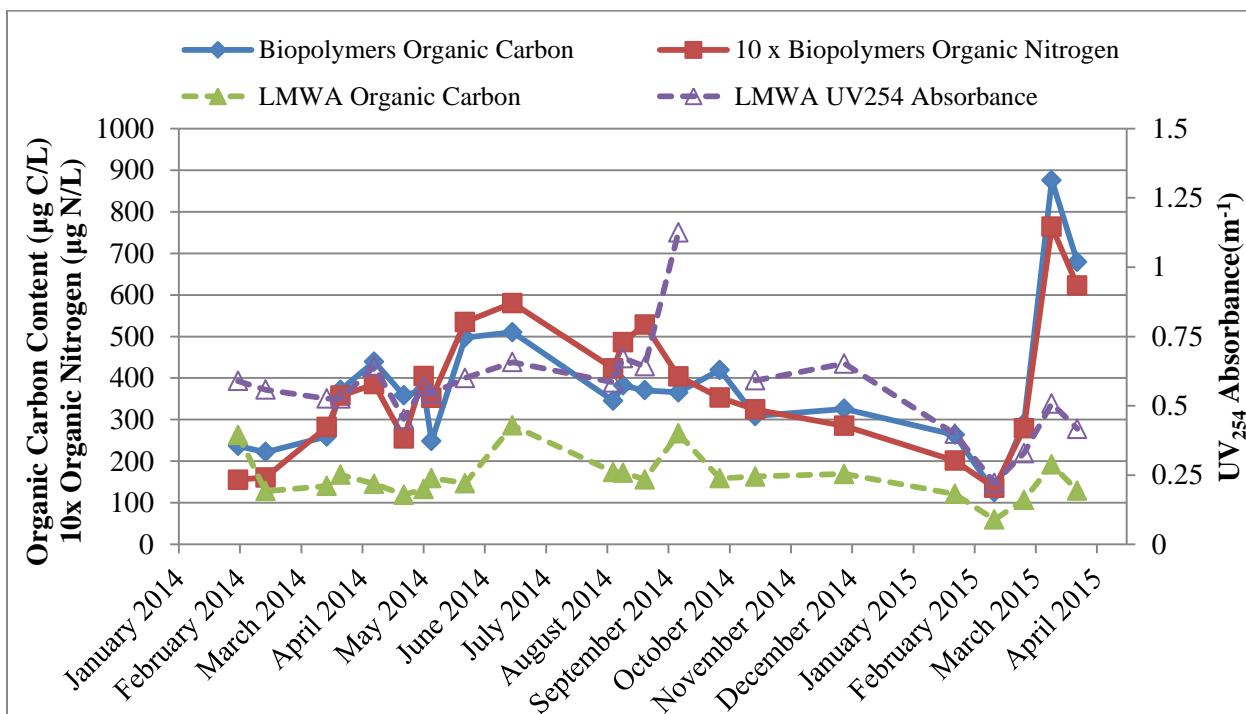
Figure 4-13 Seasonal changes in LC-OCD biopolymers and low molecular weight acids (LMWA) fractions concentrations in the river raw water

4.5 Conclusions

AOC is an important parameter to study the biological stability of drinking water. In this study, a published AOC method using flow cytometry and an indigenous bacterial community as inoculum to account for the natural heterogeneity of the microbial communities encountered in real life was optimized. The modified method was used to monitor AOC changes in a long term study on an impacted water source. In addition, flow cytometry was used to measure the dynamics of the microbial water quality. The presented AOC and cell counting methods are both reliable techniques that were successfully adapted to a new ecological system compared to the system for which these methods were originally developed. The two modified methods may also be used as monitoring tools in new studies looking to improve unit performance in drinking water treatment processes. The main conclusions are as follows:

- Preparation of the natural inoculum is a key component of the AOC method. This study found that a reliable natural inoculum with a good growth yield could only be obtained by

using the same natural water as growth media for the bacterial community. Nutrient limitations largely affected the growth of the natural inoculum when testing other water matrices. The bacterial yield on acetate was nearly half of the value obtained in natural river water for these other water matrices.

- Growing the natural inoculum from the same water sources at different seasons over the year had no effect on the inoculum growth on acetate. The method is therefore suitable for long term studies where the preparation of a new inoculum is required periodically. The validity of the AOC inoculum was tested and the prepared inoculum yield was not affected within a 4 month storage period.

- Combined filter sterilization and heat treatment was necessary to sterilize the river water used in this study, mainly due to the presence of LNA bacteria which passed through the 0.2 μm membrane filters.

- The AOC results from the flow cytometry method gave similar results to the standard plate count AOC method except for ozonated water samples which had higher AOC values in the standard AOC method possibly due to the high growth of NOX bacteria used in standard AOC method on the present ozonation by-products along with the differences in the yield coefficients of the P17 and NOX bacteria on acetate compared to the river indigenous bacteria.

- NOM fraction analysis showed that the natural inoculum could consume a wider range of organic molecules including both biopolymers and LMWA fractions. This is compared to low consumption of LMWA fraction only for P17 and NOX pure strains used in the standard AOC test.

- The modified AOC method using indigenous bacteria and flow cytometry provided reliable results with lower variability in a long-term study of river water.

- Flow cytometry could also provide reliable total cells count data from the river water, and could distinguish between HNA and LNA groups of bacteria. HNA bacteria responded more rapidly to an increase in nutrients or water temperature than did LNA bacteria. Also HNA bacteria were affected by a drop in water temperature more than LNA bacteria, suggesting that HNA bacteria are more sensitive to changes in environmental conditions.

- LC-OCD biopolymers seemed to be related to bacterial activities in the river as they were correlated with the total cell count in the river, but they were not directly correlated to the observed AOC.

Chapter 5

Influence of Seasonal Variations and Operating Conditions on Drinking Water Biofilter Performance and Attached Biomass

5.1 Summary

   A pilot-scale dual-media drinking water biofilter was used to study the effect of biofilter EBCTs on NOM removal and biomass characteristics under summer and winter conditions. Bulk DOC, specific fractions of the NOM and AOC were used as indicators of the biofilter performance. Flow cytometry was also used to measure the net removal of bacterial cells by the biofilters. A comprehensive protocol was used to characterize biofilter biomass, including biomass activity and the composition of EPS, to understand how the biofilter biomass may be linked to biofilter performance and affected by temperature changes. Both the large molecular weight biopolymers and the low molecular weight acids fraction of NOM, as well as the easily biodegradable AOC, were effectively removed by the filters at warm water conditions. Although low water temperature significantly reduced biofilter performance, there was still some removal of AOC and the NOM biopolymers and acids fractions at cold water temperatures below 7ºC. Average cellular ATP content was found to be a good indicator of the drop in biofilter performance at cold water temperatures which was not detected using a single biomass parameter such as bulk media ATP or biofilm cell count using flow cytometry.

5.2 Introduction

Biological filtration has been used in drinking water treatment for several decades in different ways such as slow sand filtration, river bank filtration and conventional biofiltration with pre-ozonation. In principle, any granular media filter operated in the absence of a disinfectant residual, both in the feed or backwash water, would act as a biofilter because active biomass would grow on the filter media and consume BOM. Potential benefits of biological filtration include the reduction of BOM to improve the biological stability of the treated water, along with a reduction in disinfection by-products precursors, chlorine demand and water corrosion potential (Urfer et al., 1997). BF_{WP} is a more recent application of biological filtration, where biologically active media filters are used as a pre-treatment step to improve water quality and target certain types of organic molecules to improve the performance of subsequent treatment units (Huck et al., 2015). BF_{WP} can efficiently reduce the concentration of large molecular weight organics (i.e. biopolymers) which are responsible for fouling of low pressure membranes (Hallé et al., 2009). Biofiltration can also reduce the easily biodegradable organics and limit biofouling of high pressure membranes (Griebe and Flemming, 1998).

NOM consists of a large pool of organic molecules which exist in the different surface or ground water sources. NOM is naturally occurring in the environment from plant or microbial sources, or as an outcome of domestic, industrial or agricultural activities (Prévost et al., 2005). A sub-fraction of NOM is BOM which can be degraded by aquatic microorganisms, and is approximately 17 to 40% of the bulk NOM in rivers (Servais et al., 1987). BOM includes different types of molecules such as humic substances, proteins, amino acids, carbohydrates and organic acids, which largely differ in their molecular weight and their utilization rate by aquatic microorganisms (Prévost et al., 2005). The large molecular weight fraction of NOM is defined as biopolymers, and is commonly linked with biofouling of low pressure ultrafiltration membranes (e.g. Chen et al., 2014). Also, biopolymers have been linked to transparent exopolymer particles (TEP) in water (Villacorte et al., 2009) which can trigger high pressure membrane biofouling (Bar-Zeev et al., 2015). Humic substances are the major fraction of aquatic NOM and have a lower molecular weight than biopolymers (Huber et al., 2011). Humic substances are known to have low biodegradability (Prévost et al., 2005), unlike biopolymers which can be easily degraded by aquatic bacteria as shown in **Chapter 4** and in the literature (e.g. Huber, 2002). The lower molecular weight NOM compounds include amino acids, carboxylic acids and mono sugars, and typically are degraded more easily by microorganisms.

Different methods have been used to measure biofilter performance in terms of BOM removal. BOM is commonly measured using a method based on DOC consumption due to microbial activities, and is known as BDOC. Bulk DOC removal has been used as an indicator of the performance of BF_{WP} as a biological process, and was reported to be removed with drinking water biofilters to different extents (Hallé, 2009; Hallé et al., 2009; Huck and Sozański, 2008; Huck, 2000). A different method to measure NOM removal is based on biomass regrowth due to substrate utilization known as AOC (Huck, 1990). AOC has been linked to biofouling and biofilm formation in distribution systems (Hijnen et al., 2009; Prévost et al., 2005). Recently, modern advanced methods for NOM characterization such as size exclusion chromatography (Huber et al., 2011), fluorescence spectroscopy (Baker, 2001), and field flow fractionation (Giddings, 1993; Pifer and Fairey, 2012) have been applied to better understand NOM composition. Using these methods, more information about the chemical structure, characteristics and molecular weight of BOM can be obtained and used to better understand NOM removal by biofilters.

To better understand biofilter performance, the biofilter attached biomass needs to be monitored so that its potential relationship to performance can be determined As well, providing a benchmark value for biofilter biomass can determine if there are any changes to the biomass and microbial community due to operational changes or environmental conditions (Evans et al., 2013b). Different biomass indicators have been used to evaluate attached biofilter biomass, such as ATP (Magic-Knezev and van der Kooij, 2004), phospholipids (Wang et al., 1995), biomass total direct cell count (Servais et al., 1994), biomass hydrolase enzyme activity (Le Bihan and Lessard, 1998) or respirometric methods (Urfer and Huck, 2001). To date, these biomass indicators have not been quantitatively linked to biofilter performance. EPS is a major component of bacterial biofilms, which attaches the bacteria to the surface of the media grains and accommodate extracellular enzyme activities to degrade dissolved or particulate organics (Flemming and Wingender, 2010). Few studies have investigated EPS levels or composition in drinking water biofilter attached biofilms (Elhadidy et al., 2015; Stoquart et al., 2013), and more work is still needed to understand their relevance for evaluating biofilter performance.

In this study, an automated dual-media BF_{WP} pilot plant was used to investigate the removal of BOM within biofilters using different contact times at both high and low water temperature conditions. A comprehensive protocol for the characterization of biofilter attached biomass was used to determine the amount of active biomass, along with the amount and composition of the biofilm EPS, within the

different biofilters and over the biofilter depth. Flow cytometry was used as a method to determine true volumetric cell count of the biofilm attached cells compared with planktonic cells within the biofilters. At the same time, NOM characterization techniques such as LC-OCD, fluorescence spectroscopy and AOC were used to determine the removal of specific NOM fractions that had a direct relationship to biofilter performance. AOC was tested using a modified method employing a natural microbial inoculum to better measure the effect of BF_{WP} on treated water biological stability. Using these analytical techniques, the effects of biofilter contact time as a design parameter, and water temperature as an operational parameter, were compared with biofilter performance and biofilter attached biomass to identify possible relationships.

5.2.1 Development of a suitable research platform to perform biofiltration research studies

A suitable research platform was needed for the current study. The NSERC Chair in Water Treatment at the University of Waterloo had a pilot scale BF_{WP} facility located at the Mannheim water treatment plant. The old facility was not suitable for the current study for numerous reasons and the pilot plant facility had to be completely redesigned, constructed and commissioned to overcome these limitations which included:

- The old pilot feed lines, effluent lines and backwash lines were made from flexible PVC lines which compromise the results of the study. Flexible plastics can potentially leak trace organics which can be degraded by bacteria (van der Kooij, 1992) and affect the water quality especially if a sensitive analytical method such as AOC is used. All lines needed to be changed to hard PVC.

- The old pilot plant biofilter columns were made from clear PVC but the pilot parts were glued together using organic polymers which can be a source of contamination as well. PVC welding was found to be a better method to build biofilter columns.

- The old pilot plant biofilter columns were operated in declining rate mode. In declining rate mode, the filter surface loading rate starts at the design loading rate after biofilter backwash then as the filter gets clogged the effluent flow rate starts to drop and the surface loading rate starts dropping. This declining rate operational mode would affect any findings about the effect of biofilter EBCT at constant loading rate. Automated flow

87

controllers were needed to automatically adjust the biofilter effluent flow rate to achieve a constant surface loading rate.

- The capacity of the pilot plant had to be increased to accommodate the current research project along with other research projects from the other research group members. As part of this upgrade, a central roughing filter was designed to have the same feed water for all biofilter instead of using small separate roughing filters from the old pilot plant.

- Online sensors were needed to better study the biofilter performance.

A new pilot plant was constructed to meet those requirements and the details of the pilot plant are provided in **Appendix C**.

5.3 Materials and Methods

5.3.1 Experimental setup and sample collection

A pilot scale BF_{WP} plant was used for the study, as is described in more detail in **Appendix C**. The pilot plant design, construction and operation were shared tasks between me and fellow graduate student Brad Wilson. The pilot plant was located in a full scale drinking water treatment facility and used the same feed water (Grand River). Briefly, the river raw water first passed through a roughing filter consisting of 10 cm of crushed gravel to reduce particle loading on the biofilters. The water was fed to two biofilters using a centrifugal pump with a magnetic sealed drive to prevent possible contamination. Biofilter A (BF (A)) consisted of 20 cm of anthracite over 20 cm of sand with 10 cm of gravel base. Biofilter B (BF (B)) consisted of 20 cm of anthracite over 60 cm of sand with 10 cm gravel base. The effluent from BF (B) was fed under gravity flow into a 40 cm sand column to have a total sand depth of 100 cm in biofilter C (BF (C)). The hydraulic surface loading rate for all three filters was kept constant at 3.1 m/h using digital flow controllers. As a result the EBCT for BF (A), BF (B) and BF (C) were 8, 16 and 24 min, respectively.

The biofilters were backwashed approximately every 48 h to recover excessive head loss development within the filters beyond the capacity of the flow controllers, to ensure a constant hydraulic loading rate. The backwash procedures are described in **Appendix C**, and included combined compressed air and sub-fluidization water backwash to achieve collapse pulse conditions for 3 min to improve backwash efficiency (Amirtharajah, 1993). Afterwards, the bed was backwashed

only with water at 100% bed fluidization for 10 min to remove trapped particles within the bed. The backwash flow was then gradually reduced to stratify the bed after the end of the backwash. Details of the backwash procedure and its effect on biofilter performance are available elsewhere (Wilson, 2015).

5.3.2 Water and biofilter media sampling

Water samples were collected 24 h after the backwash in the middle of the filtration run. Raw water before the roughing filter, roughing filter effluent downstream of the feed pump, and BF (A), BF (B) and BF (C) effluent samples were collected in 1 L AOC clean glass bottles. The cleaning protocol for the sample bottles is described in detail in **Chapter 4**. The clean bottles were rinsed three times with the sample water before filling. The samples were transported and stored at 4ºC in the dark.

Media samples were collected right after collecting water samples. The biofilter feed line was turned off and the filter column was drained. Media sample ports (as described in **Chapter 3**) were used to collect media samples from the center of the column. A total of 30 cm^3 from each sample location were collected and stored as described in **Chapter 3 and Figure 3-1**. Media samples were collected at the interface between sand and anthracite (20 cm deep) in both BF (A) and BF (B) Sand and anthracite in these samples were separated using a stainless steel 2 mm sieve as described in **Chapter 3**. Media samples were also collected at the bottom of BF (B) (60 cm deep) at the top of the extension column of BF (C) (total of 85 cm deep). Media samples were stored at 4ºC in the dark for analysis.

5.3.3 Water quality analysis

Online sensors were used to monitor the water temperature, pH and turbidity of the biofilter influent and effluent water, as described in **Appendix C**. TOC was measured using unfiltered water samples, and samples for DOC were filtered using pre-rinsed 0.45 μm PES Supor ® membrane disc filters (Pall Corporation, USA). TOC and DOC samples were preserved at pH 2 using 85% phosphoric acid (Sigma Aldrich, USA) and stored at 4ºC, and analyzed within 3 days using a wet oxidation standard method using an Aurora 1030W TOC Analyzer (OI Analytical/Xylem Inc., USA). . The UV_{254} absorbance of 0.45 μm filtered water was determined in 1 cm path length quartz glass cuvettes using a Cary 300 UV-visible spectrophotometer (Agilent Technologies, Inc., USA). TOC, DOC and UV254 analysis were performed by fellow graduate student Jangchuk Tashi. AOC was determined as described in **Chapter 4** based on a new method employing a natural microbial community inoculum

and flow cytometry (Hammes and Egli, 2005). The yield of the natural bacterial inoculum in this experiment was 1 x 10^7 cells / µg C as acetate. Other methods used to characterize NOM in water (LC-OCD and FEEM) are described in section 3.5. The total planktonic cell count in water samples was done as described in **Chapter 4**, using a standard method for flow cytometry cell counting (SLMB, 2012) and a Partec Cube 6 flow cytometer (Partec NA, NJ, USA).

5.3.4 Attached Biomass Extraction and Analysis

The ATP content of the biomass attached to the media was measured using a commercial ENLITEN ATP kit as described in **Chapter 3**. EPS and cell extraction from the media was done using a cation exchange resin extraction protocol as described in **Chapter 3**. Cell concentrations were measure by flow cytometry as described in **Chapter 3**. EPS carbohydrates were determined using a phenol sulfuric acid method (DuBois et al., 1956), and proteins were measured with a bichronic acid method using the Pierce Micro-BCA Protein Kit (Fisher Scientific, USA), as described in **Chapter 3.**

5.3.5 NOM Characterization techniques

Fluorescence spectroscopy and LC-OCD analysis was used to characterize both the aquatic DOM composition and the biofilm EPS extract. Fluorescence spectroscopy was done using a Cary Eclipse Fluorescence Spectrophotometer (Agilent Technologies, USA). All measurements were done using quartz cuvettes with 10 mm path length and PMT voltage of 750 V. Water samples were filtered using 0.45 µm PES Supor ® membrane disc filters (Pall Corporation, USA) then measured. EPS samples were measured diluted in Milli-Q water to avoid having any saturated peaks in the protein like substances region. Fluorescence measurements were done by fellow graduate student Fei Chen and Dr. Monica Tudorancea, who then provided me with the raw data files. A typical FEEM plot of natural water is shown in **Figure S1** of the **Appendix D**, and a typical plot of extracted EPS is shown in **Figure 3-4** (**Chapter 3**). Each matrix included 301 individual emission intensity values (within the 300 – 600 nm emission range at 1 nm increment) at sequential 10 nm increments at excitation wavelengths between 250 nm and 380 nm. These range values were used in previous studies (Chen et al., 2014; Peldszus et al., 2011) to characterize natural organic matter in the same surface water source (Grand River) that was used to feed the biofilters. In the resulting FEEM plot, the humic acid-like substances response was measured at the excitation / emission pair of 270/460 nm (FEEM-C). The fulvic acid-like substances response (FEEM-B) was determined at the excitation / emission pair

of 320/415 nm. The protein-like substances response (FEEM-A) was determined at the excitation / emission pair of 280/330 nm, and it was used as an indicator of the protein content of the samples (Peiris et al., 2010).

LC–OCD (DOC-Labor Dr. Huber, Germany) analysis was done for extracted EPS as described in **Chapter 4** and for water samples as described in **Chapter 4**. A typical LC-OCD chromatogram for aquatic DOM is shown in **Figure S1** of **Appendix B**, and for extracted EPS is shown in **Figure 3-5** (**Chapter 3**). For the extracted EPS, the bulk EPS can be divided into three main fractions according to their apparent molecular weight as described in **Chapter 3**. For aquatic DOM, the bulk DOM is divided according to their molecular weight to several fractions as described by Huber and co-workers (2011) and explained in **Chapter 4**. Each fraction was integrated using ChromCALC commercial software (DOC-Labor Dr. Huber, Germany). LC-OCD measurements were done by Dr. Monica Tudorancea, who provided me with the raw data files for analysis.

5.4 Results and discussion

The pilot scale BF_{WP} testing facility was used to study the impact of three different biofilter EBCTs and water temperature on the biofilter media attached biomass and biofilter performance. Removal of BOM fractions within the three parallel filters was monitored using LC-OCD and fluorescence spectroscopy. A modified AOC method using flow cytometry was applied to monitor the removal of the primary substrate to determine the water biological stability after biofiltration.

5.4.1 Feed water quality

The biofilter feed water quality was monitored using different online sensors during the study period (August 2014 to March 2015). The data for turbidity, temperature and DOC are as shown in **Figure 5-1,** and the range of each parameter is shown in **Table 5-1**. Three different sampling events to assess the biofilter biomass and NOM removal were done in the period between early August to mid-September 2014, when the water temperature ranged between 20 ℃ and 23℃. One more sampling was done early October as the water temperature started to drop but was still relatively high at 17 ℃. During that warm temperature period, the turbidity ranged between 3 and 6 NTU with some spikes due to major rainfall events. To test the effect of low water temperature, three more sampling events were done between early December 2014 to mid-February 2015, as the water temperature ranged between 3 and 7 ℃. There was a major turbidity spike in late November due to a major snow melt.

Feed water DOC dropped from 6 to 5 mg C/L after the water temperature dropped to 5°C. Sampling was not done during the transition period between the high and low water temperatures (October to December), as the main objective was to assess the process performance at high temperatures during summer conditions and at low temperatures during winter conditions.

Table 5-1 Summary of the water quality parameters for the feed water within the two phases of the study at warm and cold water conditions

Parameter	Unit	Warm Water Condition (n=4)		Cold Water Condition (n=3)	
		MIN	MAX	MIN	MAX
Temperature	°C	17	23	2.3	6.9
Turbidity	NTU	2.6	9.7	1.2	9.9
TOC	mg C/L	5.7	7.0	5.1	7.4
DOC	mg C/L	5.9	6.8	5.1	7.2
UV254	cm^{-1}	0.181	0.218	0.133	0.145
LNA Bacteria	Cell/mL	1.9×10^6	3.0×10^6	1.4×10^6	2.1×10^6
HNA Bacteria	Cell/mL	1.0×10^6	1.7×10^6	7.6×10^5	1.1×10^6
Total Cell Count	Cell/mL	9.0×10^5	1.4×10^6	6.2×10^5	9.4×10^5
AOC	µg C/L	181	237	147	238
Biopolymers OC	µg C/L	482	525	309	435
Biopolymers ON	µg N/L	41	106	21	34
Humics OC	µg C/L	2856	4608	3047	4151
BB OC	µg C/L	754	957	609	913
LMWA OC	µg C/L	156	267	122	172
LMWN	µg C/L	453	575	505	546
FEEM Protein-Like Response	I.U	47.8	52	41.3	50.8
FEEM Humic Acid-Like Response	I.U	321	381	288	360
FEEM Fulvic Acid-Like Response	I.U	325	428	337	418
Total Phosphorus [a]	mg P/L	0.025	0.047	0.031	0.093
Ortho – Phosphate [a]	mg P/L	0.009	0.049	0.02	0.051
Ammonia / Ammonium [a]	mg N/L	0.1	0.1	0.11	0.581
Nitrate [a]	mg N/L	1.33	2.5	2.93	4.82
Alkalinity [a] (as $CaCO_3$)	mg /L	193	254	249	286
Hardness [a] (as $CaCO_3$)	mg/L	241	287	287	327
Total Dissolved Solids [a]	mg/L	308	379	369	454

[a] These parameters were provided by the Regional Municipality of Waterloo as measured by the treatment plant staff

Exact Sampling Dates (Temperature)

August 07, 2014 (22.7°C), August 21, 2014 (21°C), September 11, 2014 (21°C), October 02, 2014 (18.4°C), December 04, 2014 (6.7°C), January 29, 2015 (2.8°C) and February 16, 2015 (2.8°C)
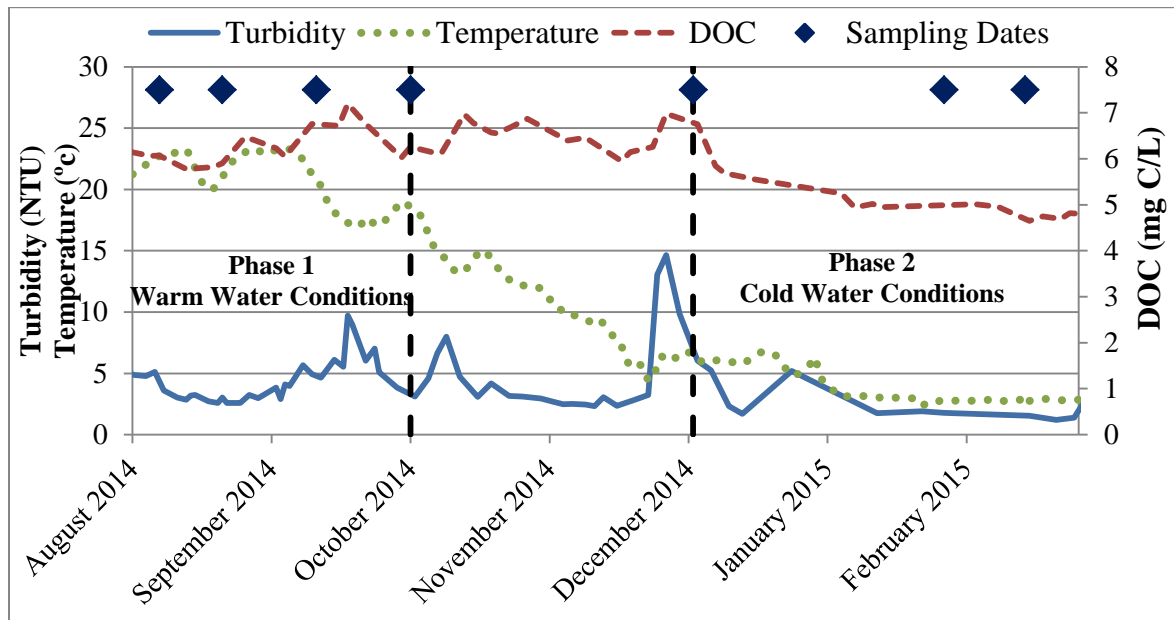
Figure 5-1 Feed water quality over the study period and the different sampling dates

5.4.2 Biofilter Biomass Trends

5.4.2.1 Biomass Activity and Biofilm Cell Count

ATP has been recently used as a monitoring parameter for the activity and amount of attached biofilter biomass as it has been directly correlated with cell count (Evans et al., 2013a; Magic-Knezev and van der Kooij, 2004). Another biomass parameter is the biofilm cell count, which is a direct measure of the attached biomass. Flow cytometry is a more recent tool to perform a true volumetric cell count for the biofilm bacteria, as explained earlier in **Chapter 3.** A sample of the density plots obtained for biofilter feed and effluent water and biomass samples is shown on **Figure 5-2**. Prior to sampling the biofilter media, the pilot plant was in operation for four months (April to August 2014) to acclimate the media. In addition, before pilot plant start-up, the biofilter media was pre-acclimated in upflow reactors for 6 months using the same feed water at a very low flow rate to allow bacteria to colonize the media surface and initiate biofilm growth. Details of the pre-acclimation process are described elsewhere (Wilson, 2015). Therefore, it was expected that the biofilter operational period before the study began was long enough to fully acclimate the biofilters before doing any water or media sampling. However, the measured bulk media ATP content was found to increase at each

sample depth over the course of the study, as shown in **Figure 5-3-a**. As described in **Chapter 3**, media samples taken from 20 cm depth in both biofilter A and B were collected from the intermixing zone, and sand and anthracite particles in these samples were separated by sieving and analyzed separately. Based on ATP data, sand was found to have more biomass per unit volume compared to anthracite when they are sampled at the same depth within the filters. This is attributed to the larger specific surface area of sand compared to anthracite which allowed more sites for biomass attachment. Biofilm cell count results had more variability compared with ATP, but in general it also had an increasing trend over time as shown in **Figure 5-3-b**. This can indicate that the attached biofilm on the biofilter media was still in the growth phase. Bulk media ATP increased linearly regardless of water temperature over the study period of 7 months (11 months after pilot plant start-up) as shown in **Figure 5-4-a,** but this trend was more pronounced in samples collected from the top of the filter compared with those at the bottom. For 16 different full scale biofiltration facilities, ATP values ranging from 100 to 10,000 ng ATP / cm^3 media were measured depending on the feed water quality, biofilm age and the used biofilter pre-treatment (Evans et al., 2013a; Pharand et al., 2014). The reported ATP values in this study are in this range and the attached biofilm has not yet reached its maximum or steady state ATP levels or biofilm cell count. Interestingly, even with the large drop in water temperature in the last three sampling events (i.e. T<7ºC), the biofilm bulk ATP content and cell count were noticeably higher than the samplings done during warm water conditions (i.e. T>17ºC).
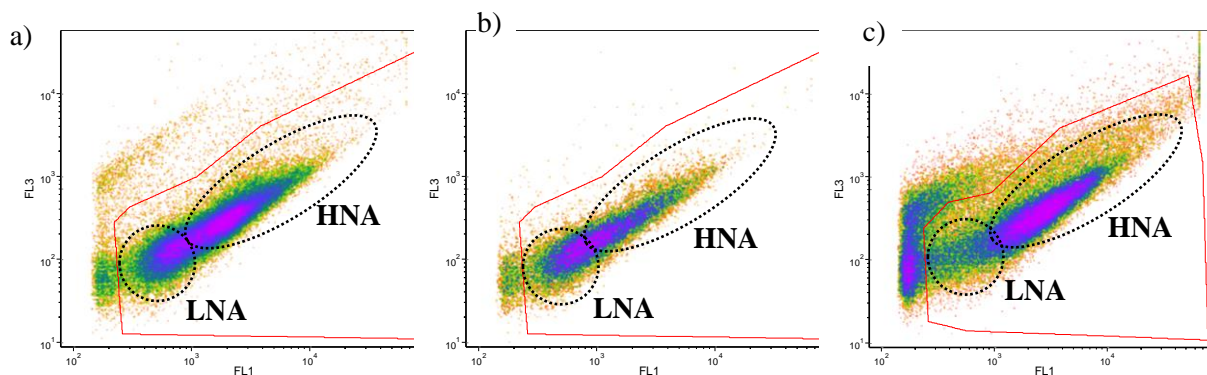
Figure 5-2 Typical density plot of green fluorescence (FL1) and red fluorescence (FL3) and the used electronic gate for raw river water (a), biofilter effluent (b), and extracted biofilm bacteria (c) showing LNA bacteria and HNA bacteria regions
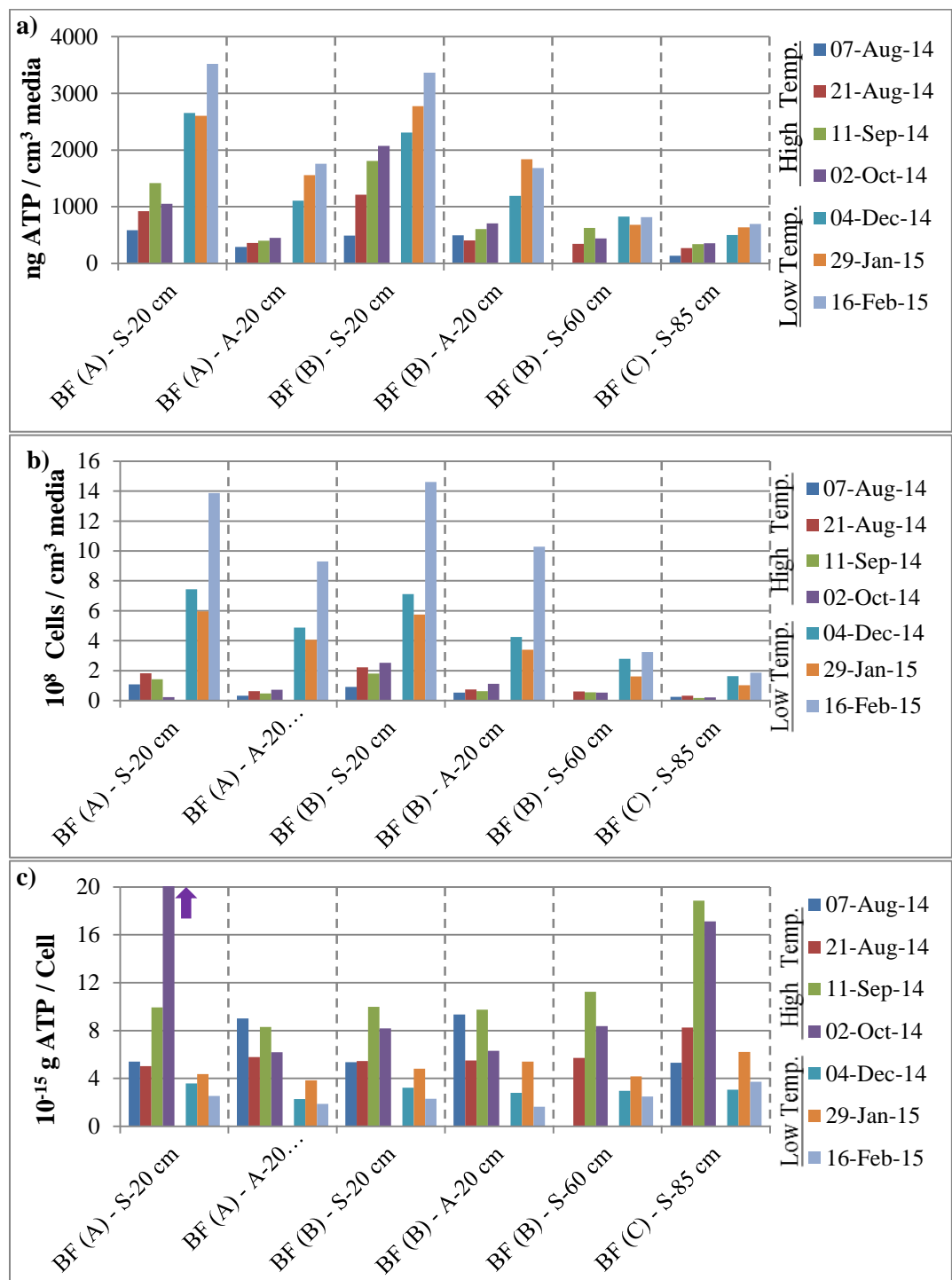
Figure 5-3 Attached biofilter biomass characterization over the study period; (a) ATP content , (b) biofilm cell count and (c) cellular ATP content
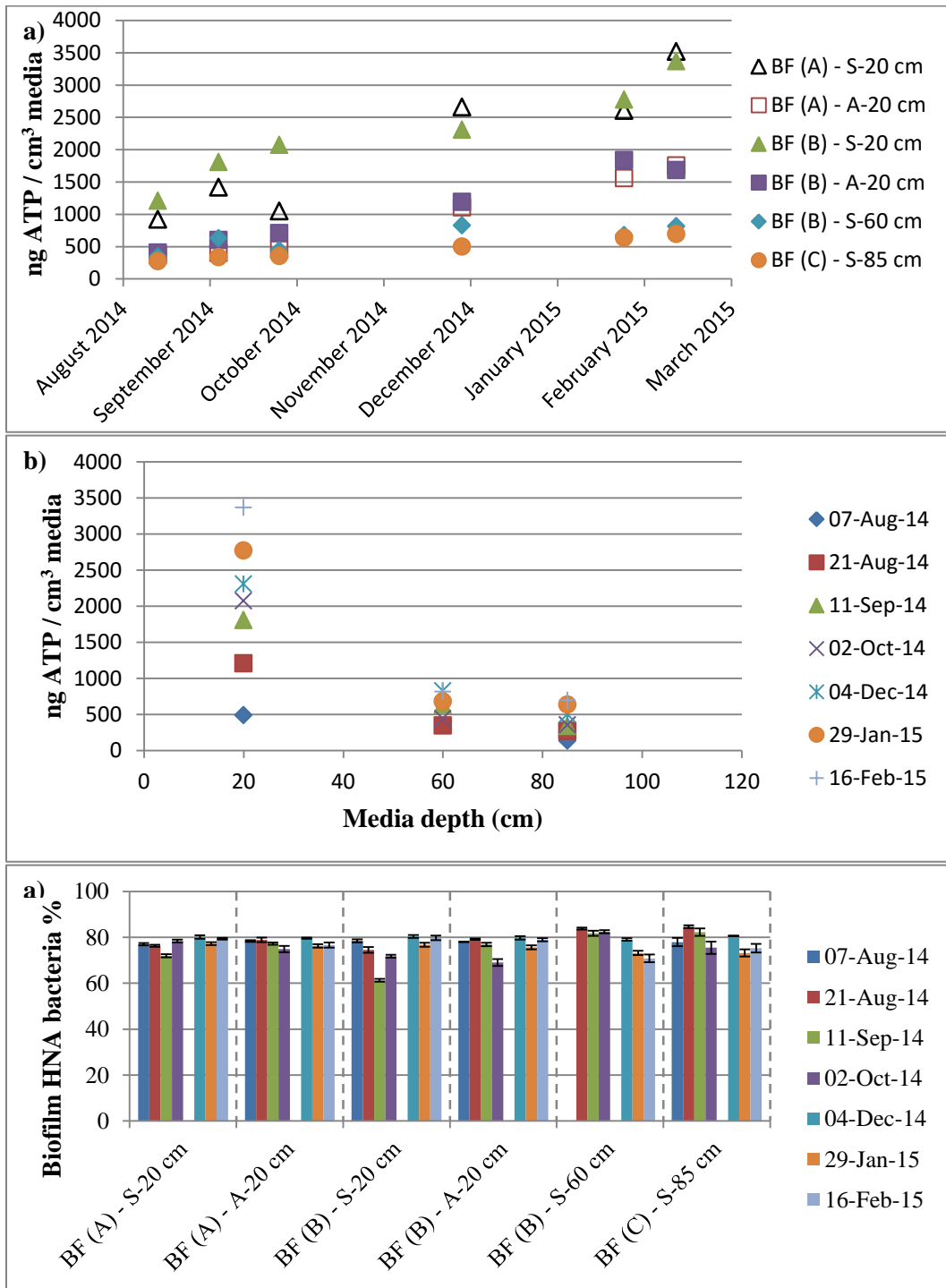
Figure 5-4 Bulk media (a) ATP, (b) ATP profiles over the depth of BF (B) and BF (C), and (c) percent of HNA bacteria in the biofilm flow cytometry population over the study period

Another possible effect of water temperature on the biofilter biomass is the possible change in the composition of the biofilm microbial community as reported in literature (Moll et al., 1999) or any possible changes in the nutrient levels or composition in the biofilter feed water. Flow cytometry can provide various descriptors for the bacterial population. As described in **Chapter 3**, flow cytometry is able to separate the microbial population detected into HNA and LNA groups. Using the technique, one descriptor that can assess the microbial community is the ratio of HNA and LNA bacteria. The ratio of HNA bacteria compared with the total cell count determined using flow cytometry was stable at 80% over the study period as shown in **Figure 5-4-c** regardless of the temperature change, and HNA bacteria seem to be the major fraction in the bacterial biofilms.

Results for BF (A) and BF (B) obtained at 20 cm bed depth showed similar ATP values and trends (**Figure 5-4-a)** between the sand and anthracite media samples. Biofilm cell counts between the two filters were also similar as shown in **Figure 5-3-b**. This indicates that the two filters are suitable to study the effect of the biofilter EBCT on biofilter performance, as both filters have the same feed water along with similar biomass distributions. Biofilm biomass was also assessed over the depth of biofilter B and C. The data shows that the biofilter media ATP declined exponentially ($R^2 > 0.9$) over the depth of BF (B) and BF (C) (n=3) as shown in **Figure 5-4-b** indicating a possible first order decay of biomass over the biofilter depth. According to the observed exponential decay of biomass over the biofilter depth, the total biomass expressed as cell count existing within the first 40 cm of the bed (i.e. 0 to 40 cm deep) would be approximately 3.3 times higher than the next 40 cm of the bed (i.e. 40 to 80 cm deep) and nearly 11 times higher than the last 40 cm of the bed (i.e. 80 to 120 cm). A similar trend was reported for the same biofilters during their acclimation period as shown in **Chapter 3.** Also, these results are similar to those in the literature for biofilter media ATP (Velten et al., 2011) or biomass phospholipids (Urfer and Huck, 2001) probably due to a nutrient gradient over the biofilter depth.

The average cellular ATP content was also calculated by dividing the bulk media ATP by the total cell count for each sample, and results are shown in **Figure 5-3-c**. It is clear that regardless of the overall increase over time in bulk media ATP or biofilm cell count, the average cellular ATP content in the low water temperature conditions is significantly lower than the values during high water temperature conditions (unpaired t-test, α=5%) for most of the media sampling ports as shown on **Table S3** in **Appendix D**. The BF (A) sand sample obtained on October 2014 was an outlier possibly due to a problem with the EPS extraction process as a very low cell count was observed for that

sample compared to previous samples at the same sampling port. Cellular ATP content is an important parameter to determine the state of the bacterial cells. Cellular ATP is known to increase rapidly during the exponential growth phase of bacterial cells until it reaches a maximum during the stationary phase, and then it starts dropping when the cells reach the decay phase (Martin et al., 1980). ATP molecules are the energy currency for all bacterial cells as they provide the energy supply for cellular enzymatic activities and other cell activities, including being a precursor for ribonucleic acid (RNA) synthesis (Schneider and Gourse, 2004). This indicates the importance of monitoring this value. Cellular ATP values of Enterobacter aerogenes bacteria were also reported to be affected by low temperature (<5℃) when stored in glucose mineral solution or in skimmed milk (Theron et al., 1987). This observed drop in cellular ATP content with lower water temperatures may be attributed to a drop in cellular activities or the state of the bacterial biofilm as it is reaching the decay phase. The latter is less likely as the biofilm cell count was still increasing as shown earlier. The change in cell activity might be a more reasonable explanation as low water temperature conditions in drinking water biofilters were reported to affect the activity of the attached biomass as measured by the hydrolase enzyme activity method (Le Bihan and Lessard, 2000) or the glucose respiration method (Laurent et al., 1999) which would limit the degradation of organic molecule.

5.4.2.2 Biofilm EPS Composition

The total protein and carbohydrates content of the EPS (**Figures 5-5-a, 5-5-b**) did not show a continuous increase over time similar to ATP or biofilm cell count. Instead, both proteins and carbohydrates levels on media taken from all of the sampling ports were highly dependent on the water temperature except for the samples collected deeper in BF (B) (i.e. 60 cm depth) and BF (C) (i.e. 85 cm depth). During either the warm or cold water temperature phases, the EPS proteins or carbohydrates were relatively stable on media collected at each location in the biofilters. Also, the average EPS protein and carbohydrates content at cold water temperatures were significantly higher than the values at warm water temperatures. Previous studies have also reported that low water temperatures enhanced bulk biofilm EPS production for lactic acid bacteria (Degeest et al., 2001) and a marine *Pseudoalteromonas* isolate (Nichols et al., 2005). Increased EPS carbohydrate levels in biofilters were linked to increased filter bed head loss (Evans et al., 2013a), however, this was not linked to changes in biofilter performance.
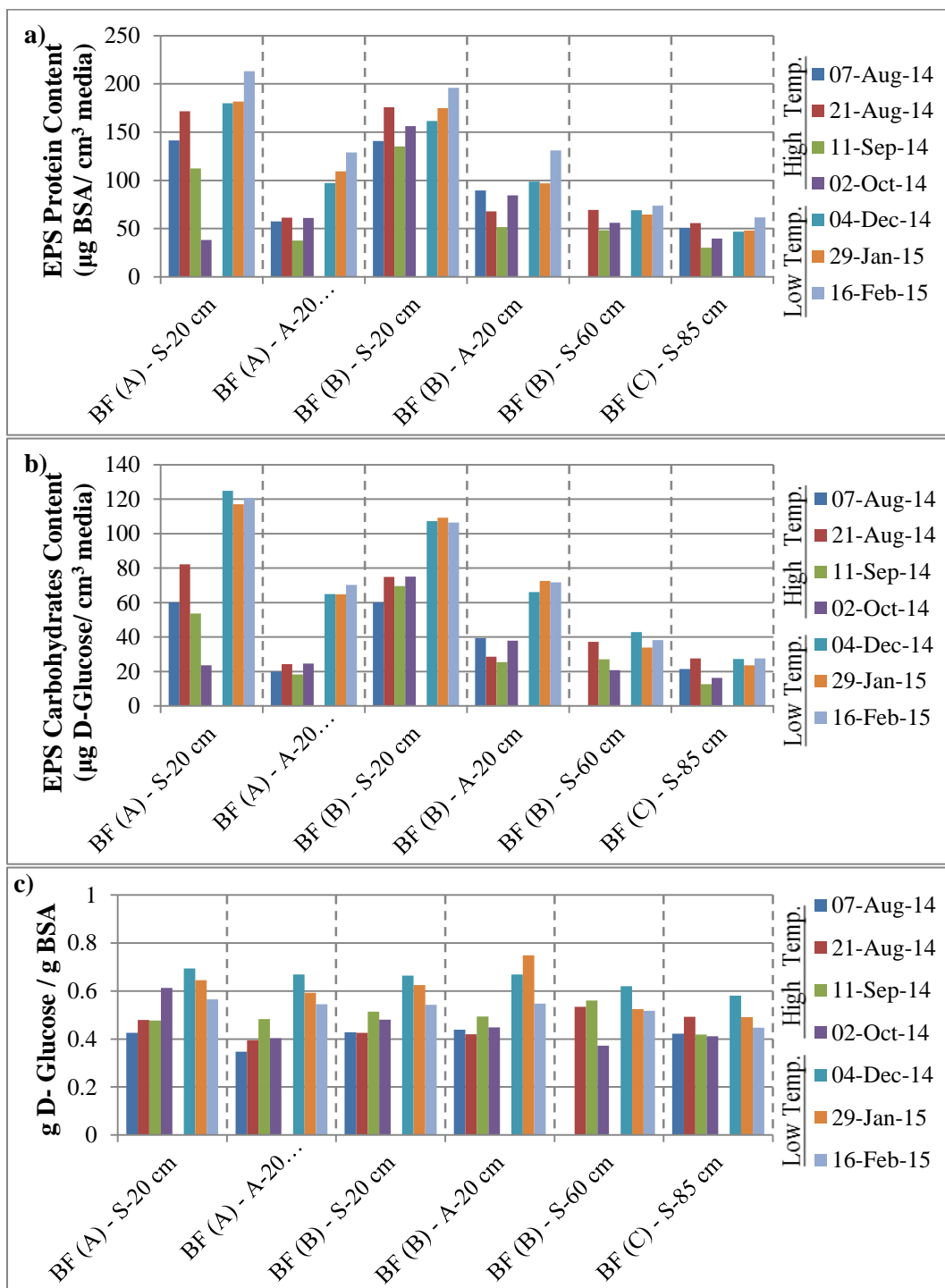
Figure 5-5 Characterization of the extracted EPS over the study period; (a) total protein content, (b) total carbohydrate content and (c) the ratio of carbohydrates to protein
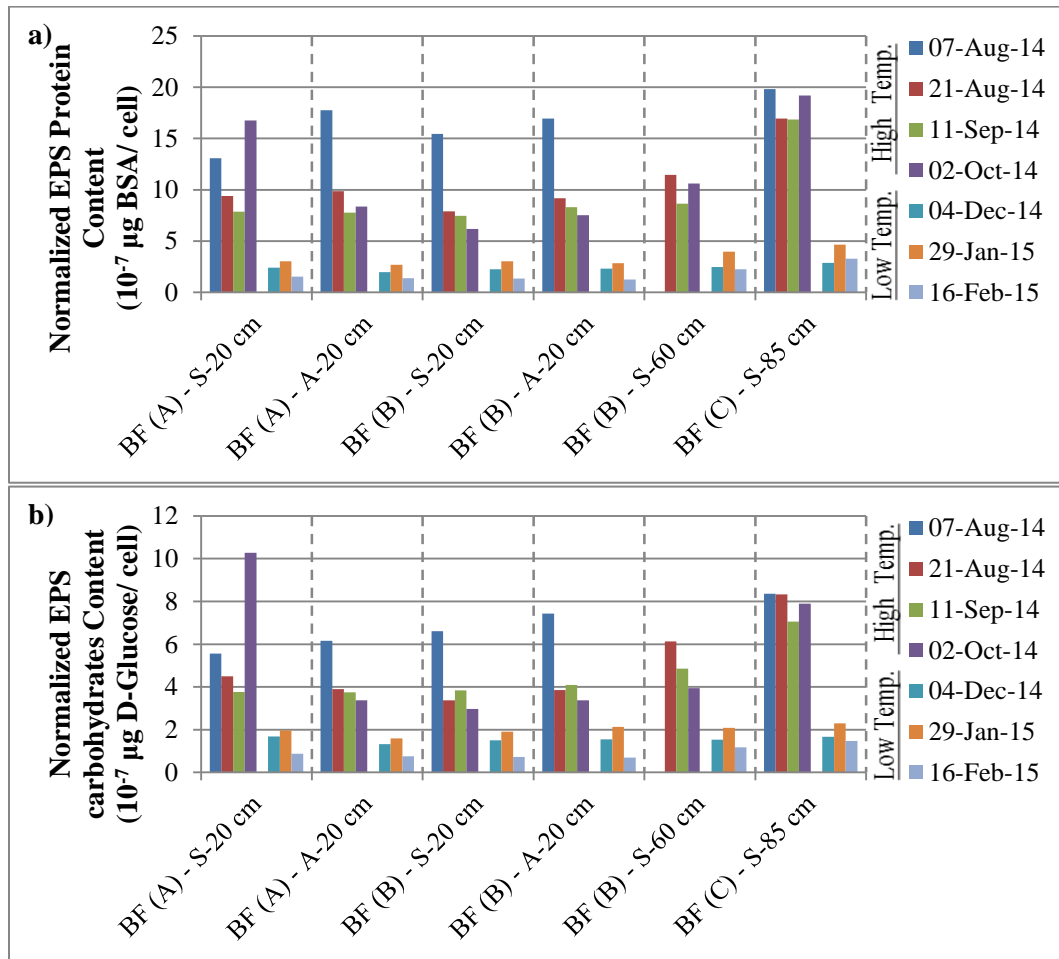
Figure 5-6 Specific EPS (a) protein and (b) carbohydrates production for biofilm bacteria

The EPS data can also be studied by observing the carbohydrate to protein ratio as shown in **Figure 5-5-c,** which was significantly higher during cold water conditions (unpaired t-test, α=5%) as shown on **Table S3** in **Appendix D**. Nichols and co-workers (2005) also found that the polysaccharides content of the EPS was higher at low water temperatures. A possible explanation for the relative increase in EPS carbohydrates production compared to proteins is the reduction of nutrients, as was reported for attached biofilms in a soil media (Leon Morales et al., 2007). However, this explanation does not seem likely since the AOC and inorganic nutrient levels remained high in the biofilter feed water during the cold water conditions, as shown in **Table 5-1**. If the biofilm cell count is used to normalize the observed carbohydrates and protein content as shown in **Figure 5-6-a and Figure 5-6-b**, the specific EPS protein and carbohydrate content per cell was significantly lower during the cold

water conditions (unpaired t-test, $\alpha=5\%$) as shown on **Table S3** in **Appendix D**. Michalowski (2012) also observed different trends for bulk EPS protein or carbohydrates and their normalized values per cell for drinking water biofilms. This was attributed to changes in gene expressions of biofilm cells due to biofilm maturation or changes in substrate utilization preference which affected the biofilm hydrolytic enzyme activity. Similar results were reported for pure strain biofilms (Sauer and Camper, 2001; Sauer et al., 2002). Based on this, the observed drop in EPS proteins and carbohydrates per cell during the cold water temperature can be attributed to changes in the biofilm enzyme activity which is in agreement with the drop in cellular ATP content show on **Figure 5-3-c**.

For the data collected within each sample date, both EPS proteins and carbohydrates content had a decreasing trend over the biofilter depth, similar to the biofilm ATP content results (**Figure 5-4-b**). This was expected, since it was previously shown that there was a high correlation among the different components of the biofilm matrix as discussed in **Chapter 3**. Additionally, sand samples had significantly higher EPS total proteins and carbohydrates content compared with the anthracite samples, again similar to the ATP or cell count data, which was attributed the higher specific surface area of sand compared to anthracite.

LC-OCD analysis was used to further characterize the carbon content of the extracted biofilm EPS, by fractionation of the EPS pool of molecules into three sub-groups based on their molecular weight (high, intermediate and low MW fractions defined here as HMW EPS, IMW EPS and LMW EPS respectively) as described in **Chapter 3**. Fluorescence spectroscopy was also used to study the nature of the EPS molecules, also as described in **Chapter 3**. EPS total organic carbon content measured by LC-OCD (sum of all MW fractions) (**Figure 5-7-a)** and EPS protein-like FEEM response (**Figure 5-7-b)** were slightly higher during the cold water conditions compared to the warm water condition, which is in agreement with the results of the EPS total carbohydrates and proteins data measured using colorimetric methods as shown in **Figure 5-5**. Also, the EPS total organic carbon content and FEEM protein-like response had a declining trend over the depth of the biofilter, and both were higher on sand compared with anthracite media (**Figure 5-7-a, 5-7-b**), again similar to the total carbohydrates and protein data in **Figure 5-5**.
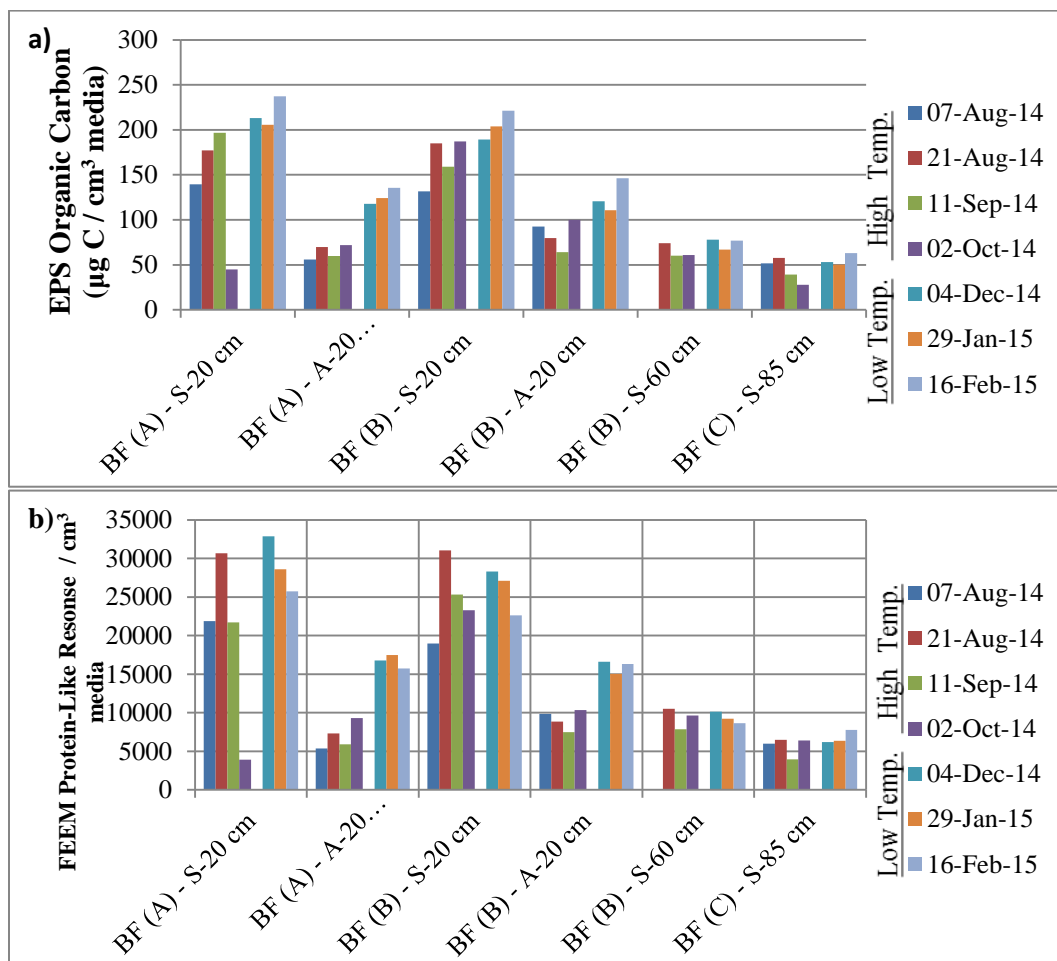
Figure 5-7 LC-OCD measured (a) total organic carbon of the extracted EPS and (b) FEEM protein-like substances response

For the HMW EPS (> 13 kDa) fraction, the organic carbon content remained relatively stable both in warm and cold water temperature conditions as shown in **Figures 5-8-a** (with data for each sample shown in **Figure S-2b** in **Appendix D**) regardless of the increase in EPS total organic carbon content. Since the LC-OCD can measure both organic carbon and nitrogen compounds, the C/N ratio could also be determined for each fraction (as described in **Chapter 3**). Results showed that the carbon to nitrogen ratio of the HMW fraction was also found to be stable at 3.66 ± 0.52 g C/g N (n=41) in samples collected over both warm and cold water conditions as shown on **Figures 5-8-b** (with data for each sample shown in **Figure S-2c** in **Appendix D**). This supports the results in **Chapter 3**, where this fraction was linked to EPS total protein content and was assumed to include extracellular

bacterial enzymes. In contrast, both IMW EPS (2 to 13 kDa) and LMW EPS (< 2 kDa) fractions significantly increased in cold water temperature conditions compared to warm water conditions as shown in **Figure 5-8-a** and **Figures S-3a, 4a** in **Appendix D**, which would explain the overall increase in the total EPS organic carbon content. Similar the HMW fraction, there was no significant different in the C/N ratio of the IMW fraction between warm and cold temperature conditions. The C/N ratio could not be measure for the LMW fraction because as inorganic nitrogen species interfere with this fraction as they elute at a similar time window. The increase in IMW EPS was also accompanied by an increase in the humic acid-like and fulvic acid-like FEEM responses observed using fluorescence spectroscopy as shown on **Figures 5-9-a, 5-9-b**. Also aquatic humic-like substances in the river water elute at a similar time window to the IMW EPS explained in **Chapter 3** so the observed increase in IMW EPS OC can be attributed to an increase in humic substances. Humic substances, are highly aromatic organic molecules with low biodegradability (Flemming and Wingender, 2010). They are the main contributor to the allochthonous NOM in surface waters, which can be incorporated within the biofilm through adsorption (Jahn and Nielsen, 1998; Nielsen et al., 1997) or they can be formed within bacterial biofilms due to enzymatic degradation and repolymerization of plant matter (Wingender et al., 1999b). The observed increase in humic substances could possibly be attributed to their lower degradation in the cold water condition so they start accumulating within the biofilm or this can be attributed to changes in the biofilm EPS but no information is available in literature regarding the presence and role of humic substances in the EPS matrix of attached biofilter biomass.
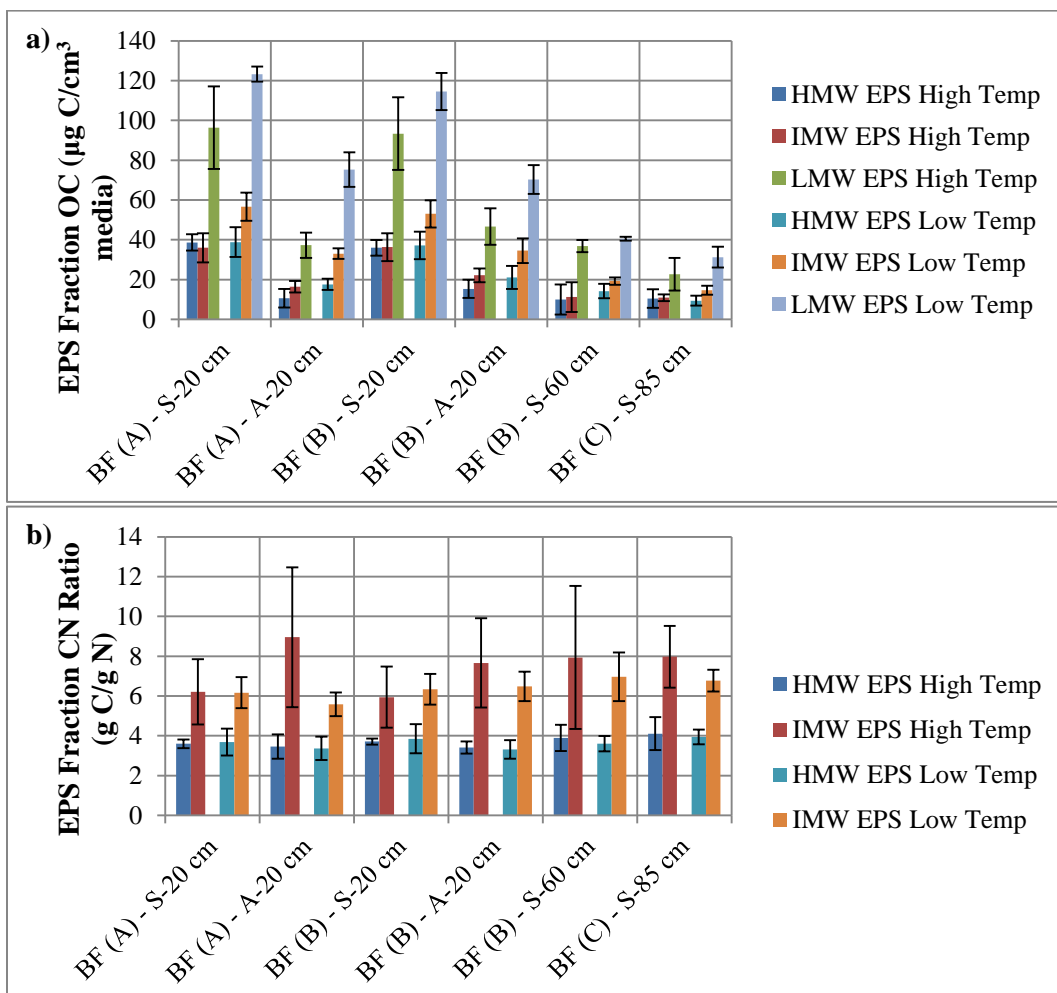
Figure 5-8 Average (a) organic carbon content of the LC-OCD defined HMW, IMW and LMW EPS fractions and (b) carbon to nitrogen ratio of HMW and IMW EPS fractions with errors bars showing standard deviation (n = 4 for high water temperature samplings, n=3 for low water temperature samplings).
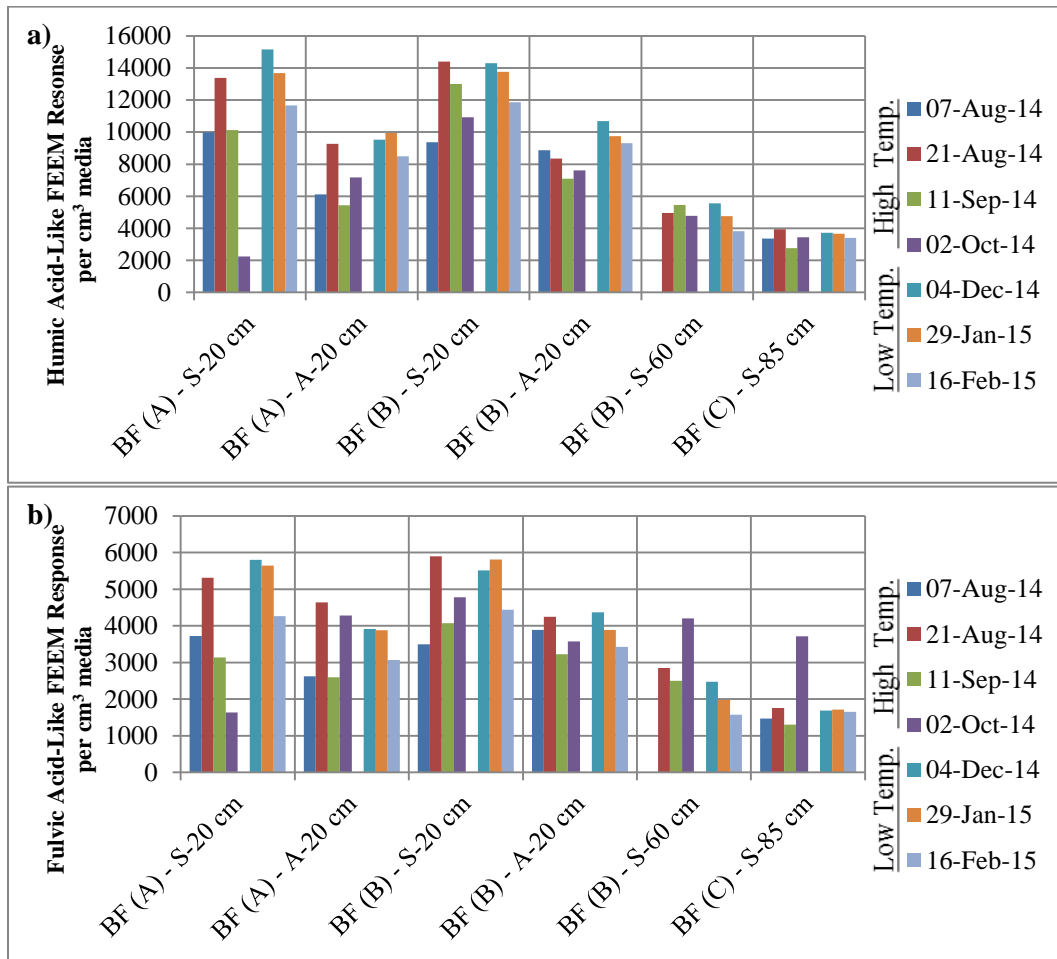
Figure 5-9 Extracted biofilm EPS (a) humic acid-like FEEM response, (b) fulvic acid-like FEEM response over the study period

5.4.3 Biofilter Performance

The biofilter performance in removing certain parameters of importance for downstream treatment units and water quality was determined. Net cell removal was measured to determine biomass loading on subsequent treatment units. A second parameter measured was AOC, which is representative of the ability of biofilters to remove easily biodegradable compounds and improve the biological stability of the finished water as a biofouling control strategy. DOC was also used as an indicator of the bulk NOM removal which is commonly used in the literature. Among the different NOM fractions, the high molecular weight biopolymers fraction and FEEM protein-like substances response were used as performance indicators, as they have been linked to both low pressure membrane

106

fouling (e.g. Chen et al., 2014) and biofouling (Villacorte et al., 2009). Humic-like substances measured using LC-OCD, and humic acid-like or fulvic acid-like FEEM responses were also used as performance indicators, and although they are expected to be less removed within the biofilters, humic substances have been linked to DBP formation (e.g. Zheng et al., 2015) and membrane organic fouling, especially in the presence of divalent cations (Hong and Elimelech, 1997; Katsoufidou et al., 2005). Low molecular weight compounds such as organic acids or neutral compounds were of lesser importance in the BF_{wp} used in this study and low molecular weight acids were expected to be primarily consumed in the river by fresh water bacteria as shown in **Chapter 4**.

5.4.3.1 Net Reduction of Bacterial Cells

The three biofilters BF (A), BF (B) and BF (C) had a design EBCT of 8, 16 and 24 min, respectively. Flow cytometry was used to measure the total cell count in the feed and effluent of each filter. Total cell count was also divided into LNA and HNA bacteria as discussed in **Chapter 4,** to understand if net reduction of those two sub-populations will change due to the seasonal change in the fresh water microbial community or due to the water temperature. Net reductions of total cell counts through the three biofilters are shown in **Figure 5-10-a**. The observed cell reduction is the net product of the removal of planktonic cells and the release of any microbial cells from the biofilter attached biomass or biofilm detachment. The three biofilters achieved between 50% to 70% removal of the total cell count during the warm water conditions. Increasing the EBCT from 8 to 24 min improved the removal of microbial cells by 10 to 15 percentage points. The majority of the cells were likely trapped in the top part of the biofilter, since BF (A) removed nearly 55% of the feed water total cell count, and the additional bed depth in either BF (B) or BF (C) improved removals by only 6 and 11 percentage points, respectively. No significant differences were observed between BF (A) and BF (B) However BF (C) provided significantly higher net cell reduction (paired t-test, α=5%) as shown in **Table S1** in **Appendix D**. That would indicate that the removal of bacterial cells is not the same over the biofilter depth. The removed cells can represent a continuous supply of fresh cells to the bacterial biofilm on the media. HNA bacteria were better removed than LNA bacteria as shown on **Figures 5-10-b** and **5-10-c**. HNA bacteria were reduced by 64% to 75%, while LNA bacteria were reduced by 45 to 57% within the three biofilters. HNA bacteria are reported to have a larger cell volume than LNA bacteria (Wang et al., 2007), so they are expected to be better removed by the filter. HNA

bacteria were found to represent nearly 80% of the biofilm cell count as shown on **Figure 5-4-c** and explained earlier in this Chapter in the section 5.4.2.

During cold water conditions below 7ºC, the observed net cell reduction dropped significantly (unpaired t-test, $\alpha=5\%$) as shown in **Table S2** in **Appendix D**. Net cell reduction ranged from 11% to 35% with no effect of EBCT. Hallé (2009) reported a similar decrease in total cell count removal at low temperatures within dual media biofilters, however HPC removal was not affected .Interestingly, the total cell count of the EPS attached to the filter media was higher at cold temperatures (**Figure 5-3**), which suggests that cell transfer and attachment to the media was not responsible for the seasonal different in cell removal. The LNA fraction of the bacterial community was more affected by the temperature drop than the HNA fraction as shown on **Figure 5-10-b** and **5-10-c**. The average removal of LNA bacteria dropped by nearly 30 to 50% as the water temperature dropped, while HNA bacteria removal dropped by only 25 to 40%. The drop in water temperature did not only affect the overall total cell count net removal but also affected the composition of the effluent water population by affecting its HNA and LNA fractions in different ways.
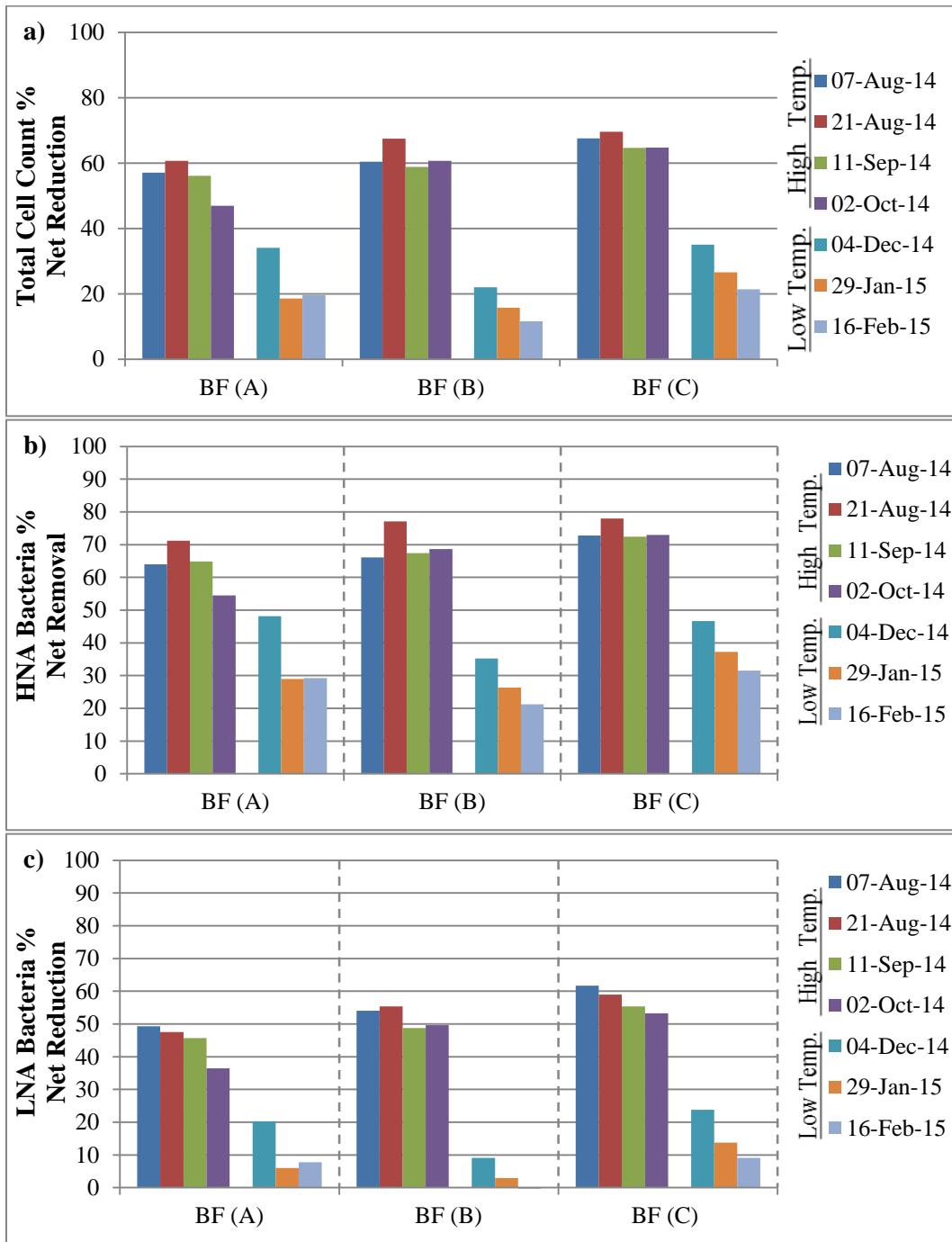
Figure 5-10 Performance of the different biofilters over the study period; (a) total cell count percent reduction, (b) HNA Bacteria percent reduction and (c) LNA Bacteria percent reduction

5.4.3.2 DOC Removal

DOC removal can be used as an indicator for the removal of bulk NOM within the biofilters; however the BF_{WP} system used in the current study is expected to attain lower DOC removal compared to conventional biofilters preceded with clarification and ozonation as a pre-treatment. The observed DOC removals (**Figure 5-11-a**) show that at warm water temperatures, DOC removals ranged from 10% to 20% for the three filters. BF (B) with a 16 min EBCT had approximately a 3 percentage point increase in DOC removal over BF (A) with an 8 min EBCT. BF (C) with the additional 8 min EBCT had a 3 percentage point higher DOC removal than BF (B). The three filters were significantly different than each other (paired t-test, α=5%) as shown in **Table S1** in **Appendix D**. This observed DOC consumption profile is due to the nature of the biofilter as a plug flow packed bed bioreactor, where the organic substrate is controlling the degradation of the organic matter (Huck and Sozański, 2008). BOM removal within biofilters is believed to be a first order model which explains this smaller increase in DOC removal with increasing EBCT (Huck et al., 1994; Urfer et al., 1997). Additionally, the stable DOC removal throughout a season indicated that the biofilters were operating at steady state regardless of the observed linear increase in bulk media ATP or biofilm cell counts shown on **Figures 5-3-a** and **5-3-b**. This shows that DOC removal was not affected by the increase in attached biofilter biomass. Therefore, an increase in ATP or biofilm cell count beyond a certain optimal level would not have a direct relationship to biofilter performance in terms of DOC removal. Earlier studies on conventional biofilters should than only a minimum amount of biomass is needed to achieve a stable biomass removal within the biofilters (Urfer et al., 1997; Wang et al., 1995).

As the water temperature dropped below 7ºC, the observed DOC removal significantly dropped and ranged between 6% and 8% (unpaired t-test, α=5%) as shown in **Table S2** in **Appendix D**, which is nearly half of the observed removal at warm water temperatures. At cold temperatures, doubling the biofilter EBCT in BF (B) compared to BF (A) increased DOC removal by nearly 1%, and a similar increase was observed in BF(C) compared to BF (B). Several other studies also reported lower DOC removal at lower temperature ranges (Evans et al., 2013a; Fonseca et al., 2001; Huck, 2000; Laurent et al., 1999). The observed drop in DOC removal at low water temperatures may be attributed to lower enzyme activity and mass transport limitations at low water temperatures, as has been reported by (Urfer et al., 1997). The observed DOC removal by each of the three filters was stable within the cold or warm sample phase, which indicates that the biofilters microbial communities rapidly adapted to the cold water temperature. In summary, biofilter EBCT increase beyond 8 min was not beneficial

at either at low or high water temperature, as it yielded only a small increase in DOC removal. The studied biofilters were still able to remove DOC below 7ºC, but the observed removal was less than half of its value at high water temperatures above 17ºC.
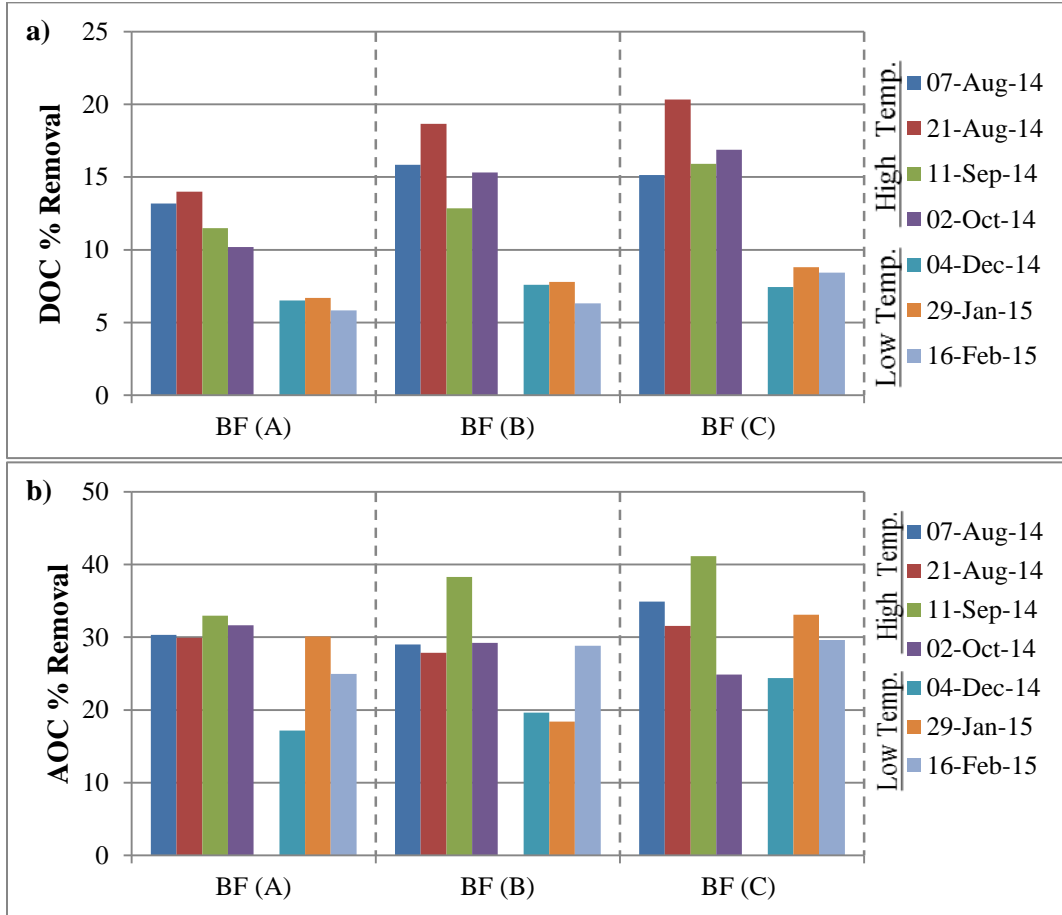
Figure 5-11 Performance of the different biofilters over the study period; (a) DOC percent removal and (b) AOC percent removal

5.4.3.3 AOC Removal

AOC is assumed to measure the easily biodegradable NOM fraction which can be utilized by bacterial cells for regrowth purposes, which makes it a significant parameter to study water biological stability (Huck, 1990). AOC has been found to be efficiently reduced in conventional biofilters, mainly after the spike in AOC concentration following ozonation (Evans et al., 2013a; Huck, 2000; Pharand et al., 2015; Wang et al., 1995). The removal of AOC within the biofilters in the current

study is shown in **Figure 5-11-b**. During warm water temperature conditions, AOC removal was quite stable for all three biofilters and nearly 30% AOC removal was obtained. BF (A) and BF (B) both had an average removal of 31% over the four sampling events at warm water conditions compared to 33% for BF (C). The three biofilters were therefore operating at steady state conditions as can be determined using both AOC and DOC removals. Biofilter EBCT did not seem to affect the AOC removal at the EBCT range used in the current study as no significant differences were observed among the three filters (paired t-test, $\alpha=5\%$) as shown in **Table S1** in **Appendix D**. According to the first order kinetic model for AOC removal within drinking water biofilters developed by Zhang and Huck (1996a, 1996b), AOC removal would vary greatly at relatively short EBCTs as interpreted by the dimensionless EBCT used in that model but for higher EBCTs such as the ones used in the current study; minor differences in AOC removals among the used filters would be expected. During cold water conditions, AOC removal dropped slightly with the studied biofilters (**Figure 5-11-b**) as no statically significant differences were observed for any of the studied filters (unpaired t-test, $\alpha=5\%$) as shown in **Table S2** in **Appendix D**. BF (A) and BF (B) had average AOC removal of 23%, which was only 8percentage points lower than warm water removal values. BF (C) which had an average removal of 29%, which was 4 percentage points lower than warm water conditions. Both BF (A) and BF (B) had a higher drop in AOC removal at cold temperatures compared to BF (C), showing that BF (C), which had the longest EBCT of 24 min, was the least affected by the temperature change. This shows that the advantage of a longer EBCT is that AOC removal can be kept at its maximum value even during seasonal temperature changes. Similar conclusions were found for conventional biofilters by other studies (Prévost et al., 1992, 2005, 1990).

5.4.3.4 Net Removal of NOM fractions

Size exclusion chromatography and fluorescence spectroscopy were also used as more advanced techniques to study the removal of specific NOM fractions and to better characterize the observed removal of the bulk DOC. By using those advanced techniques, more information will be available to determine how direct biofiltration can be used as a pre-treatment for other treatment technologies such as low and high pressure membrane filtration.

5.4.3.4.1 Net Removal of High Molecular Weight Biopolymers and Protein-like substances

The large molecular weight fraction of the NOM, commonly described as biopolymers, includes different types of molecules such as polysaccharides and proteins (Huber et al., 2011). Biopolymers play an important role in drinking water treatment and especially for membrane filtration applications. Biopolymers are reported to be a major foulant for low pressure membranes (e.g. Chen et al., 2014; Hallé et al., 2009; Peldszus et al., 2011). Also biopolymers were found to be linked to TEP (Villacorte et al., 2009) which are believed to contribute to high pressure membrane biofouling (Bar-Zeev et al., 2015).

Biopolymers concentration in the biofilter feed water ranged between 0.31 and 0.53 mg C/L (average concentration 0.45 mg C/L), and was 7.3% of the DOC in the water (**Table 5-1**). The average biopolymers concentration during cold water conditions was 0.36 mg C/L and this is significantly lower than the average biopolymer concentration during warm water conditions of 0.51 mg C/L which can be attributed to increased bacterial activity with the river during warm water conditions. This seasonal effect of biopolymers concentration in the Grand River water previously shown by (Croft, 2012; Pharand et al., 2015). The removal of the biopolymer fraction as determined by LC-OCD using both organic carbon and organic nitrogen detection are shown on **Figures 5-12-a**, 5-**12-b**. During warm water temperatures, biopolymers OC and ON removal were high at above 50% for all three biofilters, indicating that biopolymers were highly biodegradable (**Figure 5-12-a and 5-12-b**). Biopolymer removal by the three filters were significantly different than each other (paired t-test, α=5%) as shown in **Table S1** in **Appendix D**. A similar conclusion was reported previously in **Chapter 4** and in the literature (Huber, 2002). BF_{WP} was previously found to be successful in removing biopolymers (Hallé et al., 2009). EBCT was found to have a noticeable impact on biopolymer removal. BF (B) had a 6 to 20 percentage points higher biopolymer OC removal compared to BF (A) as the EBCT increased from 8 to 16 min. BF (C) had only an additional 3 to 9 percentage points increase in biopolymer OC removal due to the increase in EBCT from 16 to 24 min. On the other hand, biopolymer ON removal increased by 10 to 30% in BF (B) compared to BF (A) and by 20% to 25% in BF (C) compared to BF (B). At the longest tested EBCT of 24 min, the average removal was 68% for the biopolymers OC and 83% for the biopolymers ON, indicating a possible preference for the protein fraction of the biopolymers.

During cold water temperatures, the removal of the biopolymers OC and ON content dropped significantly in all of the tested biofilters (unpaired t-test, α=5%) as shown in **Table S2** in **Appendix**

D, and removal values were more variable. BF (A) achieved nearly 18% to 27% OC content removal while ON content removal was 0 to 37%. BF (B) had a significantly higher removal for OC content at 25 to 40%, while ON content removal ranged between 7 to 31%. For BF (C), the OC content removal was about 26 to 45% and ON removal was 16 to 46%. This shows that even at cold temperatures, longer EBCTs still resulted in higher removal of biopolymers OC, as BF(C) achieved an average removal of 36% compared to 30% for BF (B) and 23% for BF (A). However, there was less effect of EBCT on the removal of biopolymers ON at cold compared to warm temperatures, and the results are more scattered possibly due to the lower concentration of biopolymers ON during cold water conditions as show on **Table 5-1.**
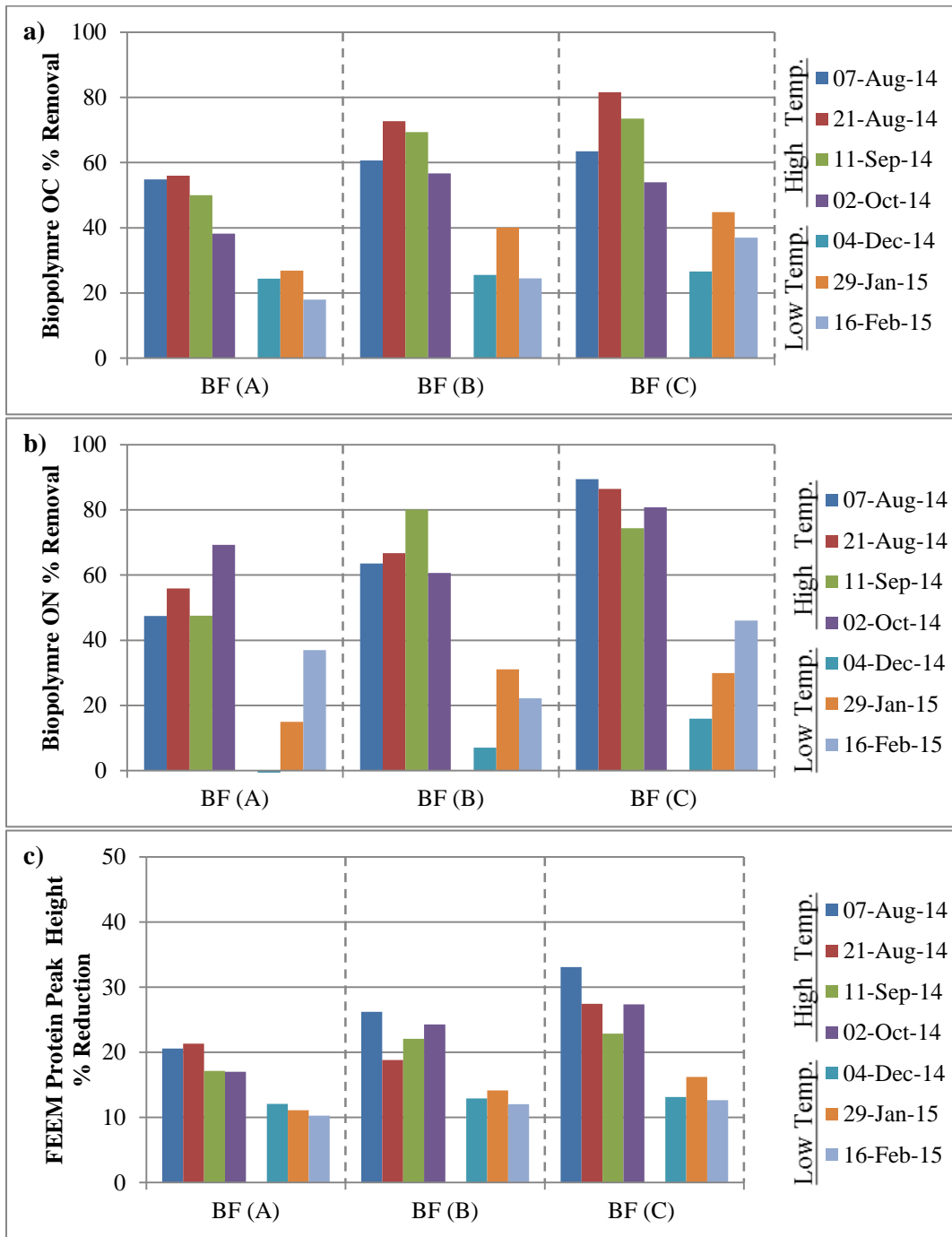
Figure 5-12 Biofilter performance characterized by percent removal of (a) LC-OCD biopolymer fraction organic carbon content, and (b) organic nitrogen content; and (c) removal FEEM protein like substances response percent reduction

Fluorescence spectroscopy provides an alternative method to study the removal of protein-like matter by the biofilters, but the measurement principles differ from LC-OCD. For LC-OCD, size exclusion chromatography is used to separate the molecules based on their apparent MW into fractions, and then the OC or ON concentration is measured using separate detectors. Fluorescence spectroscopy is applied directly to the bulk sample, and determines the amount of certain fluorophores that are associated with certain types of molecules. Protein-like substances in surface water sources have a distinct response in the FEEM at an excitation / emission wavelength of 280/330 nm (Peiris et al., 2010) which is characteristic for the amino acid tryptophan. Percent reduction in the protein like-substances (FEEM-A) of biofiltered water is shown on **Figure 5-12-c** and significant differences were observed among the three filters (paired t-test, α=5%) as shown in **Table S1** in **Appendix D**. BF (A) average removal was 19% compared to 23% for BF (B) and 28% for BF (C). This shows that EBCT had an effect on the removal of protein-like substances, but again that most of the observed peak reduction happened within an 8 min EBCT (BF (A)), and the additional increase in EBCT through extension of the filter bed depth was not directly related to increased protein removal. During cold water conditions, the reduction of the protein like substances FEEM response dropped significantly. BF (A) achieved only 11% average removal compared to 13% and 14% for BF (B) and BF (C) respectively. There was lower removal of the FEEM-A peak at colder temperatures in each biofilter, and no obvious effect of biofilter EBCT on removal. FEEM protein-like substances response was reduced to a lesser extent than the other indicator of protein-like substances, which is the organic nitrogen content of the biopolymers LC-OCD fraction (**Figure 5-12-c**). This can be attributed to the differences between LC-OCD and fluorescence spectroscopy. LC-OCD fractionates NOM based on molecular weight then the mass concentration of each fraction is quantified unlike fluorescence spectroscopy which detects certain fluorophores present in different types of molecules so differences among the two analytical methods is expected.

5.4.3.5 Net Removal of Humic Substances

Humic-like substances compromise the main fraction of the DOM in most surface waters (Huber et al., 2011) but they have low biodegradability as shown on **Chapter 4** and in literature (Huber, 2002). In the Grand River water used to feed the biofilters, the humic substances peak measured by LC-OCD ranges from 2.85 to 4.60 mg C/L (average of 3.6 mg C/L), and was 58 % on average of the DOC in the river (**Table 5-1**). .Humic substances were previously found to be removed by BF_{WP} biofilters to a

low extent (Hallé et al., 2009). The removal of humic like substances as determined by LC-OCD is shown on **Figure 5-13**, and results showed that removals were highly variable and no significant differences were observed among the filters (paired t-test, α=5%) as shown in **Table S1** in **Appendix D**. During warm water conditions, the humic substances were removed by 3 to11% within the three studied biofilters. There was somewhat higher removal in BF (B) and BF(C) compared to BF (A). During cold water conditions, the humic substances removal dropped to be in the range of 0 to 4%, and there were no obvious differences among the three filters. Obviously, the biodegradable fraction of humic substances was less removed at such cold water temperature due to the overall drop in biomass activity due to the drop in temperature.

Fluorescence spectroscopy can further identify the two main contributors to humic substances which are fulvic acid-like (FEEM-B) and humic acid-like substances (FEEM-C). In the Grand River, the response for fulvic acid-like and humic acid-like substances response were similar as their average values were 323 and 368 A.U, showing that the two types of humic-like substance were present at similar levels in the river. There were no seasonal differences in the both FEEM responses. The fulvic acid-like substances (FEEM-B) response was reduced by 3 to 8% during warm water conditions as shown on **Figure 5-13-b** of the supplementary material Humic acid-like substances had a lower percent reduction which was only 1 to 4% as shown on **Figure 5-13-c** of the supplementary material. Both fulvic and humic-like substances showed a small increase in BF (B) and BF(C) compared with BF (A). During cold water conditions, reduction in either fulvic acid-like or humic acid-like substances peaks ranged from 0 to 5% but most of the samples were below 2% with no consistent differences among the three biofilters. Overall, results show that humic-like substances removal as determined using both LC-OCD and fluorescence spectroscopy were negligible at cold water conditions with no significant improvements due to EBCT increase. However at warm water conditions there was a low but measurable removal of humic substances and a small but consistent effect of EBCT on removal. Also both LC-OCD and fluorescence spectroscopy provided very similar values for the removal of humic substances, unlike the measured FEEM protein-like substances (FEEM-A) and LC-OCD biopolymers removal as explained earlier.

Figure 5-13 Biofilter performance characterized by percent removal of (a) LC-OCD humic substances fraction organic carbon content , and (b) FEEM fulvic acid like content percent reduction and (c) FEEM humic acid like content percent reduction (c)

118
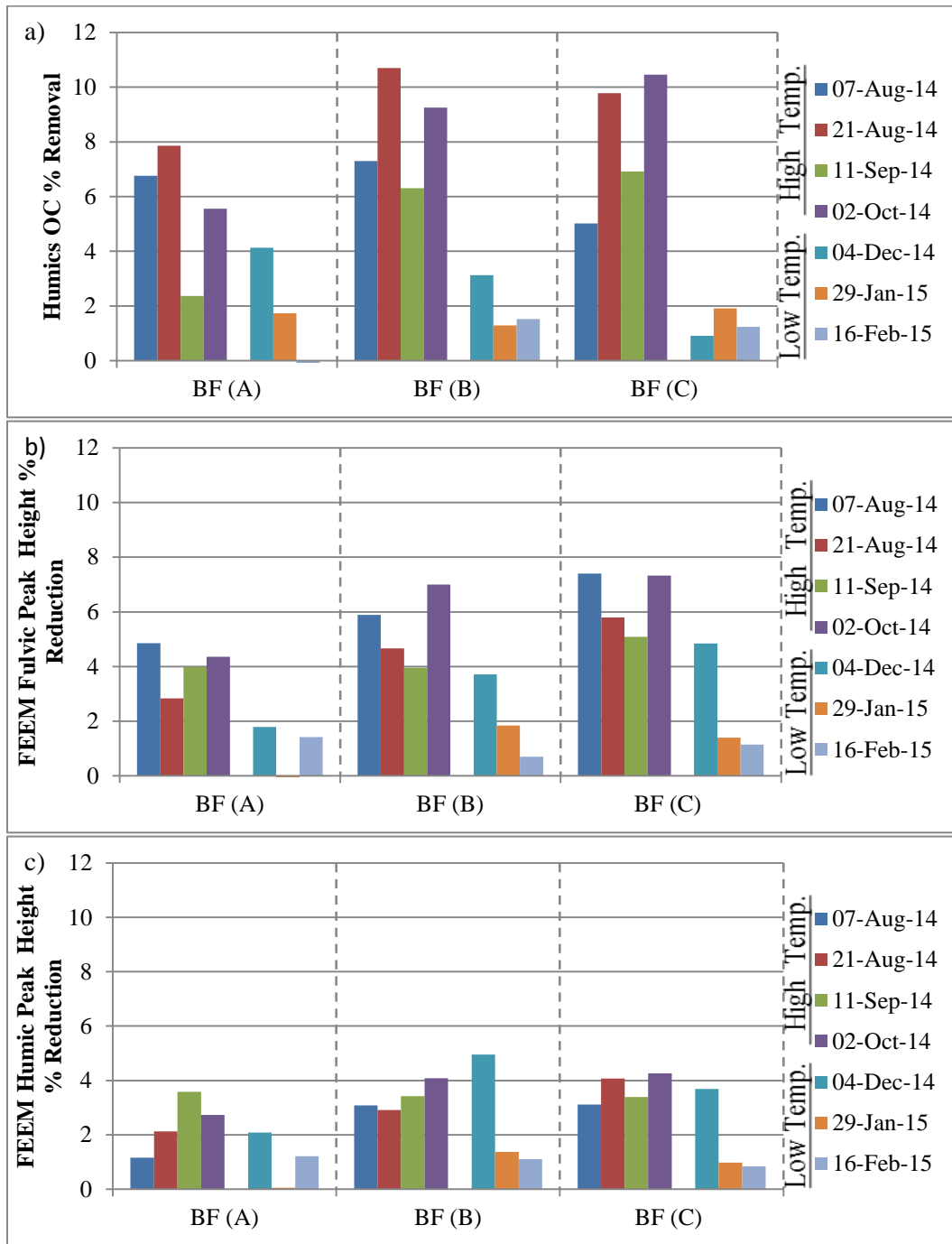
5.4.3.6 Net Removal of Low Molecular Weight NOM Fractions

Low molecular weight NOM fractions include both low molecular weight acids and neutrals. The LMWA made up 3% of the DOC in the raw water, while the LMWN fraction made up 8.3% of DOC (**Table 5-1**). The LMWA fraction is highly biodegradable as discussed in **Chapter 4** and in literature (Huber, 2002). Ruhl and Jekel (2012) showed that acetate and pyruvate would elute in this fraction. The LMWA fraction has also a visible peak in the UV_{254} absorbance chromatograph, showing that this fraction can also include some monomers of humic-like substances (Huber et al., 2011). LMWA organic carbon content was efficiently reduced by 10 to 35%, and LMWA UV_{254} absorbance was reduced by 10 to 20% as shown on **Figure 5-14-a and 5-14-b** of the supplementary material. The removal of LMWN OC ranged between 0 to 25% but at some cases negative removal was measured (Figure 10c) .For both LMWA and LMWN fractions, there was high variability in removal values, and the observed scattering in the results can be attributed to the data analysis software for the LC-OCD chromatographs, which makes integration of these low molecular fractions difficult. As a result, there were no observed trends in removal of either fraction with EBCT or temperature. During cold water conditions, LMWA OC content removal dropped to be 5 to 30%. The average removal was approximately 10% with no obvious differences among the three filters so EBCT had no obvious effect on the observed removal. Similarly for LMWA UV absorbance reduction ranged between 2 to 25% with an average removal of approximately 5% with no obvious differences among the three biofilters. Another remark is the difference among the removal of LMWA organic carbon and UV_{254} absorbance which indicate that the LMWA fraction is a complex fraction that have both low molecular acids which have a simple structure with no aromatic rings along with some monomers for humic like substances which are primarily responsible for the UV absorbance due to their aromatic structure.
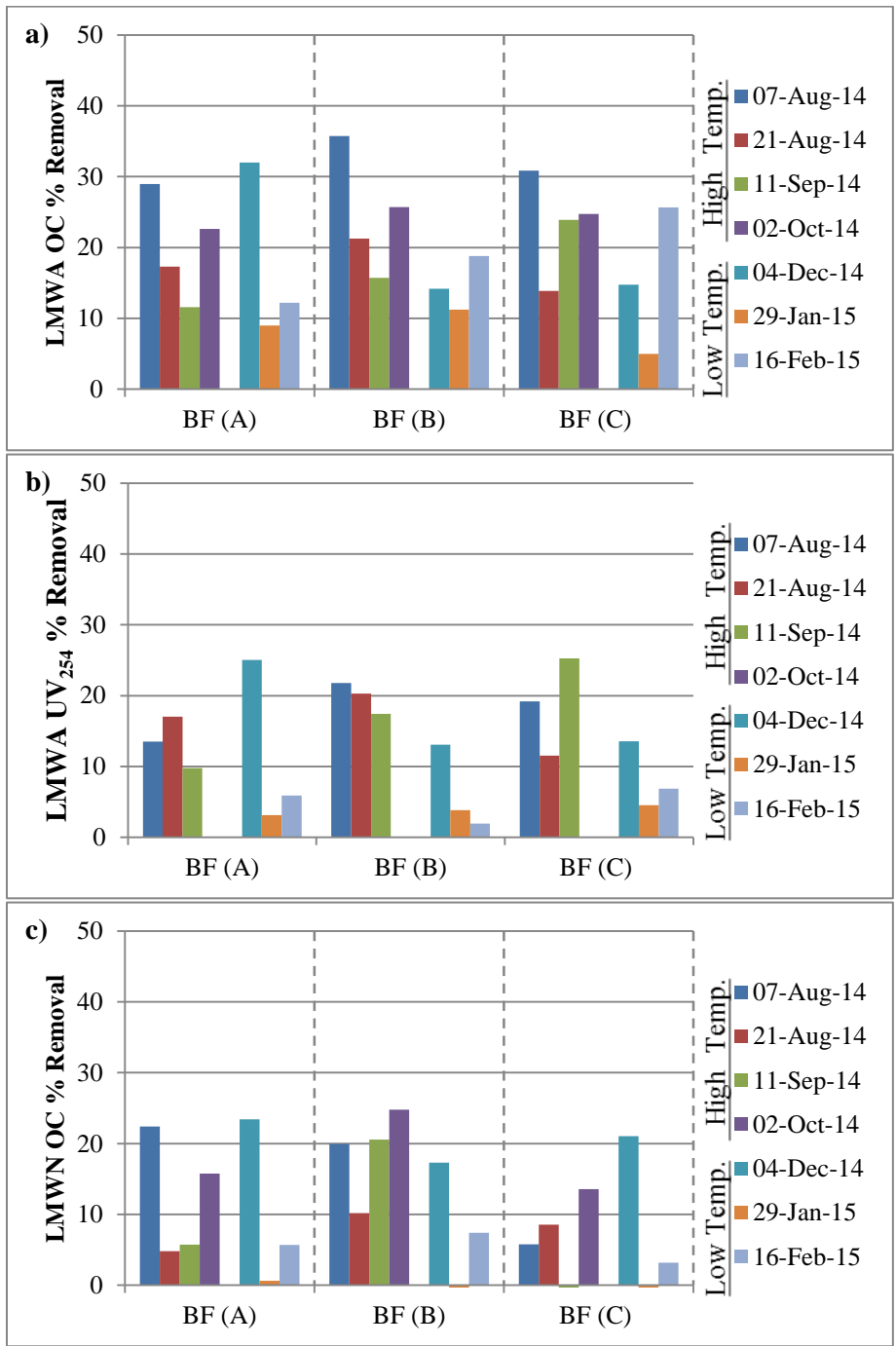
Figure 5-14 Percent removal of (a) LC-OCD low molecular weight acids fraction organic carbon content, and (b) UV absorbance and (c) low molecular weight neutrals OC content over the study period

5.4.4 Relationship between biofilter NOM removal and biomass measurements

In general, the different NOM fractions measured in this study were efficiently removed within the studied biofilters. The highest removals were obtained for the high molecular weight biopolymers and protein-like substances. AOC was also removed efficiently within the filters. There was lower removal of the humic substances likely due to their lower biodegradability. Also, there was low and highly variable removal of the low molecular weight compounds as measured by LC-OCD, likely due to difficulties in measuring these compounds using this method. Water temperature could greatly affect the observed removals for DOC and biopolymers. Although AOC was removed efficiently within the filters, it was less affected by the drop in water temperature, possibly due to the rapid biodegradability of this fraction. Biomass parameters such as biofilm ATP content, biofilm cell count or EPS composition per unit volume of filter media showed an opposite trend with water temperature compared to NOM removal. Instead, each of these parameters was found to increase in the biofilters at cold water temperatures. This shows that biofilter performance in terms of NOM removal was not related to the bulk attached biomass parameters measured in the filters. This suggests that minimum amount of attached biofilter biomass is actually required to operate the biofilter at a steady state condition, and therefore the bulk biomass parameters are less helpful in studying changes in biofilter performance. However, an important finding of this study was found when ATP was measured on a per cell basis (ATP divided by the total cell count) as the average cellular ATP content decreased at cold water temperatures compared with warm water (**Figure 5-3-c**), and similarly the EPS carbohydrates and protein content per cell were lower at cold water temperatures (**Figure 5-6**). The relationships between the average cellular ATP content within each of the filters and biofilter performance are shown on **Figures 5-15**, **5-16** and **5-17**. For the three filters, DOC, AOC and biopolymers percent removal increased as the average cellular ATP content increased over the study period. This shows that the metabolic state of the biofilms could be measured on a per cell basis (for example as ATP), and could be a suitable parameter to predict biofilm performance. However, before this can be used as a benchmark value, additional data from other biofilters would need to be obtained.
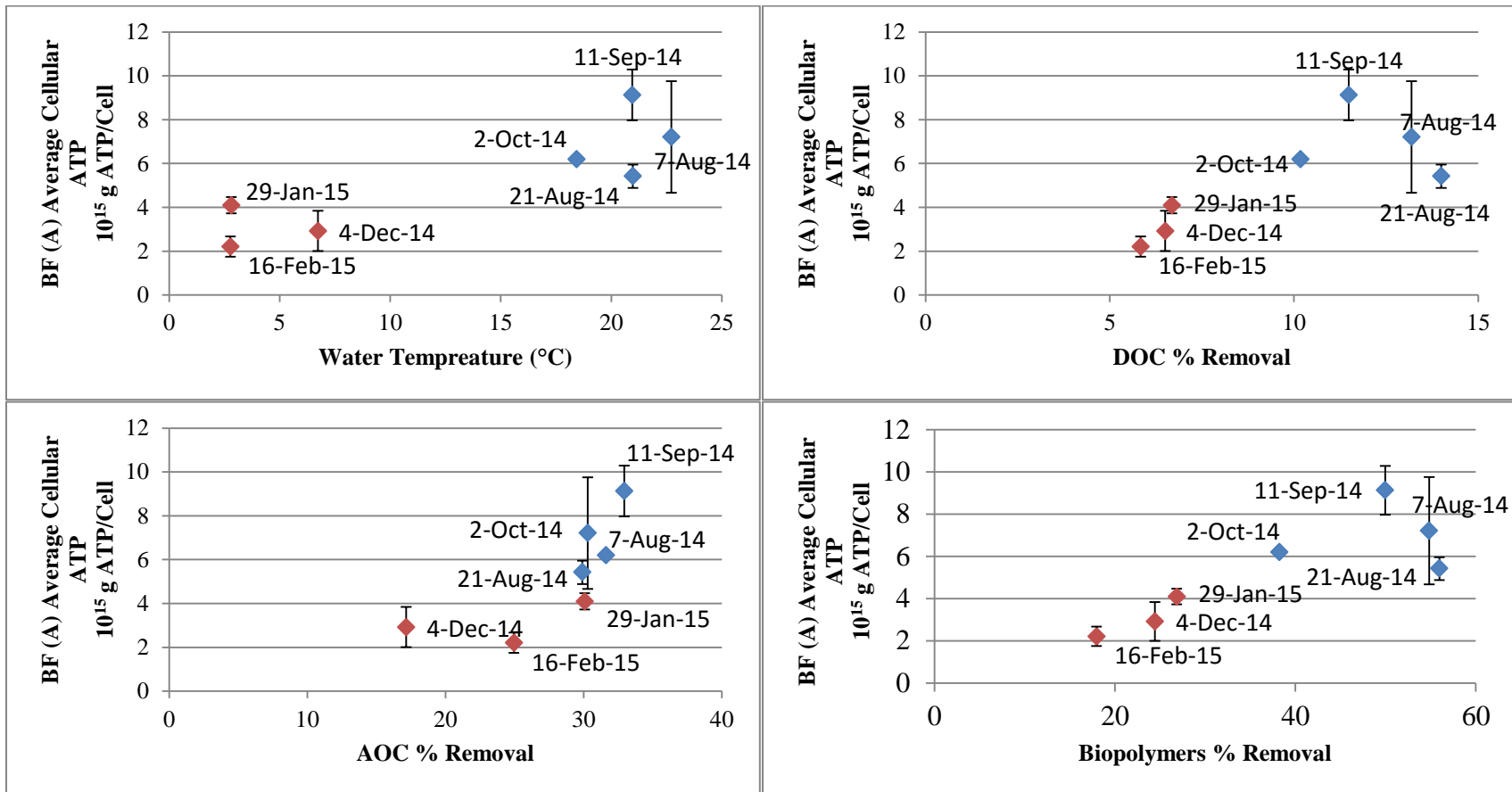
Figure 5-15 The relationship between BF (A) average cellular ATP content for the different media samples (n=2) and (a) the biofilter feed water temperature , (b) observed DOC removal, (c) observed AOC removal and (d) observed biopolymer removal . Red symbols indicate low water temperature samplings and blue symbols indicate high water temperature samplings. Error bars represent standard deviation of the cellular ATP content for the different media samples within the filter (n=2)
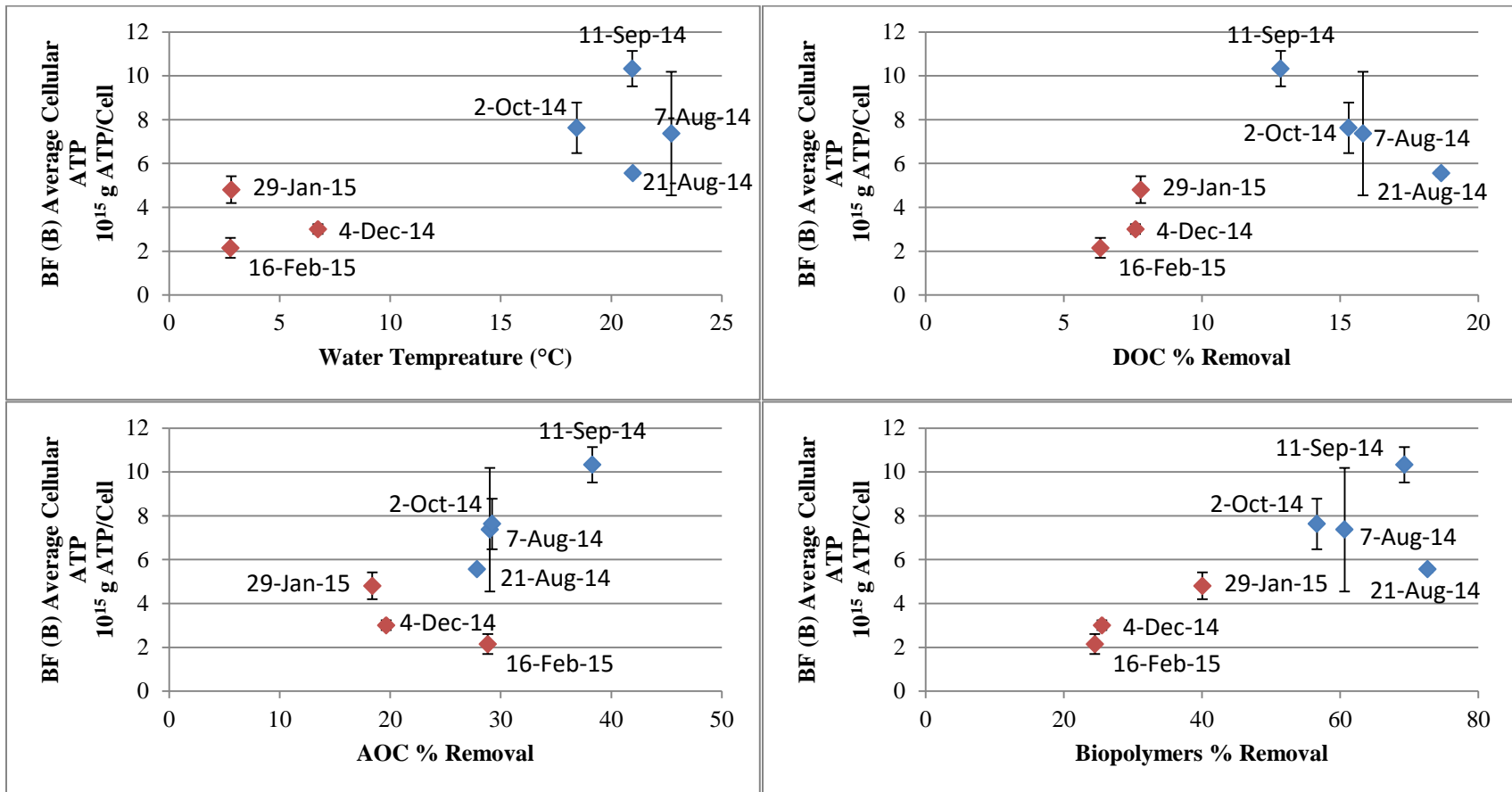
Figure 5-16 The relationship between BF (B) average cellular ATP content for the different media samples (n=3) and (a) the biofilter feed water temperature , (b) observed DOC removal, (c) observed AOC removal and (d) observed biopolymer removal . Red symbols indicate low water temperature samplings and blue symbols indicate high water temperature samplings. Error bars represent standard deviation of the cellular ATP content for the different media samples within the filter (n=3)

123
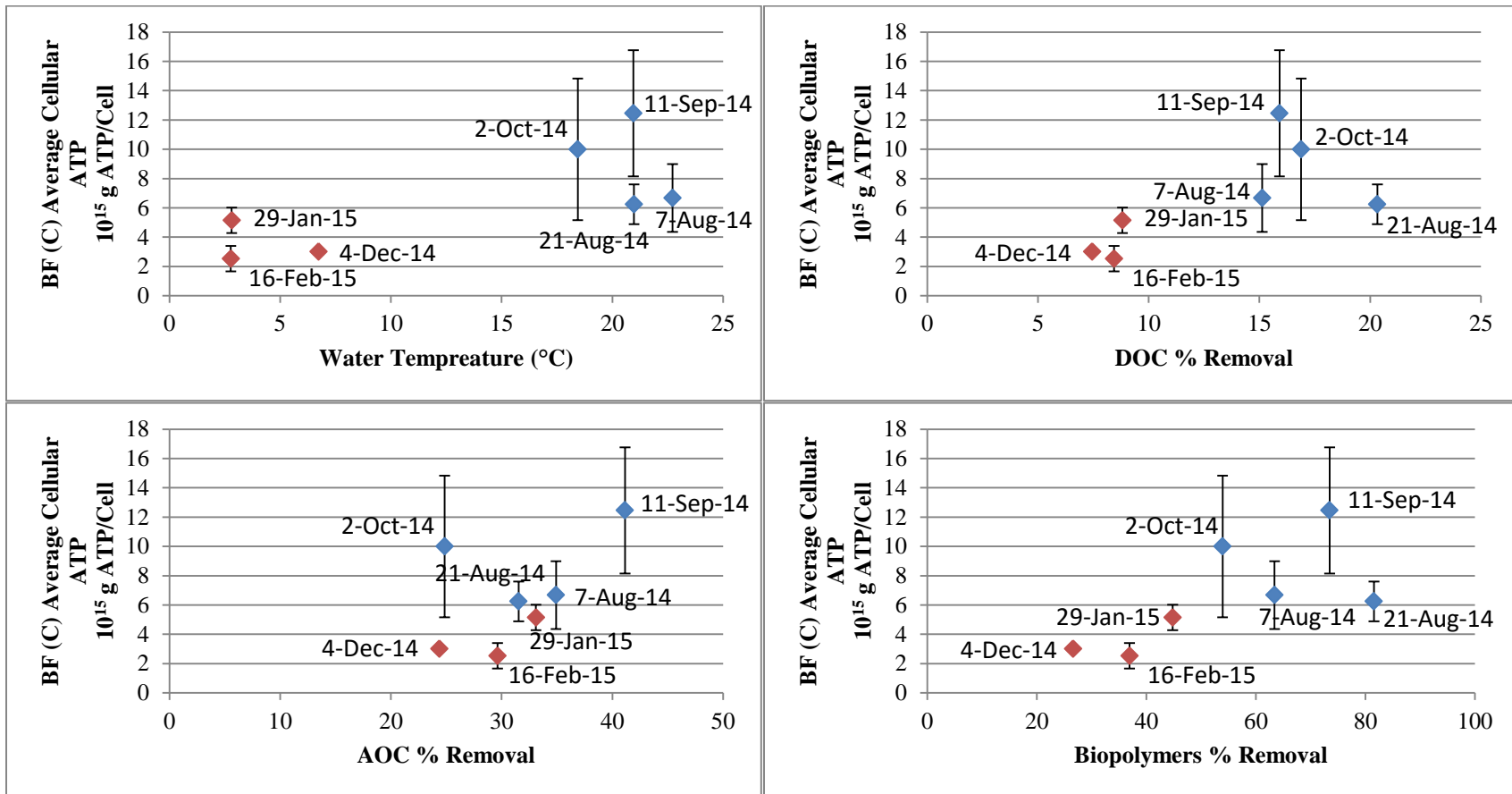
Figure 5-17 The relationship between BF (C) average cellular ATP content for the different media samples (n=4) and (a) the biofilter feed water temperature , (b) observed DOC removal, (c) observed AOC removal and (d) observed biopolymer removal . Red symbols indicate low water temperature samplings and blue symbols indicate high water temperature samplings. Error bars represent standard deviation of the cellular ATP content for the different media samples within the filter (n=4)

124

5.5 Conclusions

BF_{WP} is a promising green pre-treatment technology for drinking water treatment. The current study evaluated the effect of design EBCT and water temperature on the performance of pilot scale biofilters. This research would provide the basis for further testing at a larger scale to be able to implement BF_{WP} as a pre-treatment technology for full-scale drinking water operations. Also, the study aimed at identifying possible linkages between biofilter biomass characteristics to the observed biofilter performance. This can lead to a better way to investigate the state of the biofilter biomass and the operational state of the biofilter. Main conclusions of the current study are:

- Both bulk biofilter media ATP and biofilm cell count alone are informative methods to study the biomass of the biofilter, however both methods were not directly related to the observed biofilter performance (i.e. DOC or AOC removal).

- The bulk amount of the biofilm EPS and its individual components were accurately monitored and were found to decline over the biofilter depth, similar to the trend for other biofilter biomass parameters such as ATP and biofilm cell count.

- Determining the average cellular ATP content was an informative technique and was able to reflect the drop in attached biomass activity and / or possible changes in the microbial community as the water temperature dropped. The cellular ATP content was related to biofilter performance in terms of DOC and biopolymer removal.

- The amount of the bulk biofilm EPS and its protein or carbohydrate content was mainly dependent on the water temperature being higher at colder water temperature regardless of the increase in biofilm ATP content.

- The ratio of EPS carbohydrates to proteins slightly increased as the water temperature dropped, possibly due to changes in microbial community.

- All of the different NOM fractions measured were reduced through the biofilters, but high molecular weight biopolymers including both proteins and polysaccharides showed the highest removal, even at low water temperatures. This further proves that BF_{WP} is suitable pre-treatment for low pressure membranes as biopolymers are their major foulant.

- AOC was efficiently removed within the filters, and the longer biofilter EBCT of 24 min was able to buffer the effect of the extreme cold water conditions. BF_{WP} is a promising technology for

125

membrane biofouling control in high pressure membranes, as they can provide a robust pre-treatment to degrade easily biodegradable organics at extreme water conditions.

- Humic-like substances, known for their low biodegradability were removed to some extent, especially under warm water conditions, but their removal was negligible under cold water conditions.

- Low molecular weight LC-OCD defined NOM fractions were efficiently removed in the different temperature ranges, but results were highly variable.

- EBCT as a design parameter had a significant effect on the biofilter performance, mainly for biopolymers and AOC removal. However, the top part of the biofilter seems to be the most active and responsible for most of the observed removal of these fractions. Increasing biofilter EBCT beyond 8 min should be studied wisely to weigh the cost and the benefits that can be obtained.

- Cold water conditions affected not only NOM net removal, but also it caused a reduction in the net reduction of the total cell count of the biofiltered water as well.

Chapter 6

Using Community-Level Physiological Profiling (CLPP) to Study Seasonal and Spatial Differences in Microbial Community Composition in Drinking Water Biofilters

6.1 Summary

BF_{WP} is a green biological treatment process to remove BOM present in natural surface waters that can potentially foul drinking water treatment membranes. Biofilter-attached biomass is a key component of the biofiltration process so good understanding of the biofilter biomass characteristics and microbial community composition is necessary to get a better understanding of the biofilter performance. Community-levels physiological profiling (CLPP) is an interesting tool for studying microbial community composition by investigating their carbon substrate utilization patterns (CSUPs) data using Biolog EcoPlates. In this chapter, biomass samples from three different biofilters at different depths within the filter along with freshwater biomass were used to study spatial changes in microbial community composition over the filter depth and among parallel filters. Also samples were collected at different water temperatures to understand the effect of feed water temperature and potential changes in feed water quality on the microbial community composition. These results can be correlated to the observed biofilter performance and the biomass activity and EPS profiles observed in **Chapter 5**. Based on those results, microbial community maximum rate of substrate utilization (μ_m) was found to be a more representative descriptor for CSUPs data than the maximum optical density (A). Using μ_m as a descriptor for both hierarchical clustering and principal component analysis (PCA) multivariate statistical analysis techniques yielded more representative results of the microbial community differences results than using A as a descriptor. Based on the obtained results, raw water was obviously different for the biofilter biomass microbial community and some seasonal changes in raw water microbial community were observed as well. Microbial community composition for the biofilter biomass during warm and cold water temperature conditions was obviously different. No obvious differences in the microbial community on sand and anthracite samples obtained at the same biofilter depth were observed during high and low water temperature conditions however the microbial community on the sand samples obtained at different depths in the filters were slightly different. The drop in biofilter performance observed in cold water

127

conditions is likely related to a combination of the observed drop in biomass activity as discussed in **Chapter 5** along with changes in biofilm microbial community.

6.2 Introduction

BF$_{WP}$ as a drinking water pre-treatment technology that involves the use of a media filter without any antimicrobial agents in the biofilter feed or backwash water, to allow for biofilm growth on the surface of media particles to degrade BOM. Different substances forming the BOM pool of molecules diffuse within the biofilm or get trapped within the biofilm structure, where they are subject to bacterial enzymatic activity and degraded by the biofilm microbial community. Biofilter biomass is usually studied using general biomass parameters (e.g. total cell amount) to ensure that a sufficient amount of biomass is present in the filter, however, such an approach was not fully able to explain changes in biofilter performance as discussed in **Chapter 5** and in the literature (Evans et al., 2013a; Magic-Knezev and van der Kooij, 2004; Pharand et al., 2014; Velten et al., 2007). Another approach for studying the relationship between biofilter biomass and biofilter performance is through the characterization of the microbial community composition. The diversity of the biofilm microbial community can be directly related to the biofilm stability as an ecosystem (McCann, 2000), as it will be protected through its functional redundancy (Yachi and Loreau, 1999).

Methods for studying the biofilter microbial community structure can include molecular biological techniques such as sequence analysis, and also indirect profiling methods such as denaturing gradient gel electrophoresis (DGGE) (Boon et al., 2011) or arbitrarily primed polymerase chain reaction (AP-PCR) (Moll et al., 1998). Other methods based on cellular component analysis include phospholipid-derived fatty acids (PLFA) profiles (Moll et al., 1999, 1998). An alternative method to examine microbial communities is the CLPP technique. In CLPP, the ability of the microbial community to utilize different types of carbon substrates, defined as CSUPs data are used as indicators of the microbial community composition. The CLPP technique has been widely applied to various types of environmental samples, and has been used to characterize biofilms in freshwater systems (Massieux et al., 2004) and drinking water biofilters (Moll et al., 1998). CLPP seems to be particularly suited to study the changes in biofilter biomass, since this method depends on nutrient utilization patterns and is likely more directly linked to changes in BOM removal through the biofilters.

Drinking water biofilter performance was found to be significantly reduced at colder water temperatures, as shown in **Chapter 5** and in the literature (Evans et al., 2013a; Liu et al., 2001; Moll et al., 1999; Pharand et al., 2015; Urfer et al., 1997). This can be attributed to drop in biomass activity (Laurent et al., 1999) and / or some changes in the biofilm microbial community (Moll et al., 1999). Moll and co-workers (1999) showed that the biofilter biomass microbial community structure as shown by PLFA profiles was clearly different at 35, 20 and 5°C and over the biofilter depth. A similar community structure gradient over the depth of a pre-ozonated GAC biofilter was reported by Boon and co-workers (2011) using DGGE analysis of the 16S rRNA gene. In that study, the maximum BOM removal in the middle of the biofilter was found to correspond with the highest community richness. Moll and co-workers (1998) also showed that the number of carbon substrates utilized during CSUPs analysis declined over the media depth in biofilters receiving both ozonated and non-ozonated water, and that this trend was greater in the filter receiving ozonated water. This shows that the nature of BOM in the feed water can have an effect on the microbial community composition.

In this study and as part of the biofilter performance study presented in **Chapter 5**, the microbial communities in the biofilter biomass were assessed using Biolog EcoPlates (Biolog, CA, USA)` . Biolog EcoPlates were used as a simple and fast method to look at the functional diversity of the microbial community. Biolog EcoPlates use 31 carbon substrates commonly used as nutrients by soil bacteria. Substrates are provided in a microplate format, and substrate utilization is easily measured spectrophotometrically based on reduction of a tetrazolium dye to formazan. The main objectives are to study the effect of seasonal water temperature changes on the biofilter microbial community, and to study the changes over the biofilter depth. Different descriptors for the obtained CSUPs, such as substrate rate of colour development (utilization rate; $\mu_{m)}$ or the maximum colour value (A) were investigated to determine the most suitable way to analyze CLPP results. The relationship of the results obtained to the observed biofilter performance was also investigated.

6.3 Materials and Methods

6.3.1 Sample Preparation

The water and media samples were obtained from the biofilter performance study presented on **Chapter 5**. Samples of the pilot plant media and the raw water feeding the biofilters were obtained on August 2014, September 2014 and October 2014 to represent biofilter biomass during warm water conditions.

The average daily water temperature was 23.3, 21 and 18.5°C for the three sample dates, respectively. Samples from the pilot plant media and raw feed water were sampled on December 2014, January 2015 and February 2015 to represent biofilter biomass at cold water conditions. The average daily water temperature was 6.7, 2.5 and 2.8°C for the three sample dates, respectively. On each sample date, media samples were collected at different biofilter depths at 20 cm, 60 cm and 90 cm as described in **Chapter 5**. For media samples, EPS extraction of the attached biofilter biomass was done according to the described method in **Chapter 3**, and the resuspended cell pellet was used for CLPP analysis. After flow cytometry total cell count of the resuspended cell pellet, the sample was further diluted to a final concentration of 1×10^6 cell/mL using 0.2 μm filtered and autoclaved 6mM PBS. For raw water, 4×5 mL of each sample was centrifuged at 10,000 ×g for 20 min and then the supernatant was decanted. The cell pellet was resuspended in autoclaved 0.2 μm filtered PBS to a concentration of 1×10^6 cell/mL, according to the flow cytometry total cell count of the water. Each diluted sample was used to inoculate a 96 well Biolog EcoPlate™ microplate, using 150 μL per well, then incubated in the dark at 20°C. As the bacteria present in each well consumed the substrates present during the respiration process, the tetrazolium dye present in each well was reduced to formazan and the developed colour was detected photometrically at a wavelength of 590 nm using a ChroMate® 4300 microplate reader (Awareness Technology, Inc., USA). The colour development was recorded at 2, 3, 4, 8, 10, 11, 14 and 21 days.

Each Biolog Ecoplate contained 31 different substrates, each in triplicate wells, along with three blanks (containing no substrate). The substrates used are shown in **Table 6-1,** and the classes of compounds are polymers, carbohydrates, amino acids, carboxylic acids, amines, phosphorylated compounds and esters. The measured absorbance for each well was corrected by subtracting the average of the blanks. The corrected average absorbance of each substrate over time was determined as shown on **Figure 6-1**. Both the maximum colour intensity (A) and the maximal rate for colour development (μ_m) for each substrate were used as metrics for multivariate statistical analysis, to study the differences among the different microbial communities as described by Verschuere and co-authors (1997). In certain cases when the maximum intensity was the first recorded data point, the microbial community was assumed to start consuming the substrate at time zero and a straight line was fitted between the origin and the first data point to determine μ_m. The obtained A and μ_m data sets are available in **Appendix E**.
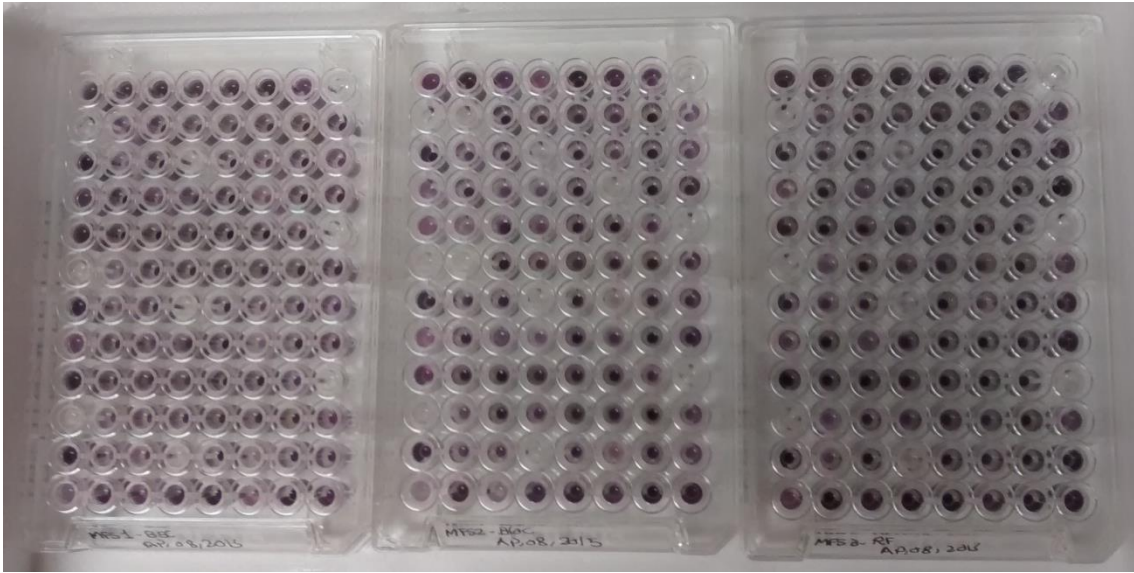
Figure 6-1 Biolog EcoPlate colour development for different biofilm samples
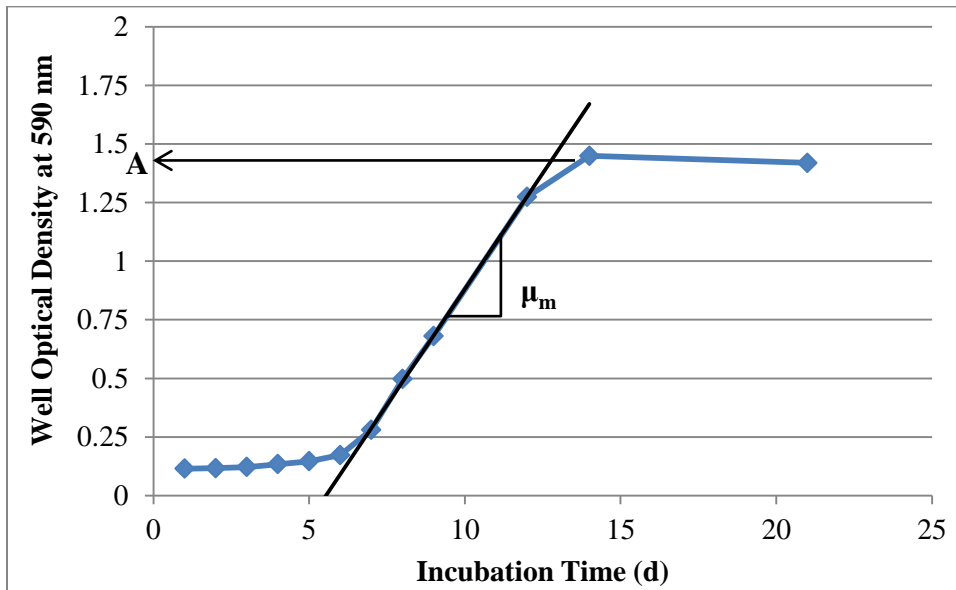
Figure 6-2 Schematic of the model used to fit the obtained Biolog Ecoplate data for a single substrate, showing maximum optical density (A), maximum rate of colour development (μm)

Table 6-1 Nutrients used in the Biolog EcoPlates

Category	Nutrient	Symbol
Polymers	Tween 40	POLY1
	Tween 80	POLY2
	α-Cyclodextrin	POLY3
Carbohydrates	Glycogen	CARB1
	D-Cellobiose	CARB2
	α-D-Lactose	CARB3
	β-Methyl-D-Glucoside	CARB4
	D-Xylose	CARB5
	i-Erythritol	CARB6
	D-Mannitol	CARB7
	N-Acetyl-D-Glucosamine	CARB8
Phosphorylated compounds	Glucose-1-Phosphate	POSPH1
	D,L-α-Glycerol Phosphate	POSPH2
Esters	PyruvicAcid MethylEster	ESTER1
Carboxylic Acids	D-Glucosaminic Acid	CAACID1
	D-Galacturonic Acid	CAACID2
	γ-Hydroxybutyric Acid	CAACID3
	Itaconic Acid	CAACID4
	α-Ketobutyric Acid	CAACID5
	D-Malic Acid	CAACID6
	D-Galactonic Acid γ-Lactone	CAACID7
	2-Hydroxy Benzoic Acid	CAACID8
	4-Hydroxy Benzoic Acid	CAACID9
Amino Acids	L-Arginine	AMACID1
	L-Asparagine	AMACID2
	L-Phenylalanine	AMACID3
	L-Serine	AMACID4
	L-Threonine	AMACID5
	Glycyl-L-Glutamic Acid	AMACID6
Amines	Phenylethylamine	AMINE1
	Putrescine	AMINE2

6.3.2 Multivariate Statistical Analysis

Project R, a free statistical analysis software (R Core Team, 2015), was used to analyze the CSUPs results obtained from the Biolog Ecoplates, to classify the different microbial communities into sub-groups. An unweighted pair-group method using arithmetic averages (UPGMA) was performed on the Euclidean distances of the maximum colour intensity (A) and the maximal rate for colour development (μ_m) data sets. Additionally, principal component analysis (PCA) was also applied on the multivariate data set, to ordinate the different samples into a reduced 2D space while representing the maximum allowable amount of variance within the data set. PCA analysis was also performed on both A and μ_m data sets. PCA groups the multivariate data set with (n) dependent variables into (n) orthogonal components, to maximize the amount of variability explained by only few components. This allows a better investigation of the data set in a reduced space in order to visualize similarities between samples.

6.4 Results and Discussion

Biofilter media samples were collected from the dual-media biofilters located at the Mannheim Water Treatment Plant. The samples were collected at different depths over the biofilter to understand the possible changes in the microbial community due to the expected nutrient gradient. Also, samples were collected from both sand and anthracite media at the same filter depth, by sampling at the intermixing zone. This was done to determine if the type of biofilter media can affect the attached microbial community. Also, the effect of water temperature on biofilter performance was investigated by comparing the microbial community CSUPs for samples collected during warm and cold water conditions.

6.4.1 Hierarchical Clustering Analysis

Hierarchical clustering was applied on both the A and μ_m data sets. The obtained dendrogram for the substrate utilization rate (μ_m) data set is shown on **Figure 6-3**, and shows that the samples clustered in 6 different apparent groups. The first group G1 included all the raw river water samples used to feed the biofilters from the different sampling events along within two samples from BF(C). It was found that both the raw water and BF (C) samples had slow substrate utilization rates compared with the other biofilter samples. In fact, colour development on plates containing biomass from the BF (A) and BF (B) media was very rapid, with high absorbance values for the majority of substrates occurring within 10 days. For raw water samples, colour development was very slow and required 20 days before colour development reached its maximum value. BF(C) samples also had slower colour development compared to the other

133

biofilter samples. The second group G2 included most of the samples obtained at warm water conditions during August, September and October. This can be linked to the stable performance of the biofilters in removing DOC and NOM fractions during warm water conditions as reported on **Chapter 5**. The next four groups are G3, G4, G5 and G6, which included samples from December, January and February sampling events respectively. This shows that during cold water conditions, there was a change in the microbial community, possibly due to the adaption of the biomass to the cold water conditions. Laurent and co-workers (1999) found the biofilter biomass activity dropped significantly in response to the drop in water temperature, then increased again as the biomass adapted to the cold water conditions. **Figure 6-3** also shows that samples collected from the same depth of BF (A) and BF (B) were similar, which would be expected as the parallel filter had the same loading rate. These results are similar to the biofilter performance data presented in **Chapter 5**. The data set for the maximum absorbance (A) was also used for clustering analysis is shown in **Figure 6-4**. The first two groups G1 and G2 included the raw water samples in similar way to the clustering dendrogram for μ_m data set. It is clear that there were differences between raw water biomass and biofilter biomass using both descriptors for CSUPs data. The third group G3 included most of the samples obtained from the sampling events on August, September and October samples (i.e. during warm water conditions). This is also similar to the finding of the μ_m data set. The next three groups G4, G5 and G6 included the samples from the three sampling events on December, January and February during cold water conditions. Some differences among the different sampling events can be observed in a similar manner to the μ_m data. A general observation is that there were more samples that did not fall into a specific group in the A data set compared to the μ_m data set. Also, analysis based on the A data set could not group the samples from BF (C) differently from the rest of the samples. Apparently, μ_m as a descriptor for the CSUPs data was a more suitable parameter than A, and could better separate the samples and explain the differences among them. A more detailed comparison among the two descriptors was also done using a more advanced statistical technique such as PCA analysis, as shown next.

134
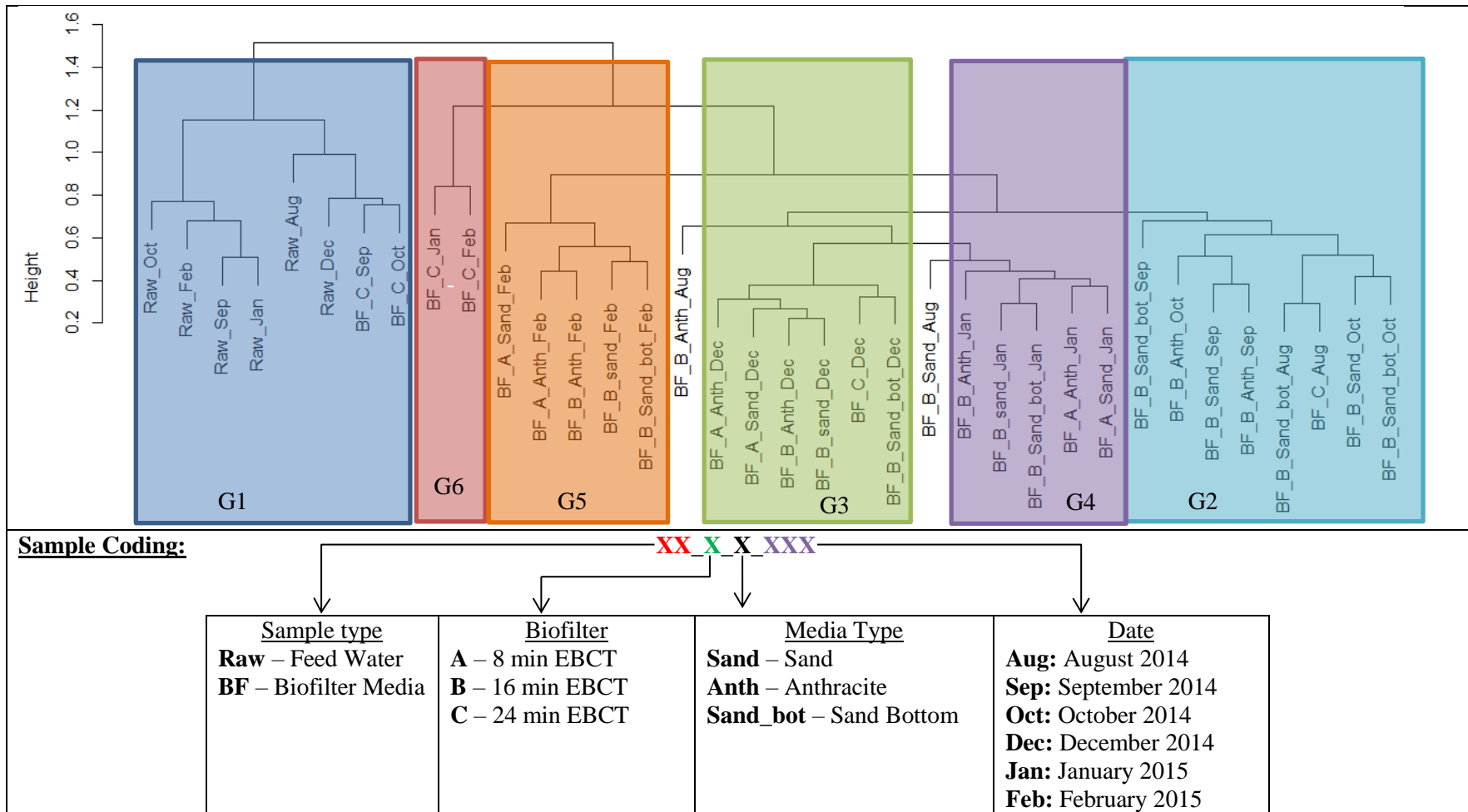
Figure 6-3 Hierarchical clustering dendrogram of the maximum rate of colour development (μₘ) data set of the CSUPs for biofilter and freshwater biomass
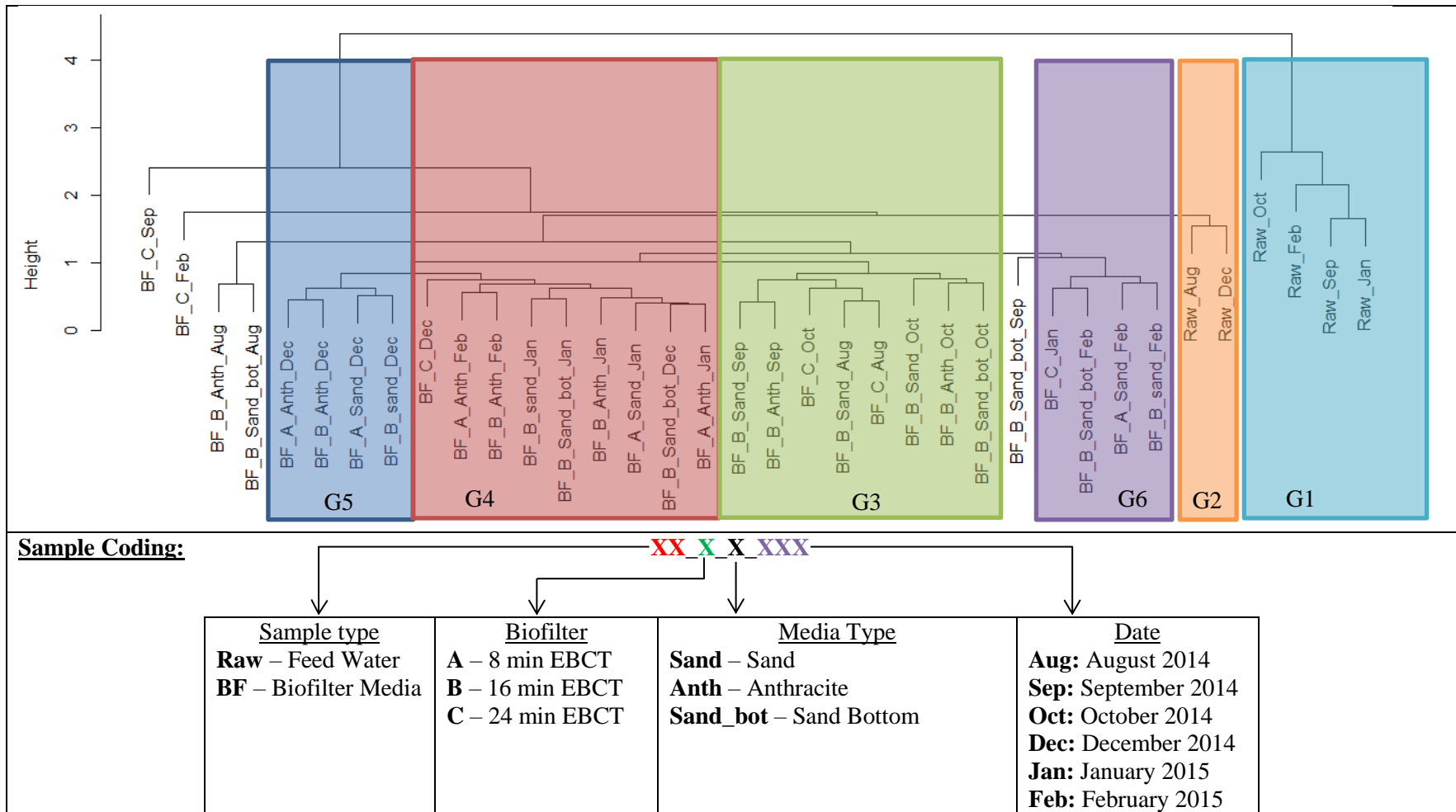
Figure 6-4 Hierarchical clustering dendrogram of the maximum colour intensity (A) data set of the CSUPs for biofilter and freshwater biomass

6.4.2 PCA Analysis

PCA uses an advanced multivariate statistical analysis technique, which can represent a multivariate data set such as the CSUPs in a reduced space of two to three dimensions, instead of 31 dimensions as in the case of CSUPs data. Each principal component (PC) would represent a different proportion of the total variability within the studied data sets (e.g. Legendre and Legendre, 2012). Project R statistical analysis software was used to perform PCA on the A and μ_m data sets, and the code used is shown in **Appendix E**. The obtained PC accounted for different proportions of the total variability as shown in **Figure 6-5**. For the μ_m data set, PC1, PC2 and PC3 account for 58%, 17% and 5% of the total variability, respectively, and the three PCs combined accounted for 80% of the total variability. For the A data set, PC1, PC2 and PC3 accounted for 74%, 6% and 5% of the total variability respectively, and the three PCs combined accounted for 85% of the total variability. As a result, both PCA models could account for a large proportion of the total variability by investigating 3 PCs only.
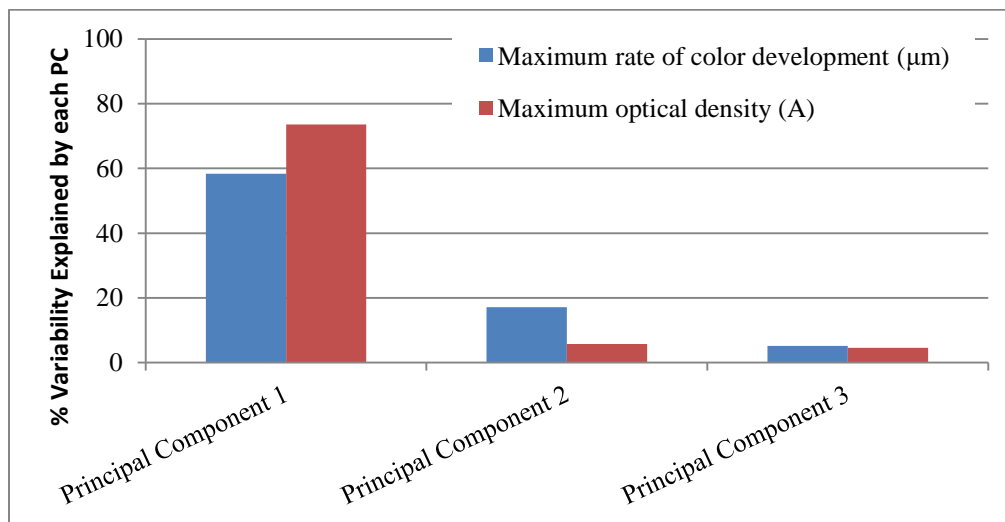
Figure 6-5 Percent variability of the first three principal components in both PCA models

The obtained PCA model can be used to study the correlation among the different samples using PCA biplots with different combinations of PCs. The species scores of the PCA model for any two PCs can be plotted in a biplot to understand the relationship among the samples (e.g. **Figure 6-6-a**). PCA biplots can also provide information about the relationship between the original variables (i.e. different carbon sources in Biolog EcoPlates) and the obtained PCs along with the relationship among the different samples (e.g. **Figure 6-6-b**). The red arrows indicate the different types of carbon sources, and their

relation can be evaluated visually using the angle between the PC and the variable; the smaller the angle, the stronger the correlation would be.

Figure 6-6 PCA biplot for (a) PC1 and PC2 of the maximum rate of colour development (μ_m) data set showing samples score and (b) variables correlation with PCs (b)

The PCA biplot using the μ_m data set (**Figure 6-6-b)** shows that all the different variables had a good correlation with PC1, indicating that PC1 could represent the overall trend of the samples and account for the largest proportion of the variability, as discussed earlier. By investigating the PC1-PC2 biplot on **Figure 6-6-a**, raw water samples clustered together far from the rest of the samples, and PC1 separated them from the biofilter biomass samples. This shows that the raw water samples had a lower rate of growth than the biofilter biomass samples as shown by the original data before performing the PCA analysis in **Appendix E**. The fact that the raw water samples did not group based on season indicates that the microbial community did not shift based on temperature over the 7 month study period, even though there was a wide temperature range of 23 to 2 °C. This was also observed in the consistency of the AOC inoculum yield on acetate as shown in **Chapter 4**, and the apparent stability of the freshwater microbial community also supports the use of a natural AOC inoculum prepared in different seasons, that would be required for long term studies. **Figure 6-6** also showed that most of the samples obtained from BF (C) (90 cm) grouped separately, which confirmed the fact that those samples were significantly different than the samples obtained at the top of the filters. This shows that the microbial community deeper in the biofilter was different that the biofilter top, which is in agreement with the findings from Moll and co-workers (1998) obtained on biofilters with or without prior ozonation. This can be attributed to the nutrient gradient over the biofilter depth (Boon et al., 2011).

No clear differences can be observed between sand and anthracite samples within a sampling event, and also the samples at the bottom of BF (B) (60 cm) were not significantly different than the top of the filter. Moll and co-workers (1998) found that the samples obtained over the depth of a biofilter without prior ozonation consumed nearly the same types of substrates regardless of the depth, unlike biofilters with ozonated water; however, that study evaluated if the substrate was used or not without evaluating the degree of substrate utilization. The PC1-PC2 biplot (F**igure 6-6-a)** also shows that the biofilter samples from cold water sampling events clustered together. In addition, PC2 could separate biofilter samples from each of the three cold water sampling events clearly, which can be attributed to the adaption of the biofilter biomass to the cold water temperature, as indicated by the arrows on **Figure 6-6-a**. This is in agreement with findings of Laurent and co-workers (1999) who found that the biomass activity dropped drastically due to sudden drop in water temperature but the media samples acclimated at cold water condition (10°C) had higher activity than the media acclimated at high water temperature (20°C) indicating the ability of the biofilter biomass to adapt to the cold water conditions.

139

To examine the other major PCs, the biplot of PC1 and PC3 is shown on **Figure 6-7-a**. By including PC3, there was better separation of the two groups of biofilter media samples taken at warm and cold water temperatures. Also, raw water and BF (C) samples could still be separated from the rest of the samples, as PC1 was still used in the model. Additional insight on the variability can be obtained by investigating both PC2 and PC3 as shown in their biplot on **Figure 6-8-a**. Warm and cold water condition biofilter samples could still be nicely separated due to PC3 as expected. By including PC2, the differences among the three cold water sampling events were obvious and could be separated. However, in the PC2/PC3 biplot, raw water samples and BF (C) samples were no longer separated from the rest of the samples as PC1 was not present. PC3 was able to reflect the differences between warm and cold water samples, which accounted only for 5% of the total variability, and indicated that the differences due to water temperature change was only a small portion of the total variability.
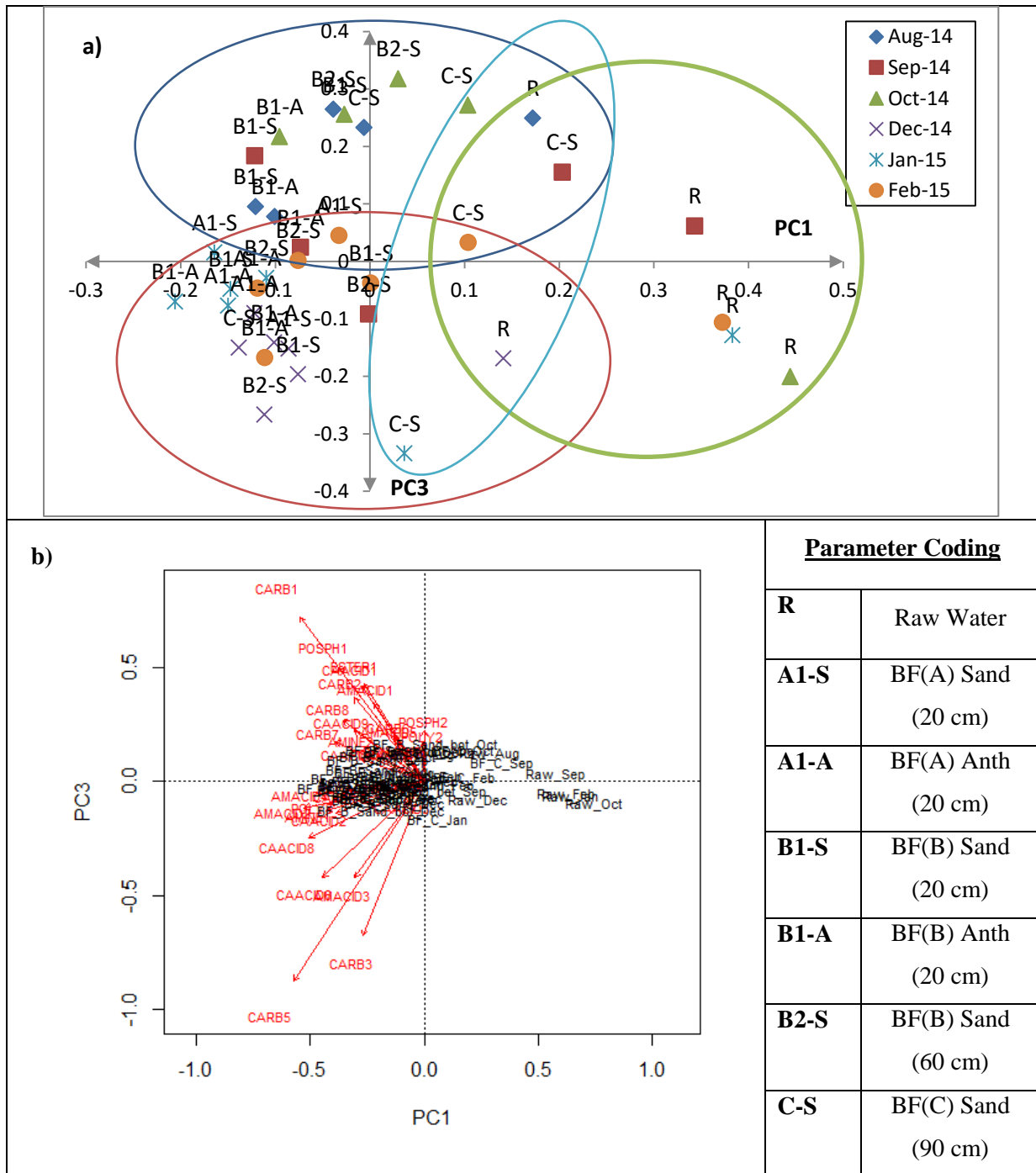
Figure 6-7 PCA biplot for (a) PC1 and PC3 of the maximum rate of colour development (μ_m) data set showing samples score and (b) variables correlation with PCs
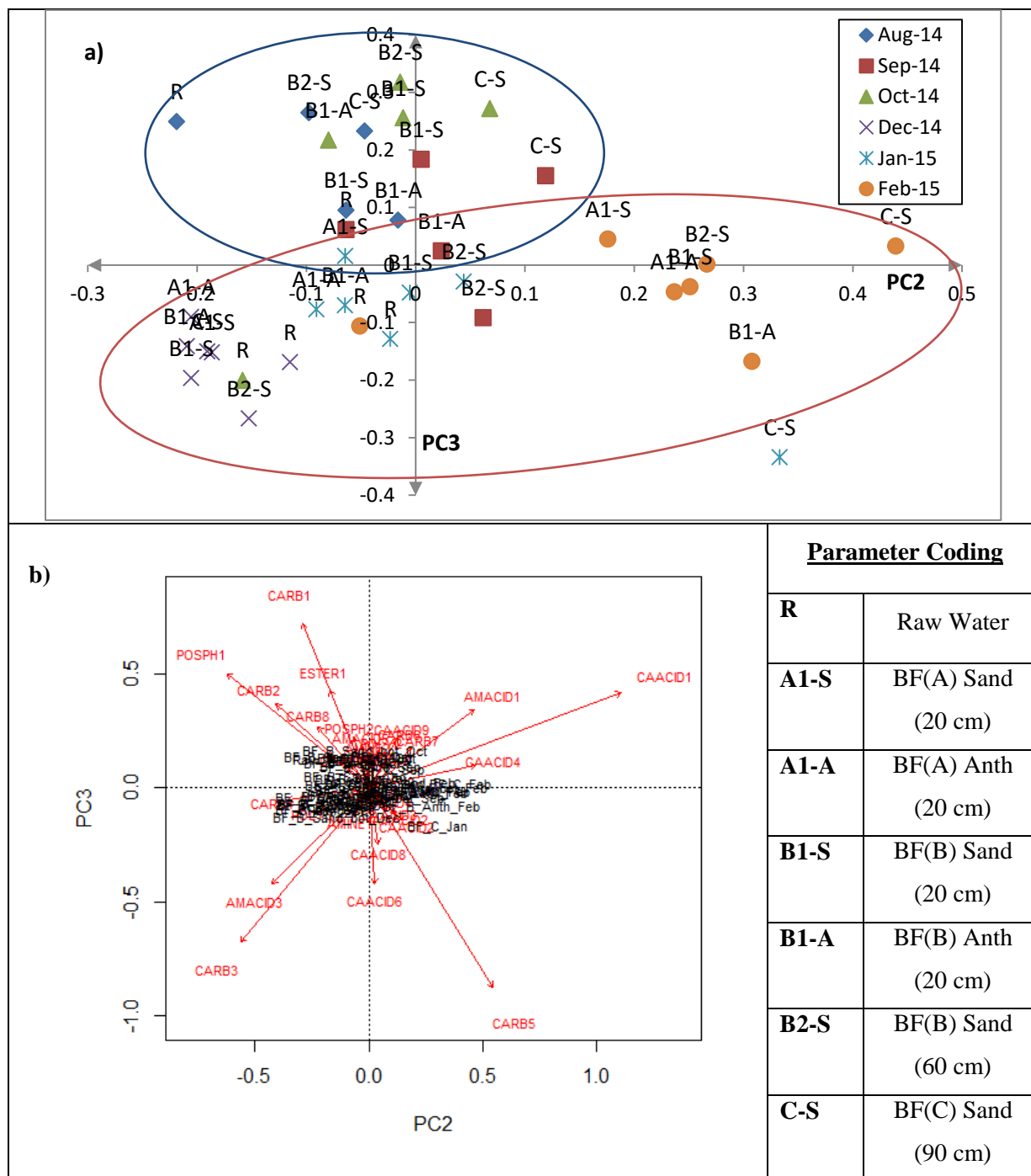
Figure 6-8 PCA biplot for (a) PC2 and PC3 of the maximum rate of colour development (μ_m) data set showing samples score and (b) variables correlation with PCs

For the maximum absorbance (A) data set PCA model, PC1 accounted for most of the total variability (74%). PC2 and PC accounted for only 6% and 5% of the variability. The biplot of PC1 and PC2 is shown in **Figure 6-9**. In similar way to the μ_m PCA model, raw water samples were well separated from the biofilter biomass samples using PC1. Apparently, for this data set PC1 was also indicative of the overall functional diversity of the microbial communities. PC2 was able to separate biofilter biomass samples taken at warm and cold water conditions. Similar separation of warm and cold water conditions can be observed by studying the biplot of PC2 and PC3 shown on Figure 6-10. PC3 could also provide some separation of cold and warm water conditions by investigating the biplot of PC1 and PC3 as shown on **Figure 6-11**. This confirms the findings of the PCA model using the μ_m data set, showing that the differences among the cold and warm water conditions is only a small portion of the total variability between samples..
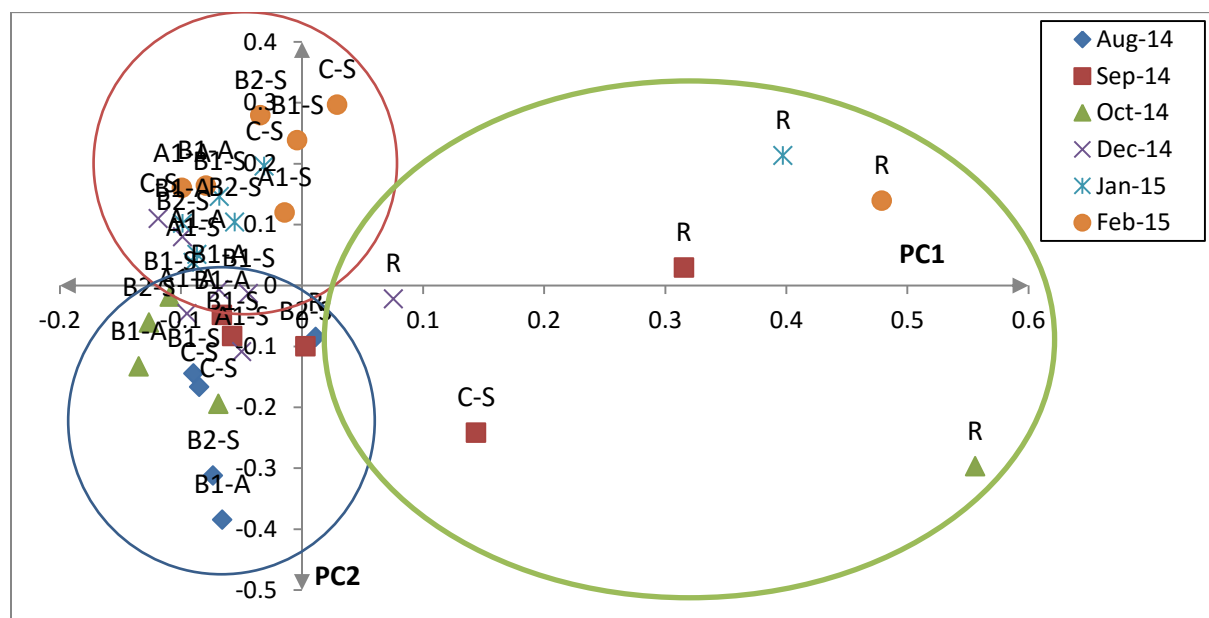
Figure 6-9 PCA biplot for PC1 and PC2 of the maximum colour density (A) data set showing sample scores
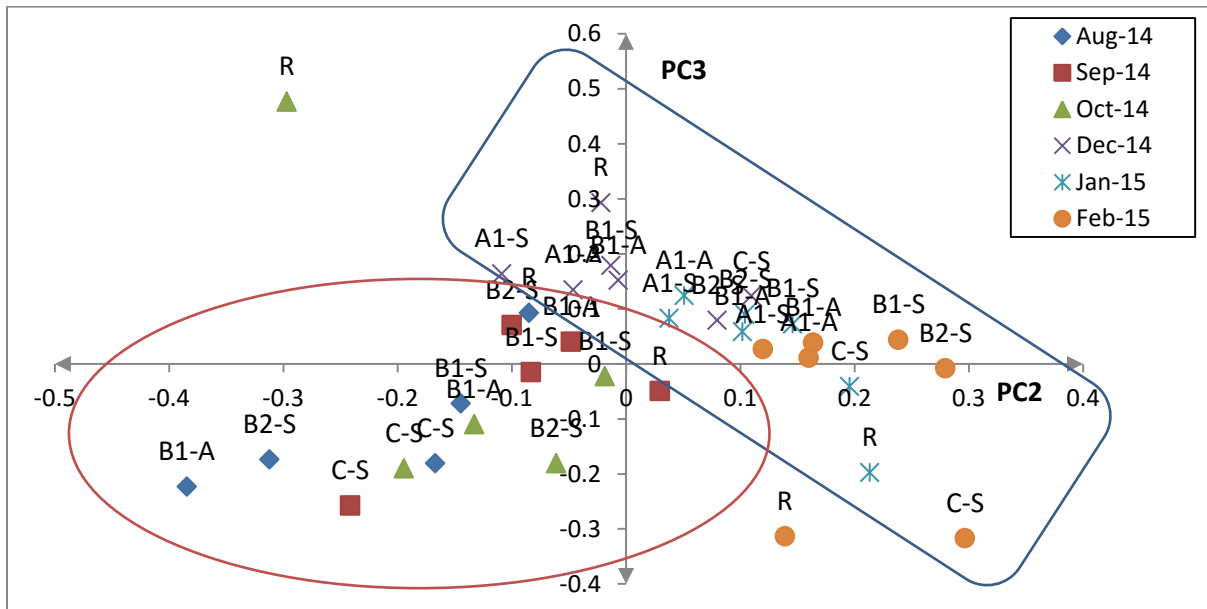
Figure 6-10 PCA biplot for PC2 and PC3 of the maximum colour density (A) data set showing sample scores
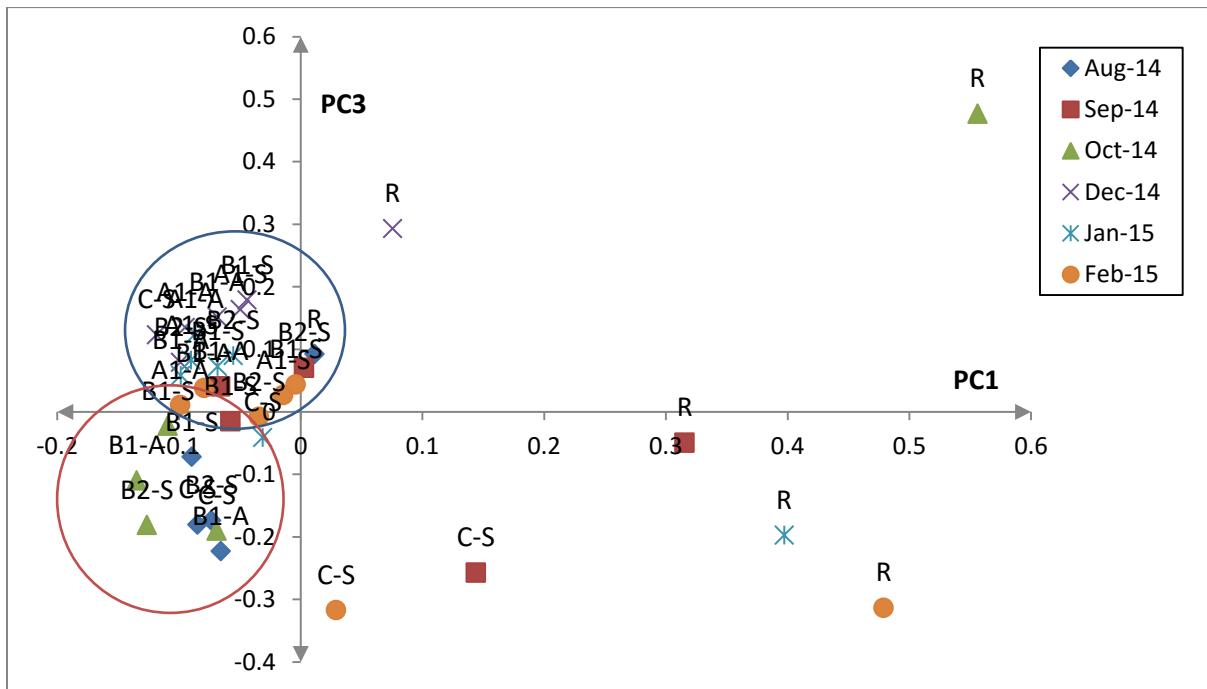
Figure 6-11 PCA biplot for PC2 and PC3 of the maximum colour density (A) data set showing sample scores

6.5 Conclusions

The current study aimed at investigating the differences in biofilter and freshwater microbial community functional diversity using samples collected as part of the biofilter performance study presented on **Chapter 4**. The study used CLPP techniques as they depend on the utilization of different carbon sources by the microbial community in the sample, which can be related to biofilter activity and BOM removal. By applying multivariate statistical analysis techniques, differences among the samples were observed, indicating differences in the microbial community functional diversity. Main conclusions are:

- Both hierarchical clustering and PCA were successful techniques in analyzing CSUPs data to investigate possible differences in microorganisms among the different samples.

- Freshwater (raw water) biomass was clearly different than the biofilter biomass using both hierarchical clustering and PCA analysis. PCA analysis showed some differences among the samples over the course of the study, but those differences could not be explained by the change in water temperature. The microbial populations in the raw water samples showed a much slower rate of substrate utilization compared with those in the biofilter samples.

- For hierarchical clustering, the maximum rate of colour development (μ_m) was better than the maximum optical density as a descriptor for the CSUPs results.

- The biofilter biomass samples collected from BF (C) at a total depth of 90 cm grouped separately from the rest of the biofilter biomass samples collected higher in the filter (at 20 and 60 cm), and had a slower rate of substrate utilization. This can be attributed to the observed nutrient gradient over the depth of the filter. This difference was observed using both μ_m and A as descriptors.

- No clear differences were observed between sand and anthracite samples from Bf (B) and BF (A) collected at the same samples depth, showing that the type of biofilter media had no effect on the microbial community activity or composition as measured by the CLPP technique.

- Samples at the middle of BF (B) at a total biofilter depth of 60 cm were not significantly different than the samples collected from 20 cm in the same filter.

- The differences among cold and warm water sampling events were observed using PCA, however, this difference accounted for only a small portion of the total variability within the data set.

- PCA models using μ_m were able to detect differences between the different sampling events, but only at the cold water conditions. This could be because the biofilter biomass was gradually

145

adapting to the environmental stress of the cold water temperature. The fact that no significant differences were observed among the sampling events done at warm water condition can be explained by the stable performance of the biofilter in this phase as explained in **Chapter 5**.

- The data suggests that the observed change in biofilter performance due to the drop in water temperature, as shown in **Chapter 5,** would be mainly attributed to a change in biomass activity, with only a small contribution due to a change in the in biofilter biomass microbial community as only small differences were observed among the samples at the high and low water temperature.

Chapter 7

Biological Filtration as a Pre-Treatment to Control Nanofiltration Membrane Biofouling

7.1 Summary

BF_{WP} is a promising pre-treatment technology for membrane applications. It is a green technology that can limit the use of chemicals and reduce the treatment process energy requirements. BF_{WP} can reduce membrane fouling, including high pressure membrane biofouling which is one of the main operational problems for NF membranes. A pilot scale BF_{WP} facility was used to test biofouling reduction of NF membranes using MFS test units. Biofilters with either 8 or 16 minute EBCT were able to reduce the observed increase in ΔFCP due to biofouling compared to a control without pre-treatment. The performance of the16 min EBCT BF_{WP} biofilter was similar to that of a full-scale conventional biofilter with extensive chemical pre-treatment, as no increase in ΔFCP was observed in both MFS units. Biofiltration was able to control the amount of accumulated biomass in the MFS units. BF_{WP} was also able to increase the time period needed until a significant increase in ΔFCP was detected. Furthermore, biofiltration was able to decrease the biofouling rate and resulted in a lower terminal ΔFCP at the end of the experiment. The developed biofilm in the MFS units fed with biofiltered water had lower biofilm cell count and EPS compared to the MFS units fed with raw water, which is consistent with the observed ΔFCP results. Additionally, biofiltration affected the microbial community of the developed biofilms in the MFS units based on their CSUPs data using Biolog EcoPlates. In general, BF_{WP} can extend the service life of high pressure spiral wound NF membrane elements by reducing biofouling.

1. Introduction

High pressure membrane filtration is a water treatment technology that is becoming more frequently used in water treatment, mostly in desalination and water reuse applications. High pressure membranes include both NF and RO membranes. NF membranes are mainly used to remove divalent cations from water along with DOC, synthetic organics, pathogens and taste and odour causing compounds (Bergman, 2007). Biofouling is a major operational problem for NF membranes, and happens when bacterial biomass starts growing within the feed channel of the membrane module causing reduced productivity. Biofouling can increase head loss within the membrane elements thereby increasing the pressure drop along these elements, enhance concentration polarization, increase module cleaning frequency, and eventually reduce membrane lifetime (Flemming et al., 1997). Therefore, fouling control is one of the key research topics for the high pressure membrane industry. Control strategies include membrane surface modification (Mansouri et al., 2010), improved cleaning protocols (Hijnen et al., 2012) or pre-treatment of feed water (van der Kooij et al., 2010). Pre-treatment of the feed water seems to be a sound alternative, as frequent membrane cleaning can shorten the membrane lifetime significantly (Bergman, 2007), and newer membrane material research still needs further validation before commercializing new products (Mansouri et al., 2010). Conventional surface water pre-treatment, including coagulation and sedimentation, was not found to be a successful biofouling control strategy (Baker et al., 1995; Schneider et al., 2005). However, biological treatment such as biologically active filtration is a promising pre-treatment technology for biofouling control. Griebe and Flemming (1998) showed that a sand biofilter with an EBCT of 40 minutes could efficiently reduce membrane biofouling by decreasing the amount of attached biomass on the membrane using settled river water. Van der Kooij (2010) concluded that single step conventional biofiltration or slow sand filtration can increase the membrane service time before cleaning to control biofouling.

BF_{WP} is a form of biofiltration where the media filter is used without any pre-treatment such as coagulation/sedimentation /ozonation that is commonly used with conventional biofiltration. In BF_{WP} raw water is fed directly to the biofilter may be preceded by a roughing filter to remove larger particles and to mitigate high turbidity events. BF_{WP} can effectively remove BOM present in the biofilter feed water as discussed in **Chapter 5** and in the literature (Huck and Sozański, 2008; Persson et al., 2006). BOM includes organic molecules that can serve as a substrate for the biofilm bacteria that cause biofouling in the NF modules. AOC is the easily biodegradable organic matter mainly used for bacterial regrowth

(Huck, 1990), and was found to be mainly composed of low molecular weight organics (Hem and Efraimsen, 2001). AOC was found to greatly affect membrane biofouling even at very low concentrations (i.e. 1 μg C/L) (Hijnen et al., 2009). Vrouwenvelder and van der Kooij (2001) reported excessive biofouling rates when the AOC of the membrane feed water exceeded 80 μg C/L. Other than the AOC fraction, BOM includes different NOM fractions that vary in molecular weight and source (Prévost et al., 2005). Biopolymers are the largest molecular weight NOM fraction and include both proteins and polysaccharides, and its main source is thought to be EfOM or bacterial activities within the surface water source (Huber et al., 2011). Biopolymers concentration in surface water was found to be highly correlated with the concentration of TEP (Villacorte et al., 2009), and especially the colloidal part of the freshwater TEP (Villacorte et al., 2015). TEP are sticky molecules than have an important role in the initial stages of biofilm attachment and growth which trigger membrane biofouling (Bar-Zeev et al., 2015; Berman and Holenberg, 2005; Berman et al., 2011). Biopolymers were found to be a highly biodegradable fraction as discussed in **Chapter 3,** and **Chapter 5** showed that BF_{WP} could remove both biopolymers and AOC at both high and low water temperatures. Others have also shown that BF_{WP} was an efficient pre-treatment to remove biopolymers (Hallé et al., 2009) and AOC (Persson et al., 2006).

Biofouling can be defined as biofilm growth on the membrane and feed spacer (Vrouwenvelder et al., 2009a). Biofilms are composed of two main components; bacterial cells and EPS. Bacterial cells compromise only 10% of the biofilm mass while EPS accounts for the remainder (Flemming and Wingender, 2010). EPS gives the biofilm its 3D structure and it includes a variety of molecules that determine the biofilm's physical and functional properties. EPS components include proteins, polysaccharides (i.e. carbohydrates), humic substances and extracellular DNA (Wingender et al., 1999b). The relationship among the different biofilm components and biofouling development is not well understood. However, attached biomass measured as biofilm cell count or ATP has been shown to be directly related to biofouling. For example, a biofilm cell count of 3×10^7 cell/cm^2 was shown to be sufficient to cover a membrane surface (Flemming and Schaule, 1988), and a value of 1×10^8 cell/cm^2 was indicative of severe biofouling (Flemming et al., 1993). ATP content of the biofouling layer was also reported to be directly correlated with observed biofouling rates, with ATP values above 10 ng ATP/cm^2 found to cause more than 100% increases in ΔFCP (Vrouwenvelder et al., 2008). Overall biofilm thickness was found to be directly correlated to biofouling rates, and a biofilm thickness of more than 20 μm was found to trigger biofouling (van der Kooij et al., 2010). In addition, high amounts of specific

components of the biofilm EPS, specifically polysaccharides (i.e. carbohydrates), were related to excessive biofouling (Fonseca et al., 2003; Gabelich et al., 2004).

In this study, BF_{WP} was tested as a promising pre-treatment technology for biofouling control of nanofiltration membranes. Pilot-scale filters were used on a challenging surface water source with high turbidity and organic loading. Two biofouling experiments were performed to test the efficiency of the technology at varying water temperatures. Also, a direct comparison of two different biofilter EBCTs was carried out to evaluate the significance of EBCT as a biofilter design parameter. A full-scale conventional biofilter was also tested to compare BF_{WP} as green per-treatment technology to biofiltration with extensive pre-treatment. To understand the role of biofiltration in biofouling control, the different components of the developed biofilms, such as bacterial cells and EPS, were quantified. CLPP, as described by Weber and co-authors (2008), was also used as a basic method to determine possible differences in the biofilm microbial community composition of the membrane biofilms . In this way, the underlying biofouling control mechanisms could be investigated, which is necessary for process optimization and for providing the necessary design criteria for biofilters as a biofouling control strategy.

7.2 Materials and Methods:

7.2.1 Experimental Setup

MFS test unit was used to investigate NF membrane biofouling. The MFS was developed at the Technical University of Delft by Dr. Hans Vrouwenvelder (Vrouwenvelder et al., 2006) to test the biofouling of high pressure membranes. The used MFS unit (Global Membrains, Netherlands) was made from PVC with a poly(methyl methacrylate) (PMMA) top to visually inspect the used membrane during operation. A schematic of the first MFS setup (UW MFS) is shown on **Figure 7-1-a**. The MFS is a flow cell that operates without permeation (i.e. vertical velocity component), and it houses a 20×4 cm membrane and feed spacer coupon to simulate the flow field in spiral wound membrane elements. The design flow rate was 16 L/h to achieve a cross flow velocity of 0.16 m/s which is commonly used in full-scale installations. The thickness of the flow cell is 0.93 mm, which is adequate to contain both a membrane and a feed spacer of the same total thickness. The rest of the components of the MFS test unit were sourced from local suppliers and assembled at the University of Waterloo. The membrane was a TS80 NF membrane (TriSEP Inc., USA), which is a thin layer composite aromatic polyamide membrane with an average divalent salt (i.e. $MgSO_4$) rejection of 99% and monovalent salt (i.e. NaCl) rejection of 93%

according to the manufacturer. The membrane thickness was 150 μm. The spacer was a PP diamond shaped spacer (DelStar Technologies Inc., USA). The spacer thickness was 0.031 inch (780 μm) and it had 9 strands per inch (SPI). A magnetically sealed centrifugal pump (EW-72012-10, Walchem, Iwaki America Inc., USA) was used to pump water at a maximum pressure of 32 PSI from a 20 L PVC collection tank (Figure 1-a). A 40 μm PP cartridge filter (Pentek DGD-5005-20, Pentair Canada Inc., Canada) placed after the pump was used to filter out large particles that can damage the MFS components or cause particle accumulation within the MFS unit and result in excessive head loss development or affect the biofilm development. A mechanical pressure controller (KPR1EFC417A20000, Swagelok, Canada) was used to control the feed pressure at 22 PSI, to prevent degassing and the formation of excessive air bubbles in the MFS feed water. A precise metering valve (SS-4L, Swagelok, Canada) was installed downstream of the MFS unit to set the flow at 16 L/h. A digital Pelton wheel flow meter (FLR1009, Omega, USA) was used to measure the flow rate and record it to a data logger (HOBO H22, Onset Computer Corporation, Canada). The temperature of the MFS unit effluent was measured using a digital temperature sensor (TMB-M002, Onset Computer Corporation, Canada). The MFS ΔFCP (i.e. head loss along the MFS unit) was measured using a differential pressure transducer (JD series, Honeywell , USA) with a detection range of 10 PSI and a resolution of 0.02 PSI. The initial ΔFCP (ΔFCP_0) for the membrane and spacer was 1.1 PSI. The different components of the MFS system were connected using polytetrafluoroethylene (PTFE) dark flexible tubing (Cole Parmer, Canada) to limit contamination of the feed water with trace organics commonly present in other types of flexible tubing (Parker and Ranney, 1996). Three parallel MFS units were built and used to test the biofouling on three different types of water. The MFS units were connected to the biofiltration pilot plant described in **Chapter 4**, to compare the biofouling rate of raw water and biofiltered water. The flow of each MFS unit was manually adjusted every 24 h back to the design flow rate and the ΔFCP value was recorded manually.

A more advanced system was also used to test membrane biofouling, and these experiments used the same type of membrane and spacer. The commercial bench-scale system (MFS-Minos unit, Convergence, Netherlands) with automated digital flow control capability is shown on **Figure 7-1-b**. The Convergence MFS flow cell had the same width and channel depth as the UW MFS setup from the TU Delft, but the length of the cell was with 12 cm a bit shorter. Two of these Convergence MFS systems were used to test two different types of feed water simultaneously. The units had remote control capabilities to allow constant monitoring of system performance. The feed water to the units was also filtered through 40

micron PP cartridge filters (Pentek DGD-5005-20, Pentair Canada Inc., Canada) and the feed pressure was kept at 22 PSI using a back pressure regulator (KBP1E0D4A5A20000, Swagelok, Canada). The pump was a positive displacement pump, unlike the centrifugal pump used in the UW MFS setup. The initial unit ΔFCP was 0.9 PSI. Unlike the first testing system, the on-line temperature sensor in the Convergence Minos system was installed upstream of the feed pump, which caused an underestimation of the actual temperature in the test cell by approximately 2°C, since the water would be warmed up due to the friction within the high pressure pump. The two Convergence MFS units were installed on the full-scale treatment train of the Mannheim Water Treatment Plant, and fed using either the raw water or the full-scale biofilter effluent. The data logger in the Convergence unit installed on the effluent line of the full-scale conventional biofilter stopped working towards the end on the biofouling experiment (850 h), but was fixed on the last day of the experiment (980 h) and a few more data points were recorded. Photos of both setups are shown in **Figure S1** of **Appendix F**.
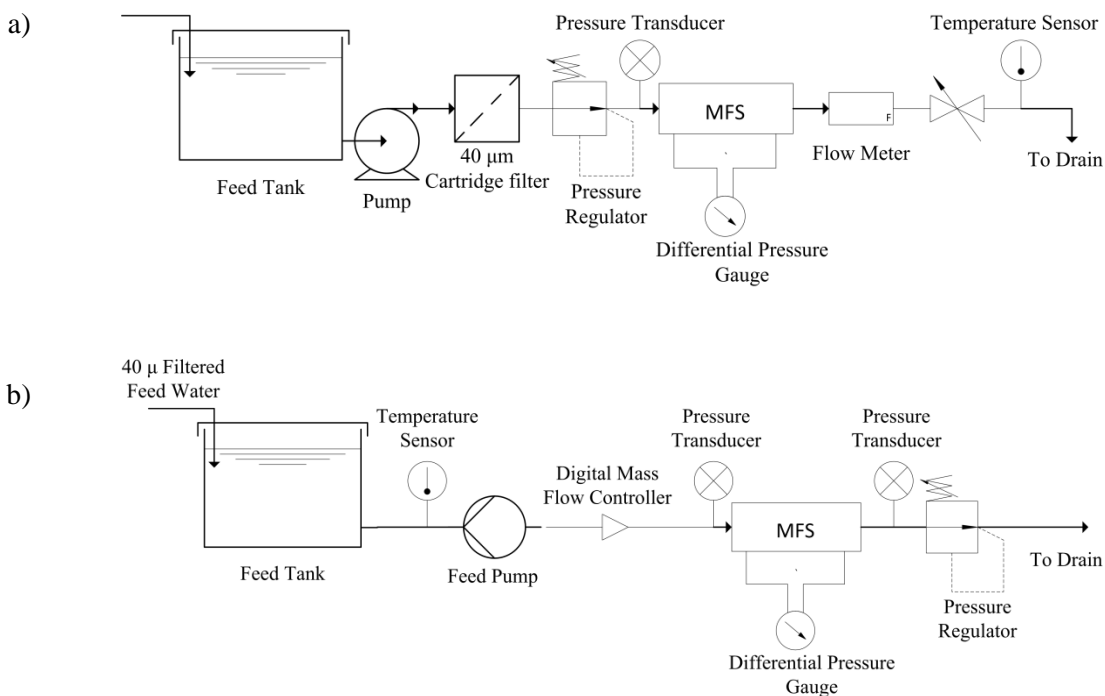
Figure 7-1 Schematic of (a) the UW membrane fouling simulator (MFS) test units or (b) Convergence Minos MFS unit (b)

7.2.2 Biofouling Experiments and Feed Water Quality

The UW MFS systems with manual flow controllers were used to test the biofouling potential of the raw (Grand River) and biofiltered water from the BF_{WP} pilot plant located at the Mannheim Water Treatment Plant described in **Chapter 4**. Two experiments were performed at different seasons to test the effect of raw water temperature on membrane biofouling. The first experiment was done in September 2014 when the water temperature was high (15 to 21°C). The first MFS unit was operated using raw water and the other two units were operated using the effluent of BF (B) which had an EBCT of 16 minutes to test the reproducibility of the measured biofouling rates. The second experiment was done in January 2015 when the raw water temperature was low (6 to 10°C). Raw water, BF (B) effluent and BF (A) effluent (8 minute EBCT) were tested using the MFS units to determine the effect of biofilter EBCT and low water temperature on the biofouling rates.
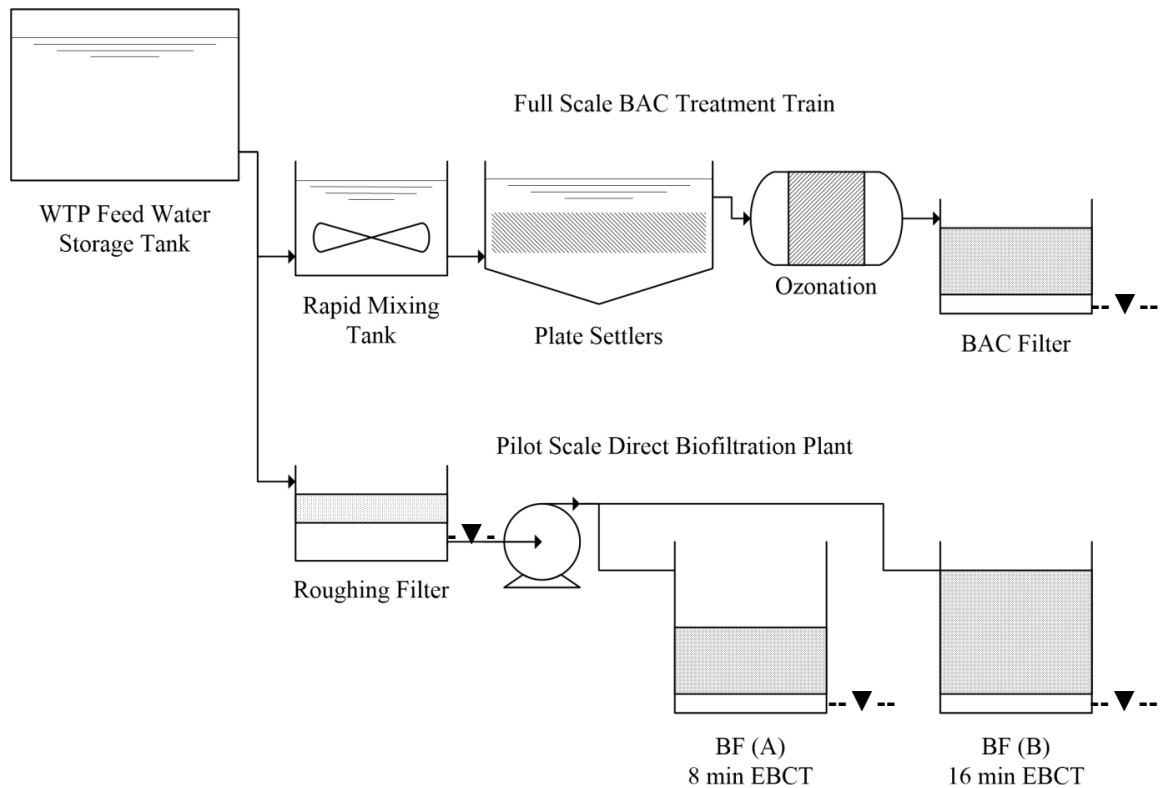
Figure 7-2 Schematic of the full scale water treatment plant (WTP) and the used direct biofiltration pilot plant showing the water sampling locations (--▼--)

The automated Convergence MFS test units were used to compare biofouling using the same raw water (Grand River) with the effluent of the Mannheim full-scale conventional biofilter #1. The filter depth was 1.07 m of GAC and 0.3 m of sand. The design EBCT for the filter was 10 min. The full-scale biofilter was preceded by a coagulation system using poly aluminum chloride (PACl) and a high rate plate settler. Also, an ozone dose of 2.5 to 3.0 mg O_3/L was applied before the filters, and residual ozone was quenched before the conventional biofilter. The conventional biofilter effluent before disinfection was used to feed the second Convergence MFS unit. A process flow diagram for the Mannheim full-scale plant and the BF_{WP} pilot plant is shown on **Figure 7-2**. **Table 7-1** shows the list of the water quality parameters monitored in the current study, and the methods for each parameter are described in **Chapter 4**. Water quality analysis was done every 2 weeks over the course of each biofouling experiment, and was measured for the raw water and each of the biofilter effluents.

Table 7-1 A list of the measured water quality parameters used for the study. Details of the methods are reported in Chapters 4 and 5

Temperature
Turbidity
Total Organic Carbon (TOC)
Dissolved Organic Carbon (DOC)
Ultraviolet light absorbance 254 nm (UV254)
Flow Cytometry:
Flow Cytometry Total Cell Count
LNA Bacteria count
HNA Bacteria count
Assimilable Organic Carbon (AOC)
Liquid Chromatography Organic Carbon Detector (LC-OCD) Analysis
Biopolymers Organic Carbon (OC)
Biopolymers Organic Nitrogen (ON)
Humics OC
Building Blocks (BB) OC
Low Molecular Weight Acids (LMWA) OC
Low Molecular Weight Neutrals (LMWN) OC
Fluorescence Spectroscopy
FEEM Protein-Like Response (FEEM A)
FEEM Humic Acid-Like Response (FEEM B)
FEEM Fulvic Acid-Like Response (FEEM C)

7.2.3 Membrane Autopsies

As the different MFS units were operated, biofouling started to develop as microbial biofilm started growing on the membrane surface. The experiments were terminated after the ΔFCP in any of the operated parallel units increased above 100% of the ΔFCP$_0$, which is defined as an indicator of excessive biofouling in this study. The first MFS experiment in September 2014 was terminated after 703 h (30 days) and the second MFS experiment in January 2015 experiment was terminated after 1008 h (42 days). At the end of each experiment, the feed pump to the MFS unit was switched off and the top of the MFS unit was removed. The fouled NF membrane and spacer were transferred using tweezers to a clean sterile glass container filled with the same feed water as the MFS unit. The glass containers were sealed and stored in the dark then transferred to the laboratory. The membrane and spacer were then cut using a scalpel into ten equal coupons (4×2 cm) over the length of the unit in the direction of the water flow using a machined template module fabricated at the University of Waterloo as shown in **Figure S2** in **Appendix F**. The membrane and spacer coupons sampled from the same location were stored in the MFS feed water in sterile plastic 10 mL PP tubes and stored at 4°C for ATP analysis and EPS extraction. The membrane and spacer were analyzed together so the analyzed biomass is the total biomass from the membrane and spacer. The analysis was done within 24 h after sample collection. A schematic showing the used membrane and spacer samples for each analysis is shown in **Figure S3** in **Appendix F**.

For the longer UW MFS units (20 cm length), a total of 6 coupons were analyzed for ATP and EPS (2 coupons for each assay, taken at start, middle and end of the feed channel). Two coupons were frozen right away in empty PP sterile tubes and stored at -80°C for future molecular biology, which was beyond of the scope of this study. Two more coupons were shipped to collaborators on the project to for further analysis using confocal surface laser microscope (CLSM), which is also not discussed in this study. For the shorter Convergence MFS units (15 cm length), a total of 4 coupons were analyzed for ATP and EPS (2 coupons each, taken at start and end of the feed channel). The remaining two coupons were used both for analyzing microbial community composition and CLSM analysis. A schematic showing the used membrane and spacer samples for each analysis is shown in **Figure S4** in **Appendix F**.

7.2.4 Biofilm Analysis

7.2.4.1 ATP Analysis

For ATP analysis, the membrane and spacer coupons were gently rinsed twice using the effluent of BF (B) to remove any loosely attached biomass. The rinsed membrane/ spacer were transferred to a sterile 15 mL PP sterile centrifuge tube. 5 mL of a commercial cell lysis buffer (Ultralyse 7, LuminUltra Technologies, NB, Canada) was added to lyse the bacterial cells and release the intercellular ATP. The tubes were vortexed at maximum speed for 1 minute. ATP measurements were then done in triplicate as described for the ATP method for biofilter biomass analysis in **Chapter 3**.

7.2.4.2 Biofilm EPS Extraction and Cell Count

The EPS extraction method used for the NF membranes/spacers was developed earlier in this study, and was similar to the CER extraction method described in **Chapter 3**. For EPS extraction, the membrane and spacer coupons were gently rinsed twice using BF (B) effluent to remove any loosely attached biomass. The membrane was rinsed two more times using 6 mM PBS to prevent any contamination NOM present in the BF (B) effluent. The membrane and spacer were then moved to a sterile 15 mL PP centrifuge tube and 12 mL of 0.2 µm filtered 6 mM PBS was added. Three 4 mm diameter acid washed glass beads (OPS Diagnostics LLC, USA), along with 1 g of rinsed CER, were added to the centrifuge tube. The tubes were loaded horizontally in a vortex mixer and vortexed at maximum speed for 1 h to detach the biofilm and dissolved the EPS. The tubes were then left stationary for a few seconds to settle the CER, and then the supernatant was transferred using a sterile pipette into sterile 5 mL micro centrifuge tubes. The tubes were centrifuged at 10,000 ×g for 20 min to harvest the bacterial cells. The supernatant was removed and filtered through a 0.2 µm PES syringe filter into an AOC clean 45 mL glass vial and stored at 4°C for further analysis. The cell pellets were resuspended and pooled in a final volume of 2 mL of autoclaved 0.2 µm filtered 6 mM PBS and stored at 4°C for further analysis. To determine the efficiency of the biomass extraction, the membrane and spacer coupons after EPS extraction were rinsed using 6 mM PBS then the remaining ATP content on them was determined as described above. The EPS total carbohydrates and proteins were analyzed using the phenol sulfuric acid and bicinchoninic acid photometric methods, respectively, as described earlier in **Chapter 3**. Also LC-OCD and fluorescence spectroscopy were used to analyze the composition of the biofilm EPS as described in **Chapter 3**. For the biofilm cell count, the

resuspended cells were diluted 1:10 in autoclaved sterile 6 mM PBS, then stained using SYBR Green I nucleic acid stain and counted using flow cytometry as described in **Chapter 3**.

7.2.4.3 Community Level Physiological Profiling (CLPP)

CLPP analysis of the MFS biofilm and feed water was done based on CSUPs in BIOLOG^{TM} EcoPlates (Biolog Inc., USA). For biofilm samples, the resuspended cell pellet after EPS extraction was diluted in autoclaved 0.2 μm filtered PBS to a concentration of 1×10^4 cell/mL, based on the flow cytometry total cell count. For MFS feed water, 4×5 mL sample of the feed water was centrifuged at 10,000 $\times$g, then the supernatant was decanted. The cell pellet was resuspended in autoclaved 0.2 μm filtered PBS to a concentration of 1×10^4 cell/mL according to the total cell count of the water before centrifugation. The Biolog EcoPlates analysis was done in the same way described in **Chapter 6**. Project R, a free statistical analysis software (R Core Team, 2015), was used to analyze the CSUPs results obtained from the Biolog Ecoplates to classify the functional diversity of the different microbial communities using hierarchical clustering or PCA techniques as described in **Chapter 6**.

7.3 Results and Discussion

Membrane biofouling is an important operational problem encountered during the use of high pressure spiral wound membrane elements. Biological filtration can efficiently remove nutrients to limit biofilm growth within the membrane modules and potentially reduce biofouling. In this study, both a pilot scale BF$_{WP}$ plant and a full-scale conventional biofilter were used to control biofouling in parallel MFS units. Both the pilot-scale and full-scale biofilters were located at the same municipal water treatment plant and were fed using the same river water.

7.3.1 Water Quality and Biofilter Performance

7.3.1.1 Experiment 1 (September 2014)

A summary of the water quality for the feed water to the MFS biofouling experiment operated on September 2014 is shown in **Table 7-2**. For this experiment, only the UW MFS units (**Figure 7-1-a**) were used. The first MFS unit was operated using raw water and the second and third MFS units were both operated using BF (B) effluent to test the reproducibility of the treatment. The raw water temperature in September ranged between 15 and 21°C, while the BF (B) effluent was 2°C higher (17 to 23 °C) due to warming of the water as it flowed through the biofilter media. Hourly average temperatures of both

streams are shown on **Figure S5** of **Appendix F**. The river water temperature range was 2 to 25°C as shown on **Figure S3** in **Appendix B**. High temperatures would be expected to promote bacterial growth and biofilm formation and result in fast biofilm growth within the MFS units.

Table 7-2 Summary of the water quality parameters for the feed water to the different MFS units used for the first biofouling experiment on September 2014 (n=4)

Parameter	Unit	Raw Water		Biofilter (B) Effluent		
		MIN	MAX	MIN	MAX	% R
Temperature	°C	15	21	17	23	NA
Turbidity	NTU	3.1	6.7	0.25	0.43	93±1
TOC	mg C/L	5.71	7.10	5.01	6.18	13.8±2.4
DOC	mg C/L	5.95	7.02	5	6.131	13.8±3
UV254	cm^{-1}	0.1729	0.218	0.1587	0.2025	7±1.2
LNA Bacteria	Cell/mL	1.1×10^6	1.4×10^6	5.5×10^5	7.0×10^5	50±2
HNA Bacteria	Cell/mL	1.5×10^6	1.6×10^6	4.7×10^5	5.3×10^5	68±3
Total Cell Count	Cell/mL	2.8×10^6	3.0×10^6	1.0×10^6	1.3×10^6	60±3
AOC	μg C/L	185	232	132	171	30±9
Biopolymers OC	μg C/L	320	425	90	160	67±14.3
Biopolymers ON	μg N/L	35	69	13	20	68±5.7
Humics OC	μg C/L	3760	4880	3525	4385	8.1±2
BB OC	μg C/L	927	1112	830	930	9.6±3.7
LMWA OC	μg C/L	160	273	110	240	19±8.8
LMWN	μg C/L	440	525	410	470	9.5±11.2
FEEM Protein-Like Response	I.U	50	52	36	39	26±4
FEEM Humic Acid-Like Response	I.U	357	428	343	409	4±0.6
FEEM Fulvic Acid-Like Response	I.U	321	382	298	357	6±2

The river raw water had relatively high turbidity, but BF (B) efficiently removed 93% of the raw water turbidity, indicating that the biofilter was efficiently performing its basic task as a media filter without coagulant addition. Additionally, DOC removal within the filter was nearly 14%, which is similar to results for the same filter measured between August and October 2014 as reported in **Chapter 5**. Also similar to results in Chapter 5, the best removed LC-OCD fraction was the biopolymer fraction, with an average removal of 67% for both the organic carbon (OC) and organic nitrogen (ON) content of this

fraction. Average removals of the other LC-OCD fractions were lower, and on average were 19% for the LMWA and below 10% for the humics, humic building blocks and LMWN. Fluorescence spectroscopy yielded similar results to the LC-OCD data. The protein-like substances response (FEEM A) was efficiently reduced by the filter (average removal 26%), and can be linked to the biopolymer organic nitrogen removal, since proteins are a main contributor to the biopolymers fraction (Huber et al., 2011). Humic acid-like (FEEM B) and fulvic acid-like (FEEM C) substances were removed below 10%.

AOC can largely influence biofouling rates, as AOC can be readily utilized by the biofilm bacteria attached to the membrane surface. (Hijnen et al., 2009) showed that increasing acetate concentrations between 1 and 25 μg C acetate /L were related to an increase in the biofouling rate in MFS units, and an acetate concentration beyond 25 μg C acetate /L caused an exponential increase in biofouling rates. Earlier studies reported a maximum AOC value of 10 μg C acetate /L to achieve biological stability in drinking water distribution systems as measured using the standard AOC method (van der Kooij, 1992). The Grand River used in the current study had a high AOC level (180 to 230 μg C acetate /L) using the flow cytometry AOC method presented in **Chapter 4**, but BF (B) was able to efficiently remove AOC by approximately 30%. Additionally, BF (B) was able to reduce the total cell count by 60%, which can result in a significant reduction of the fresh biomass loading on the membrane surface. HNA bacteria were better removed than LNA bacteria, with removal values of 68% and 50%, respectively. HNA were previously found to form the majority of the biofilm population on media samples from the same biofilter as shown in **Chapters 3** and **5**.

7.3.1.2 Experiment 2 (January 2015)

For the second MFS experiment on January 2015, raw and biofiltered water quality are shown on **Table 7-3**. For this experiment, the raw river water temperature was lower at 6 to 10°C. The effluent of both BF (A) and BF (B) had a higher temperature of 10 to 15 °C. The temperature range in this experiment is approximately 5°C lower than that of the first MFS experiment on September 2014. This drop in temperature was expected to cause slower biofilm growth and biofouling development. However, lower water temperatures can also affect biofilter performance, since it was previously shown in Chapter 5 that there was less removal of dissolved organics at colder temperatures. The biofilter performance as a biofouling control pre-treatment technology was therefore tested under winter conditions, and its overall performance was expected to drop at this lower temperature. BF (A) had an EBCT of 8 min (total depth 40 cm), while BF (B) had an EBCT of 16 min (total depth 80 cm). Comparing the two biofilters can show

whether biofilter EBCT can affect the obtained biofouling rates. BF (A) and BF(B) had a very similar hourly average temperature range as shown on **Figure S6** of **Appendix F**.

BF (A) and BF (B) efficiently removed turbidity by 71 and 79%, respectively (**Table 7-3**), which was lower than the turbidity removal by BF(B) obtained during the first experiment (93%) (**Table 7-2**) due to the drop in water temperature. This decrease in biofilter performance can be attributed to the effect of the water temperature on the transport of colloidal and particulate material within the biofilter bed, and as a result it would affect the attachment efficiency of particulates and colloids within the filter. BF (B) had a higher turbidity removal than BF (A) by approximately 8% due to the increase in filter depth. DOC removal was nearly the same within both filters. It was approximately 10%, which is slightly lower than the observed DOC removal in the first experiment (14%). In the second experiment, biopolymers OC was still the best removed fraction, with removals of 27% and 32% in BF (A) and BF (B), respectively, but this was about ½ the value of the first experiment. Biopolymers ON or FEEM A removals were the same among the two filters, indicating that removal of protein-like substances was not affected by the increase in EBCT. The FEEM A removal by BF (B) was also lower compared with the first experiment. The remaining LC-OCD fractions were removed similarly by the biofilters, but to a lower extent than the biopolymers. These results had some high variability as shown by the high standard deviation values. Water temperature did not affect the removal of the humics/humic building blocks or the LMWA and LMWN fractions which becomes apparent when comparing their values in **Table 7-2** and **Table 7-3**.

AOC was efficiently reduced within both filters, and an average AOC removal of 29 and 34% was achieved in BF(A) and BF (B), respectively (**Table 7-3**). The observed AOC removal within both the biofilters varied significantly during the experiment as it ranged from 5% to 63% (n=5), which makes it harder to compare the filters. The variability can be attributed to the large change in water quality due to the spring run-off that happened by the end of March 2015 as discussed earlier in **Chapter 4** as the AOC values increased nearly by 400%. Total cell count reduction by the biofilters was also affected by the temperature drop, and removal was reduced to approximately 35% in both filters. HNA was still reduced by the biofiltration step at a greater extent compared to the LNA bacteria. HNA bacteria were removed in BF (B) by 50% compared to 14% for LNA bacteria.

Table 7-3 Summary of the water quality parameters for the feed water to the different MFS units used for the second biofouling experiment on January 2015 (n=5)

Parameter	Unit	Raw Water		Biofilter (A) Effluent			Biofilter (B) Effluent			Full Scale BAC		
		MIN	MAX	MIN	MAX	% R	MIN	MAX	% R	MIN	MAX	% R
Temperature	°C	6	10	10	15	NA	9	15	NA	4	7	NA
Turbidity	NTU	1.17	7.34	0.37	1.88	71±9	0.31	0.93	79±11	0.05	0.12	96±3
TOC	mg C/L	5.12	7.77	4.84	6.93	9±4	4.78	6.59	10±6	3.20	4.24	41±4
DOC	mg C/L	5.12	7.64	4.82	6.83	10±5	4.80	6.61	10±5	3.13	4.26	42±4
UV254	cm^{-1}	0.132	0.145	0.13	0.144	1±1	0.13	0.143	1±1	0.036	0.04	73±1
LNA Bacteria	Cell/mL	6.2×10^5	1.5×10^6	5.7×10^5	1.2×10^6	17±6	5.9×10^5	1.1×10^6	14±10	1.2×10^4	3.6×10^4	98±1
HNA Bacteria	Cell/mL	7.6×10^5	3.4×10^6	5.0×10^5	1.6×10^6	46±12	4.6×10^5	1.4×10^6	50±21	8.0×10^3	3.7×10^4	98±1
Total Cell Count	Cell/mL	1.4×10^6	4.9×10^6	1.1×10^6	2.8×10^6	34±11	1.1×10^6	2.6×10^6	36±18	2.4×10^4	7.3×10^4	98±1
AOC	µg C/L	166	1132	103	954	29±19	120	733	34±20	91	285	52±19
Biopolymers OC	µg C/L	125	1023	102	772	27±6.5	89	814	32.3±8.7	60	291	64.8±8.8
Biopolymers ON	µg N/L	2	70	7	61	20±8.5	3	56	20.3±9	0	19	81.3±14.7
Humics OC	µg C/L	1499	3848	1534	3614	5.5±1.5	1513	3574	4.5±3	799	1926	47.7±5.2
BB OC	µg C/L	371	873	309	923	13.3±4.7	345	862	5±2.7	325	921	4.8±5.2
LMWA OC	µg C/L	44	191	44	143	13.5±12.2	36	148	23.2±5.3	39	198	-2.9±9
LMWN	µg C/L	263	992	242	819	15.8±6.9	236	752	17.4±7	205	714	22±3.7
FEEM Protein-Like Response	I.U	45	104	41	68	9.5±0.7	40	67	10.6±2.8	8	14	81±1.4
FEEM Humic Acid-Like Response	I.U	299	354	296	350	1.4±0.5	294	346	1.4±0.9	54	73	82.6±1.7
FEEM Fulvic Acid-Like Response	I.U	266	305	260	303	1.3±0.5	259	298	1.8±1.1	44	64	83.9±1.5

A full-scale conventional biofilter was also used in the second experiment (January 2015) to test the ability of conventional biofiltration to limit membrane biofouling. This filter was preceded by extensive pre-treatment including coagulation/ sedimentation and ozonation steps. The water temperature of the raw water and the biofilter effluent used to feed the Convergence MFS units is shown in **Figure S5** in **Appendix F**. The temperature of the full scale filter effluent was nearly the same as the raw water temperature due to the high water flow in the full scale treatment train that did not allow the water to warm up. The raw water convergence unit used the raw water feeding the BF_{WP} pilot plant after the used roughing filter to reduce particle loading. The long feed line for the pilot plant and its low flow rate caused the water to warm up a bit as shown on **Figure S5** in **Appendix F.**

Full-scale pre-treatment and conventional biofilter removed 96% of the raw water turbidity, with an effluent turbidity less than 0.12 NTU. DOC was removed by 42%. These removal values were higher than the pilot-scale BF_{wp}, which was expected since the full-scale BAC has extensive pre-treatment steps (Croft, 2012). The increase in DOC removal is due to the higher removal of humic substances during pre-treatment, and resulted in 47% humic substances removal. Specific removal of NOM along the treatment train was not evaluated as part of the current study. Pre-treatment combined with BAC filtration also resulted in high biopolymer OC and ON removal at 65% and 81%, respectively. Removal of the LMWN fraction was 22%, and the LMWA fraction stayed basically the same when comparing raw water to full-scale biofilter effluent. However, LMWA are generated during ozonation and then removed by the full-scale biological filter. This process train seemed to function well as no substantial increase in LMWA was observed. These results are consistent with reported results for the same full scale train by Croft (2012). All the fluorescence components were also removed efficiently by 80% within the full-scale pre-treatment/conventional biofilter. AOC was removed by 52% from the raw water through full-scale pre-treatment/ conventional biofilter, which is better than the BF_{WP} filters; however, this is likely due to the ozonation step in the full-scale plant. Ozonation can break up complex NOM molecules into smaller molecules which result in a spike in the ozonated water AOC concentration (e.g. Hammes et al., 2006). Those ozonation by-products can be easily biodegraded by the biomass present in conventional biofilters. Finally, bacterial cells present in the raw water were removed by more than 98% as shown by the total cell count. This is likely because ozonation efficiently killed the bacterial cells in the water, causing such a significant drop in the number of bacterial cells reaching the membrane surface in the MFS unit.

7.3.2 MFS Biofouling Development

In each experiment, water was passed through the MFS flow cells and the ΔFCP was monitored continuously. Over time, the ΔFCP increased due to increased hydraulic resistance within the feed

channel of the MFS units due to biofilm growth. The ΔFCP profile over the course of the first biofouling experiment done in September 2014 is shown on **Figure 7-3**. Unit #1 was operated using the raw river water after the roughing filter, while units #2 and #3 were both operated using BF (B) effluent. Results showed that units #2 and #3 had essentially identical ΔFCP profiles over the whole experiment, showing that the treatment effect was reproducible. Unit #1 operated with the raw river water, and showed an increase in ΔFCP (i.e. > 5% ΔFCP_0) starting at 100 h of operation, and at 270 h of operation the ΔFCP increased rapidly, with a terminal increase in ΔFCP to 1.4 PSI (125% ΔFCP_0) occurring after 700 h of operation. The linear rate for ΔFCP increase by the end of the experiment between 290 and 700 h of operation was 0.07 PSI/day. For Units #2 and #3 operated using BF (B), an increase in ΔFCP (i.e. > 5% ΔFCP_0) was only observed after 460 h of operation. After 700 h of operation, the terminal increase in ΔFCP was 0.28 PSI (24% ΔFCP_0) and the observed linear rate of ΔFCP increase between 410 and 700 h of operation was 0.02 PSI/day. Biofiltration could efficiently prolong the initial acclimation phase needed to start the developing of biofouling as detected using ΔFCP monitoring.
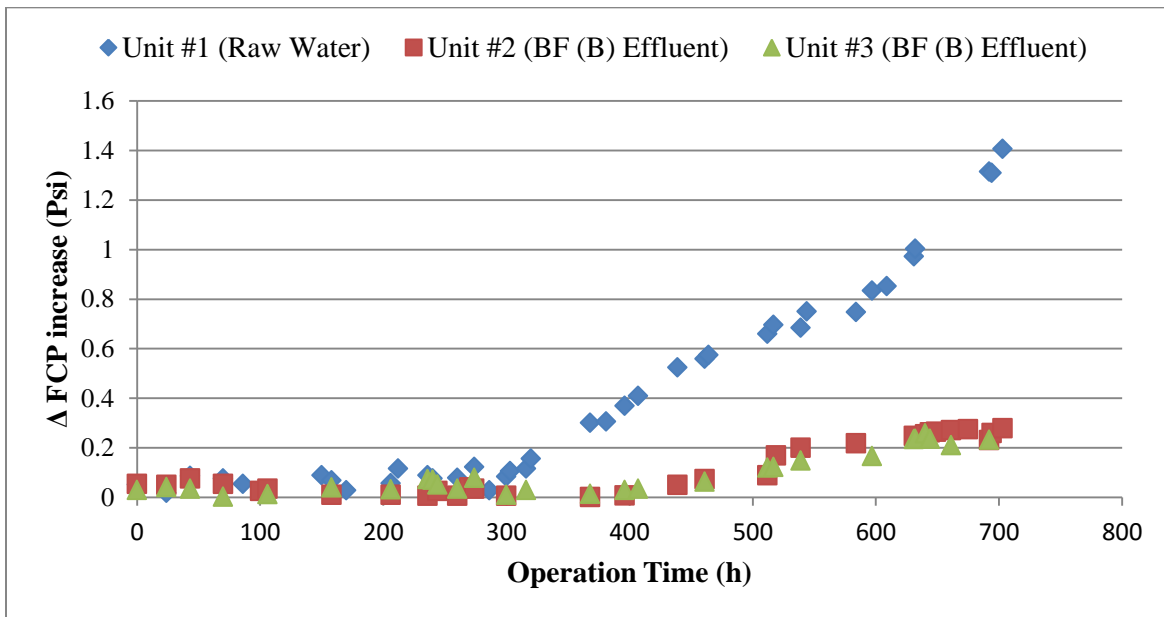
Figure 7-3 Increase in feed channel pressure drop (ΔFCP) within the feed channel of the UW MFS units within the biofouling experiment on September 2014

Differences in biofouling rates or acclimation periods can be attributed to different factors. The first factor is the possible differences in the nutrient levels such as AOC due to the biofiltration pre-treatment. A second factor is the amount and type of conditioning macromolecules present in the water such as

biopolymers or TEP which can affect the biofilm acclimation process. Although TEP was not measured in this study, Villacorte and co-workers (2015, 2009) found the TEP was correlated with biopolymer concentration. A third factor is the possible differences in the feed water microbial community which can also affect the biofilm microbial community and the biofouling rate. In the current MFS experiment, the observed difference in the initial acclimation period can be attributed to the differences in the observed biofouling rates as the biofiltered water biofouling rate was only 28% of the biofouling rate of the raw water. Results in **Table 7-2** showed that BF (B) could efficiently reduce the biopolymers and reduce biomass loading in the MFS feed water. Both of these factors could potentially explain the observed delay in the biofouling development, since biopolymers such as TEP can condition the membrane surface for bacterial attachment (Bar-Zeev et al., 2015; Berman and Holenberg, 2005). Also, BF (B) reduced the amount easily biodegradable carbon sources available in the MFS feed water, as shown by the reduction in AOC. A third explanation relates to possible differences in the microbial community composition of the biofilms that developed in the MFS feed channels fed with either raw or biofiltered water, where biofilm growth kinetics may have played a role. This final explanation was investigated using CLPP and is discussed in section 7.5.4.

The differences in biofoulant accumulation among the different MFS units were obvious by visual inspection of the MFS units as shown on **Figure 7-4**. The biofilm developed mainly on the membrane and spacer of MFS unit#1 (raw water), (**Figure 7-4-a**) and filamentous biofilm structures (i.e. streamers) that can move with the water flow were observed. This is in agreement with results in the literature for biofouling studies (Vrouwenvelder et al., 2006, 2009a) and for computational fluid dynamics (CFD) modeling (Vrouwenvelder et al., 2010). Some of the biofilm seemed to develop on the membrane away from the feed spacer, but it was not as abundant as the biofilm that formed on the spacer and particularly near the spacer intersections. For unit#2 that operated using the BF (B) effluent, the biofilm can be seen mainly on the feed spacer and not on the membrane. In this case, the developed biofilm was much less visible compared to unit#1, which can be attributed to the lower extent of biofouling. It is also possible that differences in the feed water quality, such as turbidity, could cause some particles or colloids present in the feed water to become incorporated in the biofilm and make it more visible.
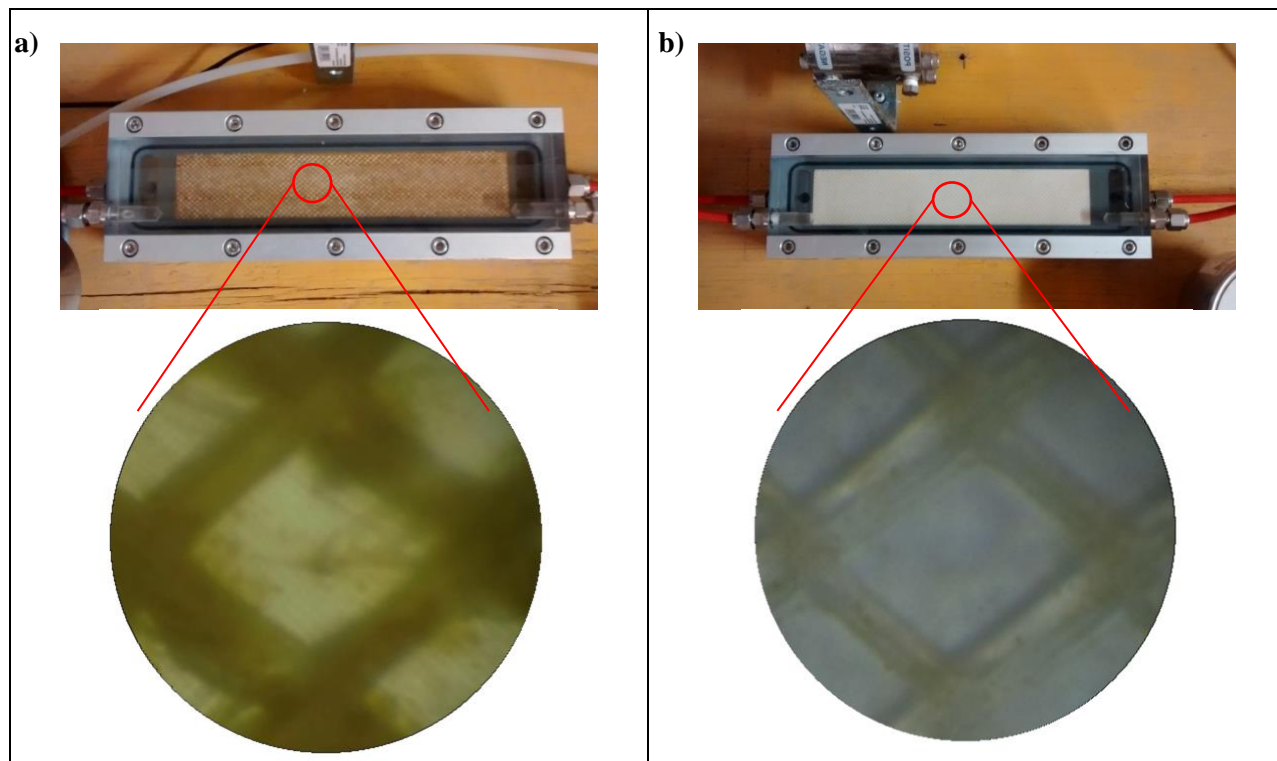
Figure 7-4 Photos of the used MFS units fed with (a) raw water (unit#1) and (b) BF (B) effluent (unit#2) during the first MFS biofouling experiment on September 2014 after 26 days of operation

In the second MFS experiment (January 2015), raw water and the effluent of BF (A) and BF (B) were used to run the three UW MFS units. The development of biofouling as indicated by ΔFCP increase for the three units is shown on **Figure 7-5**. Unit#3 was operated using the raw river water, and a significant increase in ΔFCP (i.e. > 5% ΔFCP_0) was observed at 270 h of operation, compared to 100 h in the first MFS experiment. This is likely due to the lower water temperature along with differences in water quality. After 700 h of operation, the ΔFCP started to increase linearly at a rate of 0.07 PSI/day which is identical to the rate observed in the first MFS experiment for raw water. This shows that the change in water temperature or water quality had a significant impact on the acclimation period of biofouling development, but did not affect the biofouling rate. At the end of the experiment after 1000 h of operation, the ΔFCP increased by1.14 PSI (110% ΔFCP_0), which is only slightly lower than the terminal ΔFCP in the first MFS experiment. For unit#2 fed with BF (B) effluent (16 min EBCT), no increase in ΔFCP was observed over the entire experiment (1000 h). The terminal ΔFCP at the end of the experiment was only 0.02 PSI, which is equal to the resolution of the differential pressure gauge, so no biofouling

was observed during the course of the experiment. Again, compared with BF (B) results from experiment #1 (September 2014), this shows that biofilm development in the MFS units was greatly affected by season, either due to lower water temperatures or changes in water quality.
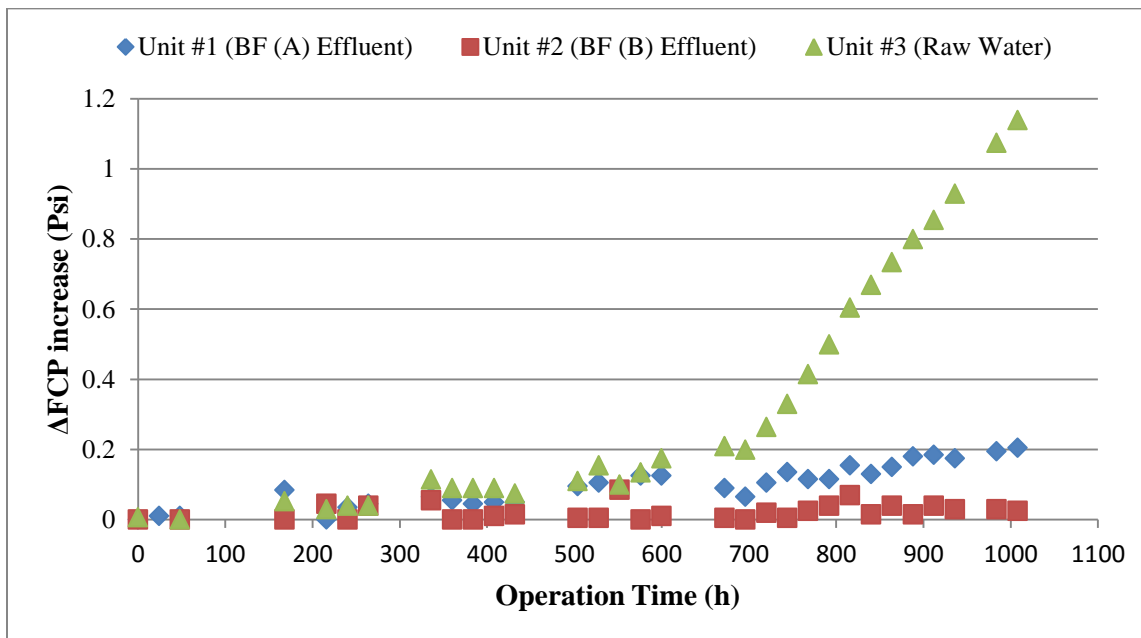
Figure 7-5 Increase in feed channel pressure drop (ΔFCP) within the feed channel of the UW MFS units within the biofouling experiment on January 2015

For unit#1 fed with BF (A) effluent (8 min EBCT), a significant ΔFCP increase was observed at 500 h of operation, which is nearly double the time observed for unit#3 fed by raw water. This occurred even though the BF (A) effluent has a slightly higher (2°C) water temperature than the raw water (as reported in **Table 7-3**) and this is similar to the observation in the first MFS experiment. The observed linear rate of ΔFCP increase was found to be 0.001 PSI/hr, which is 14% the rate for the raw water. After 1000 h of operation, the ΔFCP in the BF (A) fed unit increased only by 0.2 PSI (19% $ΔFCP_0$). In comparing MFS units fed using BF (A) and BF (B), results show that increasing the biofilter EBCT from 8 to 16 min could completely prevent an increase in ΔFCP due to biofouling. BF (B) only had slightly better water quality compared to BF (A) as shown in **Table 7-3** and both units had very similar water temperature over the course of the experiment as shown on **Figure S6** in **Appendix F**. No clear explanation for the effect of the biofilter EBCT on biofouling could be drawn based on the water quality analysis, however, biofilm analysis and microbial community composition might provide additional information.

For the comparison between raw water and full-scale-conventional biofilter using the Convergence MFS, the ΔFCP increase over the course of that experiment is shown on **Figure 7-6**. The Convergence unit#1 was fed using the raw river water after the roughing filter of the pilot plant while unit#2 was operated using the effluent of the full-scale conventional biofilter. The temperature profiles of both units are shown on **Figure S7** in **Appendix F**. An important note for the Convergence units is that the temperature is measured upstream of the high pressure pump, which causes an underestimation of the actual feed temperature to the MFS flow cell. In fact, the pump was found to increase the MFS feed water temperature by approximately 2°C, as determined by several manual measurements taken during the experiment. The biofilter effluent temperature was slightly lower the river raw water and this was because the raw water was taken from the same feed water tank as the other MFS setup; since this tank was located after the pilot plant roughing filter and feed pump it caused this slight increase in water temperature.
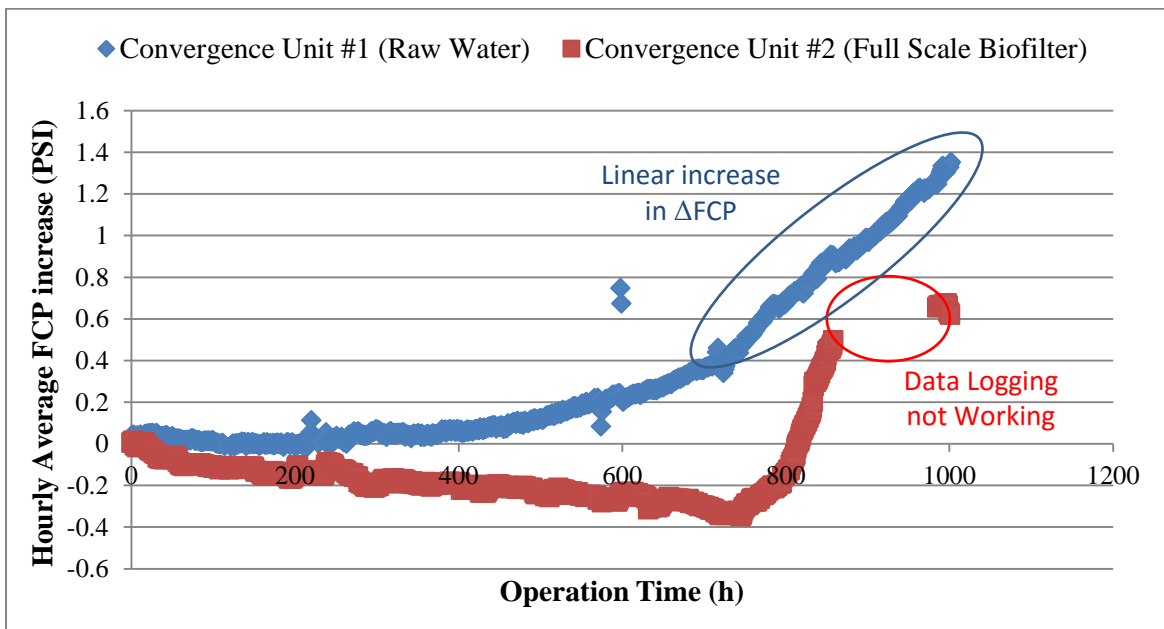
Figure 7-6 Hourly average head loss development within the feed channel of the convergence MFS units within the biofouling experiment on January 2015

For convergence unit#1 fed with raw water, a significant amount of fouling (i.e. > 5% ΔFCP_0) started to occur after 270 h of operation, which is the same as the UW MFS unit#3 that was also operated using raw water. Beyond this point, the ΔFCP increased gradually, and the linear part of the ΔFCP curve occurred

167

after 700 h of operation as indicated in **Figure 7-6**. The linear rate of ΔFCP increase was found to be 0.077 PSI/day, which is slightly higher than the observed rate of 0.070 in MFS unit#3 also fed with raw water. However, the Convergence unit is shorter (12 cm) than the standard UW MFS unit (20 cm), so if the ΔFCP rate of increase is normalized by the unit length, the Convergence unit will have significantly higher normalized rate of ΔFCP increase (0.64 PSI/m.day) than the UW MFS unit (0.35 PSI/m.day). This can be contributed to the higher nutrient flux going into the Convergence unit due to automatic flow adjustment, compared to the UWMFS unit that was adjusted manually once per day. This difference in flow adjustment method will also cause more shear force to be exerted on the biofilm in the Convergence unit, and higher shear force has been shown to increase the observed biofouling rate in MFS units (Bucs et al., 2014). At the end of the experiment after 1000 h of operation, the terminal ΔFCP increase for the Convergence unit#1 was 1.35 PSI (150% ΔFCP_0). In general, the Convergence MFS unit and the UW MFS unit had a similar acclimation period for biofouling development, but the Convergence unit had a higher rate of ΔFCP increase, which can be explained by the higher nutrient flux and shear force.

For the Convergence unit#2 fed with the effluent of the full scale conventional biofilter, the ΔFCP decreased steadily for the first 750 h of operation, then increased rapidly to a ΔFCP increase of 0.6 PSI at around 900 h of operation and remained stable until the end of the experiment. This rapid increase did not seem to be due to biofilm growth as no biofilm was visible in the test unit. The biofilter effluent had a high level of dissolved oxygen (DO) (> 10 mg O_2/L) due to ozone quenching using calcium thiosulfate which releases dissolved oxygen. The high DO concentration could have possibly affected the differential pressure transducer and caused a discrepancy in the ΔFCP readings. Membrane autopsies at the end of the experiment were used to identify if this increase was due to biofilm growth or due to a problem with the test setup, and these results are discussed in the next section.

7.3.3 Characterization of Attached Biomass

The developed biofilm on the membrane and spacer coupons was characterized to understand how the biofilm characteristics were related to the observed biofouling rates. Membrane and spacer coupons obtained at the same point in the MFS unit were analyzed together at the same time at the end on the biofouling experiment. Also the effect of biofiltration on the characteristics of the developed biofilms was investigated. The observed ATP recovery (i.e. difference in sample ATP before and after extraction over sample ATP before extraction) from the membrane samples through the EPS extraction process ranged between 92% and 98% (n=3). This shows that the extraction method could effectively remove biomass

from the membrane/spacer surface, and the characterized EPS fraction would be representative of the total biofilm mass. The average biofilm properties from the three MFS units in the first experiment (September 2014) is shown in **Figure 7-7**. Each column in the figure represents the average value of the three samples collected from the start, middle and end of the membrane/spacer. The bars on each column show the range of the value. Detailed biomass distribution data over the length of each test unit is shown in **Figure 7-8**. MFS unit#1 fed with the raw water had the highest ΔFCP increase and biofouling rate, and also had significantly higher biomass measured as either ATP content or biofilm total cell count. The biofilm cell count in unit #1 was 5×10^7 cell/cm^2 compared to 2.1×10^6 and 2.6×10^6 cell/cm^2 in units #2 and #3, respectively. Since the unit #1 cell count was higher than 3×10^7 cell/cm^2, this would indicate the biofilm is covering the whole membrane surface (Flemming and Schaule, 1988), unlike the units #2 and #3 that were fed with biofiltered water, which would be expected to have a patchy biofilm due to their lower cell count ($<3 \times 10^6$ cell/cm^2). Similarly, the average biofilm ATP content in unit #1 was 44 ng ATP/cm^2 compared to 7.6 and 7.9 ng ATP/cm^2 in units #2 and #3, respectively. The membrane/spacer samples from each MFS unit had a small range for the biofilm ATP content and total cell count, which would indicate that the biofilm formation over the MFS length did not change. EPS total proteins and carbohydrates followed a similar trend. Average EPS total protein content in unit #1 was 8.6 μg BSA /cm^2 compared to 2.3 and 2. μg BSA /cm^2 5 in units #2 and #3, respectively. Average EPS total carbohydrates in unit#1 was 3.6 μg D-glucose /cm^2, but in units #2 and #3 the total carbohydrates was below the detection limit of the phenol sulfuric acid method (1.5 ng D-glucose/cm^2). Biofilm EPS, ATP and total cell count data were all in agreement, and show that BF (B) was able to limit the overall biofilm growth within the MFS units fed with the biofilter effluent. The terminal ΔFCP increase was 125% for unit #1 compared to only 24% for units #2 and #3, which is in close agreement with the biofilm ATP and total protein content. This data was also similar to the HMW total organic carbon content of the biofilm EPS as measured by LC-OCD analysis (**Figure 7-9-a**). Observed differences in the extent of biofouling can be attributed to the accumulated biomass in the units, however no obvious differences in the biofilm relative composition can be observed. The only difference of note was that the carbon to nitrogen (C/N) ratio of the high molecular weight EPS (HMW EPS) fraction as measured by LC-OCD was slightly lower in the MFS unit#1 compared to units#2 and #3 (**Figure 7-9-b**). This fraction was linked to bacterial enzymes as discussed in **Chapter 3.** The observed drop in C/N ratio could potentially be attributed to differences in the types of bacterial enzymes existing within the biofilms in the units fed with raw versus biofiltered water.
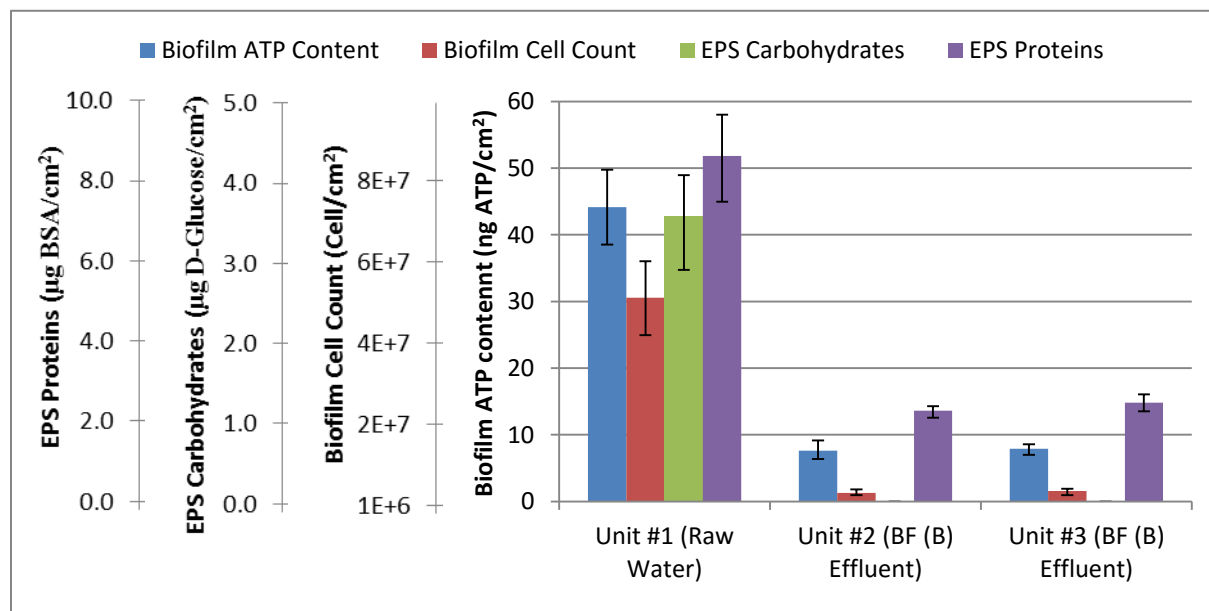
Figure 7-7 Average biofilm ATP content, cell count and total EPS proteins and carbohydrates for the biofilms developed in the UW MFS units (n=3, sampled at unit start, middle and end) for the biofouling experiment on September 2014. Error bars indicating the range over the MFS unit
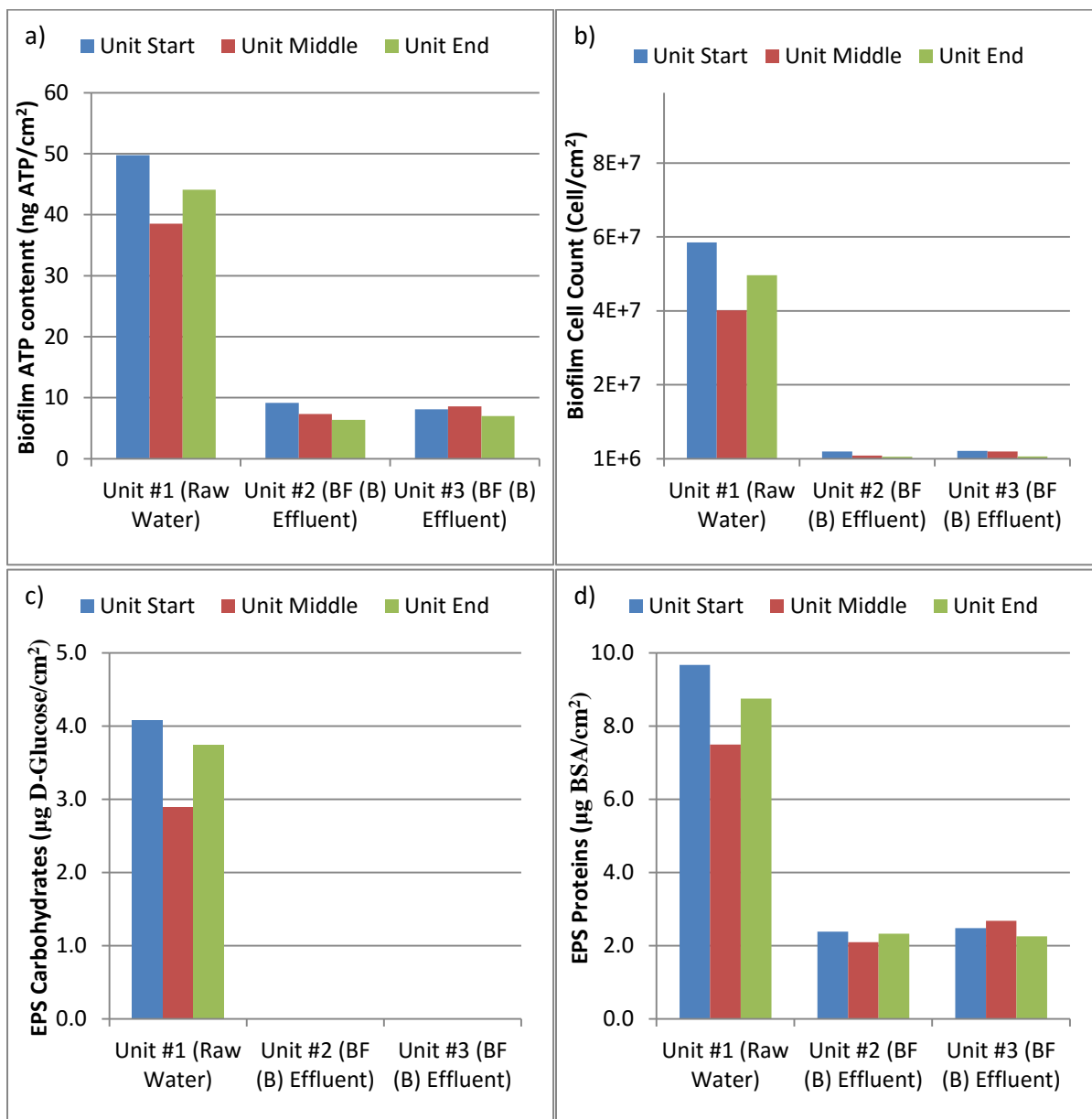
Figure 7-8 Biofilm (a) ATP content, (b) cell count, (c) total EPS carbohydrates and (d) proteins for the biofilms developed in the UW MFS units for the biofouling experiment on September 2014
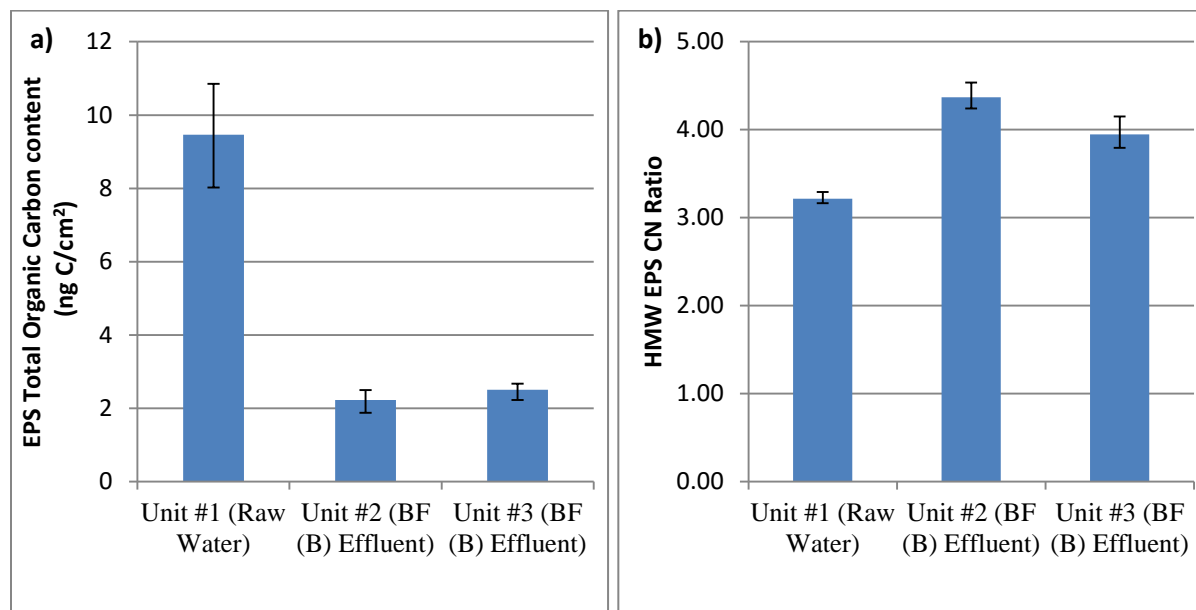
Figure 7-9 Average LC-OCD (a) total organic carbon content of the biofilm EPS and (b) the carbon to nitrogen ratio of the HMW EPS fraction (b) (n=3, sampled at unit start, middle and end) for the biofouling experiment on September 2014. Error bars indicating the range of values over each UW MFS unit

For the biofouling experiment done on January 2015, the biofilm characteristics are shown on **Figure 7-10**. Detailed biomass distribution over the length of each test unit is shown on **Figure 7-11**. Unit #3was fed using raw water and the data in **Figure 7-10** shows that there was variability in each of the measured biofilm components as shown by the large range bars. The data for each sample in **Figure 7-11** shows that there was a gradient in the amount of biomass that formed on the membrane/spacer, with higher values at the start where the feed water enters the unit. Biofilm ATP ranged from 40 ng/cm^2 at the unit start to 11 ng/cm^2 at the unit end. The ATP content at the unit start was similar to the ATP content observed for the MFS unit fed with raw water in the first MFS experiment on September 2014 shown on **Figure 7-8**. The average ATP over the MFS unit in the second experiment (22.8 ng/cm^2) was lower than the average ATP value for the first biofouling experiment (44.2 ng/cm^2), which can explain the lower terminal ΔFCP increase at the end of the second experiment. Biofilm cell count and total EPS carbohydrates and proteins had a similar trend over the unit length as well (**Figure 7-11**). For unit #1 fed with BF (A) effluent and unit #2 fed with BF (B) effluent, there was a similar gradient over the unit length but with less variability compared with unit #3 (**Figure 7-11**). The biofilm ATP content for unit#3

was higher than unit#1 which was higher than unit#2 which is in agreement with the ΔFCP increase results however the observed differences were not large enough to explain the big difference in the biofouling results. Also the average biofilm total cell count in unit#3 was approximately 2.6 times higher than the average biofilm cell count in unit#1. Unit#2 is the one that had much lower biofilm cell count and was only 7% and 17% of the average biofilm cell count in unit#3 and unit#1 respectively. Additionally, EPS total protein content was also close among the three tested units. Also no major differences can be observed with regard to biofilm total organic carbon content of the HMW EPS C/N ratio as shown on **Figure 7-12**. Main differences were observed in biofilm cell count and EPS total carbohydrates which were linked to high biofouling rates in literature (Flemming and Schaule, 1988; Fonseca et al., 2003; Gabelich et al., 2004). EPS total carbohydrates content was not detected in units #1 or #2 unlike unit#3 which had detectable concentration of carbohydrates (3.2 μg D-Glucose/cm^2) which was even similar to the EPS carbohydrates concentration observed for raw water MFS unit on September 2014 (3.6 μg D-Glucose/cm^2).
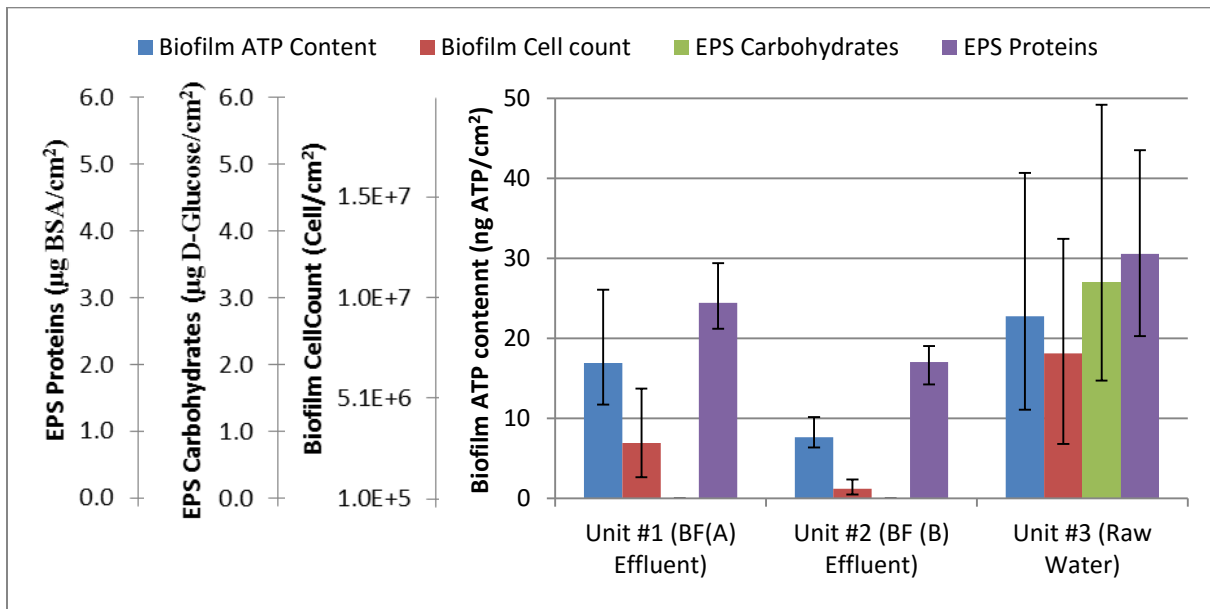
Figure 7-10 Average biofilm ATP content, cell count and total EPS proteins and carbohydrates for the biofilms developed in the MFS units (n=3, sampled at unit start, middle and end) for the biofouling experiment on January 2015 with error bars indicating the range over the UW MFS unit
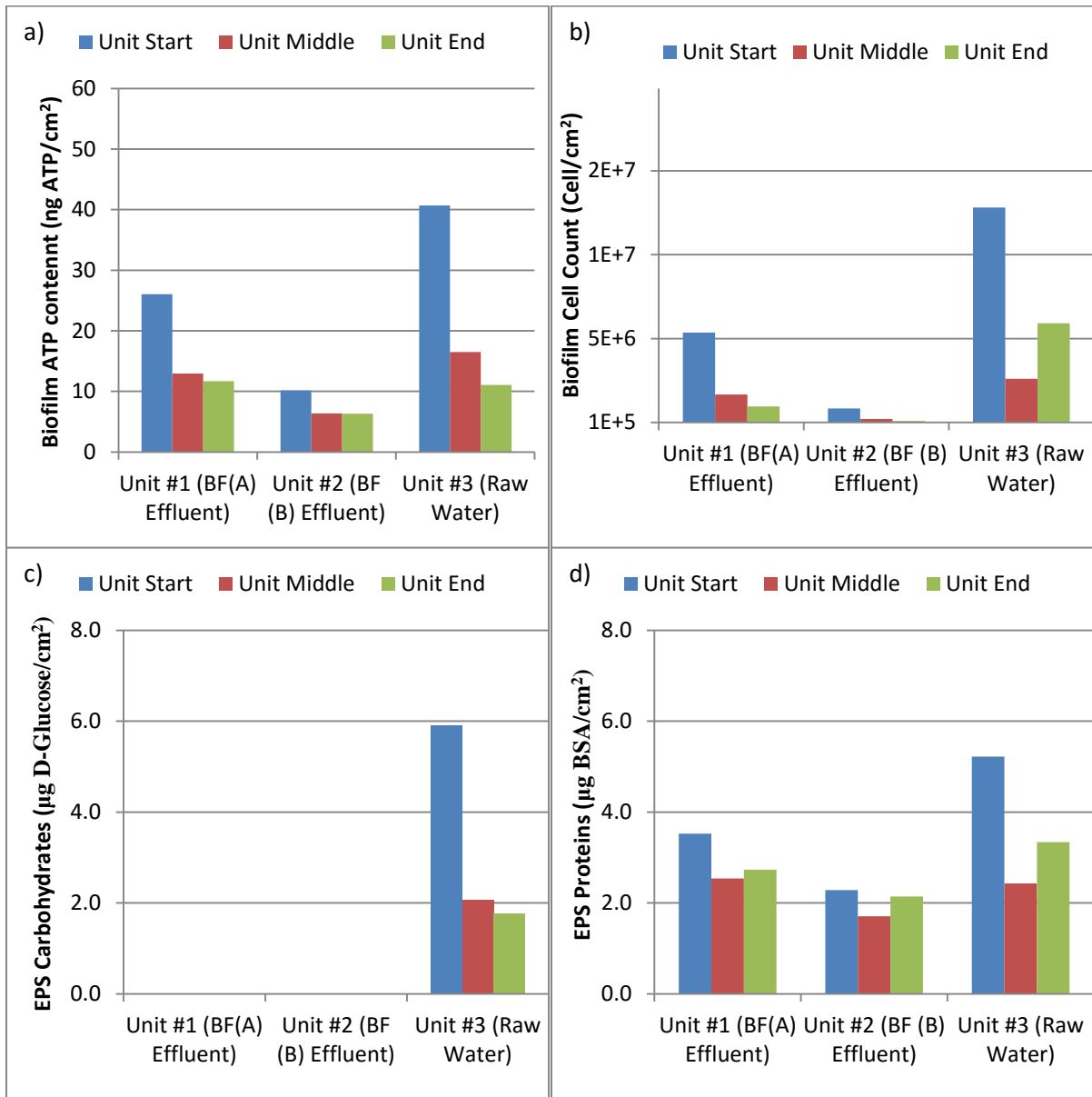
Figure 7-11 Biofilm (a) ATP content, (b) cell count, (c) total EPS carbohydrates and (d) proteins for the biofilms developed in the UW MFS units for the biofouling experiment on January 2015
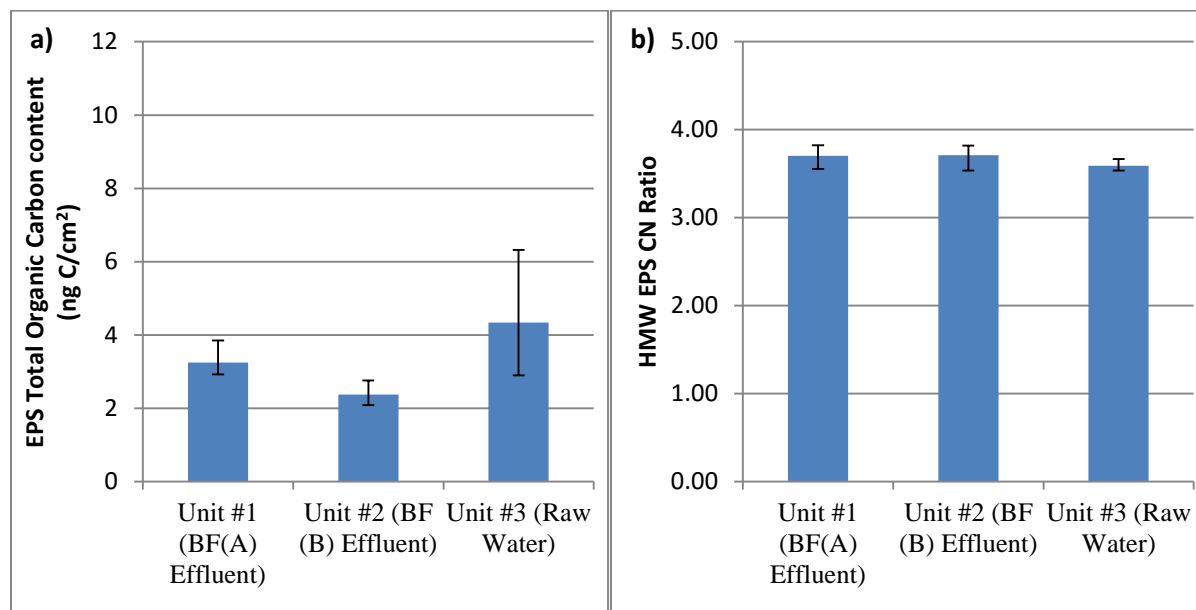
Figure 7-12 Average LC-OCD (a) total organic carbon content of the biofilm EPS and (b) the carbon to nitrogen ratio of the HMW EPS fraction (n=3, sampled at unit start, middle and end) for the biofouling experiment on January 2015 with error bars indicating the range of values over each UW MFS unit

For the Convergence MFS units, the membrane/spacer from unit#2 that was fed with the full-scale BAC effluent showed no biofouling, as each of the measured parameters were below the detection limit for each analytical methods (**Figure 7-13**). The Convergence Unit#1 fed with raw water had significantly more biomass than the UW MFS unit#3 that was operated with the same raw water, and the biofilm ATP, cell count, EPS carbohydrates and proteins were nearly twice the value. The developed biofilm on the Convergence #1 membrane/spacer seemed to be denser due to the higher biofilm cell count along with the visual inspection that showed more biomass in the convergence MFS unit, which can confirm the hypothesis that the higher nutrient flux and shear force may have resulted in the differences between both types of MFS units.
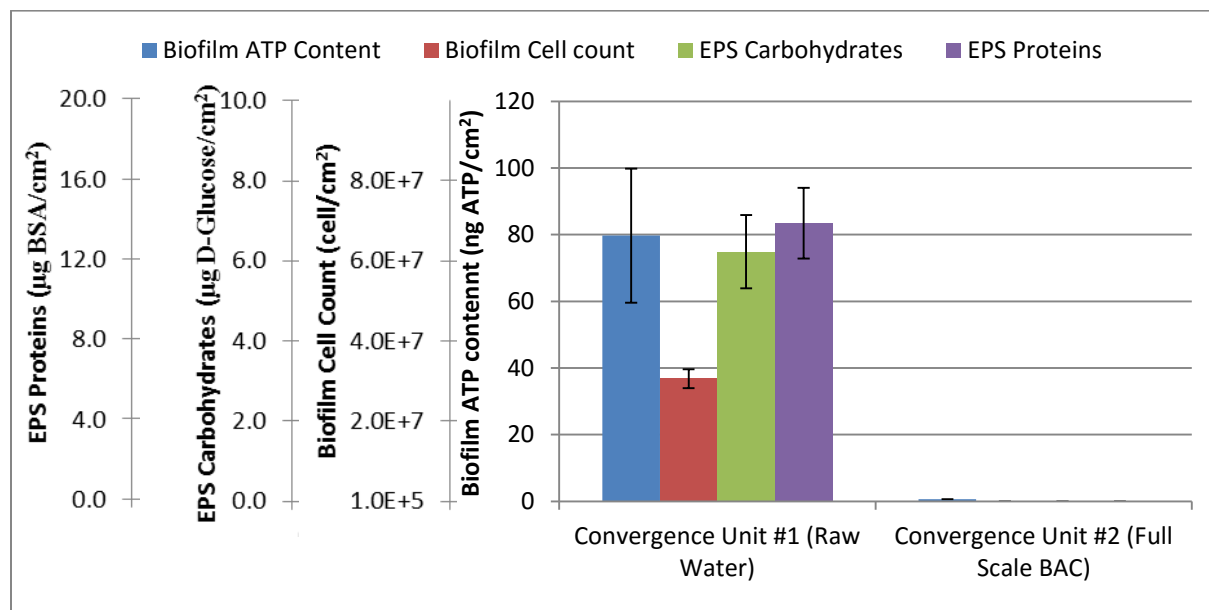
Figure 7-13 Average biofilm ATP content, cell count and total EPS proteins and carbohydrates for the biofilms developed in the Convergence MFS units (n=2, sampled at unit start and end) for the biofouling experiment on January 2015 with error bars indicating the value at the unit start and end of the Convergence MFS unit

Another interesting parameter that can be calculated for the biofilm is the cellular ATP content as shown in **Figure 7-14**. For both experiment, results showed that cellular ATP content for the biofilm samples fed with biofiltered water were higher compared to the units operated using raw water. As well, cellular ATP values were generally higher at cold water conditions (experiment #2) compared with warm water conditions (experiment #1). The observed differences show that cellular ATP content which can depend on the growth state of the biofilm or the microbial community composition, as was discussed in **Chapter 3** and **Chapter 5**. Also, similar cellular ATP values were obtained for the biofilm in the raw water Convergence MFS unit was 2.6×10^{-15} g ATP/cell compared to 3.6×10^{-15} g ATP/cell for the MFS unit#3 operated using the same raw water, which shows that the nature of the biofilm in both units were similar. This confirms that the observed difference in ΔFCP increase among the two units is mainly due to the operational mode of the unit as explained earlier.
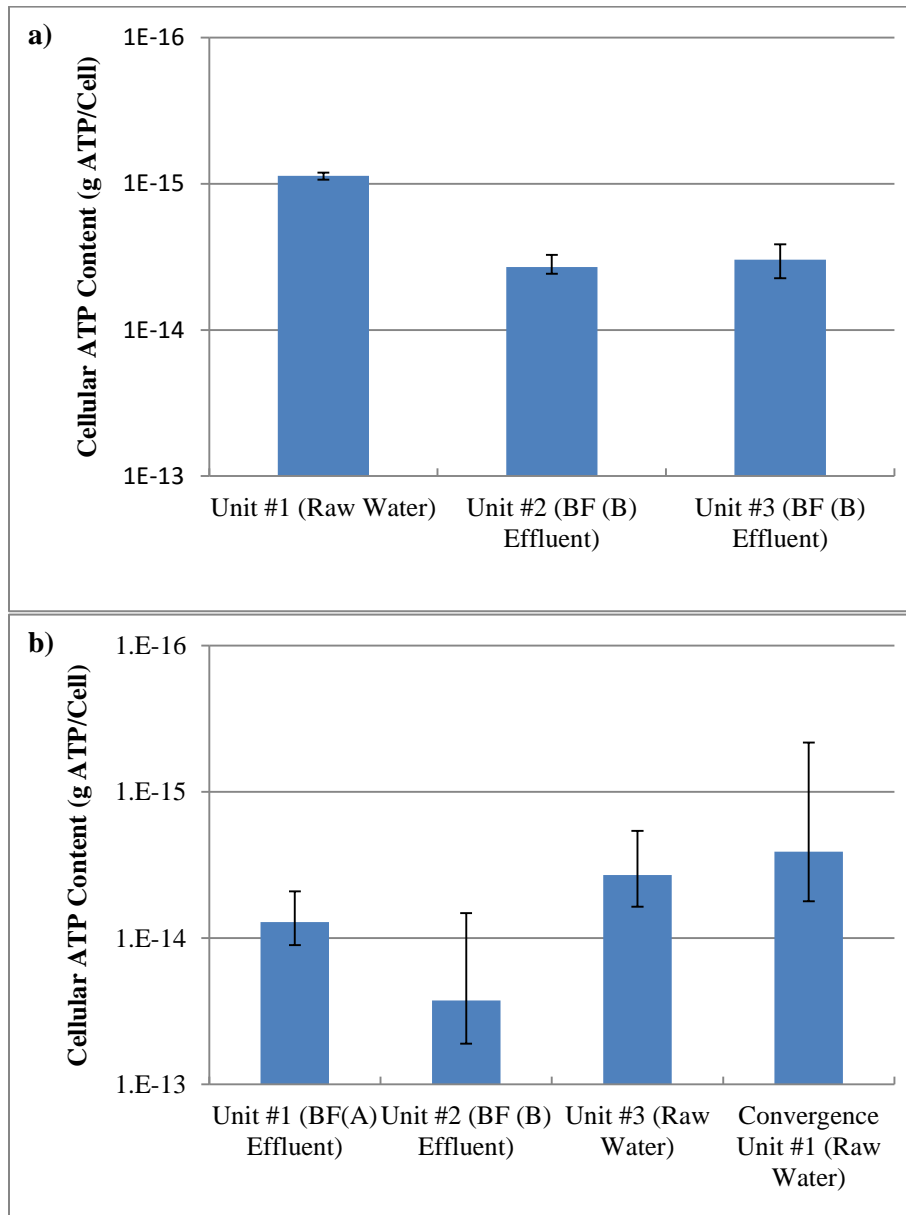
Figure 7-14 Biofilm (a) average cellular ATP content (n=3, sampled at unit start, middle and end for UW MFS units & n=2, sampled at unit start and end for the Convergence MFS unit) for the biofouling experiment on September 2014 and for (b) the experiment on January 2015. Error bars indicating minimum and maximum value

7.3.4 CLPP Results

As was discussed in **Chapter 6**, Biolog EcoPlates can be used to provide addition information on microbial communities in the environment based on the microbial community consumption of different sole carbon sources. The results from the CSUPs data obtained using the Biolog EcoPlates for MFS membrane/spacer biofilm and the feed water samples were used to classify the microbial communities and determine their similarity. The water samples were collected right before the end of the biofouling experiments and the biofilm samples were obtained through the membrane autopsies done after the experiment. Hierarchical clustering and PCA techniques were used on the data sets obtained for the maximum colour intensity (A) (**Figures 7-15** and 7-**16,** respectively) and the maximal rate for colour development (μ_m) (**Figure 7-17** and **Figure** 7-**18,** respectively).

Results based on the maximum colour intensity (A) data set and clustering analysis (**Figure 7-15**) showed that the samples clustered in 4 main groups. Group G1 included the feed water and MFS biofilm samples from the MFS unit fed with effluent from the full scale conventional biofilter, which had very low growth due to the low cell count in both of the samples. Group G2 included samples from the BF (A) and BF (B) effluents water samples from both experiments 1 and 2. Within group G2, the BF (B) effluent from both the MFS experiments were slightly different the effluent of BF (A), showing a minor effect of biofilter EBCT on the microbial community that is present in the effluent based on substrate utilization pattern. The third group G3 included the samples of the raw water. The raw water microbial community was clearly different than the biofiltered water microbial community, which shows that the biofilters were able to control the composition of microbial communities feeding the MFS units, and may have resulted in some of the observed differences with biofouling development and biofilm characteristics. The last group G4 included all the biofilm samples from both MFS experiments. Within G4, the membrane/spacer biofilm from MFS units fed with raw water in September and January, along with the biofilm from the MFS unit fed by BF (A) effluent, were more similar to each other than the biofilm samples from the MFS units fed with BF (B) effluent. These results showed that the microbial community of the biofilm developed within any of the MFS units was not directly related to the microbial community of its feed water. However, differences can be seen between the different biofilms, confirming that the observed biofouling results can possibly be due to differences in microbial community. In general, the maximum colour intensity (A) seems to be a suitable parameter to characterize the CSUPs data. PCA analysis was done on the data set, and the first principal component (PC) accounted for more than 80% of the

variability in the data set. The PCA biplot of PC1 and PC2 analysis is shown on **Figure 7-16,** and the PCA model yielded similar results as the cluster analysis.
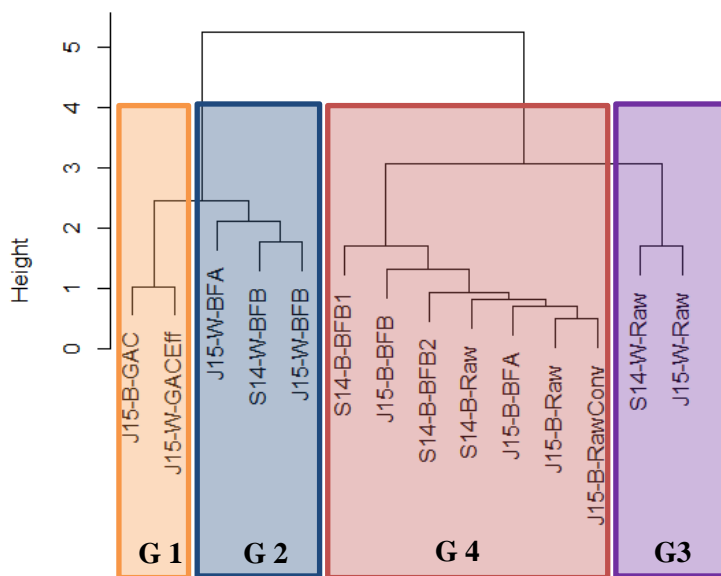
Figure 7-15 Clustering dendrogram based on the Euclidian distance for the maximum optical density (A) obtained from the Biolog Ecoplates multivariate data set including microbial communities from the membrane/spacer biofilm and planktonic bacteria
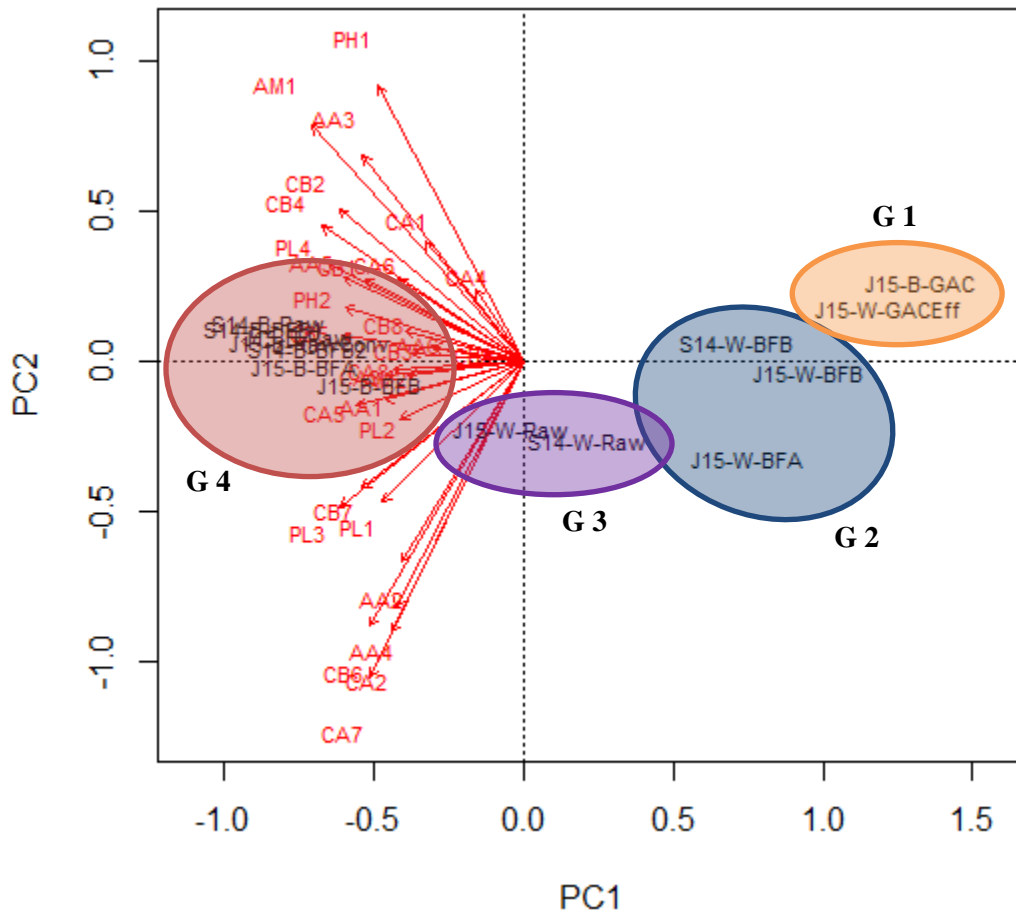
Figure 7-16 Biplot for principal components 1 and 2 for the PCA model of for the maximum optical density (A) obtained from the Biolog Ecoplates multivariate data set including microbial communities from the membrane/spacer biofilm and planktonic bacteria

For μ_m data set based on the rate of colour development, cluster analysis showed that the samples could also be divided into four groups as shown on **Figure 7-17**. The first group G1 included the microbial community in the BF (B) effluent for both MFS experiments, the effluent of the full-scale biofilter, and the biofilm from the Convergence MFS unit fed with the full scale biofilter effluent. These samples are all characterized by their low substrate utilization rate. The next group is G2 which included the microbial community in the raw water on September 2014 and the effluent of BF (A) on January 2015. This group had higher growth rates compared to the samples in group G1. The third group G3 included the biofilms of MFS units fed with raw water and BF (B) effluent in the September 2014 experiment, along with the sample of the raw water in January 2015. The last group G4 included all the biofilm samples from the

January 2015 experiment. Within G4, biofilm samples from the UW MFS and the Convergence MFS unit that were both fed with raw water clustered together. As well, the biofilm of the MFS unit fed with BF (A) clustered more closely with the raw water biofilms compared to the biofilm fed by BF (B) effluent. The data showed that by using μ_m as indicator, biofilm samples from the two MFS experiments (conducted at warm or cold temperatures) were clearly different than each other. PCA analysis was performed on the same data set, and PC1 accounted for more than 80% of the variability. The PCA biplot of PC1 and PC2 analysis is shown on **Figure 7-18.** The PCA model yielded similar results to the clustering data. Samples from groups G3 and G4 clustered in distinct groups like the clustering model, so the PCA model and the clustering results could differentiate the biofilms that developed in the two biofouling experiments. This suggests that there were differences in the microbial community due seasonal water quality between the two biofouling experiments. The remaining samples from groups G1 and G2 clustered closely together and included most of the water samples from both experiments. Again, this suggests that the microbial communities that developed on the membrane/spacer biofilms were different than that in the feed water.
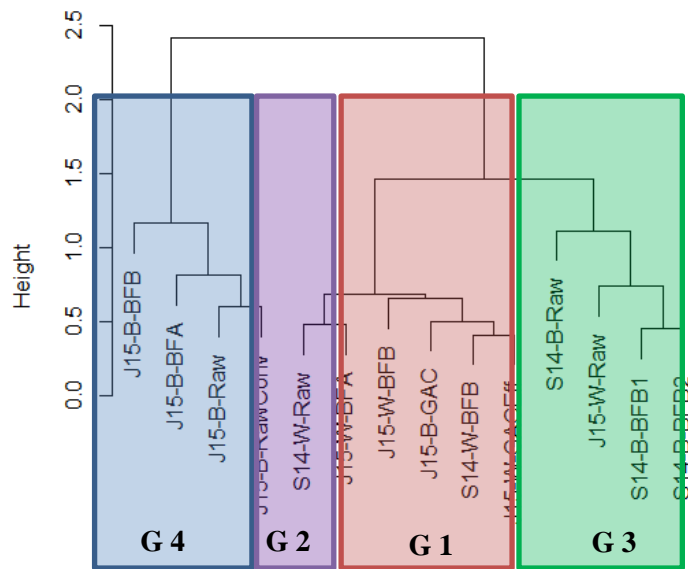
Figure 7-17 Clustering dendrogram based on the Euclidian distance for the maximum rate of colour development (μ_m) obtained from the Biolog Ecoplates multivariate data set including microbial communities from the membrane/spacer biofilm and planktonic bacteria
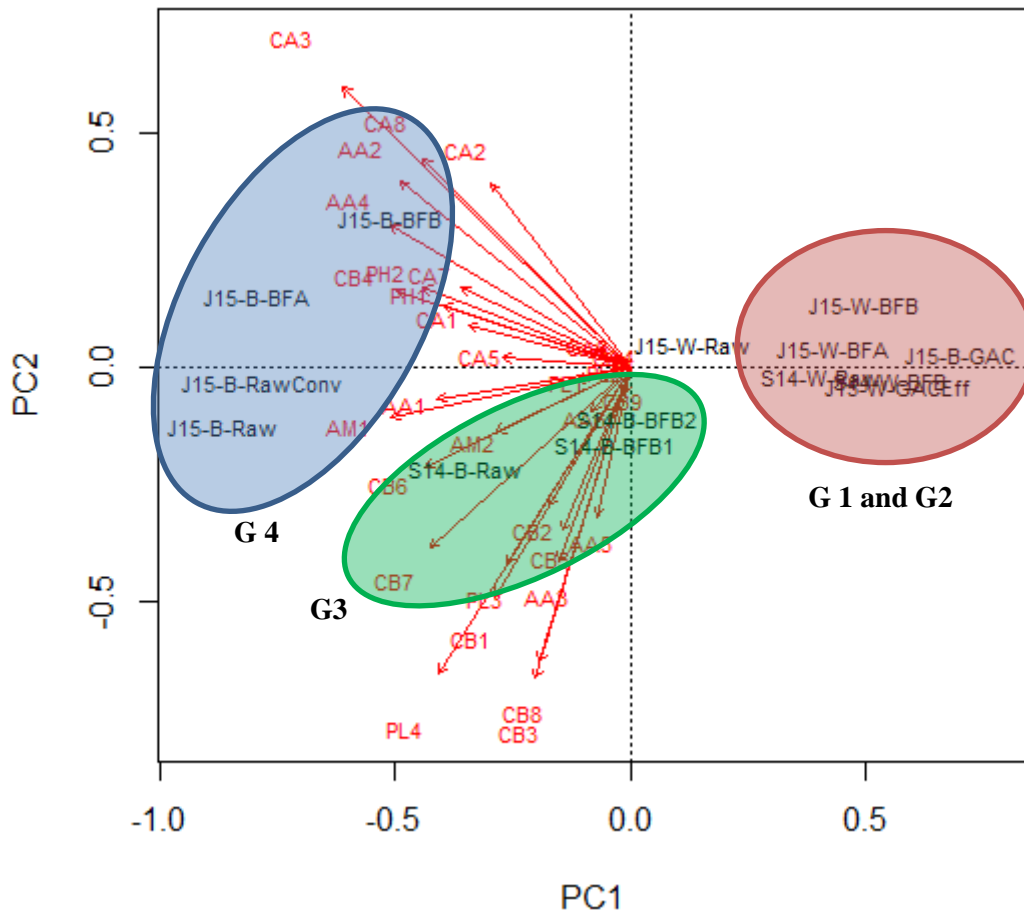
Figure 7-18 Biplot for principal component 1 and 2 for the PCA model of the substrate utilization rate data set obtained from the Biolog Ecoplates multivariate data set for different microbial communities for biofilm and planktonic bacteria

Using either A or μ_m as a descriptor of the CSUPS were advantageous and provided results that confirmed the hypothesis that the biofilm microbial community changed based on the type of feed water. The results could not provide the explanation if this difference is due to differences in the microbial community of the feed water, as none of the biofilm samples was directly linked to the corresponding MFS feed water. Another explanation for the difference in biofilm microbial community is the possible differences in the type of available nutrients in the biofilm feed water due to biofiltration.

7.4 Conclusions

BF$_{WP}$ is a promising pre-treatment technology for high pressure membrane applications. The current study aimed at testing the effect of biofiltration on the biofouling rates and the composition of the biofilm that develops in the membrane spacer, using MFS test units. In general BF$_{WP}$ pre-treatment was able to reduce biofouling rates of a nanofiltration membrane. Main conclusions of this study are:

- BF$_{WP}$ could greatly improve different water quality parameters in the feed water to the nanofiltration membranes. Water quality parameters used in the current study included turbidity, FC total cell count, DOC, AOC and biopolymers. This is particular important, as AOC is directly linked to membrane biofouling, along with HMW biopolymers which can serve as a conditioning layer that would trigger biofouling.

- At both high and low water temperatures, BF$_{WP}$ delayed the biofilm growth process and the biofouling development acclimation period was increased. BF$_{WP}$ was also able to reduce the rate of biofouling development.

- Biofiltration could reduce the amount of biomass attached to the NF membrane and spacer. Biofilm ATP, cell count and the different EPS components were all lower on the nanofiltration membrane/spacer following biofiltration pre-treatment of the feed water. EPS carbohydrates were the most affected component of the EPS, and were not detected in the EPS of biofilms fed by the biofilter effluent.

- Biofilter EBCT had an effect on membrane biofouling as BF (B) with 16 min EBCT was able to prevent biofouling completely over 1000 h compared to BF (A) which was still able to reduce the biofouling rates significantly compared to the untreated raw water.

- BF (B) with 16 min EBCT and the full-scale conventional biofilter were able to prevent biofouling development in the MFS units; however, detectable amounts of biomass were detected in the MFS unit fed by BF (B) but were insufficient to cause a ΔFCP increase.

- The EPS extraction protocol using CER was able to extract most of the biomass present on the membrane and spacer coupons as shown from the ATP recovery without affecting the biomass viability, as the cells were still able to consume the organic substrates in the Biolog EcoPlates.

- CLPP using the Biolog EcoPlates was a simple and efficient method to detect changes in the microbial communities in the different biofilm samples. Both maximum colour intensity (A) and

maximal rate for colour development (μ_m) were good descriptors for the CSUPs and statistical analysis of those data was able to detect differences among the analyzed samples.

- Both hierarchical clustering and PCA analysis were able to measure differences among the microbial communities either from MFS feed water or membrane/spacer biofilms. No direct linkage was observed between the microbial community of the MFS feed water and the biofilm developed within the unit.

- BF_{WP} altered the microbial community of the developed biofilms within the downstream MFS unit either directly by affecting the microbial community of the biofilter effluent or indirectly by modifying the nature of the available substrates or other water quality parameters.

Chapter 8

Summary, Conclusion and Recommendations

8.1 Project summary and challenges

The overarching goal of this research study was to gain a better understanding of BF_{WP} as a potential green pretreatment technology primarily for drinking water membrane applications. BF_{WP} employs biofiltration directly to a raw water source without any prior chemical addition, and it has been shown to reduce the organic and particle loading on subsequent treatment units, in addition to improving the biological stability of the treated water. Implementation of BF_{WP} will likely reduce the overall usage of chemicals such as coagulants and/or ozone which usually precede conventional biofilters. The application of BF_{WP} as a pre-treatment to control high pressure membrane biofouling might be a promising pretreatment alternative to coagulation but has not been investigated to-date. This study provides a better understanding of the BF_{WP} process capabilities and its effect on subsequent NF membrane biofouling, and therefore gives a basis to further optimize the performance of the BF_{WP} –NF process towards full scale implementation of this technology.

The first phase of the project was to develop a suitable pilot scale biofiltration and nanofiltration membrane research platform to study BF_{WP} performance. The design requirements of such a platform were described in **Chapter 5**, and detailed specifications are provided in **Appendix C**. The pilot plant was constructed in the Mannheim Water Treatment Plant in Kitchener, Ontario, which is a full-scale conventional biofiltration facility, to allow direct comparison between BF_{WP} and conventional biofiltration. Also as part of this phase, a suitable test setup to study membrane biofouling using different water streams in parallel was built, and details of this setup are provided in **Chapter 7**. The development of a suitable pilot plant for the proposed study was a critical step to ensure that reliable results could be generated. For example, no flexible plastics were used in the current pilot plant as this can cause AOC contamination. Also the use of automated flow controllers ensured that a constant surface loading rate was used to reduce any discrepancies among the different sampling events. Such design considerations are important for researchers and drinking water treatment personnel when designing pilot testing facilities or when planning future research studies.

In the second phase, a comprehensive experimental protocol was developed to study the biomass attached to the biofilter media, and advanced analytical techniques were established to measure biofilter

performance. The protocol was presented and validated in **Chapter 3**. To date, conventional biofilter biomass monitoring tools are not able to explain changes in biofilter performance, so developing a comprehensive biomass monitoring protocol and finding new biomass parameters were needed in order to study the potential relationships between biofilter biomass to performance. Such a comprehensive protocol is a key step in developing a proper understanding of the studied engineered system. The developed protocol was used to monitor an engineered system (i.e. drinking water biofilters), but it can even be applied to various natural systems such as fresh water and soil biofilms. The AOC method is also a key measure for biofilter performance, as it is an important parameter for biofouling development, and this method had to be adapted to the Grand River water quality. The modified AOC method was developed in **Chapter 4** to monitor BOM removal in the studied biofilters and to assess the biofouling potential of raw and treated waters. The modified AOC method was also used to monitor the seasonal water quality of the Grand River. The AOC method could overcome the time limitation of the standard method and at the same time employed a more representative bacterial inoculum for the studied system. This can help in making AOC a valuable tool for biofilter monitoring. As well, this improved AOC method can be applied to other drinking water treatment and distribution systems that required detailed characterization of NOM.

In the third phase of the project, the established methods from the earlier chapters were applied to monitor the performance of the pilot-scale BF_{WP} filters. The effects of biofilter EBCT and water temperature on biofilter performance in terms of BOM removal were evaluated. The biomass distribution and their composition over the biofilter depth were simultaneously measured, and potential relationships between these biomass results to biofilter performance were investigated. The results of this phase are presented in **Chapter 5**. As part of this phase, the biofilm microbial community was studied using CLPP analysis based on CSUPs. The biofilter community profile changes among the different filters and over the filter depth were evaluated at high and low water temperature conditions, and whether this could be related to biofilter performance. These results were presented in **Chapter 6**.

The results from **Chapter 5** and **Chapter 6** demonstrated the capabilities of BF_{WP} as a pre-treatment technology, and the application for BF_{WP} to reduce the biofouling potential of the river water for high pressure membranes was assessed. MFS units were used to determine the biofouling potential of raw and biofiltered water in parallel. The effects of biofilter EBCT and water temperature on the water biofouling potential were also tested. Moreover, the performance of the pilot BF_{WP} in terms of reducing biofouling

potential was also compared to that of a conventional full-scale biological filter which was preceded by coagulation and ozonation.

Several challenges were overcome in the course of the current research study:

1. A suitable research platform for biofiltration studies was needed. This required the design and construction of a new pilot plant facility, and this was done as part of this research project, in collaboration with another student in the group.

2. The Grand River is a challenging water source, and there were unexpected difficulties in adapting a flow cytometry cell count method and a modified AOC method for use with this water source. These difficulties were overcome when developing the modified AOC method.

3. The developed biofilter biomass characterization protocol had to be validated and tested on acclimated biofilter media, which had to be done after commissioning the redesigned pilot plant.

4. A biofouling test setup, namely the MFS units, had to be built and tested. The flow cells were purchased from a supplier in Netherlands, but the remainder of the components were sourced locally and assembled at the University of Waterloo as part of this project.

8.2 Summary of findings and conclusions

The study successfully characterized biofilms and monitored the performance of BF_{WP} as a promising drinking water pre-treatment technology. BF_{WP} was found to be an efficient pre-treatment for biofouling control of NF membranes.

The key overall conclusions from this thesis are followed by specific conclusions related to each phase of the study. These overall conclusions are as follows:

- BF_{WP} was an efficient pre-treatment technology for BOM removal as it was able to remove biopolymers (i.e. proteins and polysaccharides) and AOC both at low and high water temperatures. Biofilter performance was mainly affected by the drop in water temperature and biofilter EBCT had significant impact on biofilter performance as a design parameter.

- The types of methods used to assess both biofilter performance and biofilter biomass were critical for understanding and monitoring the biofiltration process. Optimization of the methods for the

used source water in the study was required in order to obtain reliable data. The incorporation of flow cytometry, EPS extraction and EPS characterization protocols, and CLPP analysis to assess community dynamics were all useful in understanding the effects of process and environmental variables on biofilter performance.

- Cellular ATP may be indicative of biofilter performance in terms of BOM removal, and therefore may provide predictive information regarding expected rates of biofouling reduction. However, these are advanced techniques that require specialized equipment and technical skill. There are certain benefits of the methods developed in this thesis that allow easier analysis and monitoring opportunities, including flow cytometer techniques.

- BF_{WP} efficiently reduced the rate of biofouling development on NF membranes and extended the acclimation time before biofouling started to develop within the MFS units, compared to untreated raw water. The advantage of using BF_{WP} as a pre-treatment for biofouling control was proven both at low and high water temperatures and was comparable to advanced pre-treatment using conventional biofiltration with prior ozonation. A simple technology like BF_{WP} was as efficient as an advanced treatment system for biofouling control, but without the use of additional chemicals and much lower energy requirements.

8.2.1 Significant conclusions related to biofilter biomass monitoring

- Newly developed parameters such as cellular ATP content, protein to carbohydrates ratio, and carbon to nitrogen ratio of different EPS size fractions, show potential for use in relation to biofilter performance monitoring. Conventional biomass parameters such as biofilm ATP and biofilm cell count were not a useful measure of biofilter performance, as they were not affected by the drop in water temperature. The latter was the reason behind their lower correlation with the observed biofilter performance parameters.

- Proteins were found to be the major fraction of the biofilm EPS in biofilters. Proteins were correlated with the HMW EPS which was mainly composed of high molecular weight protein-like substances such as extracellular enzymes.

- Flow cytometry was a useful research tool for biomass monitoring. An additional benefit of flow cytometry is its ability to provide information about biofilm composition along with its basic task

to quantify the biofilm cell count. HNA bacteria were an important fraction of the total bacterial community and they formed the main fraction in the attached biomass on the filter media.

- Biofilm bulk ATP, cell count and EPS fractions declined rapidly over the biofilter depth, which confirmed the presence of a nutrient gradient over the biofilter depth. These findings were consistent over both high and low water temperature conditions indicating a possible first order biomass decay and nutrient degradation model.

8.2.2 Significant conclusions related to the biofilter performance monitoring

- BF_{WP} can efficiently reduce the concentration of biopolymers and AOC, and can also achieve high reductions in feed water total cell counts both at low and high water temperatures. Other NOM fractions such as humic substances or low molecular weight organics had much lower removals. The biofilters achieved their intended treatment objective in reducing particle loading, fresh biomass loading and BOM loading on the subsequent treatment units.

- Biopolymers and AOC were mainly removed at the top of the filter bed at relatively short EBCTs. Longer biofilter EBCT had an effect on the observed removal but in a less proportional manner. Therefore the recommended EBCT for biofiltration will depend to a large extend on the treatment goals i.e. the target fraction of NOM for a specific treatment process train.

- Cellular ATP content was affected by the change in water temperature, which likely reflected the drop in biofilm activity. This shows the potential application of cellular ATP as a monitoring parameter to assess the biofilter biomass state of activity and to understand changes in biofilter performance.

- Cold water temperatures ($<7°C$) affected the biofilter performance, however the biofilters were still biologically active and both biopolymers and AOC were still being removed but to a lesser extent. Even the reduction in the feed water total cell count dropped significantly at the lower water temperature. This drop was related to both a change in microbial community functional diversity from the CLPP analysis and to a drop in biomass activity as shown by cellular ATP content for the biofilm.

- CLPP analysis showed that the microbial community substrate utilization patterns were found to be temperature dependent. The biofilter biomass seemed to adapt to the drop in water temperature

189

as can be interpreted from the gradual shift in the biofilter community during the cold water temperatures.

8.2.3 Significant conclusions related to the potential application of biofiltration for biofouling control

- BF_{WP} efficiently reduced the rate of biofouling development and extended the acclimation time before biofouling started to develop within the MFS units, compared to untreated raw water. The advantage of using BF_{WP} as a pre-treatment for biofouling control was proven both at low and high water temperatures.

- Biofiltration reduced the amount of biomass on the membrane in the MFS units and altered the composition of the microbial community structure as determined by CLPP analysis, when compared to units fed with raw water.

- Biofilter EBCT is a potential design parameter for biofouling control as it affected the observed biofouling rates and the amount of biomass on the membranes within the MFS units.

- Extended BF_{WP} biofilter EBCT of 16 min was able to prevent biofouling development, and this was similar to results for MFS units fed using a full-scale conventional biological filter with extensive chemical pre-treatment.

- The effect of BF_{WP} to reduce the pressure drop increase on the membrane was related to the overall reduction in biomass growth on the membranes. This can be attributed to the biofilters which reduced membrane conditioning molecules, such as biopolymers, and easily biodegradable substrate measured as AOC in the influent to the membrane units.

8.3 Implications for the drinking water treatment industry

Based on the above specific conclusions of the study, several implications for the drinking water industry were determined and they include:

1. Biological pre-treatment is a promising technology for drinking water treatment to improve surface water quality without the need for additional chemicals or increased energy costs. BF_{WP} acts as a multi barrier for particles, turbidity, bacterial cells and BOM.

2. BF_{WP} proved to be a promising pre-treatment for biofouling control for high pressure NF membranes. Together with the previously shown ability to control low pressure membrane fouling, BF_{WP} can be used as pre-treatment to prevent fouling of hybrid membrane system including both low and high pressure membranes. This treatment train would be a compact system that could provide high quality treated water for remote areas, without the need for advanced operator skills compared to conventional pre-treatment options.

3. Biofilter biomass monitoring is an essential part of the biofiltration process optimization and monitoring. Baseline biofilter biomass values should be monitored using one of the basic biomass parameters such as ATP or biofilm cell count. Advanced biomass monitoring parameters such as cellular ATP or EPS composition may be used for filter troubleshooting.

4. Biofilter performance drops significantly at cold water conditions below 7°C. Removal of turbidity, bacterial cells and NOM drops significantly and care is needed to ensure that subsequent treatment units will accommodate for that drop in unit performance.

5. Proper choice of biofilter performance parameters should be based on the overall treatment objectives. For membrane biofouling control, high molecular weight biopolymers and AOC were the most suitable parameters to monitor biofilter performance.

6. EBCT is a key design parameter for drinking water biofilters, however, this will depend on the intended application. For general BOM reduction or low pressure membrane fouling control, a short or intermediate biofilter EBCT should be adequate. For applications where improving treated water biological stability is a concern such as in the case of biofouling control, extended biofilter EBCT will be beneficial, especially in systems where a large drop in feed water temperature is expected.

8.4 Future research

1. Extend the developed biomass characterization to media samples from conventional biofilters to understand the differences between BF_{WP} and conventional biofiltration.

2. Test the yield of the natural community AOC inoculum on different types of substrates other than sodium acetate and compare the inoculum yield values over different seasons.

3. Better understand the nature of HNA and LNA bacteria in freshwater and biofilter biomass using advanced analytical techniques such as flow cytometry cell sorting.

4. Evaluate the effect of the cold water temperature on the biofilter biomass activity.

5. Test BF_{WP} as a pre-treatment for BOM removal using different surface water sources.

6. Using more advanced biofilm imaging techniques such as confocal laser surface microscopy (CLSM) determine the biofilm 3D structure and composition to fully understand the effect of biofiltration on the developed biofilm in the MFS units.

7. Use molecular biological techniques to quantify the differences in microbial community composition of biofilm samples in order to understand how biofiltration affected the community structure of the developed biofilm.

8. Prove the validity of the findings in this study using pilot scale spiral wound NF membrane test units with BF_{WP} as a pre-treatment using different types of surface waters.

9. Investigate the performance of BF_{WP} – UF – NF as a full-scale drinking water treatment train and evaluate the effect of BF_{WP} on UF organic fouling and NF biofouling.

References

Al-Halbouni, D., Traber, J., Lyko, S., Wintgens, T., Melin, T., Tacke, D., Janot, A., Dott, W., Hollender, J., 2008. Correlation of EPS content in activated sludge at different sludge retention times with membrane fouling phenomena. Water Res. 42, 1475–88.

Amirtharajah, A., 1993. Optimum backwashing of filters with air scour: a review. Water Sci. Technol. 27, 195–211.

Andersson, S., Dalhammar, G., Land, C., Kuttuva Rajarao, G., 2009. Characterization of extracellular polymeric substances from denitrifying organism Comamonas denitrificans. Appl. Microbiol. Biotechnol. 82, 535–543.

Baker, A., 2001. Fluorescence excitation-emission matrix characterization of some sewage-impacted rivers. Environ. Sci. Technol. 35, 948–953.

Baker, J., Stephenson, T., Dard, S., Côté, P., 1995. Characterisation of fouling of nanofiltration membranes used to treat surface waters. Environ. Technol. 16, 977–985.

Bar-Zeev, E., Passow, U., Romero-Vargas Castrillón, S., Elimelech, M., 2015. Transparent Exopolymer Particles: From Aquatic Environments and Engineered Systems to Membrane Biofouling. Environ. Sci. Technol. 49, 691–707.

Bereschenko, L.A., Prummel, H., Euverink, G.J.W., Stams, A.J.M., van Loosdrecht, M.C.M., 2011. Effect of conventional chemical treatment on the microbial population in a biofouling layer of reverse osmosis systems. Water Res. 45, 405–16.

Bergman, R., 2007. Reverse osmosis and nanofiltration. American Water Works Association, Denver, CO.

Berman, T., Holenberg, M., 2005. Don't fall foul of biofilm through high TEP levels. Filtr. Sep. 42, 30–32.

Berman, T., Mizrahi, R., Dosoretz, C.G., 2011. Transparent exopolymer particles (TEP): A critical factor in aquatic biofilm initiation and fouling on filtration membranes. Desalination 276, 184–190.

Boon, N., Pycke, B.F.G., Marzorati, M., Hammes, F., 2011. Nutrient gradients in a granular activated carbon biofilter drives bacterial community organization and dynamics. Water Res. 45, 6355–61.

Boretska, M., Bellenberg, S., Moshynets, O., Pokholenko, I., Sand, W., 2013. Change of Extracellular Polymeric Substances Composition of Thiobacillus thioparus in Presence of Sulfur and Steel. J. Microb. Biochem. Technol. 5, 068–073.

Bott, T.R., 2011. Industrial Biofouling: Occurrence and Control. Elsevier.

Bryers, J.D., 2008. Medical biofilms. Biotechnol. Bioeng. 100, 1–18.

Bryers, J.D., Ratner, B.D., 2004. Bioinspired implant materials befuddle bacteria. ASM News-American Soc. Microbiol. 70, 232.

Bucs, S.S., Valladares Linares, R., van Loosdrecht, M.C.M., Kruithof, J.C., Vrouwenvelder, J.S., 2014. Impact of organic nutrient load on biomass accumulation, feed channel pressure drop increase and

permeate flux decline in membrane systems. Water Res. 67, 227–42.

Camper, A.K., LeChevallier, M.W., Broadaway, S.C., McFeters, G.A., 1985. Evaluation of procedures to desorb bacteria from granular activated carbon. J. Microbiol. Methods 3, 187–198.

Chamberlain, A.H.L., 1992. The role of adsorbed layers in bacterial adhesion, in: Biofilms—Science and Technology. Springer, pp. 59–67.

Characklis, W.G., Bryers, J.D., 2009. Bioengineering report: Fouling biofilm development: A process analysis. Biotechnol. Bioeng. 102, 309–347.

Chen, F., Peldszus, S., Peiris, R.H., Ruhl, A.S., Mehrez, R., Jekel, M., Legge, R.L., Huck, P.M., 2014. Pilot-scale investigation of drinking water ultrafiltration membrane fouling rates using advanced data analysis techniques. Water Res. 48, 508–18.

Chen, M.J., Zhang, Z., Bott, T.R., 2005. Effects of operating conditions on the adhesive strength of Pseudomonas fluorescens biofilms in tubes. Colloids Surfaces B Biointerfaces 43, 61–71.

Costerton, J.W., Stewart, P.S., Greenberg, E.P., 1999. Bacterial biofilms: a common cause of persistent infections. Science (80-.). 284, 1318–1322.

Crittenden, J.C., 2005. Water Treatment Principles and Design. J. Wiley, Hoboken, N.J.

Croft, J., 2012. Natural organic matter characterization of different source and treated waters; implications for membrane fouling control. Master's Thesis, University of Waterloo.

Das, T., Sharma, P.K., Busscher, H.J., van der Mei, H.C., Krom, B.P., 2010. Role of extracellular DNA in initial bacterial adhesion and surface aggregation. Appl. Environ. Microbiol. 76, 3405–3408.

De Roy, K., Clement, L., Thas, O., Wang, Y., Boon, N., 2012. Flow cytometry for fast microbial community fingerprinting. Water Res. 46, 907–19.

Degeest, B., Janssens, B., De Vuyst, L., 2001. Exopolysaccharide (EPS) biosynthesis by Lactobacillus sakei 0–1: production kinetics, enzyme activities and EPS yields. J. Appl. Microbiol. 91, 470–477.

Dignac, M.-F., Urbain, V., Rybacki, D., Bruchet, A., Snidaro, D., Scribe, P., 1998. Chemical description of extracellular polymers: implication on activated sludge floc structure. Water Sci. Technol. 38, 45–53.

Domínguez, L., Rodríguez, M., Prats, D., 2010. Effect of different extraction methods on bound EPS from MBR sludges. Part I: Influence of extraction methods over three-dimensional EEM fluorescence spectroscopy fingerprint. Desalination 261, 19–26.

Dorner, S., Anderson, W., Huck, P., Gaulin, T., Candon, H., Slawson, R., Payment, P., 2007. Pathogen and indicator variability in a heavily impacted watershed. J. Water Health 5, 241–257.

Dreszer, C., Vrouwenvelder, J.S., Paulitsch-Fuchs, A.H., Zwijnenburg, A., Kruithof, J.C., Flemming, H.-C., 2013. Hydraulic resistance of biofilms. J. Memb. Sci. 429, 436–447.

DuBois, M., Gilles, K.A., Hamilton, J.K., Rebers, P.A., Smith, F., 1956. Colorimetric Method for Determination of Sugars and Related Substances. Anal. Chem. 28, 350–356.

Elhadidy, A.M., Van Dyke, M.I., Chen, F., Peldszus, S., Huck, P.M., 2015. Improved approach for the characterization of attached biomass and extracellular polymeric substances on granular media from

a drinking water biologically active filter. Water Res. (In Prep.

Environment Canada, 2015. Historical river flow data for the monitoring station on the Grand River near Doon (02GA048) [ON] [WWW Document].

Escobar, I.C., Hong, S., Randall, A.A., 2000. Removal of assimilable organic carbon and biodegradable dissolved organic carbon by reverse osmosis and nanofiltration membranes. J. Memb. Sci. 175, 1–17.

Escobar, I.C., Randall, A.A., 2001. Assimilable organic carbon (AOC) and biodegradable dissolved organic carbon (BDOC): complementary measurements. Water Res. 35, 4444–4454.

Evans, P.J., Smith, J.L., LeChevallier, M.W., Schneider, O.D., Weinrich, L.A., Jjemba, P.K., 2013a. A Monitoring and Control Toolbox for Biological Filtration. Water Research Foundation.

Evans, P.J., Smith, J.L., LeChevallier, M.W., Schneider, O.D., Weinrich, L.A., Jjemba, P.K., 2013b. Biological Filtration Monitoring and Control Toolbox: Guidance Manual. Water Research Foundation.

Flemming, H., Wingender, J., 2001. Relevance of microbial extracellular polymeric substances (EPSs)-Part I: Structural and ecological aspects. Water Sci. Technol. 43, 1–8.

Flemming, H.-C., 2002. Biofouling in water systems–cases, causes and countermeasures. Appl. Microbiol. Biotechnol. 59, 629–640.

Flemming, H.-C., 1997. Reverse osmosis membrane biofouling. Exp. Therm. fluid Sci. 14, 382–391.

Flemming, H.-C., Schaule, G., 1988. Biofouling on membranes-a microbiological approach. Desalination 70, 95–119.

Flemming, H.-C., Schaule, G., Griebe, T., Schmitt, J., Tamachkiarowa, A., 1997. Biofouling—the Achilles heel of membrane processes. Desalination 113, 215–225.

Flemming, H.-C., Schaule, G., McDonogh, R., 1993. How do performance parameters respond to initial biofilm formation on separation membranes? Vom Wasser 80, 177–186.

Flemming, H.-C., Wingender, J., 2010. The biofilm matrix. Nat. Rev. Microbiol. 8, 623–633.

Fonseca, A.C., Scott Summers, R., Hernandez, M.T., 2001. Comparative measurements of microbial activity in drinking water biofilters. Water Res. 35, 3817–3824.

Fonseca, A.C., Summers, R.S., Greenberg, A.R., Hernandez, M.T., 2003. Isolating and modeling critical factors governing biofouling of nanofiltration membranes. Proc. Am. Water Work. Assoc. Denver, CO.

Frølund, B., Palmgren, R., Keiding, K., Nielsen, P.H., 1996. Extraction of extracellular polymers from activated sludge using a cation exchange resin. Water Res. 30, 1749–1758.

Gabelich, C.J., Yun, T.I., Ishida, K.P., Leddy, M.B., Safarik, J., 2004. The effect of naturally occurring biopolymers on polyamide membrane fouling during surface water treatment. Desalination 161, 263–276.

Garny, K., Neu, T.R., Horn, H., 2009. Sloughing and limited substrate conditions trigger filamentous growth in heterotrophic biofilms—measurements in flow-through tube reactor. Chem. Eng. Sci. 64,

2723–2732.

Gasteiger, E., Hoogland, C., Gattiker, A., Wilkins, M.R., Appel, R.D., Bairoch, A., 2005. Protein identification and analysis tools on the ExPASy server. Springer.

Giddings, J.C., 1993. Field-flow fractionation: Analysis of macromolecular, colloidal, and particulate materials. Science (80-.). 260, 1456–1465.

Gleick, P.H., 2000. A Look at Twenty-first Century Water Resources Development. Water Int. 25, 127–138.

GRCA, 2015. Grand River Watershed Facts - Grand River Conservation Authority [WWW Document].

Griebe, T., Flemming, H.-C., 1998. Biocide-free antifouling strategy to protect RO membranes from biofouling. Desalination 118, 153–IN9.

Haddix, P.L., Shaw, N.J., LeChevallier, M.W., 2004. Characterization of bioluminescent derivatives of assimilable organic carbon test bacteria. Appl. Environ. Microbiol. 70, 850–854.

Hallé, C., 2009. Biofiltration in Drinking Water Treatment: Reduction of Membrane Fouling and Biodegradation of Organic Trace Contaminants. University of Waterloo.

Hallé, C., Huck, P.M., Peldszus, S., 2015. Emerging Contaminant Removal by Biofiltration: Temperature, Concentration and EBCT Impacts. J. Am. Water Works Assoc. 107, E364–E379.

Hallé, C., Huck, P.M., Peldszus, S., Haberkamp, J., Jekel, M., 2009. Assessing the Performance of Biological Filtration As Pretreatment to Low Pressure Membranes for Drinking Water. Environ. Sci. Technol. 43, 3878–3884.

Hamilton, R.D., Holm-Hansen, O., 1967. Adenosine triphosphate content of marine bacteria. Limnol. Ocean. 12, 319–324.

Hammes, F., Berney, M., Wang, Y., Vital, M., Köster, O., Egli, T., 2008. Flow-cytometric total bacterial cell counts as a descriptive microbiological parameter for drinking water treatment processes. Water Res. 42, 269–77.

Hammes, F., Egli, T., 2007. A flow cytometric method for AOC determination (Deliverable 3.3.1).

Hammes, F., Egli, T., 2005. New Method for Assimilable Organic Carbon Determination Using Flow-Cytometric Enumeration and a Natural Microbial Consortium as Inoculum. Environ. Sci. Technol. 39, 3289–3294.

Hammes, F., Salhi, E., Köster, O., Kaiser, H.-P., Egli, T., von Gunten, U., 2006. Mechanistic and kinetic evaluation of organic disinfection by-product and assimilable organic carbon (AOC) formation during the ozonation of drinking water. Water Res. 40, 2275–86.

Heberer, T., 2002. Occurrence, fate, and removal of pharmaceutical residues in the aquatic environment: a review of recent research data. Toxicol. Lett. 131, 5–17.

Hem, L.J., Efraimsen, H., 2001. Assimilable organic carbon in molecular weight fractions of natural organic matter. Water Res. 35, 1106–1110.

Hijnen, W.A.M., Biraud, D., Cornelissen, E.R., van der Kooij, D., 2009. Threshold Concentration of Easily Assimilable Organic Carbon in Feedwater for Biofouling of Spiral-Wound Membranes.

Environ. Sci. Technol. 43, 4890–4895.

Hijnen, W.A.M., Castillo, C., Brouwer-Hanzens, A.H., Harmsen, D.J.H., Cornelissen, E.R., van der Kooij, D., 2012. Quantitative assessment of the efficacy of spiral-wound membrane cleaning procedures to remove biofilms. water Res. 46, 6369–6381.

Hong, S., Elimelech, M., 1997. Chemical and physical aspects of natural organic matter (NOM) fouling of nanofiltration membranes. J. Memb. Sci. 132, 159–181.

Hu, J.Y., Song, L.F., Ong, S.L., Phua, E.T., Ng, W.J., 2005. Biofiltration pretreatment for reverse osmosis (RO) membrane in a water reclamation system. Chemosphere 59, 127–133.

Huber, S.A., 2002. Significance, origin, and fate of natural organic matter in boiler feedwater preparation using surface water. Ultrapure Water 19, 18–24.

Huber, S.A., Balz, A., Abert, M., Pronk, W., 2011. Characterisation of aquatic humic and non-humic matter with size-exclusion chromatography--organic carbon detection--organic nitrogen detection (LC-OCD-OND). Water Res. 45, 879–85.

Huck, P.M., 2000. Optimizing filtration in biological filters. American Water Works Association.

Huck, P.M., 1990. Measurement of biodegradable organic matter and bacterial growth potential in drinking water. J. Am. Water Work. Assoc. 82, 78–86.

Huck, P.M., Fedorak, P.M., Anderson, W.B., 1991. Formation and removal of assimilable organic carbon during biological treatment. J. Am. Water Works Assoc. 69–80.

Huck, P.M., Peldszus, S., Anderson, W.B., Chen, F., El-Hadidy, A.M., Legge, R.L., Siembida-Losch, B., Dyke, M.I. Van, Walton, T., Wilson, B., 2015. Biofiltration With and Without Pre-treatment - Are There Differences?, in: Biofilms in Drinking Water Systems. IWA, Arosa.

Huck, P.M., Sozański, M.M., 2008. Biological filtration for membrane pre-treatment and other applications: towards the development of a practically-oriented performance parameter. J. Water Supply Res. Technol. 57, 203.

Huck, P.M., Zhang, S., Price, M.L., 1994. BOM removal during biological treatment: a first-order model. J. Am. Water Work. Assoc. States) 86.

Ihssen, J., Egli, T., 2004. Specific growth rate and not cell density controls the general stress response in Escherichia coli. Microbiology 150, 1637–48.

Ishizawa, S., Yamamoto, Y., Denboh, T., Ueda, H., 2010. Release of dissolved free amino acids from biofilms in stream water. Fish. Sci. 76, 669–676.

Jago, P.H., Stanfield, G., 1989. Application of ATP determination to measure the concentration of assimilable organic carbon in water, in: Stanley, P.E., McCarthy, B.J., Smither, R. (Eds.), ATP Luminescence : Rapid Methods in Microbiology. Blackwell Scientific Publications ; Distributors, USA, Publishers' Business Services, Oxford [England]; Boston; Brookline Village, Mass., pp. 99–108.

Jahn, A., Griebe, T., Nielsen, P.H., 1999. Composition of pseudomonas putida biofilms: Accumulation of protein in the biofilm matrix. Biofouling 14, 49–57.

Jahn, A., Nielsen, P.H., 1998. Cell biomass and exopolymer composition in sewer biofilms. Water Sci. Technol. 37, 17–24.

Joret, J.C., Levi, Y., 1986. Methode rapide d'evaluation du carbone eliminable des eaux par voie biologique. Trib. du CEBEDEAU.

Kaplan, L.A., Bott, T.L., Reasoner, D.J., 1993. Evaluation and simplification of the assimilable organic carbon nutrient bioassay for bacterial growth in drinking water. Appl. Environ. Microbiol. 59, 1532–1539.

Katsoufidou, K., Yiantsios, S.G., Karabelas, A.J., 2005. A study of ultrafiltration membrane fouling by humic acids and flux recovery by backwashing: Experiments and modeling. J. Memb. Sci. 266, 40–50.

Kemmy, F.A., Fry, J.C., Breach, R.A., 1989. Development and operational implementation of a modified and simplified method for determination of assimilable organic carbon (AOC) in drinking water. Water Sci. Technol. 21, 155–159.

Kilb, B., Lange, B., Schaule, G., Flemming, H.-C., Wingender, J., 2003. Contamination of drinking water by coliforms from biofilms grown on rubber-coated valves. Int. J. Hyg. Environ. Health 206, 563–73.

Kimura, K., Amy, G., Drewes, J.E., Heberer, T., Kim, T.-U., Watanabe, Y., 2003. Rejection of organic micropollutants (disinfection by-products, endocrine disrupting compounds, and pharmaceutically active compounds) by NF/RO membranes. J. Memb. Sci. 227, 113–121.

Laspidou, C., Rittmann, B.E., 2002. A unified theory for extracellular polymeric substances, soluble microbial products, and active and inert biomass. Water Res. 36, 2711–2720.

Lauderdale, C., Chadik, P., Kirisits, M.J., Brown, J., 2012. Engineered Biofiltration: Enhanced Biofilter Performance through Nutrient and Peroxide Addition. Journal-American Water Work. Assoc. 104, E298–E309.

Laurent, P., Prévost, M., Cigana, J., Niquette, P., Servais, P., 1999. Biodegradable organic matter removal in biological filters: evaluation of the CHABROL model. Water Res. 33, 1387–1398.

Le Bihan, Y., Lessard, P., 2000. Monitoring biofilter clogging: biochemical characteristics of the biomass. Water Res. 34, 4284–4294.

Le Bihan, Y., Lessard, P., 1998. Influence of operational variables on enzymatic tests applied to monitor the microbial biomass activity of a biofilter. Water Sci. Technol. 37, 199–202.

LeChevallier, M.W., Shaw, N.E., Kaplan, L.A., Bott, T.L., 1993. Development of a rapid assimilable organic carbon method for water. Appl. Environ. Microbiol. 59, 1526–1531.

Lee, D.-Y., Lee, H., Trevors, J.T., Weir, S.C., Thomas, J.L., Habash, M., 2014. Characterization of sources and loadings of fecal pollutants using microbial source tracking assays in urban and rural areas of the Grand River Watershed, Southwestern Ontario. Water Res. 53, 123–31.

Legendre, P., Legendre, L.F.J., 2012. Numerical ecology. Elsevier.

Leon Morales, C.F., Strathmann, M., Flemming, H.-C., 2007. Influence of biofilms on the movement of colloids in porous media. Implications for colloid facilitated transport in subsurface environments.

Water Res. 41, 2059–68.

Lewandowski, Z., Beyenal, H., 2005. Biofilms: their structure, activity, and effect on membrane filtration. Water Sci. Technol. 51, 181–192.

Liu, C.X., Zhang, D.R., He, Y., Zhao, X.S., Bai, R., 2010. Modification of membrane surface for anti-biofouling performance: Effect of anti-adhesion and anti-bacteria approaches. J. Memb. Sci. 346, 121–130.

Liu, L.-F., Yu, S.-C., Zhou, Y., Gao, C.-J., 2006. Study on a novel polyamide-urea reverse osmosis composite membrane (ICIC–MPD): I. Preparation and characterization of ICIC–MPD membrane. J. Memb. Sci. 281, 88–94.

Liu, X., Huck, P.M., Slawson, R.M., 2001. Factors affecting drinking water biofiltration. Am. Water Work. Assoc. J. 93, 16.

Magic-Knezev, A., van der Kooij, D., 2004. Optimisation and significance of ATP analysis for measuring active biomass in granular activated carbon filters used in water treatment. Water Res. 38, 3971–9.

Mansouri, J., Harrisson, S., Chen, V., 2010. Strategies for controlling biofouling in membrane filtration systems: challenges and opportunities. J. Mater. Chem. 20, 4567–4586.

Martin, G., Nam, S.H., Vitrac, O., Reinbold, M., 1980. Utilisation de l'adenosine triphosphate dans les systemes d'epuration biologique. Variation de la teneur en A.T.P. de boues activees en regimes continu et transitoire. Water Res. 14, 379–387.

Massieux, B., Boivin, M.E.Y., van den Ende, F.P., Langenskiöld, J., Marvan, P., Barranguet, C., Admiraal, W., Laanbroek, H.J., Zwart, G., 2004. Analysis of Structural and Physiological Profiles To Assess the Effects of Cu on Biofilm Microbial Communities. Appl. Environ. Microbiol. 70 , 4512–4521.

McCann, K.S., 2000. The diversity–stability debate. Nature 405, 228–233.

McKie, M.J., Taylor-Edmonds, L., Andrews, S.A., Andrews, R.C., 2015. Engineered biofiltration for the removal of disinfection by-product precursors and genotoxicity. Water Res. 81, 196–207.

Melo, L.F., Bott, T.R., 1997. Biofouling in water systems. Exp. Therm. fluid Sci. 14, 375–381.

Meng, F., Drews, A., Mehrez, R., Iversen, V., Ernst, M., Yang, F., Jekel, M., Kraume, M., 2009. Occurrence, Source, and Fate of Dissolved Organic Matter (DOM) in a Pilot-Scale Membrane Bioreactor. Environ. Sci. Technol. 43, 8821–8826.

Meylan, S., Hammes, F., Traber, J., Salhi, E., von Gunten, U., Pronk, W., 2007. Permeability of low molecular weight organics through nanofiltration membranes. Water Res. 41, 3968–76.

Michalowski, W., 2012. Composition, dynamics and function of extracellular polymeric substances in drinking-water biofilms. University of Duisburg-Essen.

Moll, D.M., Summers, R.S., Breen, A., 1998. Microbial Characterization of Biological Filters Used for Drinking Water Treatment. Appl. Environ. Microbiol. 64 , 2755–2759.

Moll, D.M., Summers, R.S., Fonseca, A.C., Matheis, W., 1999. Impact of Temperature on Drinking Water Biofilter Performance and Microbial Community Structure. Environ. Sci. Technol. 33, 2377–

2382.

Nguyen, T., Roddick, F.A., Fan, L., 2012. Biofouling of water treatment membranes: a review of the underlying causes, monitoring techniques and control measures. Membranes (Basel). 2, 804–840.

Nichols, C.M., Bowman, J.P., Guezennec, J., 2005. Effects of incubation temperature on growth and production of exopolysaccharides by an antarctic sea ice bacterium grown in batch culture. Appl. Environ. Microbiol. 71, 3519–23.

Nielsen, P.H., Jahn, A., 1999. Extraction of EPS, in: Wingender, J., Neu, T.R., Flemming, H.-C. (Eds.), Microbial Extracellular Polymeric Substances: Characterization, Structure and Function. p. 258.

Nielsen, P.H., Jahn, A., Palmgren, R., 1997. Conceptual model for production and composition of exopolymers in biofilms. Water Sci. Technol. 36, 11–19.

Okabe, S., Kokazi, T., Watanabe, Y., 2002. Biofilm formation potentials in drinking waters treated by different advanced treatment processes. Water Supply 2, 97–104.

Palmgren, R., Nielsen, P.H., 1996. Accumulation of DNA in the exopolymeric matrix of activated sludge and bacterial cultures. Water Sci. Technol. 34, 233–240.

Park, N., Kwon, B., Kim, S.-D., Cho, J., 2006. Characterizations of the colloidal and microbial organic matters with respect to membrane foulants. J. Memb. Sci. 275, 29–36.

Parker, L. V, Ranney, T.A., 1996. Sampling Trace-Level Organics with Polymeric Tubings. Revision. DTIC Document.

Paul, M., Park, H.B., Freeman, B.D., Roy, A., McGrath, J.E., Riffle, J.S., 2008. Synthesis and crosslinking of partially disulfonated poly (arylene ether sulfone) random copolymers as candidates for chlorine resistant reverse osmosis membranes. Polymer (Guildf). 49, 2243–2252.

Peiris, R.H., Hallé, C., Budman, H., Moresoli, C., Peldszus, S., Huck, P.M., Legge, R.L., 2010. Identifying fouling events in a membrane-based drinking water treatment process using principal component analysis of fluorescence excitation-emission matrices. Water Res. 44, 185–94.

Peldszus, S., Benecke, J., Jekel, M., Huck, P.M., 2012. Direct biofiltration pretreatment for fouling control of ultrafiltration membranes. Journal-American Water Work. Assoc. 104, E430–E445.

Peldszus, S., Hallé, C., Peiris, R.H., Hamouda, M., Jin, X., Legge, R.L., Budman, H., Moresoli, C., Huck, P.M., 2011. Reversible and irreversible low-pressure membrane foulants in drinking water treatment: Identification by principal component analysis of fluorescence EEM and mitigation by biofiltration pretreatment. Water Res. 45, 5161–70.

Pellicer-Nàcher, C., Domingo-Félez, C., Mutlu, A.G., Smets, B.F., 2013. Critical assessment of extracellular polymeric substances extraction methods from mixed culture biomass. Water Res. 47, 5564–74.

Persson, F., Heinicke, G., Hedberg, T., Hermansson, M., Uhl, W., 2007. Removal of geosmin and MIB by biofiltration-an investigation discriminating between adsorption and biodegradation. Environ. Technol. 28, 95–104.

Persson, F., Heinicke, G., Uhl, W., Hedberg, T., Hermansson, M., 2006. Performance of direct biofiltration of surface water for reduction of biodegradable organic matter and biofilm formation

potential. Environ. Technol. 27, 1037–1045.

Pharand, L., Van Dyke, M.I., Anderson, W.B., Huck, P.M., 2014. Assessment of biomass in drinking water biofilters by adenosine triphosphate. J. Am. Water Works Assoc. 106, E433–E444.

Pharand, L., Van Dyke, M.I., Anderson, W.B., Yohannes, Y., Huck, P.M., 2015. Full-scale Ozone-Biofiltration: Seasonally-related effects on NOM Removal. J. Am. Water Works Assoc. 107, E425–E435.

Pietramellara, G., Ascher, J., Borgogni, F., Ceccherini, M.T., Guerri, G., Nannipieri, P., 2009. Extracellular DNA in soil and sediment: fate and ecological relevance. Biol. Fertil. Soils 45, 219–235.

Pifer, A.D., Fairey, J.L., 2012. Improving on SUVA 254 using fluorescence-PARAFAC analysis and asymmetric flow-field flow fractionation for assessing disinfection byproduct formation and control. Water Res. 46, 2927–36.

Prest, E.I., Hammes, F., Kötzsch, S., Van Loosdrecht, M.C.M., Vrouwenvelder, J.S., 2013. Monitoring microbiological changes in drinking water systems using a fast and reproducible flow cytometric method. water Res. 47, 7131–7142.

Prévost, J., Coallier, J., Mailly, J., Desjardins, R., Duchesne, D., 1992. Comparison of biodegradable organic carbon techniques for process control. J. Water Supply Res. Tecnol. 41, 141–150.

Prévost, M., Desjardins, R., Arcouette, N., Duchesne, D., Coallier, J., 1990. Étude de la performance de filtres à charbon actif biologique (CAB) en eaux froides. Sci. Tech. l'eau 23, 25.

Prévost, M., Laurent, P., Servais, P., 2005. Biodegradable organic matter in drinking water treatment and distribution. American Water Works Association.

R Core Team, 2015. R: A language and environment for statistical computing. R Foundation for Statistical Computing, Vienna, Austria, 2012.

Redmile-Gordon, M.A., Brookes, P.C., Evershed, R.P., Goulding, K.W.T., Hirsch, P.R., 2014. Measuring the soil-microbial interface: Extraction of extracellular polymeric substances (EPS) from soil biofilms. Soil Biol. Biochem. 72, 163–171.

Rice, E.W., Bridgewater, L., Association., A.P.H., Association., A.W.W., Federation., W.E., 2012. Standard methods for the examination of water and wastewater. American Public Health Association, Washington, D.C.

Ross, P.S., Hammes, F., Dignum, M., Magic-Knezev, A., Hambsch, B., Rietveld, L.C., 2013. A comparative study of three different assimilable organic carbon (AOC) methods: results of a round-robin test. Water Sci. Technol. Water Supply 13, 1024–1033.

Rouwenhorst, R.J., Frank Jzn, J., Scheffers, W.A., van Dijken, J.P., 1991. Determination of protein concentration by total organic carbon analysis. J. Biochem. Biophys. Methods 22, 119–128.

Ruhl, A.S., Jekel, M., 2012. Elution behaviour of low molecular weight compounds in size exclusion chromatography. J. Water Supply Res. Technol. 61, 32–40.

Sathasivan, A., Ohgaki, S., 1999. Application of new bacterial regrowth potential method for water distribution system–a clear evidence of phosphorus limitation. Water Res. 33, 137–144.

Sathasivan, A., Ohgaki, S., Yamamoto, K., Kamiko, N., 1997. Role of inorganic phosphorus in controlling regrowth in water distribution system. Water Sci. Technol. 35, 37–44.

Sauer, K., Camper, A.K., 2001. Characterization of Phenotypic Changes inPseudomonas putida in Response to Surface-Associated Growth. J. Bacteriol. 183, 6579–6589.

Sauer, K., Camper, A.K., Ehrlich, G.D., Costerton, J.W., Davies, D.G., 2002. Pseudomonas aeruginosa displays multiple phenotypes during development as a biofilm. J. Bacteriol. 184, 1140–1154.

Schmidt, J.E., Ahring, B.K., 1996. Granular sludge formation in upflow anaerobic sludge blanket (UASB) reactors. Biotechnol. Bioeng. 49, 229–246.

Schneider, D.A., Gourse, R.L., 2004. Relationship between Growth Rate and ATP Concentration in Escherichia coli A BIOASSAY FOR AVAILABLE CELLULAR ATP. J. Biol. Chem. 279, 8262–8268.

Schneider, R.P., Ferreira, L.M., Binder, P., Bejarano, E.M., Góes, K.P., Slongo, E., Machado, C.R., Rosa, G.M.Z., 2005. Dynamics of organic carbon and of bacterial populations in a conventional pretreatment train of a reverse osmosis unit experiencing severe biofouling. J. Memb. Sci. 266, 18–29.

Servais, P., Billen, G., Bouillot, P., 1994. Biological Colonization of Granular Activated Carbon Filters in Drinking-Water Treatment. J. Environ. Eng. 120, 888–899.

Servais, P., Billen, G., Hascoet, M.C., 1987. Determination of the biodegradable fraction of dissolved organic matter in waters. Water Res. 21, 445–450.

Servais, P., Billen, G., Ventresque, C., Bablon, G.P., 1991. Microbial activity in GAC filters at the Choisy-le-Roi treatment plant. J. Am. Water Works Assoc. 62–68.

Sheng, G.-P., Yu, H.-Q., 2006. Characterization of extracellular polymeric substances of aerobic and anaerobic sludge using three-dimensional excitation and emission matrix fluorescence spectroscopy. Water Res. 40, 1233–9.

Sigee, D.C., 2004. Microbial Diversity and Freshwater Ecosystems, in: Freshwater Microbiology. John Wiley & Sons, Ltd, pp. 1–46.

Simpson, D.R., 2008. Biofilm processes in biologically active carbon water purification. Water Res. 42, 2839–2848.

SLMB, 2012. Determining the Total Cell Count and Ratios of High and Low Nucleic Acid Content Cells in Freshwater Using Flow Cytometry. Analysis Method 333.1, in: The Swiss Food Book. (Schweizerische Lebensmittelbuch). Federal Office of Public Health, Switzerland.

Stepanauskas, R., Farjalla, V.F., Tranvik, L.J., Svensson, J.M., Esteves, F.A., Granéli, W., 2000. Bioavailability and sources of DOC and DON in macrophyte stands of a tropical coastal lake. Hydrobiologia 436, 241–248.

Stewart, P.S., 2012. Mini-review: Convection around biofilms. Biofouling 28, 187–198.

Stewart, T., Traber, J., Kroll, A., Behra, R., Sigg, L., 2013. Characterization of extracellular polymeric substances (EPS) from periphyton using liquid chromatography-organic carbon detection–organic nitrogen detection (LC-OCD-OND). Environ. Sci. Pollut. Res. 20, 3214–3223.

Stoquart, C., Barbeau, B., Servais, P., Vázquez-Rodríguez, G.A., 2013. Quantifying bacterial biomass fixed onto biological activated carbon (PAC and GAC) used in drinking water treatment. J. Water Supply Res. Technol.

Sutherland, I.W., 2001a. Biofilm exopolysaccharides: a strong and sticky framework. Microbiology 147, 3–9.

Sutherland, I.W., 2001b. The biofilm matrix – an immobilized but dynamic microbial environment. Trends Microbiol. 9, 222–227.

Takahashi, E., Ledauphin, J., Goux, D., Orvain, F., 2009. Optimising extraction of extracellular polymeric substances (EPS) from benthic diatoms: comparison of the efficiency of six EPS extraction methods. Mar. Freshw. Res.

Theron, D.P., Prior, B.A., Lategan, P.M., 1987. Effect of minimum growth temperature on the adenosine triphosphate content of bacteria. Int. J. Food Microbiol. 4, 323–329.

Toolan, T., Wehr, J.D., Findlay, S., 1991. Inorganic Phosphorus Stimulation of Bacterioplankton Production in a Meso-Eutrophic Lake. Appl. Environ. Microbiol. 57 , 2074–2078.

Tsai, B. -N., Chang, C. -H., Lee, D. -J., 2008. Fractionation of soluble microbial products (SMP) and soluble extracellular polymeric substances (EPS) from wastewater sludge. Environ. Technol. 29, 1127–1138.

Ubertini, M., Lefebvre, S., Rakotomalala, C., Orvain, F., 2015. Impact of sediment grain-size and biofilm age on epipelic microphytobenthos resuspension. J. Exp. Mar. Bio. Ecol. 467, 52–64.

Urfer, D., Huck, P.M., 2001. Measurement of biomass activity in drinking water biofilters using a respirometric method. Water Res. 35, 1469–1477.

Urfer, D., Huck, P.M., Booth, S.D.J., Coffey, B.M., 1997. Biological Filtration for BOM and Particle Removal: A Critical Review. J. Am. Water Works Assoc. 89, 83–98.

van der Kooij, D., 1992. Assimilable organic carbon as an indicator of bacterial regrowth. J. Am. Water Works Assoc. 57–65.

van der Kooij, D., Cornelissen, E.R., Hijnen, W., 2010. Biofouling of spiral wound membranes in water treatment. WRF, Denver, CO.

Van der Kooij, D., Visser, A., Hijnen, W.A.M., 1982. Determining the Concentration of Easily Assimilable Organic Carbon in Drinking Water. J. Am. Water Works Assoc.

Van Loosdrecht, M.C.M., Eikelboom, D., Gjaltema, A., Mulder, A., Tijhuis, L., Heijnen, J.J., 1995. Biofilm structures. Water Sci. Technol. 32, 35–43.

Velten, S., Boller, M., Köster, O., Helbing, J., Weilenmann, H.-U., Hammes, F., 2011. Development of biomass in a drinking water granular active carbon (GAC) filter. Water Res. 45, 6347–54.

Velten, S., Hammes, F., Boller, M., Egli, T., 2007. Rapid and direct estimation of active biomass on granular activated carbon through adenosine tri-phosphate (ATP) determination. Water Res. 41, 1973–83.

Verschuere, L., Fievez, V., Van Vooren, L., Verstraete, W., 1997. The contribution of individual

populations to the Biolog pattern of model microbial communities. FEMS Microbiol. Ecol. 24, 353–362.

Villacorte, L.O., Ekowati, Y., Calix-Ponce, H.N., Schippers, J.C., Amy, G.L., Kennedy, M.D., 2015. Improved method for measuring transparent exopolymer particles (TEP) and their precursors in fresh and saline water. Water Res. 70, 300–12.

Villacorte, L.O., Kennedy, M.D., Amy, G.L., Schippers, J.C., 2009. The fate of Transparent Exopolymer Particles (TEP) in integrated membrane systems: removal through pre-treatment processes and deposition on reverse osmosis membranes. Water Res. 43, 5039–52.

Vital, M., Füchslin, H.P., Hammes, F., Egli, T., 2007. Growth of Vibrio cholerae O1 Ogawa Eltor in freshwater. Microbiology 153, 1993–2001.

Volk, C., Bell, K., Ibrahim, E., Verges, D., Amy, G., LeChevallier, M., 2000. Impact of enhanced and optimized coagulation on removal of organic matter and its biodegradable fraction in drinking water. Water Res. 34, 3247–3257.

Volk, C.J., LeChevallier, M.W., 1999. Impacts of the reduction of nutrient levels on bacterial water quality in distribution systems. Appl. Environ. Microbiol. 65, 4957–4966.

Vrouwenvelder, J., Vanpaassen, J., Wessels, L., Vandam, A., Bakker, S., 2006. The Membrane Fouling Simulator: A practical tool for fouling prediction and control. J. Memb. Sci. 281, 316–324.

Vrouwenvelder, J.S., Graf von der Schulenburg, D.A., Kruithof, J.C., Johns, M.L., van Loosdrecht, M.C.M., 2009a. Biofouling of spiral-wound nanofiltration and reverse osmosis membranes: a feed spacer problem. Water Res. 43, 583–94.

Vrouwenvelder, J.S., Hinrichs, C., Van der Meer, W.G.J., Van Loosdrecht, M.C.M., Kruithof, J.C., 2009b. Pressure drop increase by biofilm accumulation in spiral wound RO and NF membrane systems: role of substrate concentration, flow velocity, substrate load and flow direction. Biofouling 25, 543–555.

Vrouwenvelder, J.S., Kappelhof, J., Heijrnan, S.G.J., Schippers, J.C., Van der Kooija, D., 2003. Tools for fouling diagnosis of NF and RO membranes and assessment of the fouling potential of feed water. Desalination 157, 361–365.

Vrouwenvelder, J.S., Manolarakis, S.A., Van der Hoek, J.P., Van Paassen, J.A.M., Van der Meer, W.G.J., Van Agtmaal, J.M.C., Prummel, H.D.M., Kruithof, J.C., Van Loosdrecht, M.C.M., 2008. Quantitative biofouling diagnosis in full scale nanofiltration and reverse osmosis installations. Water Res. 42, 4856–4868.

Vrouwenvelder, J.S., Picioreanu, C., Kruithof, J.C., van Loosdrecht, M.C.M., 2010. Biofouling in spiral wound membrane systems: Three-dimensional CFD model based evaluation of experimental data. J. Memb. Sci. 346, 71–85.

Vrouwenvelder, J.S., Van der Kooij, D., 2001. Diagnosis, prediction and prevention of biofouling of NF and RO membranes. Desalination 139, 65–71.

Vrouwenvelder, J.S., van Paassen, J.A.M., van Agtmaal, J.M.C., van Loosdrecht, M.C.M., Kruithof, J.C., 2009c. A critical flux to avoid biofouling of spiral wound nanofiltration and reverse osmosis membranes: Fact or fiction? J. Memb. Sci. 326, 36–44.

Walker, J.M., 1996. The protein protocols handbook. Springer Science & Business Media.

Wang, J.Z., Summers, R.S., Miltner, R.J., 1995. Biofiltration performance: part 1, relationship to biomass. J. / Am. Water Work. Assoc. 87.

Wang, Y., Hammes, F., Boon, N., Egli, T., 2007. Quantification of the Filterability of Freshwater Bacteria through 0.45, 0.22, and 0.1 μm Pore Size Filters and Shape-Dependent Enrichment of Filterable Bacterial Communities. Environ. Sci. Technol. 41, 7080–7086.

Wang, Y., Hammes, F., Düggelin, M., Egli, T., 2008. Influence of Size, Shape, and Flexibility on Bacterial Passage through Micropore Membrane Filters. Environ. Sci. Technol. 42, 6749–6754.

Weber, K.P., Gehder, M., Legge, R.L., 2008. Assessment of changes in the microbial community of constructed wetland mesocosms in response to acid mine drainage exposure. Water Res. 42, 180–8.

Werner, P., 1985. Eine Methode zur Bestimmung der Verkeimungsneigung von Trinkwasser. Vom Wasser 65, 257–270.

Whitchurch, C.B., Tolker-Nielsen, T., Ragas, P.C., Mattick, J.S., 2002. Extracellular DNA required for bacterial biofilm formation. Science (80-.). 295, 1487.

Wilderer, P.A., Wuertz, S., Bishop, P.L., 2002. Biofilms in wastewater treatment : an interdisciplinary approach. IWA, London.

Wilson, B., 2015. Optimization of the Biofiltration / Ultrafiltration Process. Master's thesis, University of Waterloo.

Wingender, J., Jagger, K.-E., Flemming, H.-C., 1999a. Interactions Between Extracellular Polysaccharides and Enzymes, in: Wingender, J., Neu, T.R., Flemming, H.-C. (Eds.), Microbial Extracellular Polymeric Substances: Characterization, Structure and Function. Springer, p. 258.

Wingender, J., Neu, T.R., Flemming, H.-C., 1999b. What are Bacterial Extracellular Polymeric Substances?, in: Wingender, J., Neu, T.R., Flemming, H.-C. (Eds.), Microbial Extracellular Polymeric Substances: Characterization, Structure and Function. Springer, p. 258.

Yachi, S., Loreau, M., 1999. Biodiversity and ecosystem productivity in a fluctuating environment: the insurance hypothesis. Proc. Natl. Acad. Sci. 96, 1463–1468.

Yang, H.-L., Chun-Te Lin, J., Huang, C., 2009. Application of nanosilver surface modification to RO membrane and spacer for mitigating biofouling in seawater desalination. Water Res. 43, 3777–3786.

Zhang, S., 1996. Modeling biological drinking water treatment processes. University of Alberta.

Zhang, S., Huck, P.M., 1996a. Removal of AOC in biological water treatment processes: A kinetic modeling approach. Water Res. 30, 1195–1207.

Zhang, S., Huck, P.M., 1996b. Parameter estimation for biofilm processes in biological water treatment. Water Res. 30, 456–464.

Zheng, D., Andrews, R.C., Andrews, S.A., Taylor-Edmonds, L., 2015. Effects of coagulation on the removal of natural organic matter, genotoxicity, and precursors to halogenated furanones. Water Res. 70, 118–29.

Appendix A

Supplementary Information for Chapter 3

.
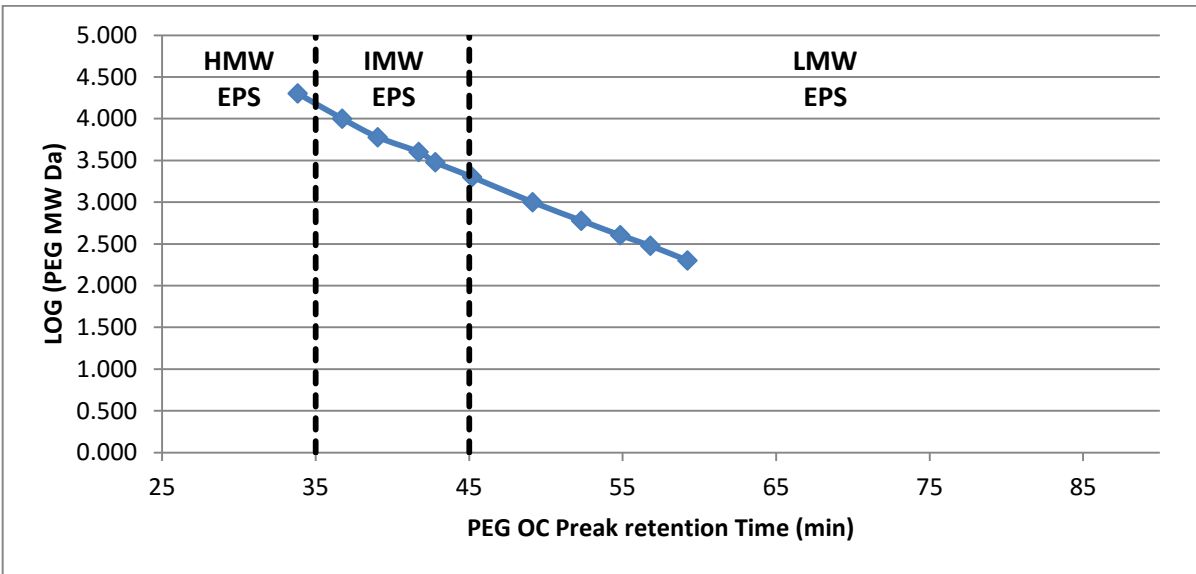
Figure S1 – Organic carbon peak retention time for standard polyethylene glycol (PEG) solutions of different molecular weights

Equation for normalizing EPS concentrations with regard to media volume

$Normalized\ EPS\ Concentration\ per\ media\ unit\ volume$

$$= \frac{concentration\ in\ EPS\ extract^1 * extract\ volume * ratio\ of\ media\ dry\ weight\ to\ wet\ weight}{sample\ dilution\ factor * bulk\ media\ density * media\ sample\ wet\ weight}$$

[1] Includes fluorescence spectroscopy response at predetermined coordinates, EPS total protein concentration, EPS total carbohydrate concentration and LC-OCD fraction concentration

Sampling Date	Biofilter	Sampling depth (cm)	Media Type	Cell Count (cells / cm³)	ATP (ng ATP / cm³)	Proteins (μg BSA / cm³)	Carbohydrates (μg D-Glucose/ cm³)	Protein Like FEEM response (A.U. / cm³)	Fulvic acid like FEEM response (A.U. / cm³)	Humic acid like FEEM response (A.U. / cm³)	HMW EPS Organic carbon (ng C/ cm³)	HMW EPS Organic nitrogen (ng N/ cm³)	HMW EPS UV Absorbance (10^{-3} x cm^{-1}/ cm³)	IMW EPS Organic carbon (ng C/ cm³)	IMW EPS Organic nitrogen (ng N/ cm³)	IMW EPS UV Absorbance (10^{-3} x cm^{-1}/ cm³)	LMW EPS Organic carbon (ng C/ cm³)	LMW EPS Organic nitrogen (ng N/ cm³)	LMW EPS UV Absorbance (10^{-3} x cm^{-1}/ cm³)
2014-04-11	Biofilter A	10	A	1.1E+08	322	34	17	1912	2432	4010	4194	1067	26	9204	1330	53	14658	4517	10
2014-04-11	Biofilter A	30	S	3.4E+08	490	62	28	4788	1981	3478	10179	2445	57	12357	2563	62	21913	8437	17
2014-04-11	Biofilter B	10	A	1.4E+08	325	35	16	2014	2682	4355	4509	1091	27	9693	1331	56	14783	4685	16
2014-04-11	Biofilter B	20	S	2.5E+08	537	67	40	5297	2120	3858	11654	2642	66	14851	2804	71	26216	8125	33
2014-04-11	Biofilter C	85	S	2.1E+08	378	62	21	4859	1748	3048	10075	2147	56	12167	2227	59	23000	7280	19
2014-05-08	Biofilter A	10	A	1.6E+08	646	62	25	4996	2775	5104	8789	2176	44	15845	2500	85	28473	20229	41
2014-05-08	Biofilter A	30	S	1.6E+08	514	64	27	5999	1905	3573	11137	2645	48	13000	2260	53	24003	17440	17
2014-05-08	Biofilter B	10	A	1.1E+08	701	60	26	5051	3049	5616	8475	2283	45	15041	2448	82	27056	19501	25
2014-05-08	Biofilter B	20	S	2.7E+08	661	111	52	11833	4874	7638	20967	4746	86	27025	4895	129	56924	40910	64
2014-05-08	Biofilter C	85	S	1.2E+08	256	59	29	5654	2553	4280	10025	2226	41	13458	2060	61	25154	21751	41
2014-05-29	Biofilter A	20	A	3.5E+08	1088	66	24	7664	3262	5992	10093	2744	50	16487	2384	77	31705	15745	0
2014-05-29	Biofilter A	20	S	1.2E+09	2158	166	102	24289	5887	12494	33816	8518	139	37949	7105	166	79398	54100	47
2014-05-29	Biofilter B	20	A	3.6E+08	782	63	24	7116	3361	6168	9535	2579	49	15950	2219	76	30318	12976	8
2014-05-29	Biofilter B	20	S	1.0E+09	1954	154	73	20632	5344	11359	31424	7515	125	35659	6246	156	71799	45826	18
2014-05-29	Biofilter C	85	S	1.4E+08	531	55	29	5351	1726	3432	8042	1946	34	11521	1307	47	21864	1952	8
2014-06-19	Biofilter A	85	S	6.4E+08	1332	143	45	19610	3814	9615	29515	6791	102	25313	5616	105	59712	26973	64
2014-06-19	Biofilter A	20	A	2.6E+08	539	61	18	7037	2537	5138	10510	2547	43	13198	2256	63	26719	10988	14
2014-06-19	Biofilter B	20	S	5.8E+08	1048	119	45	15412	3327	8208	24928	5550	83	21701	4481	90	49242	20854	63
2014-06-19	Biofilter B	20	A	1.9E+08	317	47	13	4332	3466	5944	7222	1886	36	11072	1643	61	19081	6639	23
2014-06-19	Biofilter B	60	S	2.3E+08	570	67	24	7837	1851	4148	12484	2903	45	12656	2162	46	26632	10529	33
2014-06-19	Biofilter C	85	S	1.4E+08	376	51	11	5044	1495	3117	9777	2109	33	9759	1563	40	17843	7495	18

Table S-1 – Biomass and EPS characterization results for the 21 media samples collected in this study for both sand (S) and anthracite (A)

Enzyme Name	UniProtKB id. number	Number of C atoms	Number of N atoms	C/N	MW (KDa)	Contain Aromatic Structure?
Protease	L7VS79	2114	568	3.72	48	yes
peptidase	K2EKF2	1621	435	3.72	36.8	yes
α-glucosidase	S5ZCH6	2722	741	3.67	60	yes
β-glucosidase	K4I2K9	3732	1008	3.70	84	yes
β - Xylosidase	C0INJ3	2687	755	3.56	60	yes
β-glucuronidase	H8ZT98	1233	326	3.78	28	yes
Esterase/lipase protein	M1NXW5	1402	391	3.58	32	yes
Phosphatase	W0FHD8	1323	312	4.24	28	yes
Endocellulase	F8V2V6	1842	495	3.72	40	yes
Alginate lyase	G3LI08	1566	433	3.62	35	yes
Chitinase	Q5UM79	1286	328	3.92	28	yes
Esterase	Q4TZQ3	1684	463	3.64	38	yes
Lipase	Q2KTB3	2865	772	3.71	65	yes

Table S2- Examples of enzymes commonly found in bacterial biofilm (Michalowski, 2012**). Their corresponding protein ID from the protein Resource (UniProt) and their molecular composition was generated by the ProtParam tool from the SIB Bioinformatics Resource Portal** (Gasteiger et al., 2005)

References:

Gasteiger, E., Hoogland, C., Gattiker, A., Wilkins, M.R., Appel, R.D., Bairoch, A., 2005. Protein identification and analysis tools on the ExPASy server. Springer.

Michalowski, W., 2012. Composition, dynamics and function of extracellular polymeric substances in drinking-water biofilms. University of Duisburg-Essen

Appendix B

Supplementary Information for Chapter 4
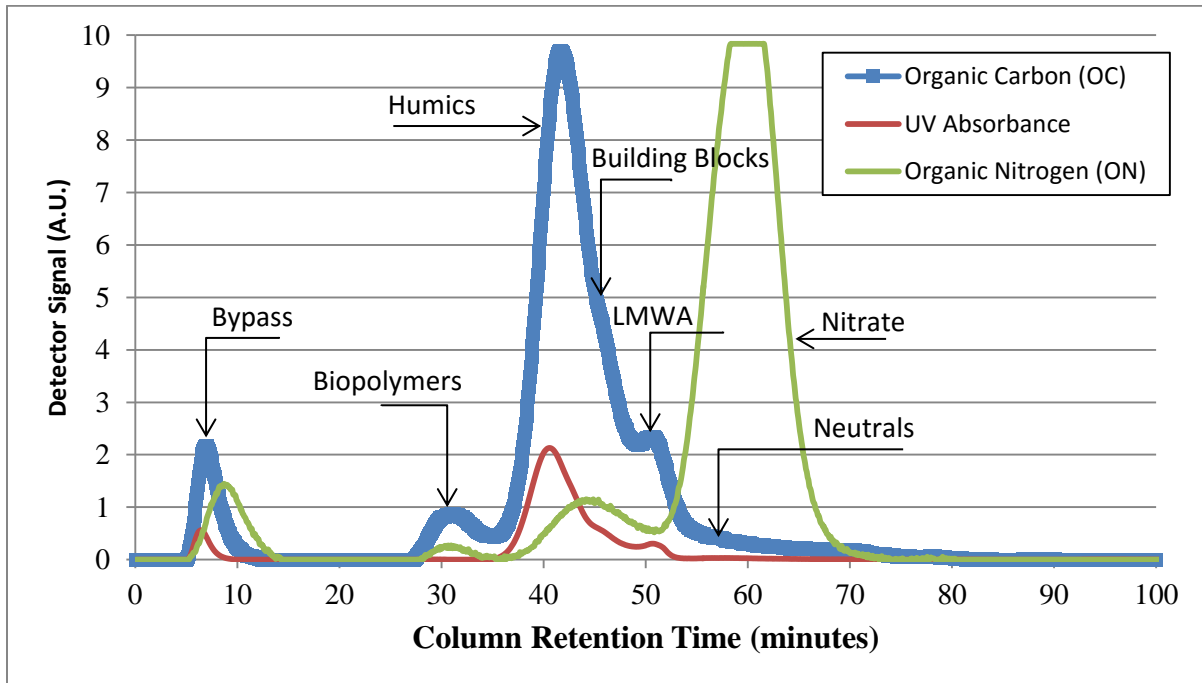
Figure S-1 – Typical raw water chromatograph using LC-OCD along with the main fractions
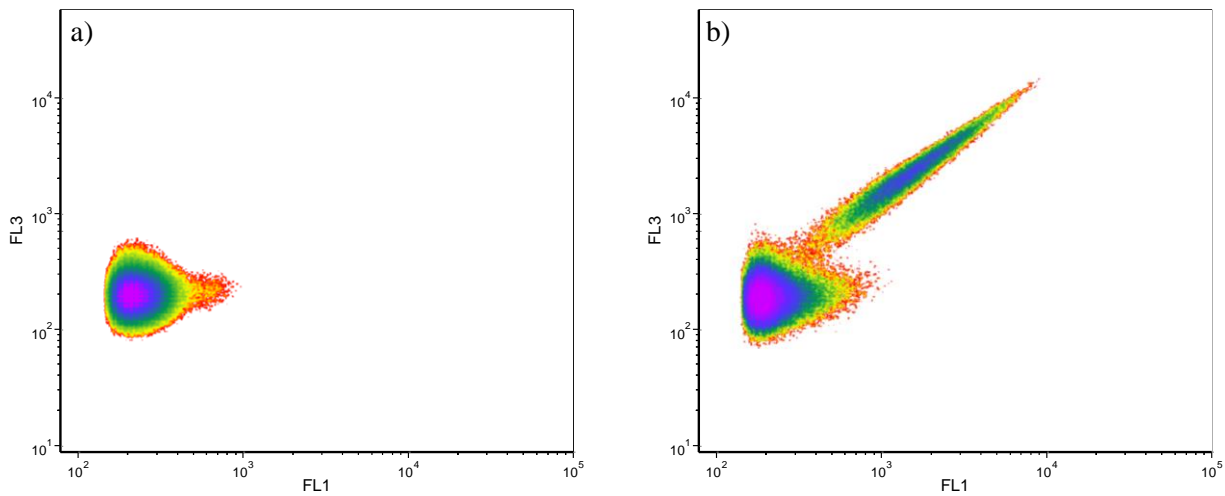
Figure S2 – Density plots for green fluorescence (FL1) and red fluorescence (FL3) for heated treated filter sterile river water using SYBR Green I nucleic acid stain after hear treatment at 60ºC for 30 min (a) and after boiling for 30 min
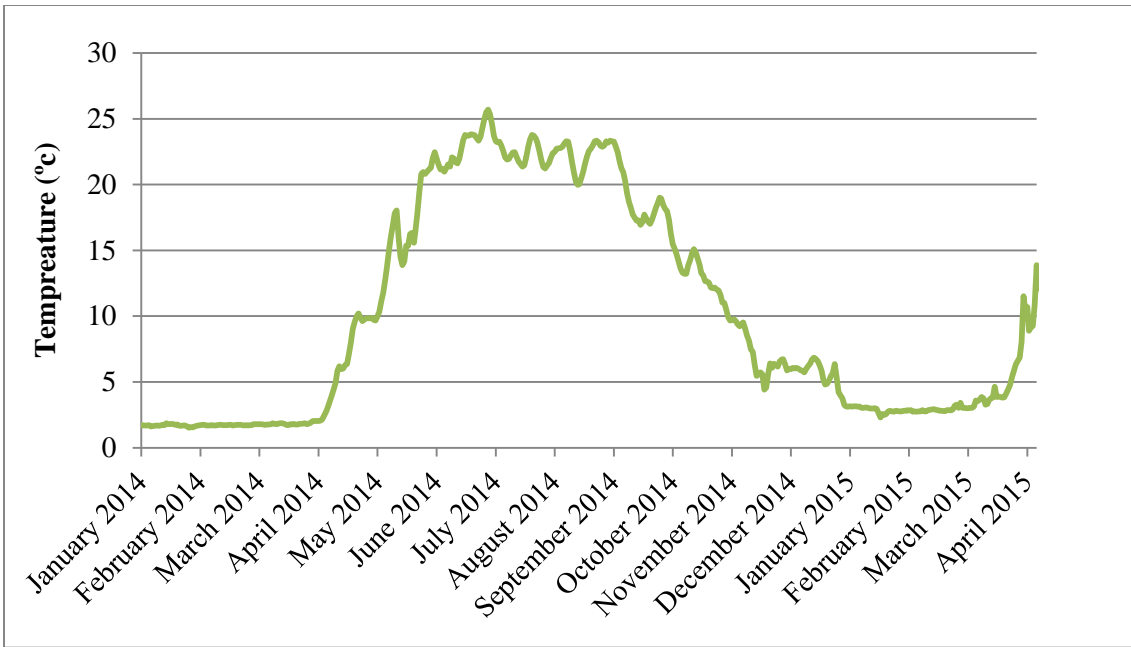
Figure S3 – Seasonal changes in river water temperature

210

Appendix C
Pilot Plant Description

1. <u>Pilot Plant Location</u>

The Region of Waterloo has a treatment plant (Mannheim WTP) that uses water from the Grand River at Kitchener, Ontario to provide drinking water for the cities of Kitchener/Waterloo. The Mannheim WTP receives its feed water from the Hidden Valley low lift pumping station (**Figure S1**). The intake of the water treatment plant consists of 4 different storage ponds to hold the river water before pumping it to the treatment plant. Mechanical mixers are used during the spring and summer season to continuously mix the stored water to control algae growth. The river water is then pumped to two large storage tanks, and these tanks are used to supply the Mannheim WTP. This WTP main raw water line, after the storage lagoons but before any chemical addition or treatment, is used to feed the biofilter pilot plant located at the same facility.
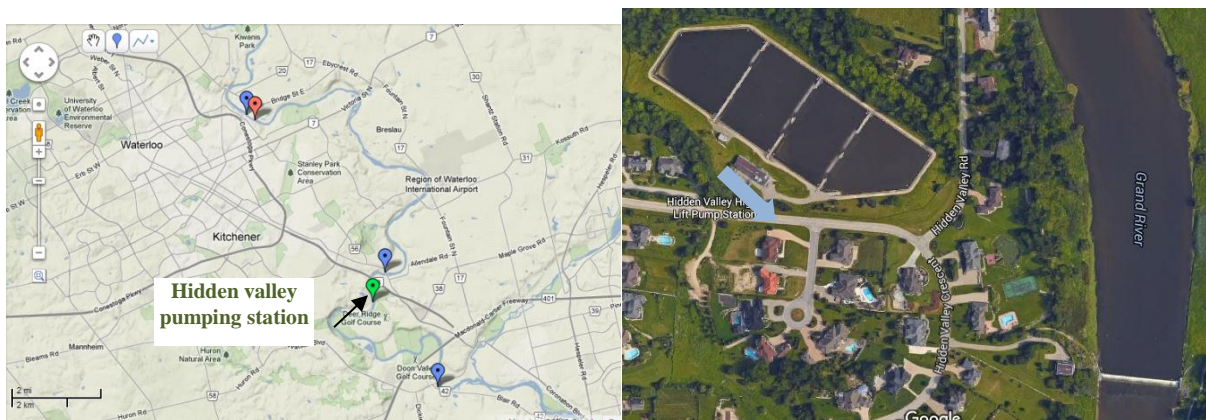
Figure S1 Map of the Grand River showing the location of Hidden Valley low lift pumping station

A biofiltration pilot facility at the Mannheim WTP was initially constructed by members of the NSERC Chair in Drinking Water Treatment in the summer of 2008 (Peldszus et al., 2012), but was substantially renovated for the current study. The previous pilot plant consisted of two anthracite\sand biofilters with EBCTs of 5 and 10 min and a surface loading rate of 5 m/h, and was operated in declined rate flow. Each biofilter consisted of 20 cm of anthracite overlaying the sand bed (20 cm and 60 cm of sand for 5 and 10 min EBCT respectively). An additional 5 min EBCT sand biofilter was used as an extension for the 10 min biofilter to achieve a total EBCT of 15 min. Upstream of each biofilter was a separate roughing filter consisting of 10 cm of gravel and 10 cm of coarse sand, which was used to partially reduce the particle loading (Peldszus et al., 2012). Within the current study, the pilot plant needed substantial upgrades to accommodate the study objectives, and also additional concurrent and future studies.

2. **Pilot Plant Component Design**

The pilot plant design and construction was a shared task with fellow graduate student Brad Wilson who also used the same pilot plant to run a study on the effect of biofilter backwash on the biofilter performance and its ability to control UF membrane fouling. The major tasks I was responsible for were as follows, and additional design information is available in Brad Wilson's thesis(2015):

2.1. **Pilot Feed water**

The pilot plant was fed using a 1 inch schedule 80 PVC pipe that connected to the main raw water line feeding the full scale water treatment plant. The feed pipe had two 50 cm clear PVC pipe sections to determine if the feed line required cleaning. To clean the feed water line, the line was divided in two sections that can be isolated and flushed at very high flow velocity to get rid of any deposits on the pipe walls.

2.2. **Roughing filter design**

One main component of the pilot plant was to have one large filter to treat the river raw water to reduce the particle loading on the biofilter which can cause excessive head loss development within the filters. The design flow rate for such a unit was 1000 L/hr. The used media in the roughing filter was 1/8 inch gravel used to retain large particles only and at the same time have high porosity and very short EBCT to prevent any biodegradation of NOM in the roughing filter. Two 5 cm layers of crushed gravel were used in the roughing filter. Four different roughing filters were designed and raw water flow was equally divided among the four filters. The roughing filter effluent was collected in one buffer tank and a magnetic sealed centrifugal pump was used to feed the water to the top of the biofilter columns. The design drawings of the roughing filter are shown on **Figures S2** and **S3**.
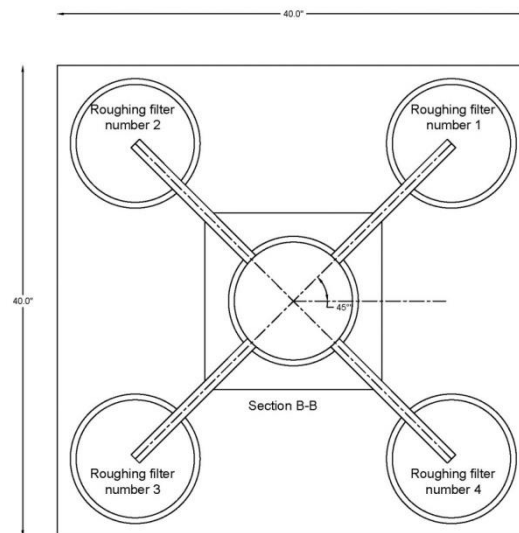
Figure S2- Design of the new pilot scale coarse media roughing filter at Mannheim WTP (Top view)

212
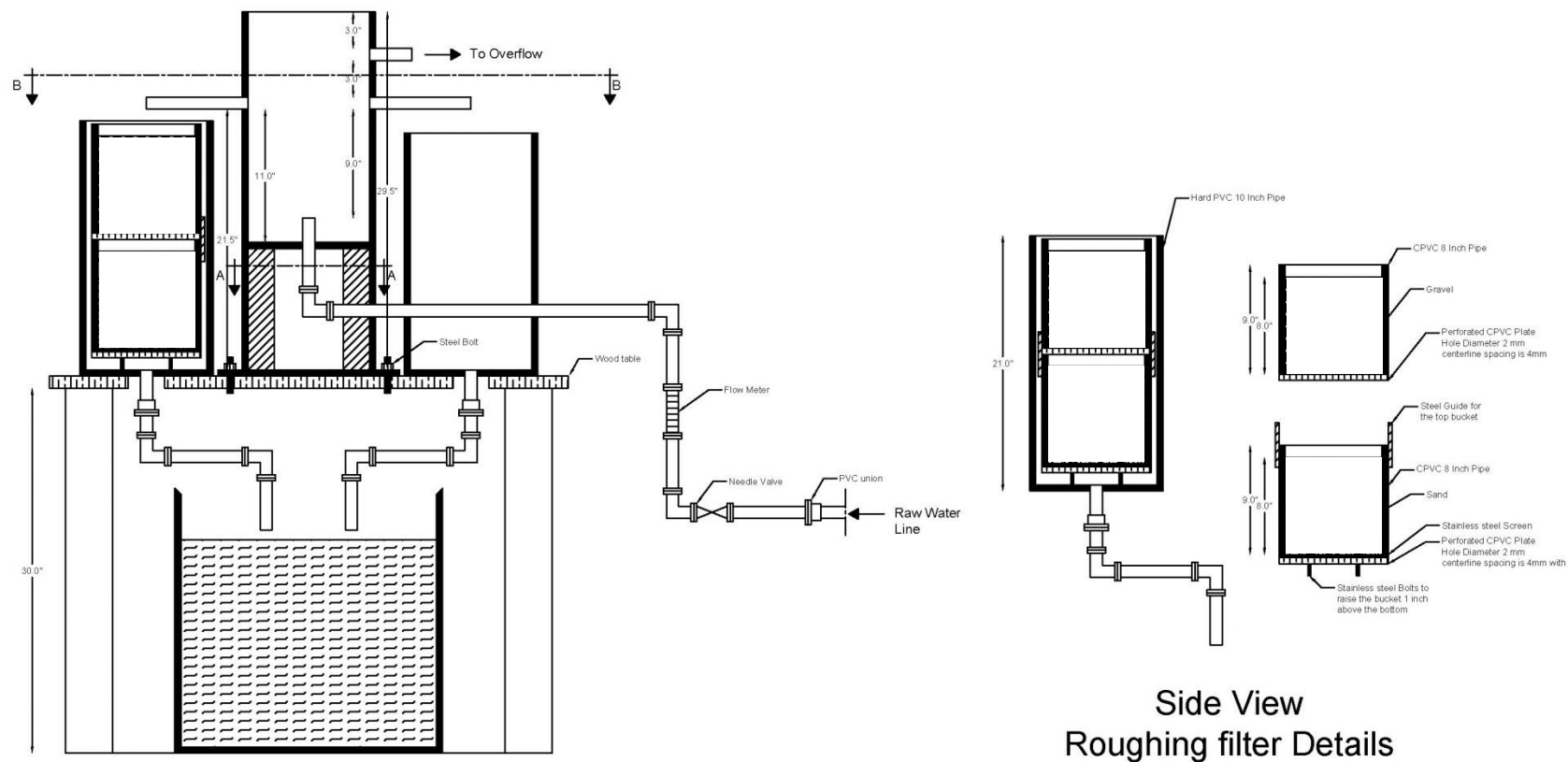
Figure S3- Design of the new pilot scale coarse media roughing filter at Mannheim WTP

2.3. **Biofilter Columns**

The new column filters used for the study were made from clear PVC to be able to visually determine the percent of bed expansion during the backwash. The design of the biofilter columns was done in way that limited the use of any glue or soft plastics that can contaminate the raw water. PVC welding was used to attached all the plastic pieces together. The bottom part of the filter include a perforated PVC plate to unformally distribute the flow over the biofilter cross section during the backwash procedures. Additionall, a conical base was used to allow for better water flow at the bottom of the filter. Several media sampling ports (1/4 inch) were drilled over the biofilter depth to allow for media sampling during the biofitlration study to characterize the biofilter attached biomass. The water depth in each filter above the filter media was 1.5 m, in order to have enough head to operate the filter for a few days. The effluent flow rate of each filter was kept constant using a custom built flow controller. The flow controller consisted of an industrial electromagnetic flow meter (ABB FEP300 Mag Meter, ABB, Canada) with a detection range of 10-500 L/h. An eletrically actuated ball metering PVC valve (Chemline Plastics, Canada) was connected to the flow meter using a PID conrtroller (Omega Canada) to adjust the PVC valve to keep the flow rate constant at 100 L/h (surface loading rate of 3.08 m/hr).

Three biofilter colums were used. BF (A) included 20 cm of anthracite, 20 cm of sand and 15 cm gravel base. BF (B) included 20 cm of anthracite, 60 cm of sand and 15 cm gravel base. The effluent from BF (B) was fed into a third biofilter BF (C) that included 40 cm sand and 15 cm gravel gravel base. In this way three filters with an EBCT of 8, 16 and 24 minutes can be achieved. To monitor the water quality, a tempreature probe (Cole Parmer Digi-Sense RTD Probe, Cole Parmer, Canada) was installed on the raw water line after the roughing filter pump. Also, each column had a pressure transducer (Model RK-68075-10, Cole Parmer, Canada) at its base to determine the headloss development with the filter columns. Low range online turbidity meters (HACH 1720E Low Range Turbidimeter, Hach, USA) were installed on the raw water line after the roughing filter pump and the bifilter columns to monitor turbidity removal within the three filters. Detailed information on the used sensors is available elsewhere (Wilson, 2015).
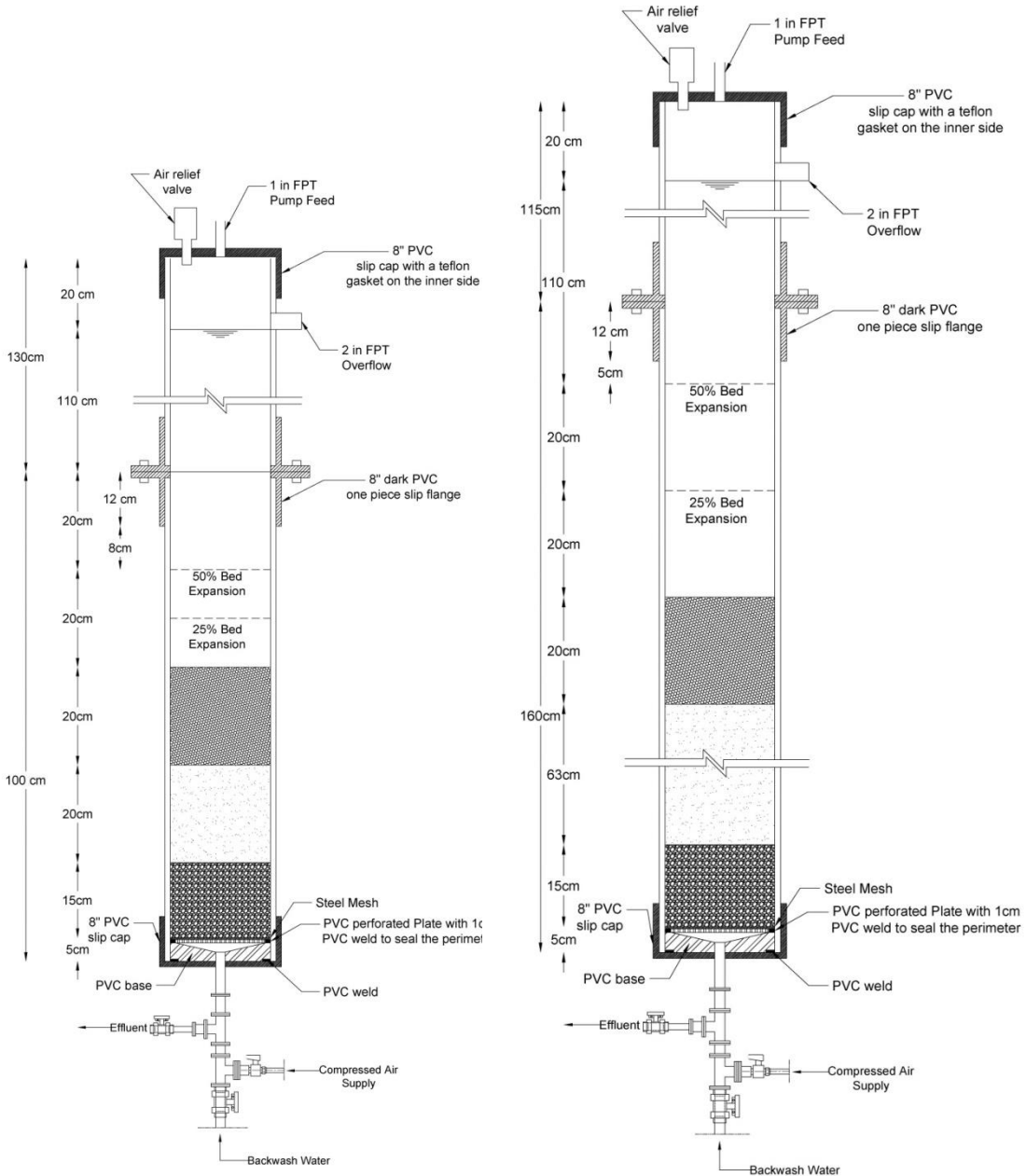
Figure S4- design of the used pilot scale biofilters A & B at the Mannheim WTP

2.4. **Biofilter waste tank**

The effluent water from the different biofilters was collected in a 1200 L PVDF tank and this tank was used for biofilter backwash. The waste water from our pilot plant leads directly into the full scale WTP filter waste line, which is sometimes pressurized during their full scale filter backwash. To solve such a problem, a second 500 L tank was connected to the biofilter effluent tank to receive its excess water. A centrifugal pump was then connected to the second waste tank to send the biofilter waste in the full scale waste line. A check valve was used to ensure no backflow into our pilot plant, and a water level controller was used to control the waste pump when the waste tank is full. A schematic of the pilot plant waste system is shown on **Figure S5**.
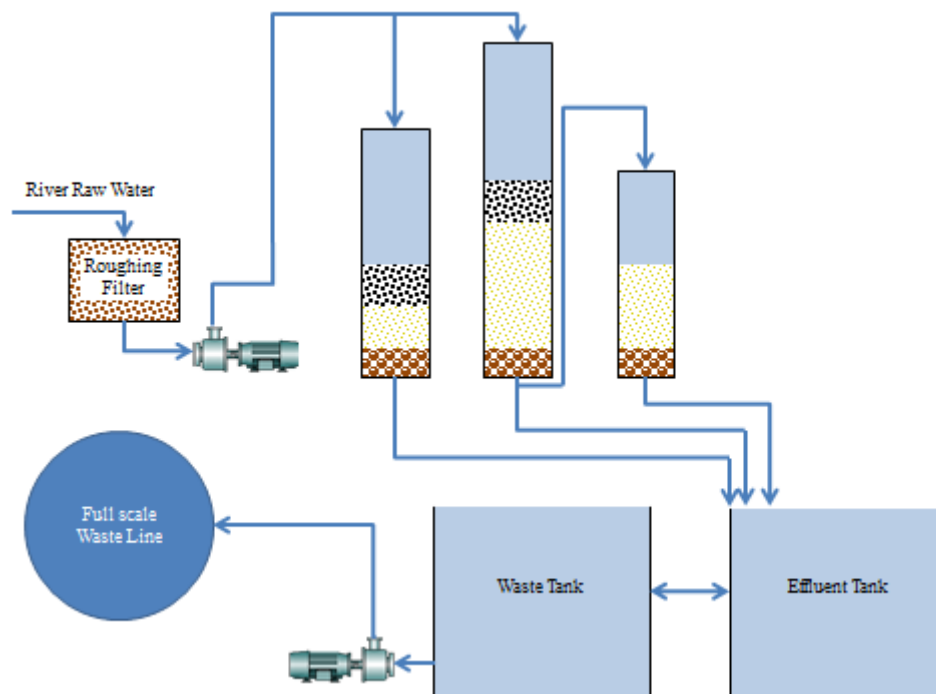
Figure S5- Schematic of the pilot plant waste system

2.5. **Media Specifications**

The biofilter media was supplied by a local distributer (Anthrafilter Media & Coal Ltd, Brantford, Ontario)**.** The media specification was as follows:

- **Sand**: Effective size of .48mm, uniformity coefficient of 1.44
- **Anthracite**: Effective size of 1.05 mm, uniformity coefficient of 1.48
- **Gravel**: 1 inch gravel

2.6. **Biofilter backwash procedures:**

The biofilter backwash procedures were as follows:

1. Isolate the biofilter feed and effluent water lines.
2. Drain the water above the filter media down to approximately 50 cm above the filter media.
3. Start the backwash by starting air scouring and sub fluidization backwash water flow for 3 minutes to achieve collapse pulsing conditions
4. Turn off the air scouring and increase the backwash flow to achieve 50% bed expansion for 10 minutes
5. Gradually turn off the backwash water to allow the media to stratify and good separation between sand and anthracite is obtained
6. Restart the filter by opening the biofilter feed and effluent water valves to resume filter operation.

Appendix D

Supplementary Material for Chapter 5

a)
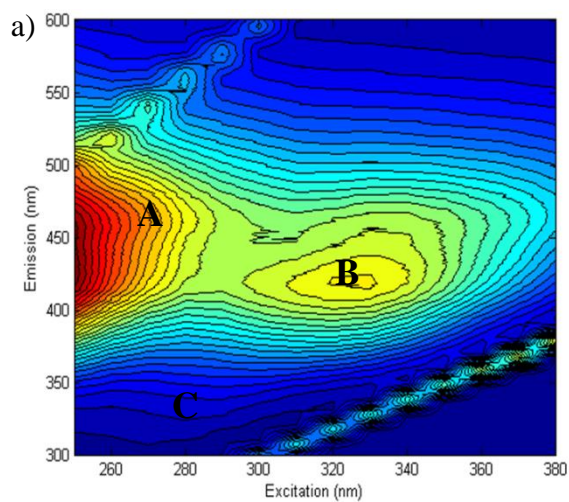
Figure S1– Typical FEEM contour plot of river water sample with humic like substances peak (A) (ex/em=270/460 nm), fulvic like substances peak (B) (ex/em=320/415 nm) and protein likes substances peak (c) (ex/em=280/330 nm)
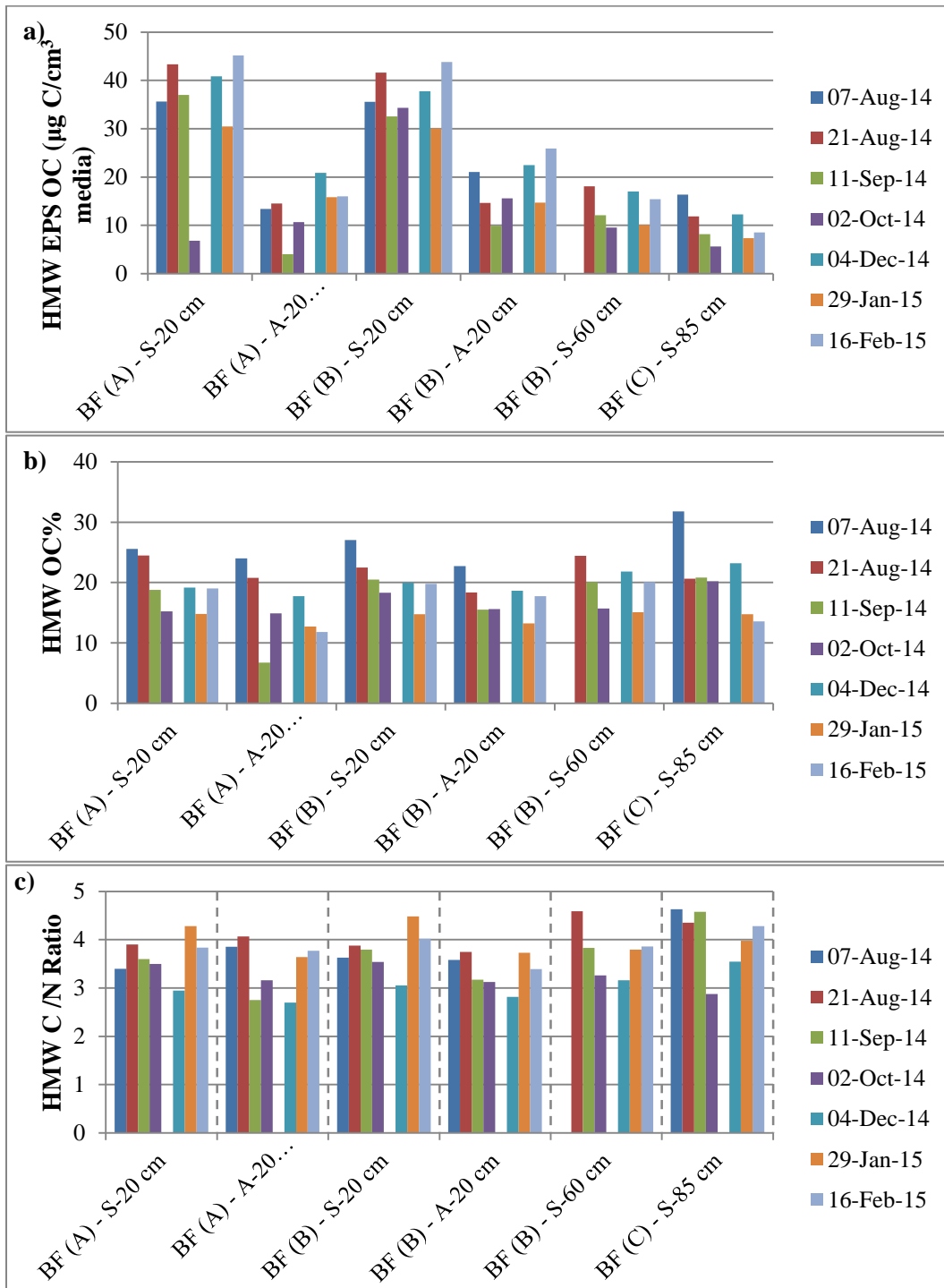
Figure S2 – Organic carbon of the extracted HMW EPS (a) the percent of total EPS organic carbon in this fraction (b) and its carbon to nitrogen ratio (c) over the study period
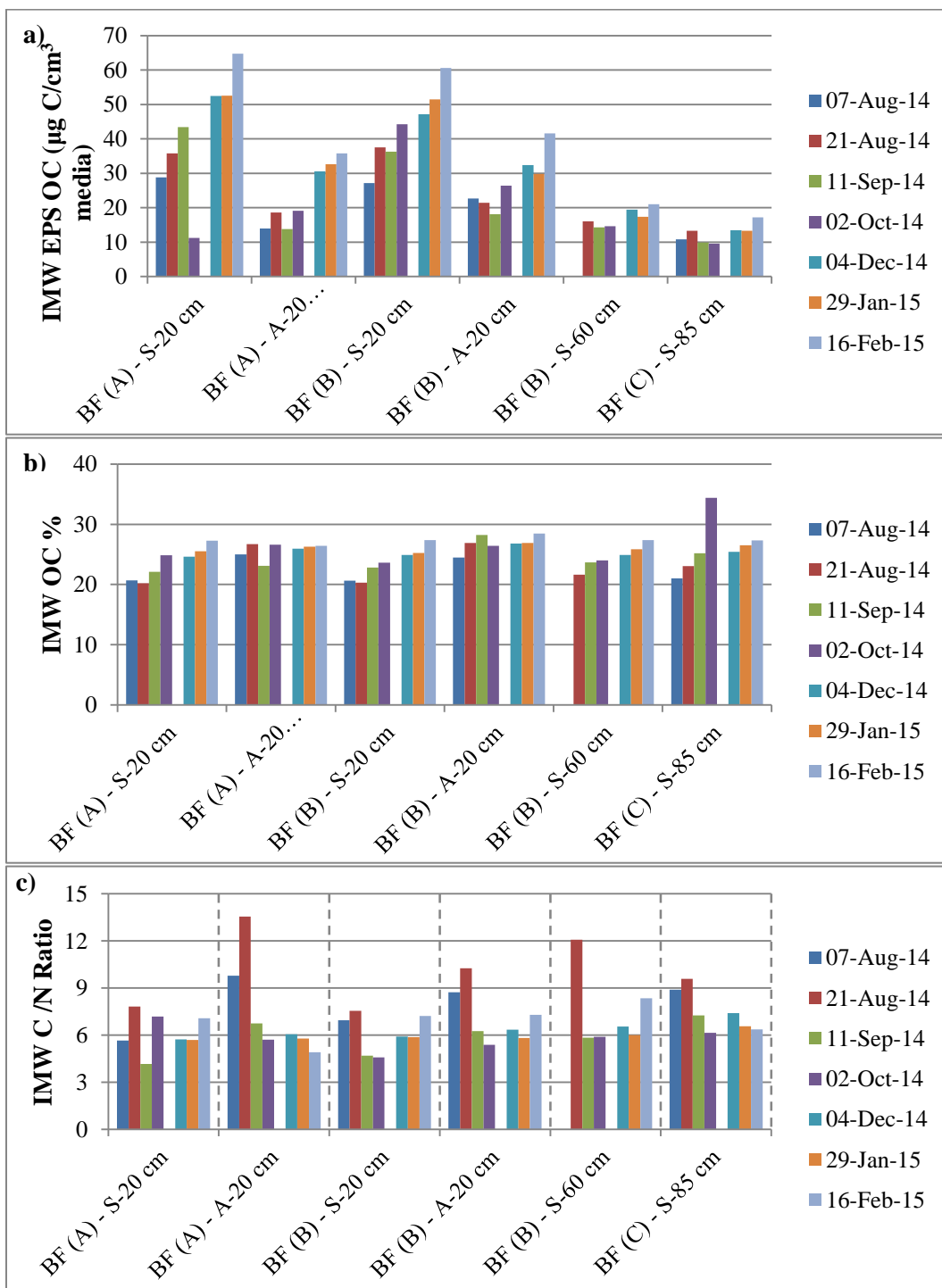
Figure S3 – Organic carbon of the extracted IMW EPS (a) the percent of total EPS organic carbon in this fraction (b) and its carbon to nitrogen ratio (c) over the study period
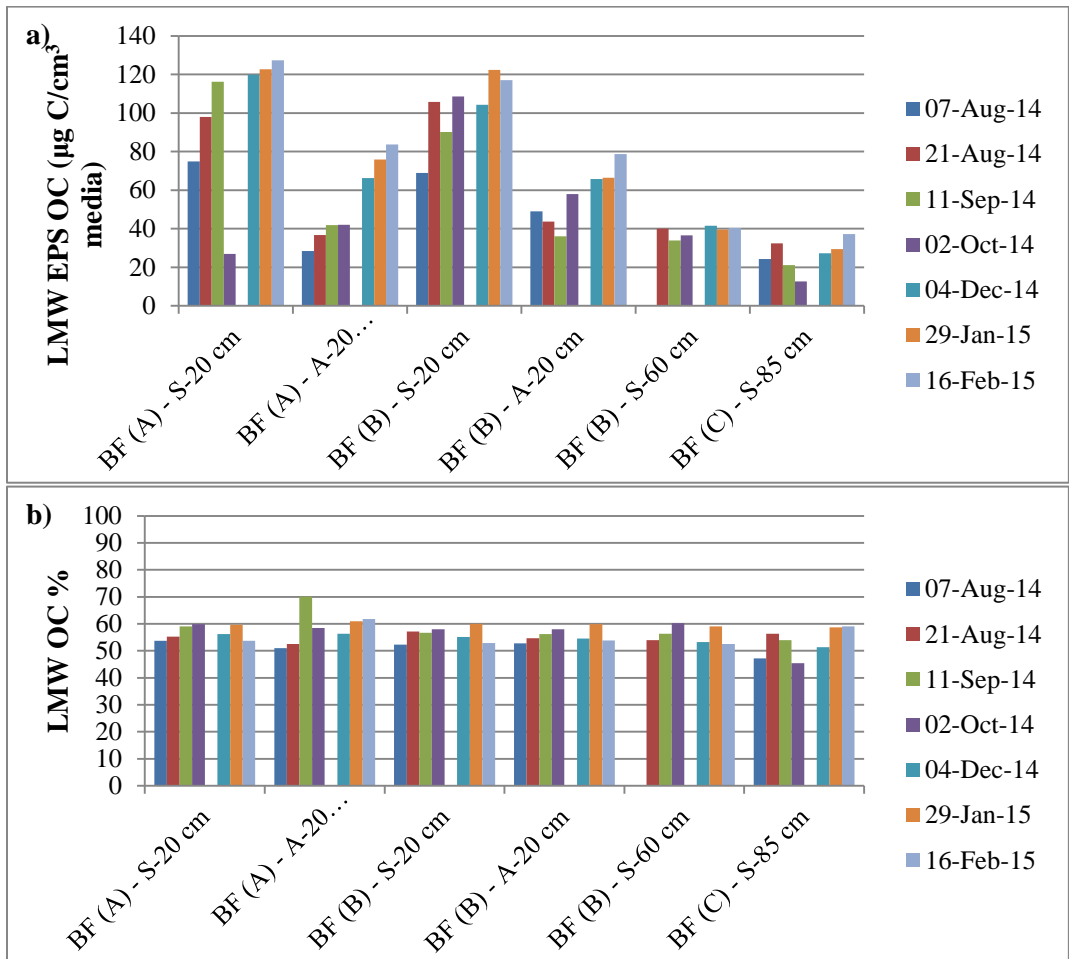
Figure S4 – Organic carbon of the extracted LMW EPS (a) the percent of total EPS organic carbon in this fraction (b)) over the study period

221

Parameter		BF (A) Vs BF (B) DF=6	BF (B) Vs BF (C) DF=6
	DOC	0.015	0.047
	AOC	0.715	0.114
LC-OCD	Biopolymers OC	0.005	0.05
	Biopolymers ON	0.170	0.033
	Humics	0.06	0.411
	LMWA	0.705	0.823
	LMWN	0.315	0.089
	Building Blocks	0.665	0.05
Fluorescence Spectroscopy	FEEM Protein	0.05	0.04
	FEEM Humics	0.03	0.77
	FEEM Fulvic	0.03	0.02
Cell Count	Total cell count	0.87	0.01
	HNA	0.97	0.01
	LNA	0.79	0.01

Table S1– P-values for the paired two sided t-test for the obtained percent removals of the different biofilter performance parameters used in study over the seven sampling events. Shaded cells indicated statistically significant differences at a 0.05 levels of significance (α)

Parameter		BF A DF=5	BF B DF=5	BF C DF=5
	DOC	0.01	0.01	0.01
	AOC	0.08	0.08	0.41
LC-OCD	Biopolymers OC	0.01	0.01	0.01
	Biopolymers ON	0.02	0.01	0.01
	Humics	0.09	0.01	0.01
	LMWA	0.76	0.12	0.26
	LMWN	0.78	0.11	0.79
	Building Blocks	0.85	0.60	0.93
Fluorescence Spectroscopy	FEEM Protein	0.01	0.01	0.01
	FEEM Humics	0.16	0.45	0.08
	FEEM Fulvic	0.01	0.02	0.02
Cell Count	Total cell count	0.01	0.01	0.01
	HNA	0.01	0.01	0.01
	LNA	0.01	0.01	0.01

Table S2– P-values for the unpaired two sided t-test for the obtained percent removals of the different biofilter performance parameters used in study during the warm water conditions (n=4) against the cold water conditions (n=3). Shaded cells indicated statistically significant differences at a 0.05 levels of significance (α)

Biomass Parameter	Cellular ATP Content	Carbohydrates to protein ratio	HMW EPS CN Ratio
BF (A) - S-20 cm	0.12	0.01	0.82
BF (A) - A-20 cm	0.01	0.01	0.85
BF (B) - S-20 cm	0.05	0.01	0.72
BF (B) - A-20 cm	0.04	0.01	0.76
BF (B) - S-60 cm	0.04	0.39	0.55
BF (C) - S-85 cm	0.10	0.13	0.75

Table S3– P-values for the unpaired two sided t-test for the obtained biomass parameters used in study during the warm water conditions (n=4) compared with cold water conditions (n=3). Shaded cells indicated statistically significant differences at a 0.05 levels of significance (α)

Appendix E

Supplementary Information for Chapter 6

<u>R code for analyzing EcoPlates data:</u>

```
#Set R software working directory

setwd('XXXXXXXX')

# Import ecopates data data set

platedata = read.table("PCA data slope.txt",header=TRUE, row.names = 1)

write.csv(platedata, "PCA result.csv")

#Load Vegan Library

library(vegan)

#Hierarchical clustering of the data set

ecdist=vegdist(platedata, method="euclidean", diag=FALSE, upper=FALSE)

range(ecdist)

hirclust=hclust(ecdist, "average")

plot(hirclust)


#PCA Analysis

write.csv(biodata, "PCA result.csv")

#Load Vegan Library

library(vegan)

#run function rda to perform PCA analysis

plateanalysis=rda(platedata, scale=FALSE, na.action = na.fail, subset = NULL)
```

```r
#run summary to get the PCA scores

ahmed=summary(plateanalysis, scaling = 0, axes = 27, display = c("sp", "wa", "lc", "bp", "cn"), digits =
max(3, getOption("digits") - 3))


#extract eigen value of axes and then convert it to a matrix and write to a .csv file

PC.eigenvalues=plateanalysis$CA$eig

ahmedmatrix= as.data.frame(PC.eigenvalues)

write.csv(ahmedmatrix, " PC_eigen_values.csv ")


#extract orthonormal site scores scores using object v

PC.speciesscore=doubsanalysis$CA$v

ahmed1matrix= as.data.frame(PC.speciesscore)

write.csv(ahmed1matrix, "PC_species_scores.csv")

#extract orthonormal species scores scores using object u

PC.sitescore=plateanalysis$CA$u

ahmed2matrix= as.data.frame(PC.sitescore)

write.csv(ahmed2matrix, "PC_Sites_scores.csv")


#generate the biplot

biplot(plateanalysis, choices = 1:2, scaling = 1,xlim=c(-1.0, 1.0), ylim=c(-1.0, 1.0))

biplot(plateanalysis, choices = 2:3, scaling = 1,xlim=c(-1.0, 1.0), ylim=c(-1.0, 1.0))

biplot(plateanalysis, choices = 1:3, scaling = 1,xlim=c(-1.0, 1.0), ylim=c(-1.0, 1.0))
```

	POLY1	POLY2	POLY3	CARB1	CARB2	CARB3	CARB4	CARB5	CARB6	CARB7	CARB8	POSPH1	POSPH2	ESTER1	CAACID1	CAACID2
Raw_Aug	1.5	1.6	1.3	1.5	1.5	1.5	1.1	1.3	1.6	1.5	1.5	0.8	0.3	1.3	1.0	1.0
BF_B_Sand_Aug	1.5	1.4	1.4	1.5	1.4	1.5	1.1	1.4	1.4	1.4	1.4	0.9	0.3	1.3	1.2	1.4
BF_B_Anth_Aug	1.4	1.4	1.4	1.4	1.4	1.5	1.1	1.4	0.3	1.4	1.4	0.9	0.3	1.3	1.2	1.3
BF_B_Sand_bot_Aug	1.5	1.4	1.4	1.5	1.4	1.5	1.0	1.4	0.8	1.5	1.3	0.9	0.3	1.3	1.3	1.3
BF_C_Aug	1.5	1.4	1.4	1.4	1.5	1.5	0.9	1.4	1.3	1.4	1.4	0.8	0.3	1.3	1.3	1.4
Raw_Sep	1.2	1.3	0.3	0.9	1.1	0.7	0.8	0.6	0.7	1.1	1.1	0.6	0.3	0.8	0.8	0.5
BF_B_Sand_Sep	1.4	1.4	1.4	1.4	1.3	1.4	0.8	1.4	1.4	1.4	1.3	0.6	0.3	1.2	1.1	1.4
BF_B_Anth_Sep	1.5	1.3	1.4	1.4	1.4	1.5	0.8	1.4	1.4	1.5	1.2	0.7	0.2	1.2	1.2	1.4
BF_B_Sand_bot_Sep	1.4	1.4	1.2	1.3	1.3	1.5	0.8	1.4	0.9	1.4	1.2	0.7	0.3	1.1	1.1	1.3
BF_C_Sep	1.2	1.2	0.5	1.3	1.3	0.4	0.7	1.2	0.0	1.4	1.0	0.6	0.2	0.9	1.1	1.2
Raw_Oct	0.2	0.8	0.1	0.0	0.6	0.7	0.5	0.0	0.0	1.3	0.3	0.2	0.2	0.5	0.1	0.3
BF_B_Sand_Oct	1.6	1.5	1.4	1.5	1.4	1.5	1.1	1.5	1.4	1.5	1.4	0.8	0.5	1.4	1.3	1.4
BF_B_Anth_Oct	1.5	1.4	1.5	1.6	1.6	1.5	1.2	1.4	1.5	1.5	1.5	0.9	0.5	1.3	1.2	1.5
BF_B_Sand_bot_Oct	1.5	1.5	1.6	1.5	1.5	1.5	1.2	1.5	1.3	1.5	1.4	0.9	0.4	1.4	1.4	1.5
BF_C_Oct	1.5	1.5	1.4	1.4	1.3	1.4	0.7	1.4	1.0	1.5	1.2	0.7	0.3	1.4	1.3	1.5
Raw_Dec	1.3	1.2	1.2	1.3	1.2	1.2	0.7	1.2	1.1	1.4	1.2	0.8	0.2	0.9	1.1	0.9
BF_A_Anth_Dec	1.4	1.2	1.4	1.5	1.5	1.6	1.2	1.5	1.3	1.5	1.3	1.1	0.3	1.3	1.3	1.3
BF_A_Sand_Dec	1.4	1.2	1.4	1.4	1.3	1.5	1.1	1.4	1.3	1.4	1.2	0.9	0.5	1.2	1.2	1.2
BF_B_Anth_Dec	1.3	1.2	1.4	1.4	1.4	1.5	1.1	1.5	1.3	1.5	1.2	1.1	0.4	1.3	1.3	1.4
BF_B_sand_Dec	1.3	1.2	1.4	1.4	1.3	1.6	1.0	1.5	1.2	1.5	1.1	0.9	0.4	1.2	1.3	1.3
BF_C_Dec	1.5	1.3	1.5	1.5	1.7	1.5	1.3	1.6	1.3	1.6	1.3	1.2	0.4	1.1	1.7	1.3
BF_B_Sand_bot_Dec	1.5	1.3	1.5	1.5	1.5	1.6	1.1	1.5	1.3	1.5	1.3	1.0	0.3	1.2	1.6	1.4
Raw_Jan	0.5	1.1	0.0	0.0	0.7	0.9	0.4	0.6	0.7	0.8	1.0	0.4	0.1	0.4	1.2	0.7
BF_A_Anth_Jan	1.5	1.3	1.6	1.5	1.5	1.6	1.0	1.4	1.4	1.5	1.3	1.0	0.2	1.1	1.5	1.3
BF_A_Sand_Jan	1.5	1.3	1.5	1.4	1.5	1.5	1.0	1.5	1.4	1.6	1.3	0.9	0.2	1.2	1.6	1.3
BF_B_Anth_Jan	1.5	1.4	1.5	1.5	1.5	1.6	1.0	1.5	1.4	1.6	1.2	0.7	0.2	1.1	1.6	1.3
BF_B_sand_Jan	1.4	1.3	1.4	1.5	1.4	1.5	1.0	1.5	1.4	1.6	1.1	1.0	0.2	1.1	1.6	1.3
BF_C_Jan	1.4	1.4	1.3	1.2	1.1	1.4	1.1	1.5	1.3	1.5	1.2	0.4	0.2	1.1	1.6	1.3
BF_B_Sand_bot_Jan	1.4	1.3	1.5	1.4	1.5	1.5	1.0	1.5	1.3	1.5	1.2	1.0	0.4	1.0	1.5	1.3
Raw_Feb	0.1	0.9	0.0	0.0	0.9	0.0	0.7	0.0	0.2	0.0	0.8	0.3	0.2	0.7	0.9	1.1
BF_A_Anth_Feb	1.5	1.3	1.5	1.6	1.4	1.4	1.1	1.5	1.4	1.6	1.4	0.8	0.3	1.3	1.6	1.5
BF_A_Sand_Feb	1.4	1.2	1.3	1.3	1.4	1.4	0.9	1.3	1.3	1.4	1.3	0.6	0.2	1.1	1.5	1.3
BF_B_Anth_Feb	1.5	1.2	1.4	1.5	1.2	1.5	1.2	1.5	1.5	1.6	1.3	0.7	0.2	1.3	1.6	1.4
BF_B_sand_Feb	1.4	1.3	1.3	1.4	1.1	1.3	1.0	1.3	1.4	1.5	1.2	0.8	0.2	1.1	1.5	1.4
BF_C_Feb	1.5	1.4	1.0	1.1	1.4	0.7	0.8	1.4	1.5	1.5	1.2	0.2	0.2	0.9	1.6	1.4
BF_B_Sand_bot_Feb	1.5	1.3	1.3	1.2	0.8	1.3	1.1	1.5	1.5	1.6	1.3	0.7	0.2	1.2	1.7	1.4

Table S1– Max AWD (A) data set for the different substrates for the samples collected in the current study (part 1)

	CAACID3	CAACID4	CAACID5	CAACID6	CAACID7	CAACID8	CAACID9	AMACID1	AMACID2	AMACID3	AMACID4	AMACID5	AMACID6	AMINE1	AMINE2
Raw_Aug	0.1	0.8	0.9	0.6	1.0	0.0	1.2	1.0	1.3	1.0	0.9	1.1	1.1	1.3	0.6
BF_B_Sand_Aug	0.2	1.3	1.2	1.4	1.2	0.9	1.3	1.3	1.5	1.4	1.2	1.4	1.1	1.3	0.8
BF_B_Anth_Aug	0.2	1.4	1.0	1.4	1.2	1.1	1.3	1.2	1.5	1.3	1.2	1.4	1.3	1.2	0.8
BF_B_Sand_bot_Aug	0.2	1.4	1.2	1.2	1.1	0.9	1.3	1.2	1.5	1.4	1.3	1.4	1.3	1.3	0.7
BF_C_Aug	0.1	1.4	1.1	1.4	1.2	0.9	1.2	1.2	1.4	1.4	1.3	1.4	1.3	1.1	0.7
Raw_Sep	0.1	0.5	0.2	0.4	0.4	0	0.7	1.1	1.1	0.2	1.0	0.8	0.7	0.0	0.5
BF_B_Sand_Sep	0.1	1.3	1.0	1.3	1.1	0.9	1.2	1.1	1.5	1.3	1.2	1.4	0.8	1.4	0.7
BF_B_Anth_Sep	0.1	1.4	1.0	1.4	1.1	0.9	1.1	1.1	1.5	1.2	1.3	1.4	0.7	1.4	0.9
BF_B_Sand_bot_Sep	0.1	1.2	0.5	1.4	0.9	0.7	1.0	1.0	1.4	1.3	1.1	1.3	0.6	1.3	0.8
BF_C_Sep	0.1	1.2	0.6	1.0	0.7	0.6	0.9	1.0	1.3	0.8	1.0	1.3	0.8	1.2	0.7
Raw_Oct	0.1	0.1	0.2	0.1	0.4	-0.1	0.0	0.4	0.4	0.0	0.7	0.1	0.1	0.3	0.1
BF_B_Sand_Oct	0.2	1.1	1.1	1.5	1.1	0.8	1.4	1.3	1.6	1.5	1.4	1.5	0.7	1.3	0.9
BF_B_Anth_Oct	0.3	1.4	1.2	1.5	1.3	1.0	1.4	1.1	1.6	1.4	1.3	1.5	1.2	1.3	1.1
BF_B_Sand_bot_Oct	0.2	1.5	0.9	1.6	1.2	0.7	1.2	1.3	1.5	1.3	1.4	1.4	1.2	1.3	1.1
BF_C_Oct	0.2	1.3	1.1	1.4	1.1	0.8	1.2	1.2	1.5	1.3	1.3	1.4	1.3	1.2	0.8
Raw_Dec	0.2	0.7	0.6	1.0	0.6	0.5	0.9	0.9	1.2	1.3	1.0	1.2	0.4	1.1	0.7
BF_A_Anth_Dec	0.2	1.1	0.9	1.4	1.3	1.2	1.4	1.2	1.4	1.3	1.3	1.4	0.6	1.4	1.1
BF_A_Sand_Dec	0.3	1.1	1.2	1.3	1.1	1.2	1.2	0.9	1.4	1.3	1.1	1.3	0.6	1.3	0.9
BF_B_Anth_Dec	0.2	1.1	0.7	1.4	1.2	1.2	1.3	1.1	1.4	1.1	1.2	1.4	0.5	1.3	0.9
BF_B_sand_Dec	0.3	0.9	0.9	1.3	1.0	1.0	1.2	1.1	1.5	1.2	1.2	1.3	0.6	1.3	0.9
BF_C_Dec	0.4	1.2	0.6	1.5	1.1	1.1	1.4	1.3	1.5	1.3	1.4	1.4	0.6	1.5	0.9
BF_B_Sand_bot_Dec	0.4	1.1	0.7	1.5	1.0	1.0	1.4	1.1	1.5	1.3	1.3	1.4	0.8	1.3	1.0
Raw_Jan	0.1	0.4	0.0	0.6	0.9	0	0.7	1.0	1.3	0.1	0.7	0.7	0.7	0.0	0.5
BF_A_Anth_Jan	0.4	1.0	0.7	1.3	1.2	1.0	1.3	1.1	1.5	1.4	1.4	1.4	0.8	1.3	0.9
BF_A_Sand_Jan	0.4	1.0	1.0	1.4	1.1	1.0	1.3	1.1	1.5	1.3	1.3	1.4	0.8	1.4	0.9
BF_B_Anth_Jan	0.3	1.1	0.6	1.4	1.2	1.0	1.4	1.1	1.5	1.4	1.4	1.5	0.8	1.4	1.1
BF_B_sand_Jan	0.4	1.0	0.8	1.4	1.1	0.8	1.3	1.1	1.5	0.9	1.4	1.4	0.7	1.4	1.1
BF_C_Jan	0.3	1.2	0.8	1.4	0.9	0.8	1.3	1.3	1.5	1.0	1.4	1.4	0.6	1.2	0.7
BF_B_Sand_bot_Jan	0.4	1.1	0.7	1.3	1.0	0.7	1.3	1.1	1.4	1.1	1.4	1.4	0.7	1.3	0.9
Raw_Feb	0.0	0.0	0.0	0.8	1.0	0.2	0.7	1.0	1.1	0.0	0.8	0.5	0.3	0.1	0.2
BF_A_Anth_Feb	0.3	1.1	0.7	1.3	1.1	0.9	1.4	1.3	1.6	1.1	1.5	1.4	0.7	1.4	1.0
BF_A_Sand_Feb	0.3	1.1	0.8	1.3	0.9	0.6	1.1	1.1	1.5	1.2	1.4	1.3	0.6	1.1	0.8
BF_B_Anth_Feb	0.3	1.3	0.6	1.3	0.9	0.8	1.3	1.2	1.5	1.2	1.4	1.4	0.7	1.4	0.9
BF_B_sand_Feb	0.3	1.1	0.3	1.3	0.9	0.6	1.1	1.2	1.5	1.0	1.3	1.3	0.6	1.2	0.8
BF_C_Feb	0.4	1.2	0.9	1.4	0.9	0.3	1.2	1.3	1.5	0.6	1.3	1.3	0.9	1.1	0.8
BF_B_Sand_bot_Feb	0.3	1.2	0.6	1.3	1.0	0.7	1.3	1.3	1.5	1.0	1.5	1.2	0.6	1.2	0.9

Table S1– Max AWD (A) data set for the different substrates for the samples collected in the current study (part 2)

	POLY1	POLY2	POLY3	CARB1	CARB2	CARB3	CARB4	CARB5	CARB6	CARB7	CARB8	POSPH1	POSPH2	ESTER1	CAACID1	CAACID2
Raw_Aug	0.3	0.4	0.4	0.5	0.5	0.2	0.3	0.2	0.2	0.5	0.5	0.3	0.2	0.8	0.1	0.3
BF_B_Sand_Aug	0.3	0.1	0.5	0.7	0.6	0.2	0.5	0.6	0.3	0.6	0.7	0.4	0.2	0.6	0.4	0.6
BF_B_Anth_Aug	0.3	0.1	0.1	0.7	0.5	0.2	0.5	0.6	0.0	0.5	0.6	0.5	0.1	0.6	0.5	0.6
BF_B_Sand_bot_Aug	0.3	0.1	0.2	0.7	0.6	0.2	0.5	0.2	0.1	0.5	0.6	0.4	0.2	0.5	0.5	0.6
BF_C_Aug	0.3	0.2	0.2	0.6	0.5	0.2	0.5	0.2	0.2	0.4	0.5	0.4	0.1	0.5	0.6	0.6
Raw_Sep	0.2	0.1	0.1	0.3	0.1	0.1	0.2	0.0	0.1	0.1	0.2	0.1	0.1	0.4	0.2	0.2
BF_B_Sand_Sep	0.3	0.2	0.4	0.7	0.5	0.3	0.4	0.4	0.2	0.5	0.5	0.6	0.1	0.5	0.7	0.6
BF_B_Anth_Sep	0.3	0.2	0.4	0.7	0.5	0.3	0.4	0.5	0.3	0.4	0.5	0.4	0.1	0.5	0.6	0.6
BF_B_Sand_bot_Sep	0.3	0.3	0.3	0.6	0.4	0.3	0.4	0.5	0.2	0.5	0.4	0.2	0.1	0.4	0.6	0.5
BF_C_Sep	0.3	0.1	0.0	0.5	0.1	0.1	0.3	0.2	0.0	0.3	0.3	0.1	0.1	0.3	0.7	0.4
Raw_Oct	0.1	0.1	0.0	0.0	0.4	0.2	0.1	0.0	0.0	0.2	0.0	0.1	0.1	0.0	0.0	0.2
BF_B_Sand_Oct	0.3	0.3	0.4	0.6	0.4	0.2	0.4	0.4	0.2	0.5	0.5	0.6	0.1	0.4	0.6	0.4
BF_B_Anth_Oct	0.3	0.2	0.5	0.7	0.5	0.2	0.5	0.5	0.3	0.5	0.6	0.7	0.2	0.5	0.6	0.6
BF_B_Sand_bot_Oct	0.3	0.2	0.3	0.6	0.5	0.2	0.4	0.3	0.2	0.5	0.5	0.5	0.2	0.4	0.6	0.5
BF_C_Oct	0.3	0.3	0.5	0.6	0.4	0.2	0.1	0.2	0.2	0.4	0.4	0.2	0.1	0.3	0.6	0.5
Raw_Dec	0.3	0.2	0.2	0.4	0.3	0.4	0.2	0.3	0.1	0.3	0.4	0.4	0.1	0.3	0.3	0.4
BF_A_Anth_Dec	0.4	0.2	0.4	0.6	0.6	0.5	0.6	0.5	0.2	0.6	0.6	0.5	0.1	0.5	0.3	0.6
BF_A_Sand_Dec	0.3	0.1	0.4	0.6	0.5	0.5	0.5	0.5	0.1	0.5	0.6	0.4	0.2	0.5	0.3	0.6
BF_B_Anth_Dec	0.3	0.2	0.4	0.6	0.5	0.6	0.5	0.5	0.1	0.5	0.6	0.5	0.1	0.5	0.3	0.6
BF_B_sand_Dec	0.3	0.2	0.4	0.6	0.5	0.6	0.5	0.5	0.1	0.4	0.5	0.5	0.1	0.5	0.3	0.6
BF_C_Dec	0.4	0.2	0.6	0.6	0.6	0.6	0.6	0.6	0.1	0.5	0.5	0.6	0.1	0.5	0.5	0.6
BF_B_Sand_bot_Dec	0.3	0.2	0.5	0.6	0.5	0.7	0.5	0.6	0.1	0.5	0.6	0.4	0.1	0.5	0.4	0.7
Raw_Jan	0.1	0.2	0.0	0.0	0.2	0.2	0.2	0.1	0.0	0.2	0.3	0.1	0.1	0.2	0.3	0.3
BF_A_Anth_Jan	0.4	0.1	0.6	0.7	0.5	0.2	0.5	0.7	0.2	0.5	0.6	0.5	0.1	0.5	0.4	0.7
BF_A_Sand_Jan	0.4	0.3	0.5	0.7	0.5	0.3	0.5	0.7	0.2	0.6	0.6	0.6	0.1	0.6	0.5	0.7
BF_B_Anth_Jan	0.4	0.2	0.6	0.7	0.6	0.5	0.5	0.6	0.2	0.6	0.6	0.5	0.1	0.5	0.6	0.7
BF_B_sand_Jan	0.4	0.2	0.4	0.7	0.5	0.4	0.5	0.7	0.2	0.6	0.5	0.5	0.1	0.5	0.6	0.7
BF_C_Jan	0.3	0.2	0.3	0.2	0.0	0.0	0.3	0.8	0.2	0.4	0.3	0.0	0.1	0.4	0.7	0.6
BF_B_Sand_bot_Jan	0.4	0.2	0.4	0.7	0.5	0.4	0.5	0.7	0.2	0.6	0.5	0.4	0.1	0.5	0.7	0.7
Raw_Feb	0.1	0.2	0.0	0.0	0.3	0.0	0.4	0.0	0.0	0.0	0.2	0.1	0.1	0.3	0.3	0.4
BF_A_Anth_Feb	0.4	0.2	0.4	0.6	0.4	0.2	0.4	0.7	0.2	0.6	0.5	0.1	0.1	0.5	0.9	0.7
BF_A_Sand_Feb	0.3	0.2	0.3	0.5	0.8	0.2	0.3	0.6	0.1	0.5	0.5	0.1	0.1	0.4	0.8	0.6
BF_B_Anth_Feb	0.4	0.2	0.4	0.5	0.4	0.2	0.4	1.0	0.2	0.6	0.4	0.1	0.1	0.4	0.9	0.6
BF_B_sand_Feb	0.4	0.2	0.3	0.4	0.3	0.1	0.3	0.7	0.2	0.6	0.4	0.3	0.1	0.4	0.8	0.6
BF_C_Feb	0.3	0.3	0.2	0.2	0.1	0.0	0.1	0.5	0.2	0.5	0.3	0.0	0.1	0.4	1.0	0.6
BF_B_Sand_bot_Feb	0.4	0.2	0.3	0.5	0.4	0.3	0.2	0.7	0.2	0.6	0.4	0.4	0.1	0.4	0.9	0.6

Table S2– Rate of colour development (μ_m) data set for the different substrates for the samples collected in the current study (part 1)

	CAACID3	CAACID4	CAACID5	CAACID6	CAACID7	CAACID8	CAACID9	AMACID1	AMACID2	AMACID3	AMACID4	AMACID5	AMACID6	AMINE1	AMINE2
Raw_Aug	0.1	0.1	0.1	0.2	0.3	0.0	0.3	0.1	0.3	0.1	0.2	0.1	0.1	0.2	0.2
BF_B_Sand_Aug	0.1	0.3	0.2	0.7	0.5	0.3	0.4	0.4	0.7	0.2	0.6	0.2	0.2	0.4	0.4
BF_B_Anth_Aug	0.1	0.4	0.1	0.7	0.5	0.3	0.4	0.5	0.7	0.3	0.6	0.3	0.2	0.4	0.4
BF_B_Sand_bot_Aug	0.1	0.3	0.1	0.5	0.4	0.3	0.4	0.4	0.7	0.2	0.5	0.2	0.2	0.5	0.3
BF_C_Aug	0.1	0.3	0.1	0.4	0.4	0.4	0.3	0.4	0.6	0.2	0.5	0.2	0.2	0.4	0.3
Raw_Sep	0.1	0.1	0.0	0.1	0.2	0.0	0.3	0.3	0.3	0.0	0.1	0.1	0.1	0.0	0.1
BF_B_Sand_Sep	0.1	0.5	0.2	0.6	0.4	0.6	0.4	0.4	0.7	0.2	0.5	0.3	0.1	0.5	0.3
BF_B_Anth_Sep	0.1	0.4	0.2	0.6	0.4	0.7	0.3	0.4	0.7	0.2	0.5	0.2	0.1	0.4	0.3
BF_B_Sand_bot_Sep	0.0	0.3	0.1	0.8	0.3	0.4	0.4	0.4	0.5	0.2	0.4	0.2	0.1	0.4	0.3
BF_C_Sep	0.1	0.3	0.1	0.2	0.3	0.1	0.3	0.3	0.4	0.1	0.3	0.2	0.1	0.2	0.2
Raw_Oct	0.1	0.0	0.0	0.0	0.1	0.0	0.0	0.1	0.1	0.0	0.1	0.0	0.0	0.1	0.0
BF_B_Sand_Oct	0.1	0.3	0.1	0.5	0.4	0.4	0.6	0.6	0.6	0.2	0.4	0.2	0.1	0.4	0.3
BF_B_Anth_Oct	0.1	0.3	0.1	0.5	0.4	0.4	0.4	0.4	0.6	0.2	0.5	0.2	0.1	0.5	0.3
BF_B_Sand_bot_Oct	0.1	0.3	0.1	0.4	0.3	0.3	0.4	0.5	0.5	0.2	0.4	0.2	0.2	0.2	0.3
BF_C_Oct	0.1	0.4	0.1	0.1	0.3	0.2	0.5	0.5	0.5	0.2	0.4	0.2	0.2	0.2	0.4
Raw_Dec	0.1	0.2	0.1	0.3	0.3	0.2	0.2	0.2	0.4	0.4	0.3	0.1	0.1	0.2	0.2
BF_A_Anth_Dec	0.1	0.3	0.1	0.6	0.5	0.3	0.5	0.4	0.7	0.6	0.6	0.2	0.2	0.5	0.4
BF_A_Sand_Dec	0.1	0.3	0.2	0.6	0.4	0.4	0.4	0.3	0.7	0.5	0.5	0.2	0.1	0.5	0.4
BF_B_Anth_Dec	0.1	0.3	0.1	0.6	0.5	0.4	0.5	0.4	0.7	0.4	0.6	0.2	0.1	0.5	0.4
BF_B_sand_Dec	0.1	0.2	0.1	0.5	0.4	0.4	0.4	0.3	0.7	0.4	0.5	0.2	0.1	0.5	0.4
BF_C_Dec	0.2	0.3	0.1	0.6	0.5	0.5	0.4	0.3	0.7	0.4	0.5	0.2	0.2	0.5	0.3
BF_B_Sand_bot_Dec	0.2	0.3	0.1	0.6	0.4	0.4	0.4	0.3	0.7	0.5	0.5	0.2	0.2	0.5	0.3
Raw_Jan	0.0	0.1	0.0	0.2	0.2	0.0	0.1	0.2	0.3	0.0	0.1	0.0	0.1	0.0	0.2
BF_A_Anth_Jan	0.2	0.3	0.1	0.7	0.4	0.5	0.5	0.4	0.7	0.4	0.6	0.2	0.2	0.5	0.4
BF_A_Sand_Jan	0.2	0.3	0.2	0.7	0.4	0.5	0.5	0.5	0.8	0.3	0.6	0.2	0.1	0.4	0.4
BF_B_Anth_Jan	0.2	0.4	0.1	0.7	0.5	0.6	0.6	0.4	0.8	0.5	0.6	0.2	0.2	0.5	0.5
BF_B_sand_Jan	0.1	0.3	0.1	0.7	0.4	0.5	0.5	0.4	0.7	0.3	0.6	0.2	0.2	0.4	0.5
BF_C_Jan	0.1	0.5	0.1	0.5	0.4	0.5	0.3	0.4	0.7	0.1	0.5	0.2	0.1	0.3	0.2
BF_B_Sand_bot_Jan	0.1	0.3	0.2	0.6	0.4	0.4	0.5	0.4	0.7	0.2	0.6	0.2	0.2	0.4	0.3
Raw_Feb	0.0	0.0	0.0	0.5	0.2	0.0	0.2	0.1	0.1	0.0	0.1	0.1	0.0	0.0	0.1
BF_A_Anth_Feb	0.1	0.4	0.1	0.5	0.5	0.6	0.5	0.5	0.7	0.2	0.6	0.1	0.1	0.5	0.3
BF_A_Sand_Feb	0.1	0.5	0.1	0.5	0.4	0.3	0.4	0.5	0.6	0.1	0.4	0.1	0.0	0.5	0.3
BF_B_Anth_Feb	0.1	0.5	0.1	0.5	0.4	0.4	0.5	0.6	0.7	0.1	0.5	0.1	0.2	0.6	0.3
BF_B_sand_Feb	0.2	0.4	0.0	0.5	0.4	0.2	0.5	0.5	0.6	0.1	0.4	0.1	0.1	0.4	0.3
BF_C_Feb	0.2	0.5	0.1	0.6	0.4	0.1	0.4	0.6	0.6	0.1	0.4	0.2	0.1	0.0	0.3
BF_B_Sand_bot_Feb	0.1	0.5	0.1	0.5	0.5	0.5	0.5	0.5	0.6	0.1	0.5	0.1	0.2	0.4	0.3

Table S2– Rate of colour development (μ_m) data set for the different substrates for the samples collected in the current study (part 2)
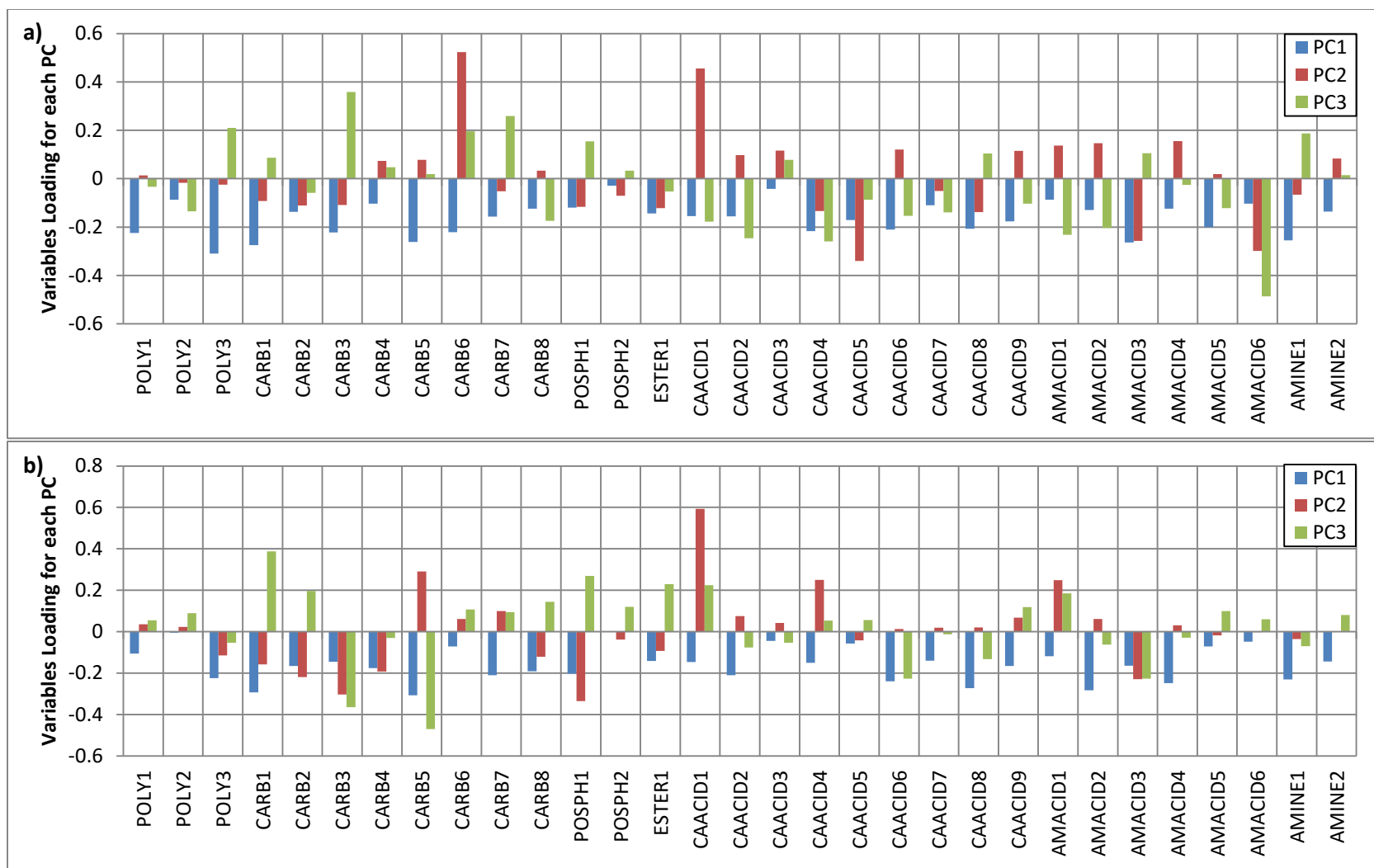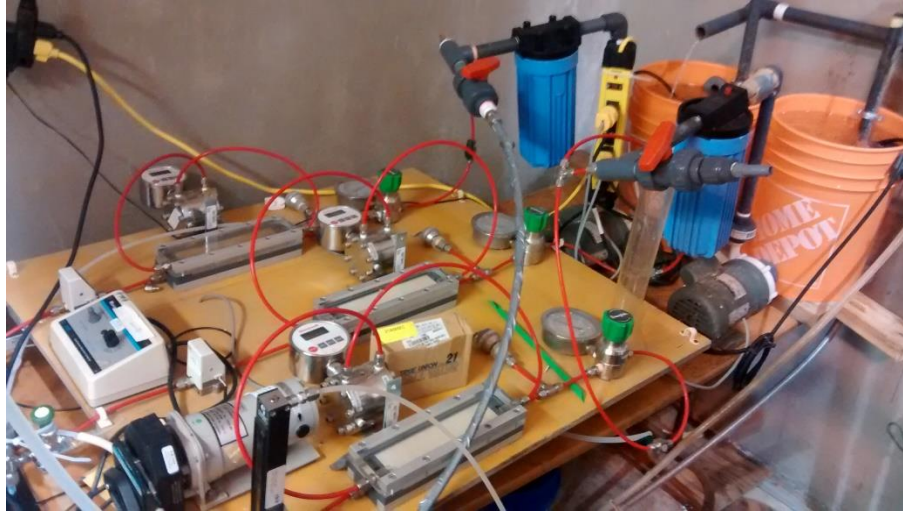
Figure S1– PCA model variable loadings for (a) the max AWD (A) data set and (b) rate of colour development (μₘ) data set

Appendix F

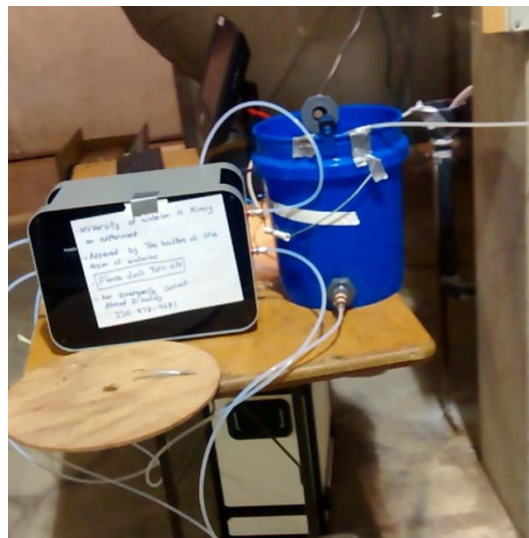## Supplementary Information for Chapter 7

a)

b)

Figure S1 – Photos of the used membrane fouling simulator (MFS) test units (September 2014) (a) and the Convergence Minos simulator (January 2015) (b)
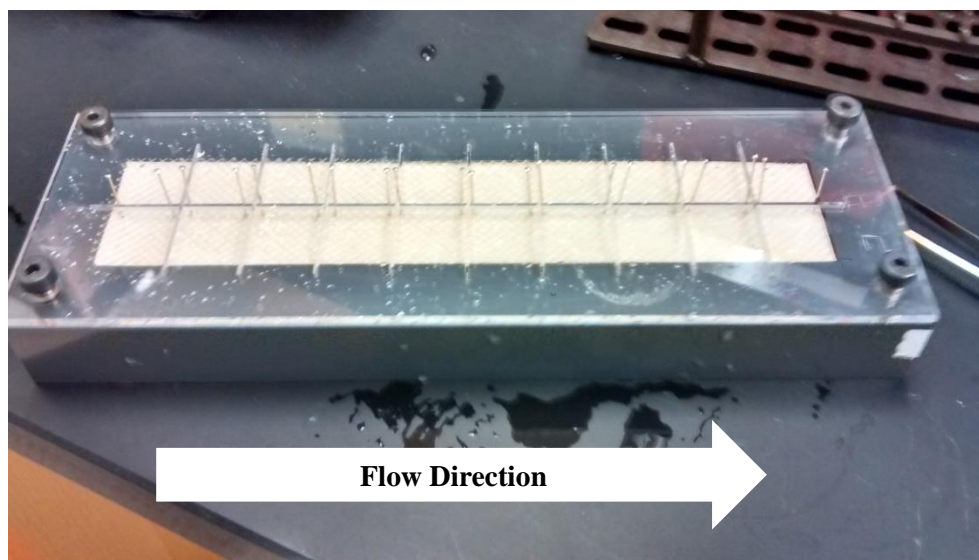
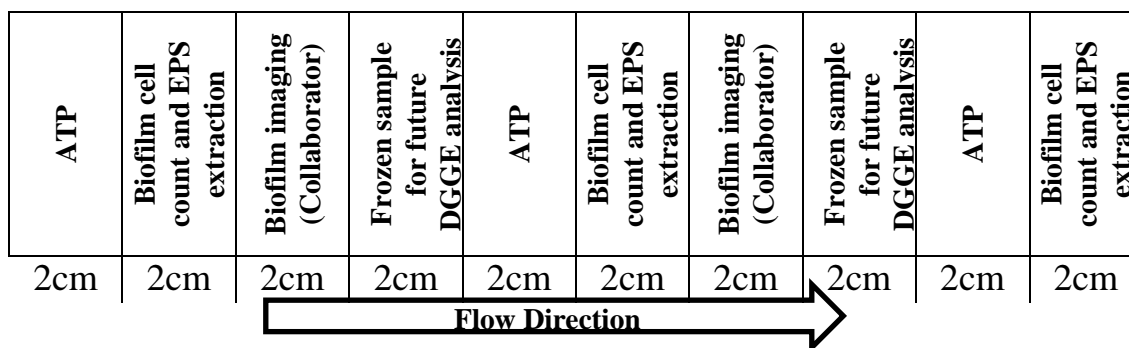**Figure S2 – Photo of the used module for cutting the membrane and spacer in equal coupons for analysis**

4 cm	ATP	Biofilm cell count and EPS extraction	Biofilm imaging (Collaborator)	Frozen sample for future DGGE analysis	ATP	Biofilm cell count and EPS extraction	Biofilm imaging (Collaborator)	Frozen sample for future DGGE analysis	ATP	Biofilm cell count and EPS extraction
	2cm	2cm	2cm	2cm	2cm	2cm	2cm	2cm	2cm	2cm

Flow Direction

Figure S3 – schematic of the used samples for each biofilm characterization technique after the membrane autopsies of the UW MFS unit

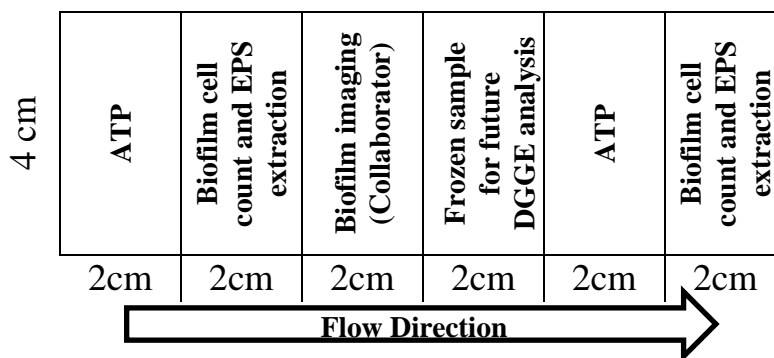| 4 cm	ATP	Biofilm cell count and EPS extraction	Biofilm imaging (Collaborator)	Frozen sample for future DGGE analysis	ATP	Biofilm cell count and EPS extraction
	2cm	2cm	2cm	2cm	2cm	2cm

Flow Direction

Figure S4– schematic of the used samples for each biofilm characterization technique after the membrane autopsies of the Convergence MFS unit
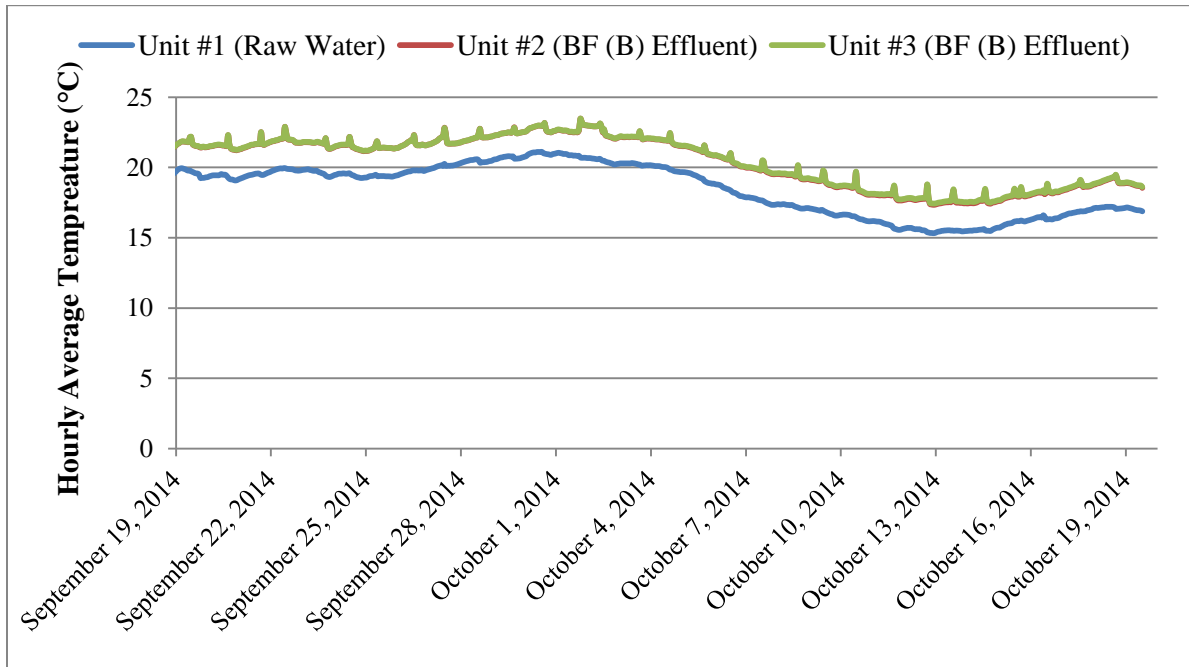
Figure S5 – Hourly average temperature for the feed water downstream of the MFS units within the biofouling experiment on September 2014
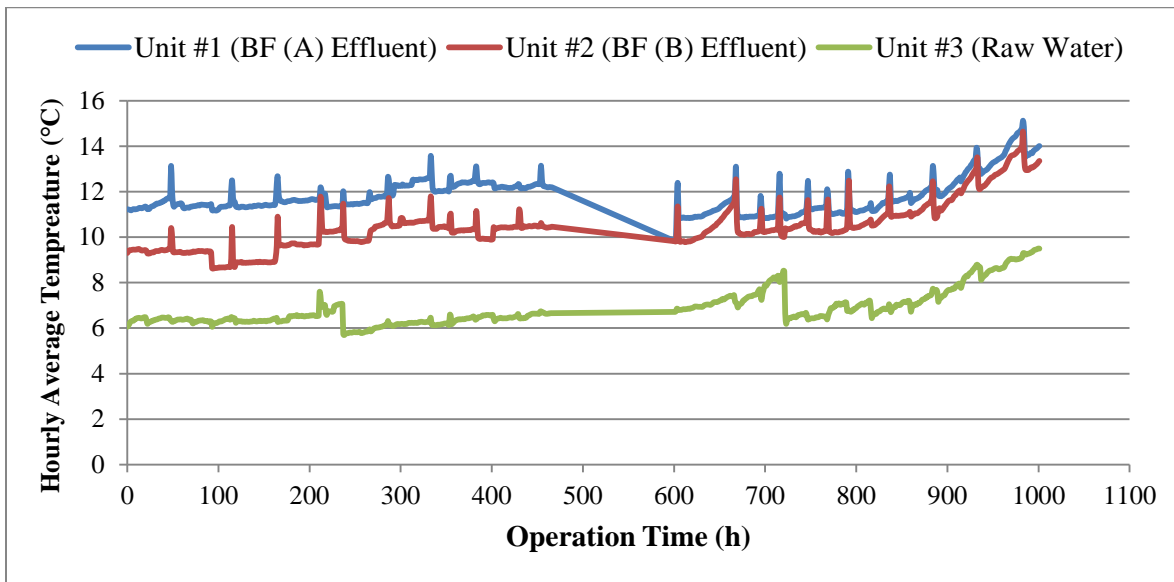

Figure S6 – Hourly average temperature for the feed water downstream of the MFS units within the biofouling experiment on January 2015
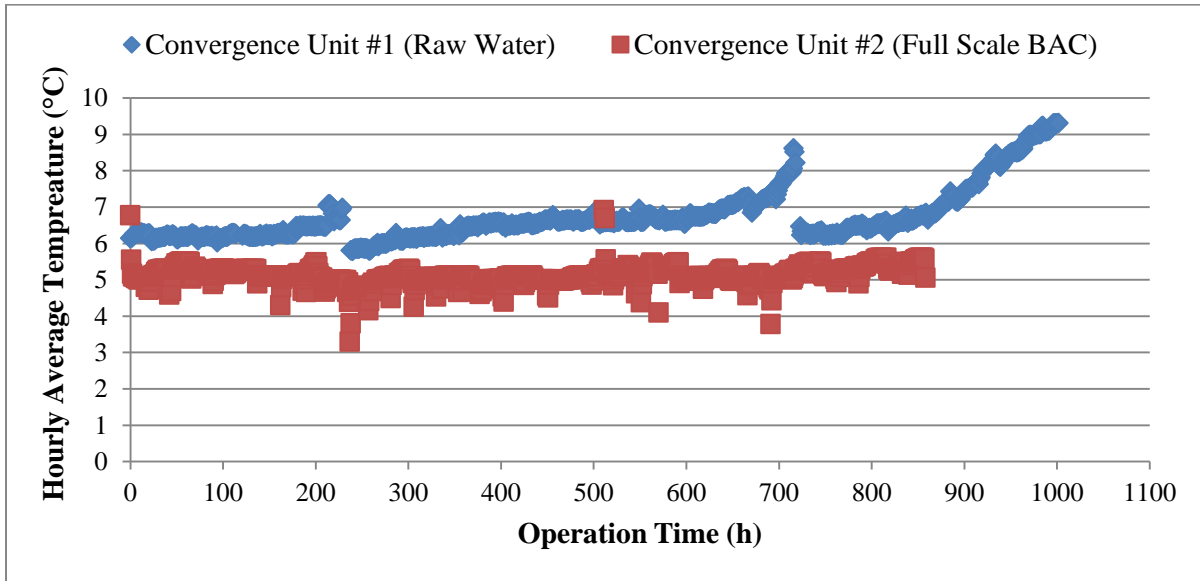
Figure S7– Hourly average temperature for the feed water upstream of the Convergence MFS units within the biofouling experiment on January 2015

XXX-X-XXX

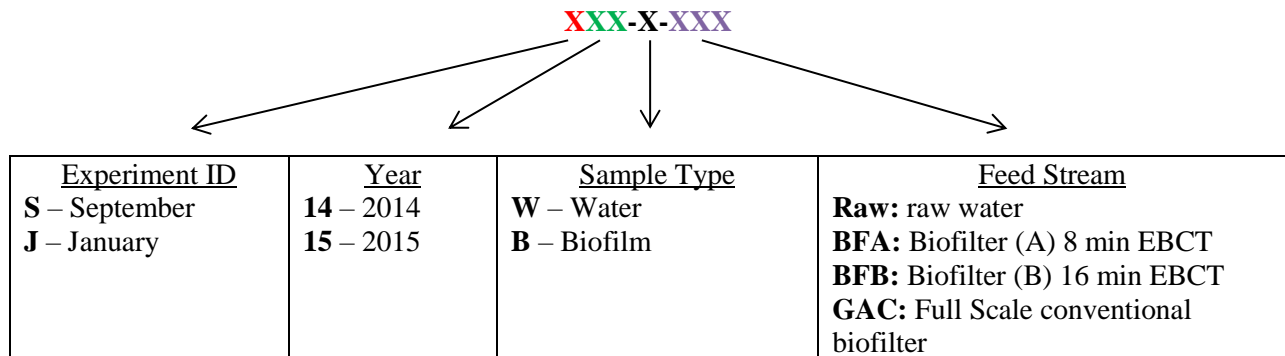| Experiment ID	Year	Sample Type	Feed Stream
S – September **J** – January	**14** – 2014 **15** – 2015	**W** – Water **B** – Biofilm	**Raw:** raw water **BFA:** Biofilter (A) 8 min EBCT **BFB:** Biofilter (B) 16 min EBCT **GAC:** Full Scale conventional biofilter

Figure S8 – Sample coding for clustering and PCA analysis